JOURNAL OF ASSOCIATED MEDICAL SCIENCES

JAMS

JOURNAL OF ASSOCIATED MEDICAL SCIENCES

THE OFFICIAL PEER-REVIEWED ONLINE JOURNAL

Volume 55 Number 3 September-December 2022 E-ISSN: 2539-6056

Journal of Associated Medical Sciences

Aims and scope

The Journal of Associated Medical Sciences belongs to Faculty of Associated Medical Sciences (AMS), Chiang Mai University, Thailand. The journal specifically aims to provide the platform for medical technologists, physical therapists, occupational therapists, radiologic technologists, speech-language pathologists and other related professionals to distribute, share, discuss their research findings, inventions, and innovations in the areas of:

1. Medical Technology
2. Physical Therapy
3. Occupational Therapy
4. Radiologic Technology
5. Communication Disorders
6. Other related fields

Submitted manuscripts within the scope of the journal will be processed strictly following the double-blinded peer review process of the journal. Therefore, the final decision can be completed in 1-3 months average, depending on the number of rounds of revision.

Objectives

The Journal of Associated Medical Sciences aims to publish integrating research papers in areas of Medical Technology, Physical Therapy, Occupational Therapy, Radiologic Technology, and related under peer-reviewed via double-blinded process by at least two internal and external reviewers.

Types of manuscript

Manuscripts may be submitted in the form of review articles, original articles, short communications, as an approximate guide to length:

- **Review articles** must not exceed 20 journal pages (not more than 5,000 words), including 6 tables/figures, and references (maximum 75, recent and relevant).
- **Original articles** must not exceed 15 journal pages (not more than 3,500 words), including 6 tables/figures, and 40 reference (maximum 40, recent and relevant).
- **Short communications** including technical reports, notes, and letters to the editor must not exceed 5 journal pages (not more than 1,500 words), including 2 tables/figures, and references (maximum 10, recent and relevant).

Peer review process

By submitting a manuscripts to Journal of Associated Medical Sciences, the authors agree to subject it to the confidential double-blinded peer-review process. Editors and reviewers are informed that the manuscripts must be considered confidential. After a manuscripts is received, it is assigned by a specific Associate Editor. The Associate Editor prepares a list of expert reviewers, which may include some suggested by the Editor-in-Chief. Authors can indicate specific individuals whom they would like to have excluded as reviewers. Generally, requests to exclude certain potential reviewers will be honored except in fields with a limited number of experts. All potential reviewers are contacted individually to determine availability. Manuscripts files are sent to at least two expert reviewers. Reviewers are asked to complete the review of the manuscripts within 2 weeks and to return a short review form. Based on the reviewers' comments, the Associate Editor recommends a course of action and communicates the reviews and recommendations to the Editor-in-Chief for a final decision.

The Associate Editor considers the comments made by the reviewers and the recommendation of the Editor-in-Chief, selects those comments to be shared with the authors, makes a final decision concerning the manuscripts, and prepares the decision letter for signature by the Editor-in-Chief. If revisions of the manuscripts are suggested, the Associate Editor also recommends who should review the revised paper when resubmitted. Authors are informed of the decision by e-mail; appropriate comments from reviewers and editors are appended.

Publication frequency

Journal of Associated Medical Sciences publishes 3 issues a year

Issue 1: January-April
Issue 2: May-August
Issue 3: September-December

Journal Impact Factor
The journal's 2017 Impact Factor is 0.237

Journal website
Homepage https://www.tci-thaijo.org/index.php/bulletinAMS/index

Journal E-ISSN:
2539-6056

Editorial Office
Faculty of Associated Medical Sciences, Chiang Mai University
110 Inthawaroros Road, Suthep, Muang, Chiang Mai, 50200
Phone 053 935072 Facsimile 053 936042

Journal of Associated Medical Sciences

Vol. 55 No. 3 : September 2022

Content

Content

Journal of Associated Medical Sciences 2022; 55 (3): 1-6

JAMS
Journal of Associated Medical Sciences

Thai-Journal Citation Index Centre (TCI) & ASEAN Citation Index (ACI)

Journal of Associated Medical Sciences

Journal homepage: https://www.tci-thaijo.org/index.php/bulletinAMS/index

Analysis of retinal nerve fibre layer thickness and optic disc parameters in patients of iron deficiency anaemia

Swati Samant[1] Suchismita Mishra[1] Smaraki Mohanty[2] Deergha Pareek[1] Srikant Kumar Dhar[3] Pradeep Kumar Panigrahi[1*]

[1]*Department of Ophthalmology, Institute of Medical Sciences & SUM Hospital, Siksha O Anusandhan (deemed to be) University, 8-Kalinga Nagar, Bhubaneswar.*

[2]*Department of Community Medicine, Institute of Medical Sciences & SUM Hospital, Siksha O Anusandhan (deemed to be) University, 8-Kalinga Nagar, Bhubaneswar.*

[3]*Department of Medicine, Institute of Medical Sciences & SUM Hospital, Siksha O Anusandhan (deemed to be) University, 8-Kalinga Nagar, Bhubaneswar*

ARTICLE INFO

Article history:
Received 28 March 2022
Accepted as revised 2 May 2022
Available online 6 May 2022

Keywords:
Iron deficiency anaemia, optical coherence tomography, retinal nerve fibre layer, peripapillary, optic disc

ABSTRACT

Background: To evaluate peripapillary retinal nerve fibre layer (RNFL) thickness and optic disc parameters in iron deficiency anaemia (IDA) patients and its correlation with various blood parameters of age and sex matched healthy controls with the help of spectral domain optical coherence tomography (SD-OCT).

Materials and methods: Cross sectional, hospital based study was done on patients with IDA and healthy patients attending departments of Ophthalmology and haematology of a tertiary referral hospital in Eastern India from June 2020 to January 2021. Comprehensive ophthalmic examination was done in all patients. Peripapillary RNFL thickness was measured using SD-OCT. Blood analysis for all patients included blood haemoglobin, serum iron binding capacity, Serum Ferritin, total iron binding capacity (TIBC), mean corpuscular volume (MCV), mean corpuscular haemoglobin (MCH) and mean corpuscular haemoglobin Concentration (MCHC).

Results: Twenty five patients with IDA and 25 age and sex matched healthy patients constituted the study and control groups respectively. Mean age of study and control groups was 40.44±5.51 and 39.12±11.60 years respectively. Strong positive correlation was noted between mean RNFL thickness and haemoglobin, serum ferritin, serum iron and serum transferrin levels. Negative correlation was noted between mean RNFL thickness and total iron binding capacity.

Conclusion: Patients with IDA in Eastern India have decreased mean peripapillary RNFL thickness. Mean RNFL thickness in different quadrants may not only be dependent on iron parameters but might also be influenced by dietary and geographical factors.

Introduction

Anaemia is a common public health problem, iron deficiency being the most common cause.[1] Women of child bearing age are particularly affected.[2] Iron is required for carrying oxygen and for normal functioning of oligodendrocytes, which play an important role in myelination.[3,4] Hence, depleted iron stores cause hypoxia and defective myelination. Hypoxia results in neuronal death through various mediators and mechanisms. As a result, retinal ganglion cells undergo damage by a compromise in normal perfusion and oxygen saturation.[5] Iron deficiency also results in dopaminergic dysfunction.[6] Retinal dopaminergic dysfunction alters receptive areas of axons and ganglion cells, which constitute retinal nerve fibre layer (RNFL).[7]

Decreased thickness of RNFL has been reported in various types of ischemic retinal diseases like diabetic retinopathy,

* **Corresponding author.**
Author's Address: *Department of Ophthalmology, Institute of Medical Sciences & SUM Hospital, Siksha O Anusandhan (deemed to be) University, 8-Kalinga Nagar, Bhubaneswar.*
** **E-mail address:** doc.pkp25@gmail.com
doi: 10.12982/JAMS.2022.017
E-ISSN: 2539-6056

glaucoma, retinal vascular occlusion, and retinopathy of prematurity. Thus decreased RNFL thickness has played a key role in diagnosis and monitoring of these diseases.[8-10] Optical coherence tomography (OCT) is a non-invasive imaging method that is widely used in the diagnosis of optic nerve and RNFL diseases.[11] The spectral domain OCT (SD OCT) technique provides faster acquisition, better resolution and improved imaging of retinal morphology than traditional OCT.[12]

In the current study, we aimed to evaluate peripapillary RNFL thickness and optic disc parameters in iron deficiency anemia (IDA) patients and its correlation with various blood parameters of age and sex matched healthy controls with the help of SD-OCT.

Materials and methods

The present study included 25 eyes of 25 adults between 20-55 years of age with iron deficiency anaemia and 25 eyes of 25 age matched healthy control subjects who had come for routine check-up procedure to Department of Ophthalmology and Hematology at a tertiary care hospital in Eastern India between June 2020 to January 2021. The study adhered to the basic tenets of Helsinki Declaration. Institutional ethical committee clearance was obtained prior to beginning the study. Informed consent was obtained from all patients before enrolling into the study.

IDA was diagnosed when serum haemoglobin (Hb) was <10 g%, serum (Sr) iron ≤50µg/dl, Sr Ferritin concentration ≤15 g µ/dl, Mean Corpuscular Volume(MCV) <80 fl/red cell and Total iron binding capacity (TIBC) ≥300. Patients with best corrected visual acuity less than 20/20, myopia or hypermetropia >4.0 D, lenticular or other ocular media opacities, evidence of glaucoma ,strabismus, history of intraocular surgery or ocular trauma, uveitis, diabetic retinopathies, vitro retinal disorders,, neurologic diseases or any systemic diseases other than IDA were excluded from the study.

A complete ophthalmologic examination was done including visual acuity assessment using Snellen's visual Acuity chart, refraction, detailed slit lamp examination for anterior segment evaluation, intra ocular pressure (IOP) measurement by Goldmann applanation tonometry and dilated fundoscopy with indirect ophthalmoscope and 20 Dioptre lens. Blood analysis for all patients included serum Hb, serum iron binding capacity, Serum Ferritin, total iron binding capacity (TIBC), mean corpuscular volume (MCV), mean corpuscular hemoglobin (MCH) and mean corpuscular hemoglobin Concentration (MCHC).

Outcome Parameters

Topcon 3D SD OCT-1 Maestro (Topcon Medical System, Tokyo, Japan) was used to obtain RNFL thickness in peripapillary region using OCT 3D optic disc cube 200×200 scan protocol. The signal strength used for analysis was >7. Average, temporal, nasal, superior and inferior quadrant RNFL measurements were noted along with disc area, rim area and Cup disc ratio. Right eyes of all the patients were arbitrarily taken for analysis.

Statistical analysis

Data were analysed using the Statistical Package for Social Sciences version 25. Independent samples t-test was used for data with normal distribution and Mann–Whitney U-test was employed for those without normal distribution. Correlation analysis was performed with Spearman's correlation test. Youden's index was calculated. $p<0.05$ was considered statistically significant.

Results

The present study included 25 patients with IDA in the study group and 25 normal patients in the control group. The mean age of study group was 40.44±5.51 (range 20-60) years. Mean age of the control group was 39.12±11.60 (20-60) years. The clinical and laboratory characteristics of cases and controls are presented in Table 1. There was no significant difference in the age, refractive status and IOP in both the groups. Significant differences were noticed in gender, Hb%, Sr Iron, Sr Ferritin, Sr Transferrin, TIBC, MCV, MCH, and MCHC.

The average disc area, rim area, cup disc ratio were same in both the study and control groups. There was no significant difference between the two groups (Table2). RNFL thickness values are presented in Table 3. There was a statistical significant difference noted in average RNFL thickness as well as RNFL thickness in superior, inferior and nasal quadrants between the two groups.

Table 1 Clinical and laboratory characteristics of the groups.

Characteristics	Study (n= 25)	Control (n= 25)	*p value*
Age	40.44±14.06	37.36±12.83	0.421
Gender			
Male	8	13	0.003
Female	17	12	
Refraction	1.12±0.52	1.17±0.42	0.459
IOP	12.487±1.808	12.607±1.827	0.81587
Hb	6.68±1.98	13.20±1.32	<0.001
Serum Iron	24.5±9.78	86.31±8.44	<0.001
Serum Ferritin	5.03±1.40	36.63±2.82	<0.001
TIBC	416.2±103.24	318.36±7.91	<0.001
Serum Transferrin	5.34±1.47	30.19±1.37	<0.001
MCV	68.79±10.33	87.89±2.41	<0.001
MCH	21.56±4.77	29.24±2.08	<0.001
MCHC	32.26±9.36	34.16±1.77	<0.001

IOP: intraocular Pressure, Hb: hemoglobin, TIBC: total iron binding capacity, MCV: mean corpuscular volume, MCH: mean corpuscular hemoglobin, MCHC: mean corpuscular hemoglobin concentration.

Table 2 Optic disc parameters of the patients and control groups.

Characteristics	Study (n= 25)	Control (n= 25)	*p value*
Rim Area	1.48±0.28	1.55±0.302	0.400
Disc Area	1.98±0.42	1.97±0.39	0.915
Cup: Disc ratio	0.43±0.16	0.40±0.19	0.255

On Correlation analysis, a strong positive correlation was noted between mean RNFL thickness and Hb, Sr Iron, Sr Ferritin and Sr Transferrin while a negative correlation was observed between mean RNFL thickness and TIBC (Table 4) (Figure 1). Positive correlation noted between superior RNFL thickness with Sr Hb, Sr Iron and Sr ferritin (r=0.16, 0.05, 0.03) Similarly positive correlation was also found between inferior RNFL thickness and Sr Hb (r=0.22). We also found a positive correlation between nasal RNFL thickness and Sr Ferritin (r=0.362).

Table 3 Peripapillary retinal nerve fibre layer thickness by SD OCT.

RNFL thickness	Study (n= 25)	Control (n= 25)	*p value*
Average RNFL thickness	85.52±13.3	105.2±4.78	<0.001
Superior quadrant	102.88±26.29	137.44±5.45	<0.001
Inferior quadrant	102.8±23.63	129.08±1.85	<0.001
Nasal quadrant	64.24±14.89	86.24±2.44	<0.001
Temporal quadrant	60.8±15.91	67.8±5.04	0.045

RNF: retinal nerve fibre layer.

Table 4 Correlation between average RNFL layer and various blood parameters.

Average RNFL thickness 95.36± 14.02 µ	Mean±SD	Correlation "r"	*p value*
Hb	9.94±3.7	0.892	<0.001
Serum Ferritin	20.8±16.1	0.770	<0.001
Serum Iron	55.4±32.5	0.688	<0.001
Serum Transferrin	17.76±12.63	0.695	<0.001
TIBC	367.28±87.71	-0.368	0.009

RNFL: retinal nerve fibre layer, Hb: hemoglobin, TIBC: total iron binding capacity.

Receiver operating characteristic (Roc analysis) shows area under the curve is 0.891 (95% ci 0.78-0.99) with a p<0.001. Youden's index was calculated. Thus, at cut off value of 97 µm of total thickness of retinal nerve fibre, sensitivity is 100% and specificity is 84% of detecting anemia.

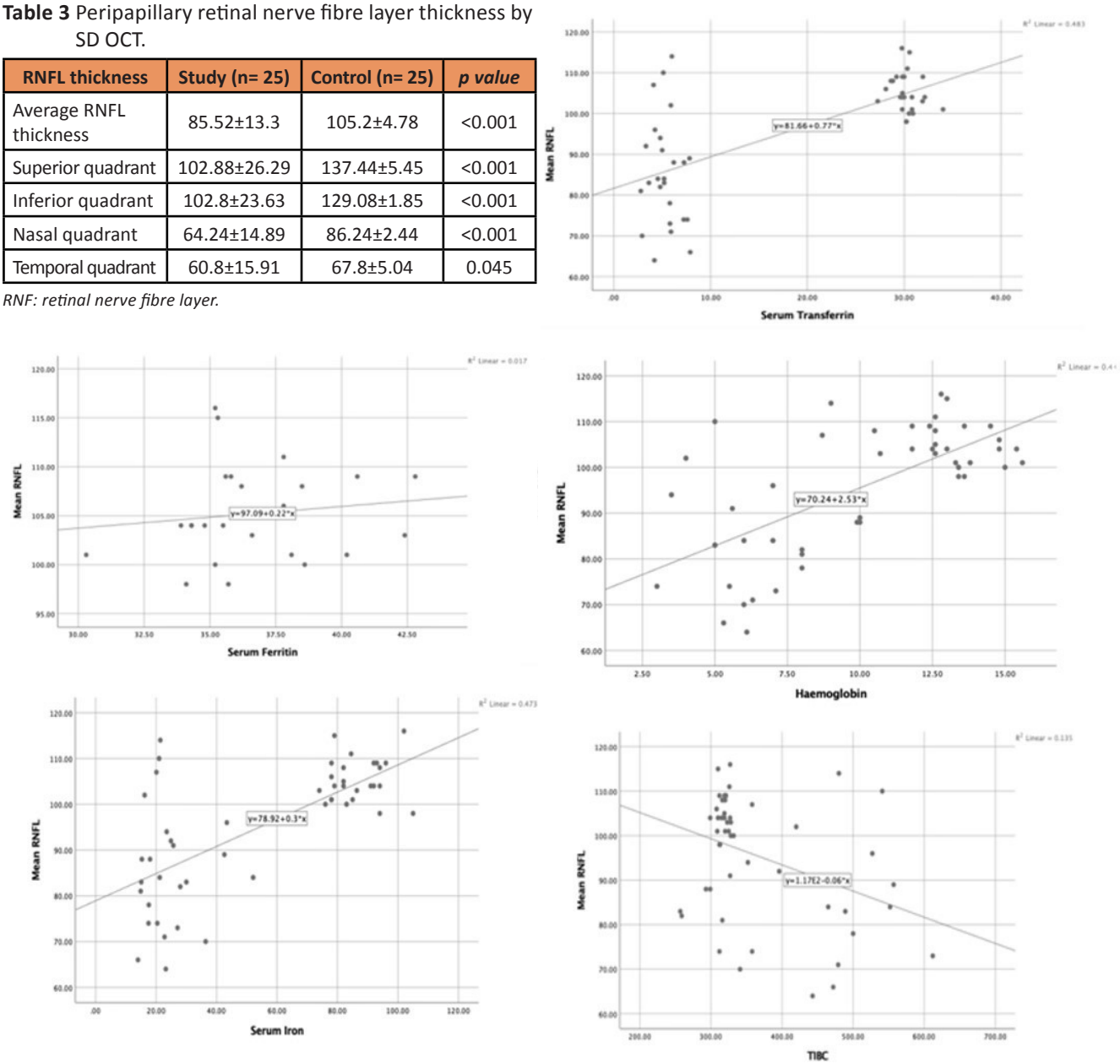

Figure 1. *Correlation analysis between retinal nerve fibre layer thickness and laboratory findings of the group.*

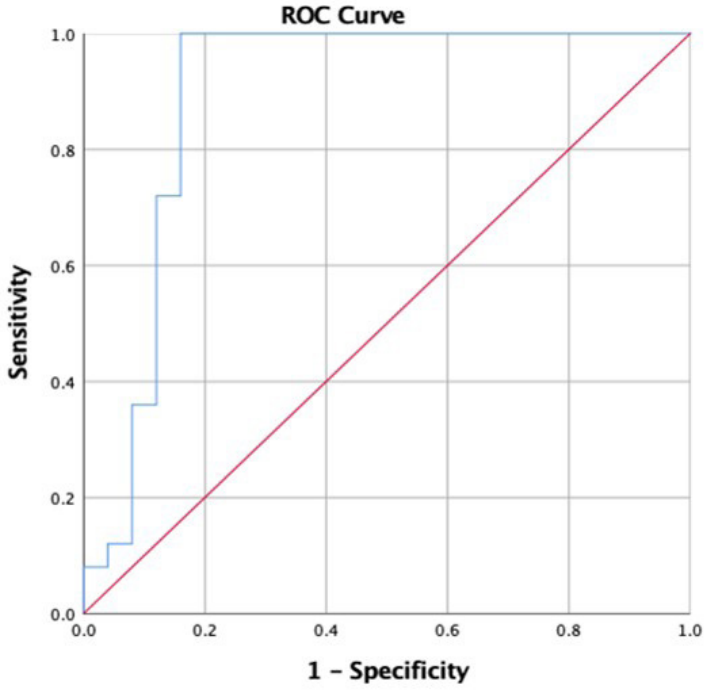

***Figure 2**. ROC Analysis.*

Discussion

IDA has been found to be the most prevalent type of anaemia worldwide.[13] It is known to cause various ocular diseases due to ischaemia.8 Decreased thickness of RNFL has been demonstrated in various ischaemic retinal diseases.[14] In our study, we have evaluated the RNFL thickness and optic disc parameters in patients with IDA. A significant (p<0.003) female preponderance was seen in our study which corroborated with other studies.[8, 15, 16] Several studies conducted in Turkish population have detected anaemia in 40-50% of the women in the childbearing age, most of which was related to iron deficiency.[17,18]

In our study mean serum Hb value (6.68±1.98 gm %) was lower and mean Serum Ferritin (5.03±1.40) was higher than in studies by Cikmazkara I *et al*[8] and Akdogan E *et al*.[16] However, Jaiswal S *et al*[3] have reported a lower mean haemoglobin and Sr Ferritin as compared to our study. Cases in our study had a higher mean Sr Iron (24.5±9.78) than that reported by Cikmazkara I *et al*.[8] However, TIBC and Sr Transferrin were similar between the two studies. Low range of Sr Hb in our study could be attributed to the direct referral of patients from Hematology Department who already had moderate to severe anemia.

Average disc area, rim area and cup disc ratio did not show any statistical significance which was similar to those reported by Cikmazkara I *et al*.[8] In our series we found IDA patients had significantly (p<0.001) thinner average, superior, inferior and nasal quadrant when compared to healthy controls. Maximum thinning was seen in nasal quadrant and maximum thickness was noted in the superior quadrant. Previous study in adult females with IDA by Moussa Eltohamy[2] showed thinning in average, superior, inferior, nasal and temporal quadrants. Study conducted by Jaiswal S. *et al*[3] on patients with IDA showed a decrease in peripapillary RNFL thickness in all four quadrants.

Various ophthalmic diseases like glaucoma are also associated with RNFL thinning along with changes in Optic Nerve Head.[19, 20] Hence, a thorough history regarding iron deficiency is vital for these disorders while taking OCT for RNFL analysis and management of such patients. Myopia and glaucoma are associated with optic nerve head changes and RNFL thining.[19, 21, 22] We could not find any significant optic nerve head changes except RNFL changes, so this should be considered while analysis of patients.

On correlation analysis between average and quadrant wise RNFL thickness with various laboratory parameters, we found a strong positive correlation between mean RNFL thickness and Sr Hb, Sr Iron, Sr Ferritin and Sr Transferrin while a negative correlation is found between mean RNFL thickness and TIBC. Positive correlation between superior RNFL thickness with Sr Hb ,Sr Iron and Sr Ferritin was noted. A positive correlation was also found between inferior RNFL thickness and Sr Hb .We also found a positive correlation between nasal RNFL thickness and Sr Ferritin. Strong correlation may be related to severe degree of anemia in our study, hence reflecting the effect of anemia on RNFL.

Cikmazkara *et al*[8] also reported a positive correlation between mean RNFL thickness and Sr Hb, Sr Iron, Sr Ferritin, and transferrin saturations, while a negative correlation was found between TIBC and mean RNFL thickness similar to us. Jaiswal *et al*[3] have reported a positive correlation between average RNFL thickness and Sr Hb and serum ferritin, and a

negative correlation was seen with TIBC. Whereas, Moussa Eltohamy[2] have reported a positive correlation between mean RNFL, Sr Hb and Sr Iron. All this studies have only compared the average RNFL with blood parameters. Akdogan *et al*[16] reported significant correlations between inferior quadrant RNFL thickness and Hb, and between nasal quadrant RNFL thickness and Sr Iron and Sr Ferritin concentrations, and TIBC which is similar to ours.

Our study has certain limitations. It has small sample size and is a hospital based study confined to Eastern India and so it does not represent typical population of India. Hence, the results of the study cannot be generalised. Larger studies from different regions are required to confirm the results obtained from our study and enhance the clinical importance of these findings. Further, duration of iron deficiency and history of blood transfusion were not taken into consideration. Moreover, the patients were not subdivided into various groups based on severity of anaemia. It is a cross sectional study and RNFL thickness was not revaluated after iron supplementation. Further studies are required to determine whether these RNFL changes can be reversed after treatment.

Conclusion

On assessment of the peripapillary RNFL thickness and optic disc parameters in IDA patients in Eastern India and comparing it to controls, it was seen that the average RNFL thickness in IDA decreases but quadrant wise it varies in different regions and is not only dependent on iron parameters but might also on dietary and geographical factors.

Acknowledgements

We would like to thank IMS and Sum Hospital, SOA deemed to be university for the facilities. Authors are grateful to the President, Prof. Manojranjan Nayak, SOA deemed to be university.

Conflict of interest

The authors declared no conflict of interest.

Source of funding

None.

References

[1]. Fairbanks VF. Iron-deficiency anemia. In: Mazza JJ, editor. Manual of Clinical Hematology. Philadelphia, USA: Lippincott Williams & Wilkins; 2002. pp. 17–38.

[2]. Soha Moussa Mohamed Eltohamy. Iron Deficiency Anemia as a risk factor for thining of peripapillary retinal nerve fibre layer thickness. International J Adv Res. 2016; 4: 1067-71.

[3]. Jaiswal SJ, Banait S, Daigavane SV. A comparative study on peripapillary retinal nerve fibre layer thickness in patients with iron-deficiency anemia to normal population. J Datta Meghe Inst Med Sci Univ 2018; 13: 9-11

[4]. Relationship of iron to oligodendrocytes and myelination. Connor JR, Menzies SLGlia. 1996; 17: 83-93

[5]. Kergoat H, Hérard ME, Lemay M. RGC sensitivity to mild systemic hypoxia. Invest Ophthalmol Vis Sci. 2006; 47: 5423-7.

[6]. Lozoff B. Early iron deficiency has brain and behavior effects consistent with dopaminergic dysfunction. J Nutr. 2011;1 41(4): 740S-6S. doi: 10.3945/jn.110.131169.

[7]. Djamgoz MB, Hankins MW, Hirano J, Archer SN. Neurobiology of retinal dopamine in relation to degenerative states of the tissue. Vision Res. 1997; 37: 3509-29.

[8]. Cikmazkara I, Ugurlu SK. Peripapillary retinal nerve fibre layer thickness in patients with iron deficiency anemia. Indian J Ophthalmol. 2016; 64: 201-5.

[9]. Lonneville YH, Ozdek SC, Onol M, Yetkin I, Gürelik G, Hasanreisoglu B. The effect of blood glucose regulation on retinal nerve fibre layer thickness in diabetic patients. Ophthalmologica. 2003; 217: 347-50.

[10]. Ozdek S, Lonneville YH, Onol M, Yetkin I, Hasanreisoglu BB. Assessment of nerve fibre layer in diabetic patients with scanning laser polarimetry. Eye (Lond) 2002; 16: 761–5.

[11]. Huang, D, Swanson, EA, Lin, CP. Optical coherence tomography. Science 1991; 254: 1178-81.

[12]. Nassif, N, Cense, B, Park, B. In vivo high-resolution video-rate spectral-domain optical coherence tomography of the human retina and optic nerve. Opt Express 2004; 12: 367-76.

[13]. Turkyilmaz K, Oner V, Ozkasap S, Sekeryapan B, Dereci S, Durmus M. Peripapillary Retinal Nerve Fibre Layer Thickness in children with Iron Deficiency Anemia. Eur J Ophthalmol 2013; 23: 217-22

[14]. Lim MC, Tanimoto SA, Furlani BA, Lum B, Pinto LM, Eliason D, et al. Effect of diabetic retinopathy and panretinal photocoagulation on retinal nerve fibre layer and optic nerve appearance. Arch Ophthalmol 2009; 127: 857-62.

[15]. F. Uzun, E. E. Karaca, G. Yıldız Yerlikaya et al., "Retinal nerve fibre layer thickness in children with β-thalassemia majorSaudi." Saudi J Ophthalmol. 2017; 31: 224-8.

[16]. E. Akdogan, K. Turkyilmaz, T. Ayaz, and D. Tufekci, "Peripapillary retinal nerve fibre layer thickness in women with iron deficiency anaemia." J Int Med Res. 2015; 43: 104-9.

[17]. Dilek I, Erkocç R, Sayarlioglu M, Ilhan M, Alici S, Turkdogan K, et al. Hematological Values And Ferritin Levels of Healthy Adult Individuals In Van City Center and Countryside. Van Med J. 2002; 9: 52–5.

[18]. Yılmaz FZ, Erdal S, Bakıcı Z, Cçınar Z. Investigation of the normal values of some haematological parameters of the adults living in the central region of Sivas. Erciyes Medical J. 2003; 25: 1-10.

[19]. Gandhi M, Dubey S. Evaluation of the Optic Nerve Head in Glaucoma. J Curr Glaucoma Pract. 2013; 7: 106-14.

[20]. Baniasadi N, Paschalis EI, Haghzadeh M, Ojha P, Elze T, Mahd M, Chen TC. Patterns of Retinal Nerve fibre Layer Loss in Different Subtypes of Open Angle Glaucoma Using Spectral Domain Optical Coherence Tomography. J Glaucoma. 2016; 25: 865-72.

[21]. Tsutsumi T, Tomidokoro A, Saito H, Hashizume A, Iwase A, Araie M. Confocal Scanning Laser Ophthalmoscopy in HighMyopic Eyes in a Population-Based Setting. InvesOphthalmol Vis Sci. 2009; 50: 5281-7.

[22]. Kamath AR, Lakshey D. Peripapillary retinal nerve fibre layer thickness profile in subjects with myopia measured using optical coherence tomography. J Clinical Ophthalmol Research. 2014; 2: 131-13.

Journal of Associated Medical Sciences 2022; 55 (3): 7-10

JAMS
Journal of Associated Medical Sciences

Thai-Journal Citation Index Centre (TCI) & ASEAN Citation Index (ACI)

Journal of Associated Medical Sciences

Journal homepage: https://www.tci-thaijo.org/index.php/bulletinAMS/index

Clinical characteristics and laboratory testing of patient with Sar CoV2 infection

Kanchana Tomanakan[1*] **Anchalee Bunbal**[2]

[1]*Department of Medical Technology, Khon Kaen Hospital, Khon Kaen Province, Thailand*
[2]*Hematology Division, Department of Medical Technology, Khon Kaen Hospital, Khon Kaen Province, Thailand*

ARTICLE INFO

Article history:
Received 9 March 2022
Accepted as revised 2 May 2022
Available online 7 May 2022

Keywords:
Sar CoV2, clinical characteristic, laboratory testing

ABSTRACT

Background: Sar CoV2, a novel coronavirus was identified as the cause of respiratory abnormality diseases COVID-19. It has no specific symptoms and the transmission occurs via respiratory droplets or contaminated surfaces. Seroprevalence studies of many diseases have been found to be useful to detect people who were exposed to infection and reveal the burden of the disease.

Objectives: This study aimed to assess the correlation between Clinical findings and laboratory testing of patients with Sar CoV2 infection as derived by RT PCR detection and to investigate serological antibody of IgM, IgG in serum of Covid19 hospitalized patients.

Materials and methods: The study was conducted on 168 patients with positive RT PCR for COVID-19 during June 2021- January 2022 in Khon Kaen Hospital. The nasopharyngeal swabs and blood samples were obtained on the day of admission. Data collection of patient's clinical symptoms and laboratory testing were recorded for statistical analysis. We performed CBC and anti Sar CoV2 (IgM,IgG) according to standard laboratory methods.

Results: The results indicated that seroprevalence of anti Sar CoV2 in COVID-19 patients was approximately 28% (47/168). The laboratory markers of CBC; as WBC, neutrophil, lymphocyte and platelet demonstrated lower significance. No correlation was observed between Ct of RT PCR with clinical signs and symptoms of COVID-19 patients. In case of RBC, Hemoglobin and Hematocrit, there were also no correlation with clinical characteristics of COVID-19 patients.

Conclusion: The study observed that WBC count and platelet count was significantly lower for some cases. However, awareness of these parameters is required, because of the large heterogeneity in test performance. From serological tests it was observed that anti Sar CoV2 is not suitable diagnosis of the acute phase of infection. Both tests can be used to help RT PCR for diagnosis of Sar CoV2 infection.

Introduction

The coronavirus disease COVID-19 has spread rapidly, resulting in high morbidity and mortality. Early on during the pandemic, WHO recommended that testing for virus should be considered for symptomatic patients as well as for those who are asymptomatic but who have been in contact with confirmed cases.[1] Sar CoV2 virus belongs to a family of enveloped RNA virus with a crown or corona like appearance.[2] The clinical signs and symptoms of COVID-19 can range from asymptomatic, mild to severe disease. The data from pooled prevalence of asymptomatic COVID-19 is about 48% and found to be higher in females than males.[3] Most patients presented with mild respiratory tract infection characterized by fever and cough (81%) while severe pneumonia

* **Corresponding author.**
Author's Address: *Department of Medical Technology, Khon Kaen Hospital, Khon Kaen Province, Thailand.*

** **E-mail address:** tomanakankanchana@yahoo.com
doi: 10.12982/JAMS.2022.018
E-ISSN: 2539-6056

has been reported in 14%. Two % was the overall mortality rate.[4] Reverse-transcription polymerase chain reaction (RT PCR) for Sar CoV2 is considered as the gold standard for diagnosis of COVID-19. In the real situation, RT PCR has not been performed widely in clinical settings because it requires special equipment, and needs highly skilled laboratory technicians. Therefore as RT PCR was a time-consuming process, alternative diagnostic tests should be performed in cases of emergency. The seroconversion of specific IgM, IgG antibodies was demonstrated in serum of patients in 4-7 days.[5] Most patients had neutralizing antibodies on day 14-20 but there was much variability. The antibodies IgG level showed positivity for 3-6 month.[6] The study of immunochromatography assay detecting IgM,IgG alone was not recommended in early phase of Sar CoV2 infection. The chest computed tomography combined with Immunochromatography assay showed sensitivity of 74.3% in asymptomatic patient and 82.4% in symptomatic patients.[7] Asymptomatic cases were defined as cases of no history of clinical signs and symptoms. Symptomatic patients exhibited clinical signs and symptoms of COVID-19: fever, nasal discharge, cough, diarrhea, dyspnea and oxygen saturation lower than 93%. The most common laboratory abnormalities were lymphopenia (63-83%), leukopenia as 9-34% and thrombocytopenia 36%.[8] Only 5-10% of COVID-19 patients progressed to severe. Then, patients in these cases were admitted to Intensive Care Unit(ICU).[9] Mortality in patients with severe and critical COVID-19 was 26%. The data showed respiratory failure was the most common cause of death in COVID-19.[10] Moreover, evaluation of laboratory parameters can be enhanced to discriminate between symptomatic and asymptomatic cases The aim of this study was to analyze laboratory abnormalities which correlated with Clinical characteristic of patients who diagnosed as COVID-19 and to assess IgM, IgG antibodies which were detected in COVID-19 patients.

Materials and methods

Study design

We conducted the present study on COVID-19 patients who were admitted and received medical treatment at Khon Kaen Hospital, Khon Kaen province, Thailand from June 2021- January 2022. All patients had RT PCR performed for Sar CoV2 using nasopharyngeal swabs and clinical information was collected from medical request records. Blood samples were taken on the same day that the RT PCR test was evaluated. We tested CBC, and serum samples were tested for IgM, IgG antibody. All methods were employed according to the manufacturer's instructions and tested as per the usual laboratory workflow.

Subjects

We enrolled 168 hospitalized patients in Khon Kaen Hospital who met the inclusion criteria of RT PCR detected with clinical data completed. The participants were categorized into 3 groups by the stage severity for COVID-19.[11,12]

Ethical statement

This study was approved by the Ethical committee of Khon Kaen Hospital. (Approved no.KEXP64008).

Laboratory methods

The nasopharyngeal swabs and blood samples were obtained on the day of admission. RT PCR were performed by automatic analyzer (Cobas 6800; Roche diagnostics GmbH) where the RT PCR assay was used to detect a conserve region in the E gene of Sar CoV2. For the complete blood count (CBC), we used the Sysmex XN series analyzer. We evaluated serum antibodies by ECLIA method using Cobas Pro (Roche diagnostics GmbH). The positive and negative controls were tested in all runs. All of the data from our study was coded as a research number.

Statistical analysis

We analyzed the quantitative data expressed as mean and range with 95% confidence interval. For the qualitative variables Chi-square testing was used to distinguish clinical characteristics and laboratory findings among asymptomatic, mild and severe cases. Statistical significance was taken as $p<0.05$.

Results

The demographic data of the 168 patients are displayed in Table 1. The mean age of our study was 48 year. Of the subjects, 43% (72/168) were male and 57% were female. All of 168 subjects were positive by RT PCR. We divided all patients into 3 groups; 87 asymptomatic cases who were taken to admit in Hospitel (Hotel serviced as hospital), 59 cases as characterized as mild and 22 cases diagnosed as severe COVID-19 and were received for treatment in ICU. Our study found that 51.8% (87/168) of RT PCR positive presented as asymptomatic. A 35.1% (59/168) of patients had mild clinical signs as fever, cough, fatigue and loss of smell. In 22 severe cases (12.1%), the patients progressed to severe pneumonia and respiratory failure.

Table 1 Demographic and clinical signs and symptoms of the study subjects.

Clinical Characteristics	n=168
RT PCR: Detected	100% (168/168)
Ct≤25	60.12% (101/168)
Ct≥25	39.88% (67/168)
Gender	
Female	57% (96/168)
Male	43% (72/168)
Age	
Mean (year)	48 (18-64)
Clinical symptoms	
Asymptomatic	51.80% (87/168)
Mild	35.12% (59/168)
Severe	13.08% (22/168)

The laboratory investigation report of the 168 patients is shown in Table 2. A PCR cycle threshold Ct<36 was defined as a positive result. In our study we were concerned about the intensity of viral RNA and investigation of Ct≤25 compared with Ct≥25 in patients who tested as RT PCR positive. The results demonstrated 60.1% of patients had Ct≤25, while 39.9% of patients had Ct≥25. When we evaluated between the 2 groups of Ct with clinical characteristics, no correlation with asymptomatic and severe COVID-19 was observed. In the case of comparing the RBC, Hemoglobin and Hematocrit with clinical group characteristics there was no significant correlation. (r=0.29-0.36) According to the data, WBC, neutrophil, lymphocyte and platelet counts were analyzed showing significant high differences between groups of asymptomatic, mild and severe cases. (p<0.05) To evaluate whether the antibody level correlated with disease severity, we observed a higher level in the severe group compared to the asymptomatic and mild cases.

Table 2 Laboratory findings of parameters in CBC (Complete blood count) and antibody detection.

Test report	Asymptomatic (n=87)	Mild (n=59)	Severe (n=22)	*p* value
CBC:				
RBC (10^6/µL)	4.7 (3.9-4.9)	4.8 (4.1-5.4)	4.5 (3.7-5.3)	0.804
Hemoglobin (g/dL)	13.2 (12.9-13.5)	13.5 (13.1-13.8)	13.4 (13.1-14.0)	0.290
Hematocrit (%)	34.9 (33.8-37.0)	36.1 (35.2-38.3)	36.3 (35.1-37.9)	0.568
WBC (10^3/µL)	5.9 (5.6-7.8)	5.7 (5.2-7.1)	5.3 (4.6-7.6)	<0.05
Neutrophil (10^3/µL)	4.6 (4.2-5.8)	5.0 (4.7-5.2)	6.3 (6.0-7.6)	<0.05
Lymphocyte (10^3/µL)	2.2 (1.6-3.1)	2.3 (2.2-2.9)	2.7 (2.6-3.6)	<0.05
Platelet (10^3/µL)	179 (157-248)	188 (186-286)	156 (165-235)	<0.05
IgM/IgG antibody to Sar CoV2	27% (24/87)	25% (15/59)	36% (8/22)	

Discussion

In our study, we analysed patients who were hospitalized in Khon Kaen Hospital during the second phase of COVID-19 outbreak. The diagnosis of COVID-19 was complicated due to the diversity of clinical symptoms. RT PCR of viral RNA is the gold standard. The limitation of RT PCR was that the initial RT PCR was not positive in patients with COVID-19 infection.[13] Several studies found the IgM,IgG antibody to protein N can be chosen for screening and estimation of seroconversion of COVID-19. However, 5-10% of convalescent individuals did not have the antibody response.[14] We observed the antibodies response in severe COVID-19 to be higher than in the asymptomatic and the mild groups. Normally asymptomatic and mild cases have a short time stay in hospital. This reason supported the study that the population failed to develop antibody against Sar CoV2. This may be from the ability to produce different immune response in infected individuals.[15]

Our study was similar to E.Ozcan. *et al*. in the year 2020.[16] The laboratory findings of the neutrophil, lymphocyte and platelet were lower when compared to normal healthy individuals. In results for 4 parameters (WBC, neutrophil, lymphocyte and platelet) for asymptomatic, mild and severe cases, we found significantly lower values for the clinical characteristics of these 3 groups.

Conclusion

From this study, we have useful information to select the test method for diagnosis of SarCoV2 infection. In situation of RT PCR positive, the associated clinical characteristics have been observed in the process of work during COVID19 pandemic in Khon Kaen hospital. The results of this study supported no significant difference in Ct ratio of viral RNA with severity of clinical signs and symptoms. Some CBC marker changes as WBC, neutrophil, lymphocyte and platelet should be considered in testing COVID19 patients.

Acknowledgements

The authors thanks Dr. Jurairat Jongthawin for her assistance of statistical analysis. I would like to thank Dr. Thananit Sangkhumkhamhang for giving me the opportunity to set up this work.

References

[1]. World Health Organization. Laboratory testing strategy recommendations for COVID-19: interim guidance. 2020. Available: http://app.who.int/iris/handle/10665/331509[Accessed 11 May 2020].

[2]. Munster VJ, Koopmans M, van Doremalen N, van Riel D, de Wit E. A novel corona virus emerging in /china: Key questions for impact assessment. N Eng J Med. 2020; 382: 692-4.

[3]. Syangtan G, Bista S, Dawadi P, Rayamajhee B, Shrestha LB, Tuladhar R, Joshi DR. Asymptomatic SAR CoV2 carriers: A systemic review and meta- analysis. Front. Public Health 2020; 8.

[4]. Sheahan TP, Sims AC, Leist SR, Schafer A, Won J, Brown AJ, et al. Comparable therapeutic efficacy of remdessivir and combination lopinavir, ritonavir and interferon beta against MERS-CoV Nat Commun. 2020; 11(1): 1-14.

[5]. Hsueh PR, Huang LM, Chen PJ, Kao CL, Yang PC. Chronological evolution of IgM,IgA,IgG and neutralization antibodies after infection with SAR-associated coronavirus. Clin. Microbiol. Infect. 2004; 10: 1062-6.

[6]. Wang Y, Li J, Li H, Lei P, Shen G, Yang C. Persistence of SARS CoV2 specific antibodies in COVID-19 patients. Int. Immunophamacol. 2021; 90 : 10727. [CrossRef] [PubMed]

[7]. Imai K, Tabata S, Ikeda M, Noguchi S, Kitahawa Y, Matuoka M, et al. Clinical evaluation of and immunochromatographic IgM/IgG antibody assay and chest computed tomograpgy for the diagnosis of COVID-19. J. Clinical Virololgy. 2020; 10493; 128: 1-4.

[8]. Guan WJ, Ni ZY, Hu Y, et al. Clinical characteristic of coronavirus disease 2019 in China. N Eng J Med. 2020; 382(18) : 1708-20.

[9]. Arentz M, Yim E, Klaff L. et al. Characteristic and outcomes of 21 Critically ill patients with COVID-19 in Washington state. JAMA. 2020; 323(16): 1612-4.

[10]. Grasselli G, Pesenti A, Cecconi M. Critical care utilization for COVID-19 outbreak in Lombardy, Italy: early experience and forecast during an emergency response [published online March 13,2020] JAMA. doi: lO.lOO/jama.2020.403l.

[11]. Huang C, Wang X, Li L, Ren J, Zhao YH,Zhang G, et al. Clinical features of patients infected with 2019 novel coronavirus in Wuhan, China. Lancet 2020; 395: 497-506.

[12]. Grasselli G, Zangrillo A, Zanella A. et al. Baseline characteristics and outcomes of 1591 patients infected with Sar CoV2 admitted to ICUs of the Lombardy region, Italy. JAMA. 2020; 323(16): 1574-81.

[13]. Guan WJ, Ni ZY, Hu Y, Liang WH, Qu CQ, He JX, et al. Clinical characteristic s of coronavirus disease. 2019 in China. N Engl J Med. 2020; 382(18): 1708-20.

[14]. Garcia-Basteiro ALG, Moncunill M, Tortjada M, Vidal C, Guinovart A, Jimenez R, et al. Seroprevalence of antibodies against Sar CoV2 among health care workers in large Spanish reference hospital. Nat. Commun.2020; 11: 3500.

[15]. Wu F, Wang A, Liu M, Wang Q, Chen J, Gu C, et al. Evaluating the association of clinical characteristics with neutralizing antibody levels in patients who have recovered from mild COVID-19 in Shanghai, China. JAMA Intern Med,2020; 180(10) : 1356-62.

[16]. Ozcan E, Yavuzer S, Borku BU, Islamoglu MS, Ikitimur H, Unal OF, et al. The relationship between positivity for COVID-19 RT PCR and symptoms, clinical finding and mortality in Turkey. 2020; doi.org/10.1080/14737159.2021.1882305.

Journal of Associated Medical Sciences 2022; 55 (3): 11-18

JAMS
Journal of Associated Medical Sciences

Thai-Journal Citation Index Centre (TCI) & ASEAN Citation Index (ACI)

Journal of Associated Medical Sciences

Journal homepage: https://www.tci-thaijo.org/index.php/bulletinAMS/index

A white cane modified with ultrasonic detectors for people with visual impairment

Pisak Chinchai[1*] Rattanaroj Inthanon[2] Kittichai Wantanajittikul[3] Supaporn Chinchai[4]

[1]Department of Occupational Therapy, Faculty of Associated Medical Sciences, Chiang Mai University, Chiang Mai Province, Thailand
[2]Rehabilitation and Traditional Chinese Medicine Center, Samitivej Chonburi Hospital, Mueang District, Chon Buri Province, Thailand
[3]Department of Radiologic Technology, Faculty of Associated Medical Sciences, Chiang Mai University, Chiang Mai Province, Thailand
[4]Department of Occupational Therapy, Faculty of Associated Medical Sciences, Chiang Mai University, Chiang Mai Province, Thailand

ARTICLE INFO

Article history:
Received 22 March 2022
Accepted as revised 30 April 2022
Available online 7 May 2022

Keywords:
White cane, assistive technology, ultrasonic sensor, visual impairment, walking locomotion

ABSTRACT

Background: A white cane is the most common equipment used by the blind for navigation. However, a cane can detect obstacles only at ground level, while many physical barriers can be at mid-body or head level.

Objectives: The aim of this study was to create a white cane with ultrasonic sensors that could detect objects at waist and head levels.

Materials and methods: Ten blindfolded participants, 5 males and 5 females, were recruited by means of purposive sampling into the study. All these participants tested the efficacy of the modified cane by walking through 3 obstacle spots; the first was a barrier at head level; the second and third were barriers at waist level. The instruments used were: 1) The Satisfaction Assessment for Assistive Devices and 2) the electrical and assembly compartments for the ultrasonic detector. The data was analyzed using descriptive statistics.

Results: The results demonstrated that all blindfolded participants could get through the three testing stations by using the modified white cane. They also revealed high satisfaction with both the usability and efficiency of the modified cane. The highest satisfaction in usability was for the size of the cane ($\bar{x}$±SD = 4.50±0.533). Participants also reported very high satisfaction with the efficiency of the cane in detecting objects at mid-body ($\bar{x}$±SD = 4.70±0.48) and head levels ($\bar{x}$±SD = 4.50±0.53).

Conclusion: All these results indicated that the modified cane with ultrasonic detectors was beneficial for detecting objects at mid-body and head levels in visually impaired people.

Introduction

The number of people who are visually impaired is increasing. In the year 2015, an estimated 36 million people around the world were blind; 217 million had moderate or severe vision impairment, and 188 million had mild vision impairment.[1] In Thailand, in the year 2019, there were 191,264 people with defective vision out of 2,058,082 people with disabilities[2] in the total population of 66,186,727.[3] This makes it the third in the country in terms of the number of people suffering from a disability.[2] Visual impairment and age-related eye diseases affect economic and educational opportunities.[4] They can also reduce the quality of life[5], and increase the risk of death in these individuals.[6, 7] Visually impaired people face many challenges in their daily lives, such as reading, cooking, socialization, transportation, exploring unfamiliar environments, and, especially, moving from place to place.[8] Navigating independently, without the assistance of others, is a major

* **Corresponding author.**
Author's Address: *Department of Occupational Therapy, Faculty of Associated Medical Sciences, Chiang Mai University, Chiang Mai Province, Thailand.*
** **E-mail address:** pisak.c@cmu.ac.th
doi: 10.12982/JAMS.2022.019
E-ISSN: 2539-6056

challenge for these people.[9, 10] The most common and accessible assistive device for individuals without vision is the white cane.[11, 12]

The white cane can detect physical barriers in front of people with visual disturbances, but only at ground level. It cannot explore aerial obstacles or architectural barriers near the middle and upper body parts of blind people, such as timber branches, suspended advertisement boards, etc., and these can be dangerous to those with blindness.[13, 14] Manduchi and Kurniawan[15] studied mobility-related accidents in 300 blind participants, and they revealed that 40% of these individuals reported head accidents at least once a year. In addition, they reported that 23% of the incidents had medical consequences. Many walking assistants have been developed for obstacle detection at the aerial level with sensor feedback signals.[16-21] Sensor-based walking aids provide people with visual impairments with information about their surroundings through an audio signal, vibration, or both.[22] Among the different sensors, ultrasonic sensors are widely used.[23] Dos Santos, *et al*.[11] developed an electronic white cane to detect objects above the waist for blind users. However, there were 3 electronic compartments affixed separately to the handle of the white cane -namely the ultrasonic sensor, the microcontroller, and the battery-and this may have caused maintenance difficulties. Kulyukin, Gharpure, and Nicholson[24] developed a walking aid for visually impaired people called RoboCart where the authors used radio frequency identification (RFID) to tag the objects. However, this system is impractical for use in real life as it is not easy to trace everything with RFID. The virtual white cane or the hand-held range sensing device[25] and the smart cane[26] are some other equipment for people with visual impairment. These also have some limitations, such as being bulky in size, uncomfortable use, and difficulties using them in public.

In Thailand, Punyanon[27] has developed ultrasonic sensor equipment that can be attached to a cap worn above the eye level of the blind persons in order to detect barriers in front of them above their waistline, and Kongkumsuk[28] has produced an ultrasonic box that is fixed to eyeglasses for persons with visual impairment to explore objects from mid-body and above. However, the equipment was bulky and the weight of it dragged down the cap and eyeglasses when the users were walking.

Researchers, therefore, were interested in the development of the white cane with ultrasonic sensors that could detect obstacles both at mid-body and at head levels. The ultrasonic detector should be attached to the handle of the white cane firmly and tidily and be easy to use. This is consistent with the Empowerment of Persons with Disabilities Act, B.E 2007, in Thailand, which states that assistive devices should be accessible by people with disabilities in order to promote independent living and a good quality of life (QOL) for these individuals.[29]

Materials and methods

The present study aimed to create a white cane with an ultrasonic sensor to detect physical barriers at waist and head levels in front of people with visual impairment. This study also investigated the effectiveness of the modified white cane and evaluated satisfaction among the blindfolded subjects using the equipment.

Participants

Ten non-visually impaired adult participants, 5 males and 5 females, were recruited by means of purposive sampling from the 4th year occupational therapy students at the Faculty of Associated Medical Sciences, Chiang Mai University, in the academic year 2020. The selection of subjects was in accordance with the inclusion criteria as follows:

Inclusion criteria

1) All senses are intact throughout the whole body. Superficial, deep, and cortical senses were tested by the 3-scale (intact, impaired, and absent) sensation examination.
2) People with a normal gait pattern. Tested by allowing subjects to walk on a 6-meter walking path.
3) Height between 151 and 190 centimeters (cm), as most people's heights are between this range.
4) Willing to participate in the research project where all subjects are required to close their eyes with eye pads on and walk in the simulation environment during the testing procedure.

Instruments

1. The Satisfaction Assessment for Assistive Devices The Satisfaction Assessment for Assistive Devices was developed by Punyanon.[27] The instrument assesses the satisfaction of users with assistive devices in two aspects: 1) the appearance of the device size, weight, and assembly compartments), and 2) the efficiency of the device (precise detection of obstacles and accurate warning signal). Scores of satisfaction are ranked from 1 to 5 in each case, in which 1 refers to very low satisfaction, 2 to low satisfaction, 3 to moderate satisfaction, 4 to high satisfaction, and 5 to the highest satisfaction.

2. Electrical and assembly compartments for the ultrasonic detector

a. one piece of ESP32 DOIT NodeMCU ESP32 circuit board
b. two pieces of HC-SR04 Ultrasonic Module Distance Measuring Transducer Sensors
c. one piece of flame retardant FR-4: used as an electrical insulator
d. two pieces of 3-volt vibration motors
e. one piece of Module Stepdown 6-30V to 5V 3A fix 5V
f. one piece of 9-volt battery holder
g. one piece of 9-volt battery
h. one piece of on/off switch (DC power)
i. one piece of 5-meter electric wire
j. The wooden electronic box
k. The white cane.

Research Procedure

The research procedure was conducted step by step as follows: 1) The research project was approved by the Ethics Committee, Faculty of Associated Medical Sciences, Chiang Mai University (CMU), Thailand (ethics clearance number: 541/2563), 2) After the ethics approval, the research team created the circuit diagram and established the electrical circuit board of the ultrasonic detector, 3) Assembled all of the electrical compartments together into a wooden box and fixed this box to the white cane, 4) The authors of this paper contacted two experts - one a specialist who works in the area of assistive technology and the other an occupational therapist who has worked with visually impaired people for more than 5 years- to evaluate and comment on the modified white cane, 5) There was a public announcement of the research project to the 4th year occupational therapy students at the Faculty of Associated Medical Sciences, CMU and they were invited to participate in the study, 6) In accordance with the inclusion criteria, we recruited 10 participants, 5 males and 5 females, 7) We set up the simulation environment for training and testing the usability and efficiency of the fabricated white cane, 8) All subjects signed the consent form prior to participating in the testing procedure, and 9) The research team and research assistants (RA) collected data during the testing process.

Development of the White Cane Modified with an Ultrasonic Detector

The development of the white cane modified with the ultrasonic detector in the present study used ultrasonic principles. The ultrasonic transmitter sends a sound wave forward, and when it hits an object, a reflective wave is sent back to the ultrasonic receiver, which is converted into a vibration signal in real-time. The development process of the modified white cane was conducted step by step as follows.

1) The circuit board (model no. ESP32 DOIT NodeMCU ESP32 DEVKIT V1 ESP-32S NodeMCU ESP-WROOM-32 Wi-Fi) and Bluetooth Dual-Core (model no. ESP-32 ESP-32S ESP-32D) were fixed to the flame retardant FR-4. The electrical circuit diagram of the ESP32 DOIT NodeMCU is shown in Figure 1.

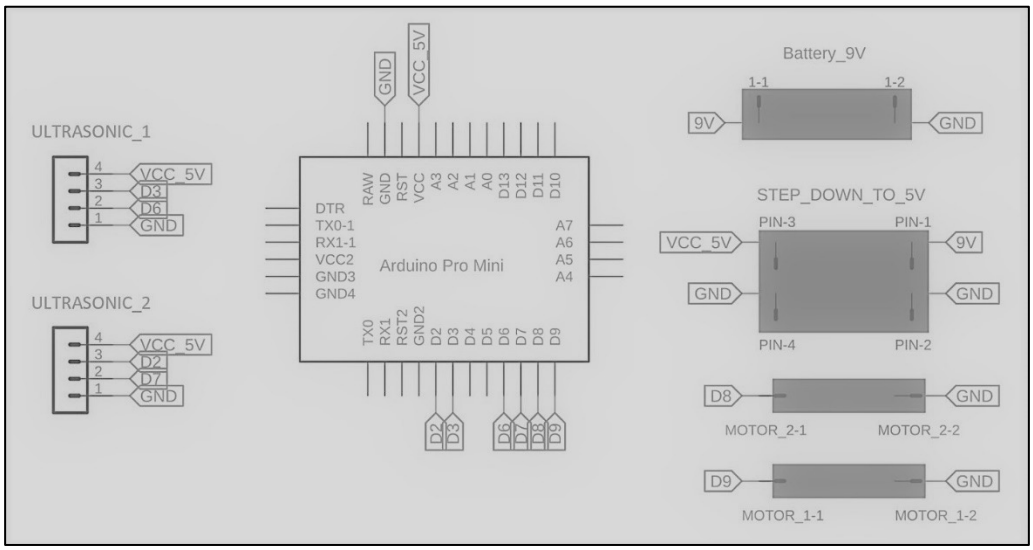

Figure 1. *Ultrasonic sensor electrical circuit diagram.*

2) Two ultrasonic sensors: module HC-SR04P, the 3-volt vibration motor and the Module Step-down 6-30V to 5V 3A fix 5V were connected to the circuit board.
3) We affixed the battery holder with a 9-volt battery and affixed the on/off DC power switch to the circuit board.
4) All of the assembly compartments were put in a small wooden electronic box (Figure 2) and attached to the handle of the traditional white cane (Figure 3). A three-dimension diagram of the wooden electronic box, which included size and shape, was shown in Figure 4. The weight of all the compartments and the wooden electronic box was 195 grams. Wooden electronic box was coated with lacquer to make it more durable. The traditional white cane has a length of 124 cm and a weight of 300 grams. The total weight of the modified white cane, therefore, was 495 grams. This cane has three main parts: a handle (grip) made from anatomic rubber, a straight aluminum shaft, and a nylon tip that is in direct contact with the object or the ground.
5) The ultrasonic sensors inside the wooden box can detect obstacles from mid-body to head level in front of the subjects. The lower sensor explored barriers at mid-body level and the upper sensor detected obstacles at head level (Figure 5). The frequency of the ultrasonic wave for the detection of objects was set at 45 kHz. It can detect both transparent and opaque objects.

Figure 2. *The wooden electronic box.*

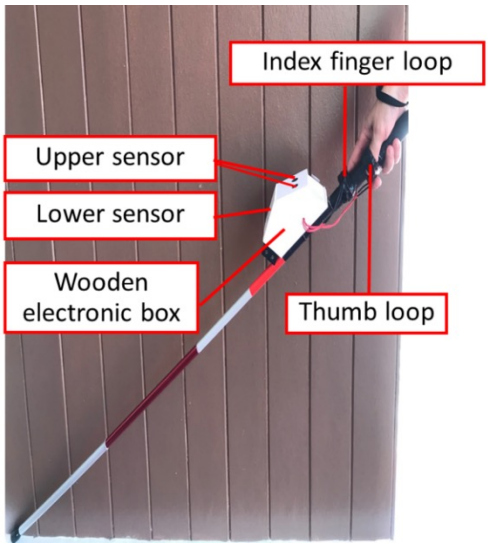

Figure 3. *A white cane with the wooden electronic box.*

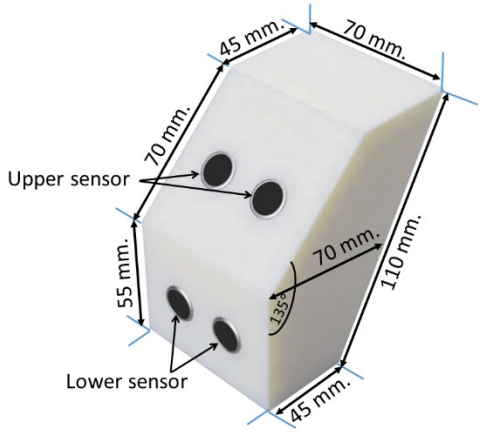

Figure 4. *A three-dimension diagram of the wooden electronic box.*

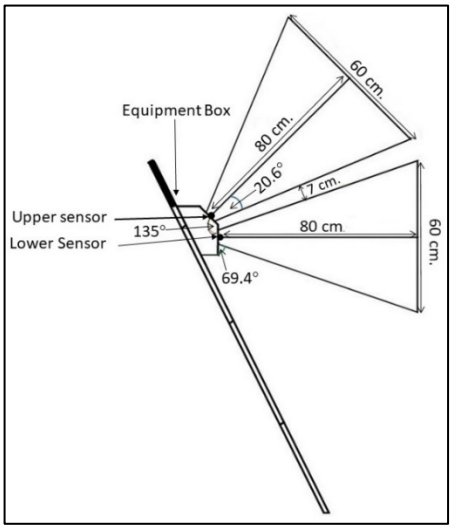

Figure 5. *Ultrasonic sensor detection degree.*

6) With a cane tilt angle of 43 degrees, the detection distance of the ultrasonic sensor was set at 80 cm in length in front of users, and 60 cm at maximum width (diameter), which meant each sensor covered an area of 2,826 cm^2 as calculated by the πr^2 formula (r=30 cm). The angle between the upper and the lower sensor was set at 135 degrees to allow the ultrasonic wave to detect objects in as much space as possible (Figure 5). However, the empty space between the detection areas of the upper and lower sensors was 7 cm wide. Users press the on/off button to start or stop the electrical circuit of the ultrasonic detector system.
7) When detecting obstacles, the sensor sends a vibration signal to the finger loops at the handle of the white cane. The index finger loop vibrates for objects at mid-body level, and the thumb loop vibrates for obstacles at head level (Figure 3).

Cost of the modified white cane with ultrasonic detector

The total price for the modified white cane with the ultrasonic detector in the present study was 800 baht (24.63 USD). This can be broken down into 1) electronic compartments and circuits, 380 Baht (11.70 USD), 2) vibration system and equipment box, 150 Baht (4.62 USD), and 3) the white cane, 270 Baht (8.31 USD). All these electronic compartments can be found in most electronic shops, and the white cane can be bought from a medical equipment shop or purchased online.

Test of the efficacy of the modified white cane with ultrasonic detectors

In the simulation testing room, we used a piece of cardboard (19 cm^2), and we hung it from the ceiling as the test's obstacle at head level. We used a pipe tree as a testing barrier at the mid-body level. There were 3 testing spots along the walking path. The first spot was the head-level testing station. The second and third spots were designed

to test reactions at waist level. The total walking distance was 8 meters, and the width of the route was 1.5 meters. Researchers used a two-inch high feature board on both sides of the path as the walking frame. The first testing station, used for testing at head level, was set at 2 meters from the starting point. The second and third stations, for testing at waist level, were set at 4 and 6 meters, respectively (Figure 6). The participants were unaware of the number of testing points in the evaluation room prior to testing.

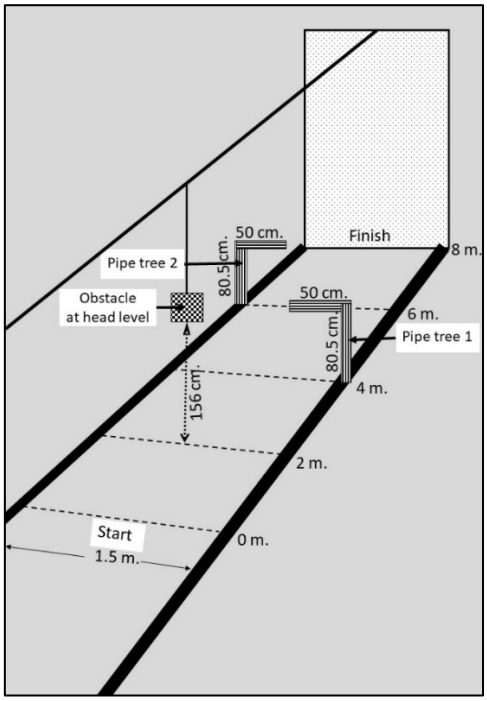

Figure 6*. A simulated path for a blindfolded walking test.*

The participants were divided into 3 groups depending on their height including:

1) For subjects who were between 151 and 160 cm, the cardboard was hung 146 cm from the floor in the middle of the walking track for head-level testing, and the pipe tree's branch, 2.2 cm in diameter, was set at 75.5 cm from the floor, protruding from the side of the testing track. The pipe tree was positioned on the right-hand side of the second testing spot but was located on the left-hand side of the third testing station. The pipe tree stood beside the simulation path where its branch protruded 50 cm into the track on the right side for the second testing spot, whereas the pipe tree branch protruded from the left side at the third testing station.
2) For subjects between 161 and 170 cm, the cardboard was hung at 156 cm from the floor in the middle of the walking track for head-level testing, and the pipe tree's branch was set 80.5 cm from the floor, protruding 50 cm into the track from the right side of testing spot number 2 and 50 cm into the track from the left side of testing spot number 3 (Figure 6).
3) For subjects between 171 and 180 cm, the cardboard was hung 166 cm from the floor in the middle of the walking track for head-level testing, and the pipe tree's branch was set at a height of 85.5 cm from the floor, protruding 50 cm into the track from the right side of testing spot number 2 and 50 cm from the left side of testing spot number 3.

All participants signed the consent form prior to the beginning of the study. They had been informed about the objectives and procedures of the research project and assured of the absence of any risks to their physical health and the possibility of leaving the study at any time. The experimental process consisted of 2 sections. Section 1 was conducted in the training room, where the obstacles at head level and at mid-body level were set up. The obstacles at head level used cardboard hung from the ceiling at 3 different heights-146, 156, and 166 cm from the floor, while the barriers at waist level used a pipe tree whose branch was positioned at the height of 75.5, 80.5, and 85.5 cm from the floor, and its branch protruded 50 cm into the path. The research team suggested participants choose a walking path that suited their height. The participants were also instructed on how to use the modified white cane and were allowed 10 minutes for familiarization. The instructions included: how to hold and position the cane (in front of the body); how to move the cane (rolling from side to side); how to turn on and off the electronic switch, and how the modified cane emits feedback as it approaches obstacles (increasing the vibration). The participants held the modified white cane in their dominant hands, kept their eyes open normally, and were instructed to walk toward the set-up obstacles at their self-selected walking speed to get familiar with the feedback vibration on their index fingers and thumbs. Section 2 was conducted in the testing room near the training room. Each subject covered both eyes with the standard eye-pads prior to entering the testing room. The research team brought the subjects into the testing venue one by one. At the start, each participant stood at the starting point in the middle of the path and could not protrude any part of their body or the modified white cane across the beginning line. They held the modified white cane in their dominant hand and waited for the researcher to inform them that they could start. All participants were also instructed not to touch the obstacles, relying only on the cane feedback, and to follow the floor path with the cane. Also, if they detected an obstacle, they had to stop and shift their steps to the right or left until the vibration signal on their finger stopped, then move forward. The research team announced, "Start walking," and the subject then walked forward at their self-selected speed.

All subjects were informed that a vibration signal occurring at the index finger indicated an obstacle at mid-body, while a vibration at the thumb indicated a barrier at head level. When the subject passed through the third station, the principal investigator informed each individual that the test was over and took off their eye pads, then asked them to leave the testing venue without a conversation with the next examinee.

Data Analysis

Descriptive statistics were used to clarify socio-demographic data, walking time, and speed, and illustrate the satisfaction in the participants on the modified white cane.

Results

There were 10 blindfolded subjects, 5 males and 5 females, who participated in the present study. The age of these participants was between 21 and 22 years old. There were 2 subjects who had a height between 151-160 cm, 5 were between 161-170 cm, and 3 were between 171-180 cm; 8 participants were right-handed and 2 of them were left-handed.

Results in the test of efficacy and satisfaction for the modified white cane are demonstrated in Table 1 and Table 2 respectively.

Discussion

Walking locomotion is important for the activities of daily living for almost all people, and evidence indicates that mobility difficulty affects social participation in persons with visual impairment.[30] It is, therefore, crucial that health professionals and responsible persons find assistive devices to promote independent locomotion for these individuals.

These tests of the efficacy of the modified white cane in 10 blindfolded subjects revealed that all participants could get through the 8-meter path with 3 testing obstacles at waist and head levels successfully. Time used for walking ranged from 65 to 103 seconds, with the average time at 85.9±13.03. The average speed in meters per second was 0.10±0.02 (Table 1). The average walking speed of participants in the present study was quite low compared to a study by dos Santos, *et al*.[11] who investigated walking speed in 31 blindfolded subjects while using an electronic and traditional white cane in an outdoor environment and revealed that subjects achieved a walking speed of 0.42-meters per second with the electronic white cane. This might be because the participants in the present study were not experienced in using the white cane beforehand and were not familiar with the condition of being blindfolded. In addition, testing was conducted only once for everyone in a limited space.

The white cane used in the present study, with an ultrasonic detector made from electronic compartments and the degree of object exploration set to a certain amount, can help people with visual disturbances walk more safely than a traditional white cane can. The ultrasonic detector can detect objects up to 80 cm in front of users, and this allows visually impaired persons to stop in time as soon as the electrical circuit transforms the feedback wave generated at the obstacle, which sends a vibration signal to the thumb or the index finger loop. In addition, the ultrasonic wave in the present study can detect barriers in front of it across a space of 2,826 cm^2, so this can protect the whole body of users. One of the key performances of walking aids for the blind is the coverage range of their object detection.[23] The ultrasonic wave also can detect transparent and opaque objects, even when the object is very small. There was an empty space between the detection areas of the upper and lower sensors of the modified white cane of 7 cm in width. However, when users swung the modified white cane left and right and stepped forward a little, the ultrasonic wave could detect the obstacles.

Table 1 Time used and walking speed in the testing of the efficacy of the modified white cane (n=10).

Subjects	Time used (seconds)	Speed (meters/second)
1	67.00	0.12
2	92.00	0.09
3	94.00	0.09
4	83.00	0.10
5	98.00	0.08
6	65.00	0.12
7	77.00	0.10
8	84.00	0.10
9	103.00	0.08
10	96.00	0.08
Average	85.9±13.03	0.10±0.02

In addition, the blindfolded participants reported high satisfaction with both the usability and efficiency of the modified white cane (Table 2). The highest score for satisfaction in usability was for the size of the wooden box on the white cane ($\bar{X}$±SD = 4.50±0.53). This might be because all the electrical compartments were arranged tidily in a small and light weight wooden box (Figure 2) and the wooden electronic box was affixed slightly below the hand-grasping point of a white cane, which did not obstruct the user's hand when they held the device (Figure 3). Kamal, Bayazid, Sadi, Islam, & Hasan[16] noted in their study regarding the walking assistants for the visually impaired that the large physical size of the tools can be an obstacle for users. All of the subjects in the present study also reported very high satisfaction on the efficiency of the modified white cane in terms of its ability to detect objects at mid-body ($\bar{X}$±SD = 4.70±0.48) and at head levels ($\bar{X}$±SD = 4.50±0.53). This could be because the ultrasonic sensor can effectively detect objects in front of the users and transform the reflective wave into a strong vibration signal sent to the index finger-loop (for barriers at waist level) or thumb-loop (for obstacles at head level). Therefore, they stopped in time before hitting the obstacles and shifted their steps to the right or left to get through. These findings are consistent with a study conducted by Islam, Sadi, Zamli, and Ahmed[23] on walking aids for visually impaired people, which revealed that the common requirements of these individuals on walking aids were proper feedback signal, light weight, easy to carry, low cost, and cosmetic suitability.

Table 2 Satisfaction on the modified white cane in blindfolded subjects (n=10).

Testing items	Mean scores of satisfactions
1. Usability	
1.1 easy to use	4.10 (0.57)
1.2 suitable size (wooden electronic box and the white cane)	4.50 (0.53)
1.3 easy to carry	4.00 (0.82)
1.4 seems strong and durable	4.20 (0.42)
1.5 seems easy to maintain	4.00 (0.82)
2. Efficiency	
2.1 detecting obstacles at head level	4.50 (0.53)
2.2 detecting obstacles at mid-body level	4.70 (0.48)

Limitations

Participants in the present study were non-visually impaired people who had never experienced being blindfolded. Therefore, research outcomes may be somewhat different from those with blind subjects who are experienced in interpreting the world using other senses. In a further study, the inclusion of the blind as participants should be considered. Another limitation was the small number of obstacle testing spots. There were only 3 barrier testing stations, and this might not be sufficient to test the efficacy of the modified white cane and get reliable measurements. Therefore, increasing the number of obstacles in the trials should be considered in the next study. In addition, recruitment of more participants into the testing procedure can enhance the reliability of the study.

Conclusion

The modified white cane with an additional ultrasonic detector in the present study could help blindfolded users detect obstacles at waist and head levels more effectively than the traditional passive white cane could. Participants also reported high satisfaction with the modified white cane in terms of both usability and efficiency.

Declaration of conflicting interests

The authors declare no potential conflicts of interest with respect to the research, authorship, and/or publication of this article.

Funding

This study was funded by the Faculty of Associated Medical Sciences, Chiang Mai University, Thailand.

References

[1] Bourne RRA, Flaxman SR, Braithwaite T, Cicinelli MV, Das A, Jonas JB, et al. Magnitude, temporal trends, and projections of the global prevalence of blindness and distance and near vision impairment: A systematic review and meta-analysis. Lancet Glob Health. 2017; 5(9): e888-e97.

[2] Matwanukul T. Situation of Persons with Disabilities 31 December 2020 (Quarterly) 2021, January 8 [Available from: https://dep.go.th/images/uploads/files/situation_sep63.pdf.

[3] National Statistical Office. Number of population from registration by age, sex and province, 2020. 2020.

[4] Eckert KA, Carter MJ, Lansingh VC, Wilson DA, Furtado JM, Frick KD, et al. A simple method for estimating the economic cost of productivity loss due to blindness and moderate to severe visual impairment. Ophthalmic Epidemiol. 2015; 22(5): 349-55.

[5] Ramrattan RS, Wolfs RCW, Panda-Jonas S, Panda-Jonas S, Jonas JB, Bakker D, et al. Prevalence and causes of visual field loss in the elderly and associations with impairment in daily functioning: the Rotterdam Study. Arch Ophthalmol. 2001; 119: 1788-94.

[6] McCarty CA, Nanjan MB, Taylor HR. Vision impairment predicts 5 year mortality. Br J Ophthalmol. 2001; 85(3): 322-6.

[7] Taylor HR, Katala S, Muñoz B, Turner V. Increase in mortality associated with blindness in rural Africa. Bull World Health Organ. 1991; 69(3): 335-8.

[8] Cardillo E, Di Mattia V, Manfredi G, Russo P, De Leo A, Caddemi A, et al. An electromagnetic sensor prototype to assist visually impaired and blind people in autonomous walking. IEEE Sensors J. 2018; 18(6): 2568-76.

[9] Alshajajeer M, Almousa MT, Al-Haija QA. Enhanced White Cane for Visually Impaired People. J Appl. Comput Sci Math. 2018; 12(26): 9-13.

[10] Jafri R, Khan MM. User-centered design of a depth data based obstacle detection and avoidance system for the visually impaired. Hum-centric Comput Inf Sci. 2018; 8(14).

[11] dos Santos ADP, Medola F, Cinelli MJ, Ramirez ARG, Sandnes FE. Are electronic white canes better than traditional canes? A comparative study with blind and blindfolded participants. Univers Access Inf Soc. 2021; 20: 93-103.

[12] Khan I, Khusro S, Ullah I. Technology-assisted white cane: evaluation and future directions. PeerJ 2018; 6: 1-27. doi: 10.7717/peerj.6058.

[13] Kim SY, Cho K. Usability and design guidelines of smart canes for users with visual impairments. Int J Des. 2013;7 (1): 99-110.

[14] Pyun R, Kim Y, Wespe P, Gassert R, Schneller S, editors. Advanced augmented white cane with obstacle height and distance feedback. 2013 IEEE 13th International Conference on Rehabilitation Robotics (ICORR); 2013.

[15] Manduchi R, Kurniawan S. Mobility-related accidents experienced by people with visual impairment. AER J. 2011; 4(2): 44-54.

[16] Kamal MM, Bayazid AI, Sadi MS, Islam MM, Hasan N. Towards developing walking assistants for the visually impaired people. 5th IEEE Region 10 Humanitarian Technology Confererence Dhaka, Bangladesh 2017. p. 238-41.

[17] Lee YH, Medioni G. Wearable RGBD indoor navigation system for the blind. In: Agapito L, Bronstein M, Rother C, editors. Computer Vision - ECCV 2014 Workshops: Part 3, vol 8927. Zürich, Switzerland: Springer, 2015. p. 493-508. doi.org/10.1007/978-3-319-16199-0_35.

[18] Penizzotto F, Slawinski E, Mut V. Laser radar based autonomous mobile robot guidance system for olive groves navigation. IEEE Latin America Transactions. 2015, May; 13(5): 1303-13.

[19] Ramadhan AJ. Wearable smart system for visually impaired people. Sensors. 2018; 18(3).

[20] Saaid MF, Mohammad AM, Megat Ali MSA, editors. Smart cane with range notification for blind people. 2016 IEEE International Conference on Automatic Control and Intelligent Systems (I2CACIS); 2016; Selangor, Malaysia.

[21] Hersh MA, Johnson MA. Assistive Technology for Visually Impaired and Blind People. London, U.K.: Springer-Verlag; 2008.

[22] Elmannai WM, Elleithy KM. A highly accurate and reliable data fusion framework for guiding the visually impaired. IEEE Access. 2018; 6: 33029-54.

[23] Islam MM, Sadi MS, Zamli KZ, Ahmed MM. Developing walking assistants for visually impaired people: A review. IEEE Sens J. 2019; 19(8): 2813-28.

[24] Kulyukin V, Gharpure C, Nicholson J, editors. RoboCart: toward robot assisted navigation of grocery stores by the visually impaired. 2005 IEEE/RSJ International Conference on Intelligent Robots and Systems; 2005.

[25] Yuan D, Manduchi R, editors. Dynamic environment exploration using a Virtual White Cane. IEEE Computer Society Conference on Computer Vision and Pattern Recognition (CVPR '05); 2005; San Diego, California.

[26] Tahat AA. A wireless ranging system for the blind long-cane utilizing a smart-phone. 2009 10th International Conference on Telecommunications; 2009; p. 111-117.

[27] Punyanon T. Navigating cap for blind people [bachelor's thesis]. Chiang Mai Province, Thailand: Chiang Mai University; 2012.

[28] Kongkumsuk K. The Navigation eye glasses for blind people [bachelor's thesis]. Chiang Mai province, Thailand: Chiang Mai University; 2014.

[29] Office of the Permanent Secretary Ministry of Social Development and Human Security. The Empowerment of Persons with Disabilities Act, B.E.2007. 2007.

[30] Alma MA, Van der Mei SF, Melis-Dankers BJ, Van Tilburg TG, Groothof JW, Suurmeijer TPBM. Participation of the elderly after vision loss. Disabil Rehabil. 2011; 33(1): 63-72.

Journal of Associated Medical Sciences 2022; 55 (3): 19-25

JAMS
Journal of Associated Medical Sciences

Thai-Journal Citation Index Centre (TCI) & ASEAN Citation Index (ACI)

Journal of Associated Medical Sciences

Journal homepage: https://www.tci-thaijo.org/index.php/bulletinAMS/index

Feasibility of inspiratory muscle training to improve pulmonary and respiratory muscle function, and for attenuating sleep apnea symptoms in children and adolescent with obstructive sleep apnea and obesity: Case report

Siramon Sornkla[1] **Nuntigar Sonsuwan**[2] **Sainatee Pratanaphon**[1*]

[1]*Department of Physical Therapy, Faculty of Associated Medical Sciences, Chiang Mai University, Chiang Mai Province, Thailand*
[2]*Department of Otolaryngology, Faculty of Medicine, Chiang Mai University, Chiang Mai Province, Thailand*

ARTICLE INFO

Article history:
Received 7 April 2022
Accepted as revised 13 June 2022
Available online 5 July 2022

Keywords:
Inspiratory muscle training, obstructive sleep apnea, children, case report

ABSTRACT

Background: Studies have demonstrated a potential risk of pulmonary and respiratory muscle dysfunction in individuals with obstructive sleep apnea (OSA) and/or obesity. Inspiratory muscle training (IMT) is an adjunct intervention designed to improve respiratory muscle strength, decrease severity of OSA, and to enhance sleep quality in adults with OSA. However, its effects on children with OSA and obesity are still largely unknown.

Objectives: This case report aims to show the feasibility and the effects of IMT on pulmonary and respiratory muscle function and sleep apnea symptoms of children and adolescents with OSA and obesity.

Case description: Four children and one adolescent who were diagnosed with OSA and classified as obesity underwent IMT with training load at 60% of the individual's maximal inspiratory pressure (MIP) for 12 weeks.

Results: No adverse effects occurred during evaluation and IMT. The participants' compliance with IMT varied from 77.4% to 100%. After 12-week of IMT, MIP and maximal voluntary ventilation (MVV) increased from baseline, varying from 8.0% to 83.5% and 0.1% to 36.1%, respectively. Scores in the Sleep Related Breathing Disorder-Pediatric Sleep Questionnaire (SRBD-PSQ) tended to decrease rapidly at week 3. Thereafter, participants responded differently toward the end of IMT. Changes in pulmonary function variables were not observed.

Conclusion: Improvements in respiratory muscle strength, endurance, and SRBD-PSQ scores occurred after IMT, suggesting the feasibility of IMT for increasing inspiratory muscle performance and for ameliorating sleep apnea symptoms in children and adolescents with OSA and obesity. However, pulmonary function was unaffected by IMT.

Introduction

Obstructive sleep apnea (OSA) is a sleep disorder characterized by partial or total upper airway occlusion that disrupts normal breathing and ventilation during sleep.[1] OSA is associated with morbidities that affect the cardiovascular, neurocognitive, and metabolic systems.[2] A prevalence of OSA, which has been observed as 2-3% in children of normal weight, can increase to 13-59% in cases of obesity.[1,3] In addition, obesity has been shown to be the strongest risk factor for developing OSA due to the contribution of excessive fat deposition on upper airway narrowing, chest wall compliance, and diaphragm function, which consequently reduced lung volume and capacity, and increased airway resistance. Additionally, an increased airway resistance or a reduction in pulmonary compliance which elevated work of breathing

* **Corresponding author.**
Author's Address: *Department of Physical Therapy, Faculty of Associated Medical Sciences, Chiang Mai University, Chiang Mai Province, Thailand.*
** **E-mail address:** sainatee.pra@cmu.ac.th
doi: 10.12982/JAMS.2022.020
E-ISSN: 2539-6056

might cause respiratory muscle dysfunction.[4-6] The coexistence of OSA and obesity have demonstrated a pronounced reduction in vital capacity, forced expiratory volume in 1 second (FEV_1), functional residual capacity, expiratory reserve volume, and total lung capacity of children with obesity. Additionally, this is the case for moderate-to-severe OSA compared to those without OSA.[7] A recent preliminary study found that respiratory muscle strength and endurance of children and adolescents with OSA and obesity were likely to be lower than the controls, but this is not statistically different (all, $p>0.05$).[8] The maximal inspiratory pressure (MIP) of this group, which refers to respiratory muscle strength are comparable to those of children with severe obesity, were inferior to normal weight individuals and thus may be considered abnormal.[9,10] These results suggested a potential risk of pulmonary and/or respiratory muscle dysfunction in children with OSA and/or obesity. Therefore, interventions that preserve airway patency and the passage of oxygen into the lungs, as well as improve pulmonary and respiratory muscle function, are required.

Many options are available to treat OSA including noninvasive positive airway pressure, adenotonsillectomy, drug treatment, oral appliances, and weight loss/exercise. However, such interventions require weighing the pros and cons regarding particular options.[11] The inspiratory muscle training (IMT) which involves breathing exercises using a pressure-threshold device becomes of interest because it has been reported to be a convenient, practical, and time-efficient program that improves MIP, severity of OSA, and sleep quality in adults with OSA.[12] However, it is unclear whether the feasibility and effects of IMT on pulmonary and respiratory muscle function in children and adolescents with OSA and obesity is suitable for those who are more likely to have obstructed airways than adults. The purpose of this case report was to report pulmonary and respiratory muscle function and sleep apnea symptoms in five cases of children and adolescents with OSA and obesity after receiving a 12-week IMT program

Case Description

Four children and one adolescent with OSA and obesity aged 10–16 years were recruited via advertisement and flyers from the Snoring Clinic of Maharaj Nakorn Chiang Mai Hospital. The inclusion criteria were diagnoses of OSA and obesity. The assessment of OSA was performed using polysomnography (PSG) (SOMNOlab-2 AASM sleep diagnostic system, Hamburg, Germany). The subjects were classified as OSA if there was a presence of obstructive sleep-disordered breathing symptoms in combination with an AHI ≥ one episode/hour[13] and classified as obesity based on standard guidelines, respectively.[13,14] The exclusion criteria included the presence of craniofacial abnormalities, underlying conditions that affect pulmonary and respiratory muscle function (e.g., sinusitis, respiratory tract infection, and rib fracture), and medication with neuromuscular side effects. The study protocol was approved by the Research Ethics Committee, Faculty of Associated Medical Sciences, Chiang Mai University (AMSEC-64FB-001) and was registered by ClinicalTrials.gov (Thai Clinical Trials Registry: TCTR20210611007). Written informed consent was obtained from participants and their parents. The participant characteristics are shown in Table 1. Based on the AHI, cases 1, 2, 3, and 5 had mild OSA and case 4 had severe OSA. All male participants had previously undergone an adenotonsillectomy and two of these (case 2 and 5) had allergic rhinitis, while the two females had no history of tonsil or adenoid hypertrophy. They were advised to maintain their usual activities of daily living and physical activity (PA) level was monitored during the study. Routine treatment including counseling for diet, PA, and drug therapy were provided by otolaryngologists. All participants performed the anthropometric variables, MIP, pulmonary function testing (PFTs), and maximal voluntary ventilation (MVV) with a 5-minute intermission between the tests in the laboratory at a temperature of 25 °C and a relative humidity of 50.5±1.3%.

Table 1 Characteristics of participants.

Characteristics	IMT (n=5)				
	Case 1	Case 2	Case 3	Case 4	Case 5
Age (years)	10	13	10	16	10
Gender	Female	Male	Female	Male	Male
BW (kg)	57.1	67.7	49.3	121.3	47.5
Height (m)	1.40	1.55	1.45	1.71	1.39
BMI (kg/m^2)	29.13	28.18	23.45	41.48	24.58
Polysomnography indices					
AHI (events/hour)	2	2.4	3	29	4.6
ODI (events/hour)	1	3.3	5	13	1.6
SaO_2nadir (%)	89	84	84	86	81
MeanSaO_2 (%)	97	97.3	97	97	97.1
Severity of OSA based on AHI	Mild	Mild	Mild	Severe	Mild
History of tonsil or adenoid hypertrophy	No	Yes	No	Yes	Yes
Adenotonsillectomy surgery	No	Yes	No	Yes	Yes
Underlying disease	No	Allergic rhinitis	No	No	Allergic rhinitis

AHI: apnea hypopnea index, BMI: body mass index, BW: body weight, ODI : oxygen desaturation index, SaO_2nadir: oxygen saturation nadir, MeanSaO_2: mean of oxygen saturation, OSA: obstructive sleep apnea

PFTs and MVV were evaluated using the Easy on-PC spirometer, software version V03b (NDD® Medical Technologies, Switzerland), according to the standardized protocols.[15] MIP was measured using a handheld mouth pressure meter (Micro RPM, Micro Medical Ltd., Rochester, Kent, UK) as previous described.[16] The Thai translated 22-items SRBD-PSQ was used to assess sleep related breathing disorders in children.[17] Parents were instructed to complete the survey queries about snoring, daytime sleepiness, and inattention. The SRBD-PSQ score was computed by the number of 'yes' answers divided by the total items answer 'yes' and 'no''. A cut-off value of 0.33 is used to identify pediatric OSA. The intra-rater reliability of MIP, PFTs, and MVV were good to excellent (the intraclass correlation coefficient, ICC>0.9, all p<0.05), except $FEF_{25-75\%}$ which was moderate (ICC=0.642, p=0.109). Body weight and percent body fat were determined using a bioelectrical impedance analyzer (Tanita BC-418, Tokyo, Japan). Height was measured using a wall-mounted stadiometer (Health-O-Meter 402 KL, IL). The validated Thai Physical Activity Questionnaire for Children and Adolescents (PAQ-A/C) was used to evaluates level and frequency of moderate to vigorous PA over the last 7 days of participants.[18] Children and adolescents completed the questionnaire by scoring the 10-item of PAQ-C and the 9-item of PAQ-A, respectively on a five-point Likert scale (5 score = higher level of PA; 1 score = lower level of PA). The summary score is the average of all question items except the last item of each PAQ that asking for other reasons that prevented the participant from engaging in regular PA. Outcomes were measured by two independent assessors at baseline and follow-ups at weeks 3, 6, 9, and 12. At baseline, the percent predicted of FVC and FEV_1, as well as MIP and MVV of our participants was found to be lower than the references values of the children and adolescents of the same age and gender of previous studies, suggesting deficits in pulmonary and respiratory muscle function.[10,19]

Participants underwent IMT using the Powerbreathe® classic light resistance (POWERbreathe® International Ltd., Warwickshire, UK). The training protocol was comprised of a 12-week home-based IMT with an initial load at 60% of the individual's MIP as recommended by previous studies.[20,21] Previous findings indicated the beneficial effects of 8-week IMT for improving the severity of OSA and sleep quality and excessive daytime sleepiness in patients with OSA.[11,20] However, a longer period effect of IMT on the severity of OSA and respiratory muscle function have never been investigated. Each participant was asked to practice IMT at the laboratory for familiarization, and heart rate (HR) was monitored. Participants were encouraged to breathe deeply and slowly. Oxygen saturation (O_2sat) and rate of perceived exertion (RPE) were measured throughout the first training session. Training loads were adjusted at every 3-week follow-up, corresponding to 60% of the new measure MIP and a symptom-limited was imposed. The training program was supervised by a professional physiotherapist. Participants were instructed to perform 80 breaths per day (10 breaths per cycle with a 1-minute rest interval for 8 cycles), 7 days a week for 12 weeks. To promote exercise adherence and safety status, each participant received a logbook to record the exercise sessions and any adverse effects that might have occurred during or after each exercise session. Adherence to the program was done via daily phone contact and/or LINE application. Flow diagram of participants throughout this study is shown in Figure 1. At the first training session, IMT caused an increased effort from RPE 0 to 4 with HR of 84 beats per minute (bpm) and O_2sat of 98% for participant case 1. Similar response of RPE with HR of 78 bpm and O_2sat of 99% for participant case 2. IMT caused an increase in RPE from 0 to 2 with HR range of 74-86 bpm and O_2sat range of 97-99% for participants case 4 and 5. Only participant case 3 had increased in RPE from 0 to 1 with HR of 75 bpm and O_2sat range of 98-100%. The initial resistive load for IMT varied among participants and the training load tended to increase by time range of 14.3- 80%, except for participant case 5 who had a constant load at 50 cmH_2O from week 3 to week 9 and increased to 60 cmH_2O for the last three weeks (Table 3). Chest pain was reported during training at the end of week 10. After decreasing training load to 50 cmH_2O, the patient could perform IMT without chest pain until week 12. During the same time, a patient went to see the doctor and was diagnosed as having recurrent adenoid hypertrophy. He has planned to do have an adenoidectomy in a few months.

Table 3 Resistive load and training volume for inspiratory muscle traning of each participant.

	Case 1				Case 2				Case 3				Case 4				Case 5			
	wk3	wk6	wk9	wk12	wk3	wk6	wk9	wk12	wk3	wk6	wk9	wk12	wk3	wk6	wk9	wk12	wk3	wk6	wk9	wk12
Load (cmH_2O)	50	70	70	90	40	50	60	60	50	60	60	70	70	80	80	80	50	50	50	60→50
Vol (breaths)	1,600	1,680	1,680	1,680	1,680	1,680	1,680	1,680	1,680	1,680	1,680	1,680	1,680	1,120	1,360	1,040	1,680	1,680	1,680	1,200
Adherence rate	98.8%				100%				100%				77.4%				92.9%			

Vol: volume, wk: week

Noted: Participant case 5 had chest pain during training at week 10, therefore the training load was reduced from 60 cmH_2O to 50 cmH_2O.

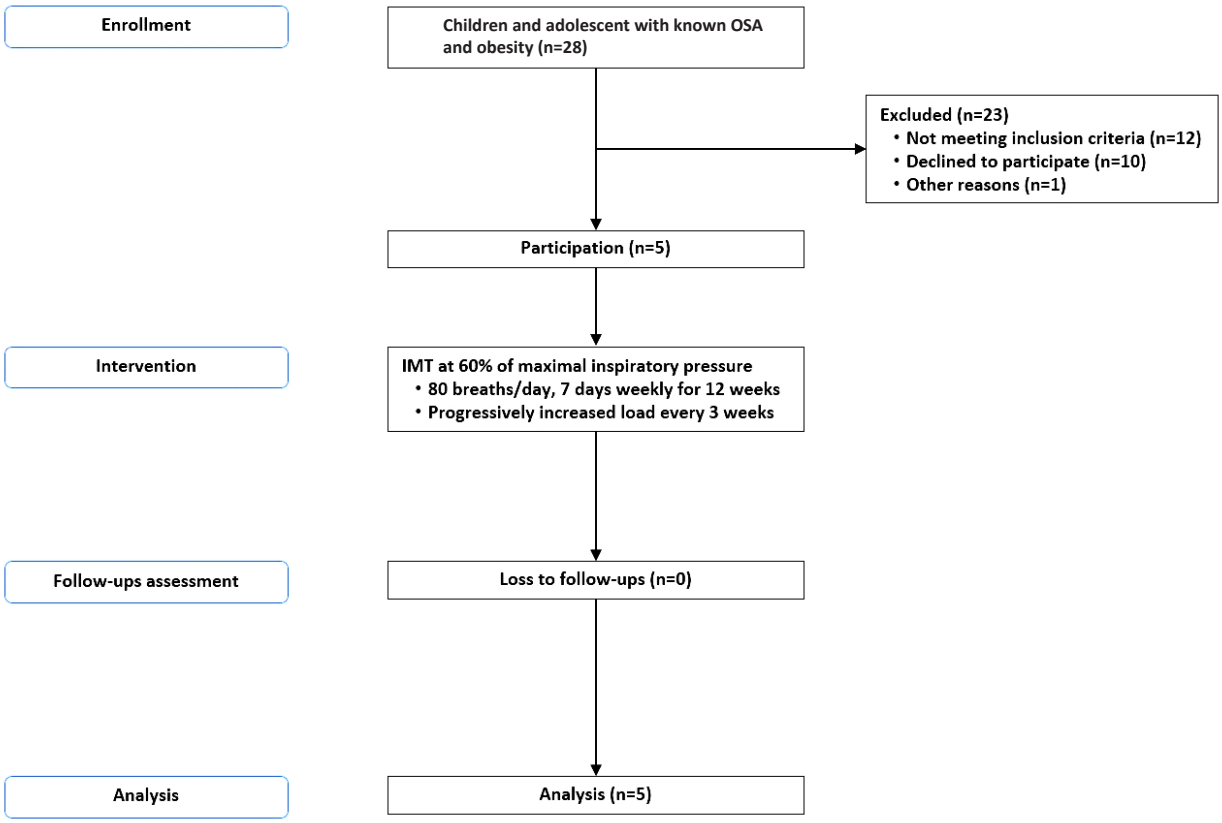

Figure 1. *Flow diagram of participants throughout intervention.*

After 12 weeks of IMT, most participants achieved adherence rate range of 92.9-100%, except participant case 4 who had low adherence to IMT (Table 3). Mean changed from baseline of MIP was 18.2 cmH_2O (20.04%), 25.6 cmH_2O (28.2%), 37.2 cmH_2O (41%), and 37.2 cmH_2O (41%) at weeks 3, 6, 9, and 12, respectively (Figure 2). Notably, MIP of participant case 5 almost unchanged from baseline values throughout the period of study. Mean changed from baseline of MVV was 4.1 L (7.1%), 2.1 L (3.6%), 4.5 L (7.8%), and 6.2 L (10.7%) at weeks 3, 6, 9, and 12, respectively (Figure 3). Sleep apnea symptoms were measured using SRBD-PSQ scores with a cut-off value of 0.33 revealed that almost participants were at high risk of OSA, except participant case 1 who had non-risk at baseline. According to the SRBD-PSQ score, participants 3 and 4 are defined as non-OSA risk after IMT at week 3 and participant case 2 at week 9. A decreased SRBD-PSQ score was observed from week 3 through the end of the study period. However, participant case 5 still had OSA (Figure 4). Variables of PFTs, anthropometry, and PAQ-C scores of all participants did not change in each period of training compared to the baseline value (Table 2). Four of the five participants informed us of their willingness to continue training after IMT completion. Some parents reported improvement of children in terms of reduced snoring after IMT.

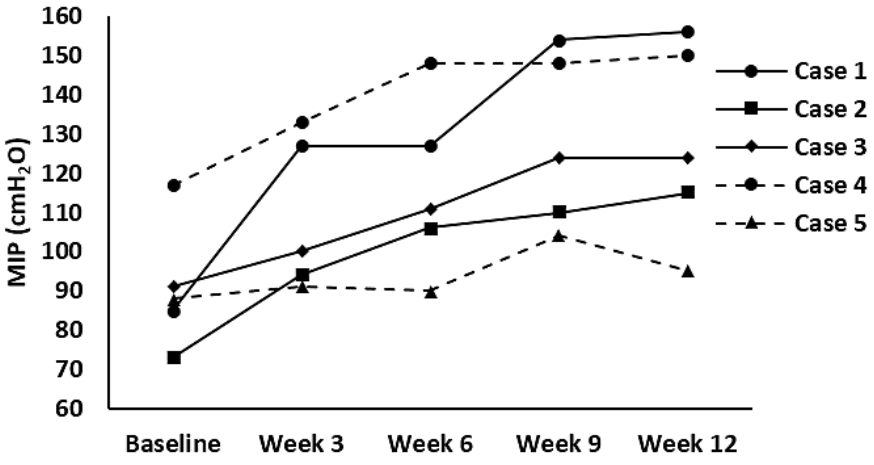

Figure 2. *Changes in the MIP from baseline to 12 weeks of IMT.*

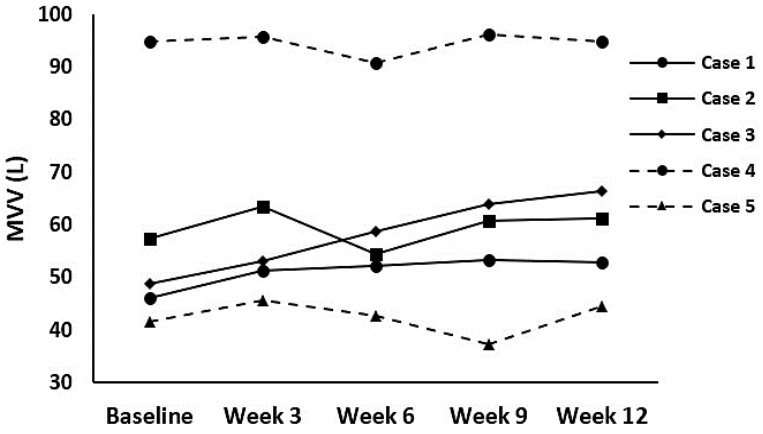

Figure 3. *Changes in the MVV from baseline to 12 weeks of IMT.*

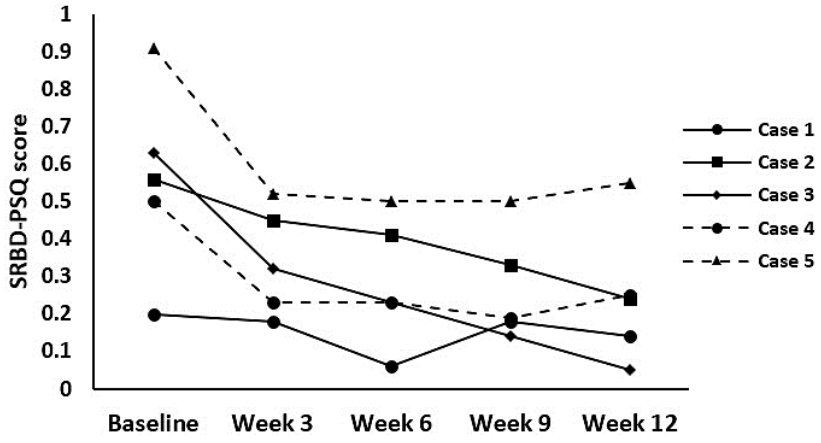

Figure 4. *Changes in the SRBD-PSQ from baseline to 12 weeks of IMT.*

Table 2 Changes in variables of pulmonary function, anthropometry and physical activity from baseline to 12 weeks of IMT.

	Baseline	Post-training			
		week 3	week 6	week 9	week 12
Pulmonary function variables					
FEV_1 (L)	2.39	2.41	2.45	2.45	2.41
	(-0.16-4.95)	(-0.01-4.82)	(-0.04-4.94)	(0.05-4.85)	(-0.16-4.99)
FVC (L)	2.80	2.86	2.90	2.87	2.82
	(-0.69-6.29)	(-0.57-6.28)	(-0.62-6.43)	(-0.49-6.22)	(-0.67-6.31)
FEV_1/FVC	0.876	0.863	0.865	0.873	0.874
	(0.71-1.04)	(0.70-1.03)	(0.71-1.02)	(0.72-1.02)	(0.73-1.01)
FEF25-75% (L)	2.72	2.71	2.82	3.00	2.87
	(0.97-4.46)	(1.54-3.88)	(1.64-4.00)	(2.10-3.89)	(1.39-4.35)
Anthropometric variables					
BMI (kg/m^2)	31.35	31.57	31.87	32.28	32.15
	(8.45-54.26)	(8.90-54.24)	(9.35-54.40)	(10.74-53.83)	(10.88-53.43)
PBF (%)	39.37	42.73	36.80	43.77	42.80
	(27.83-50.91)	(27.94-57.53)	(21.37-52.23)	(31.55-55.98)	(30.74-54.86)
Physical activity					
PAQ A/C score	1.82	2.21	2.17	1.99	2.16
	(0.27-3.38)	(0.51-3.92)	(-0.08-4.43)	(1.24-2.74)	(0.24-4.07)

Results are shown as mean and 95% confidence interval (CI), BMI: body mass index, FEF25-75%: forced expiratory flow between 25% and 75% of FVC, FEV1: forced expiratory volume in 1 second, FVC : forced vital capacity, PAQ A/C: Physical Activity Questionnaire for Children and Adolescents, PBF: percent body fat.

Discussion

Our findings showed the positive effects of the 12-week home-based IMT program on MIP, MVV, and SRBD-PSQ scores, but not for the PFTs variables. Aside from the main purposes, the observed BMI and PAQ (A/C) scores which were not altered throughout the study, affirmed that PA and BMI did not affect any positive results. These results indicated the feasibility of IMT to increase inspiratory muscle strength and endurance and for mitigating OSA symptoms in children and adolescents with OSA and obesity. In this study, initial training load varied among participants according to his/her health condition, age and gender, however IMT should be done with a symptoms limit. IMT caused an increase in RPE ranging from 1 to 4 which represented the effort as being very easy to somewhat hard and did not induce a marked decrease in O_2sat during loaded breathing. No adverse events were reported throughout the training period, except for participant 5, who experienced sharp pain on inspiration at the end of week 10. However, such a symptom immediately disappeared after reducing the training load and maintaining that load for the rest of the training period. Thus, the 12-week home-based IMT protocol of the present study was shown to be feasible and safe for further study.

In this study, the MIP was increased to week 9 of the IMT and further training up to week 12 resulted in less improvements. This was consistent with previous findings which had performed IMT for patients with chronic lung disease and healthy subjects. They found that benefits are likely to be optimal with 6-8 weeks of training.[21,22] Likewise, the MVV was increased with time, but to a lesser extent than MIP. This discrepancy may be explained by the principle of pressure-flow specificity of IMT which is proposed by Romer *et al*.[22] Moreover, each participant exhibited increased MIP and MVV at different rates, although four of five participants had mild OSA and one had severe disease (participant case 4). This reason for this discrepancy could not be determined, but could possibly be explained by the underlying disease, gender, and adherence to IMT. Three participants were male who had adenotonsillectomies prior to participating in the study, and two of them had rhinitis. At week 10 of training, one of them had recurrent adenoid hypertrophy, while participant case 4 had the lowest adherence rate of training. Such information may help researchers in designing and conducting a subsequent randomized controlled trial to establish efficacy of IMT. According to SRBD-PSQ scores, two participants were defined as non-OSA after IMT at week 3 and one at week 9. Another one showed a decrease of SRBD-PSQ scores at week 3, but OSA remained till the end of the study. These results suggested that IMT possible attributed to reduced symptoms of OSA. However, one participant was identified as non-SRBD from the beginning to the end of the study period. The inconsistent results of SRBD-PSQ score among participants suggested that further study using standard equipment such as polysomnography that assesses OSA symptoms more accurately would be more valid than SRBD-PSQ.[19]

There are several limitations in this case report that should be emphasized. The absence of a study arm involving a sham IMT intervention is relevant. Therefore, no causal inferences could be made about the IMT effects. A pilot study is warranted prior to implement on a larger scale. In addition, our IMT trial was performed on five participants who had different underlying diseases, gender, and severity of OSA. Therefore, these factors may have possibly contributed to the outcomes. Finally, a study of the long-term effects of IMT is needed to identify the optimal IMT protocol and to investigate the responses of all outcome measures.

Conclusion

Positive outcomes in inspiratory muscle strength and endurance, and SRBD-PSQ score after IMT, suggesting that IMT can be trained with the improvement of respiratory muscle function and OSA symptoms in children and adolescent with OSA and obesity.

Conflicting interests

The authors declare no conflict of interest.

Ethical approval

All procedures performed in this study involving human participants, were in accordance with the ethical standards of the institutional and/or national research committee and the 1964 Helsinki Declaration and its later amendment or comparable ethical standards. This study was approved by the Research Ethics Committee, Faculty of Associated Medical Sciences, Chiang Mai University.

References

[1] Bhattacharjee R, Kim J, Kheirandish-Gozal L, Gozal D. Obesity and obstructive sleep apnea syndrome in children: a tale of inflammatory cascades. Pediatr Pulmonol. 2011; 46(4): 313-23. doi: 10.1002/ppul.21370.

[2] Grime C, Tan HI. Sleep disordered breathing in children. Indian J Pediatr. 2015; 82: 945-55. doi: 10.1007/s12098-015-1857-5.

[3] Verhulst SL, Van Gaal LV, De Backer W, Desager K. The prevalence, anatomical correlates and treatment of sleep-disordered breathing in obese children and adolescents. Sleep Med Rev. 2008; 12: 339-46. doi: 10.1016/j.smrv.2007.11.002.

[4] Isono S. Obesity and obstructive sleep apnoea: mechanisms for increased collapsibility of the passive pharyngeal airway. Respirology. 2012; 17: 32-42. doi: 10.1111/j.1440-1843.2011.02093.x.

[5] Dehlink E, Tan HL. Update on paediatric obstructive sleep apnoea. J Thorac Dis. 2016; 8: 224-35. doi: 10.3978/j.issn.2072-1439.2015.12.04.

[6] Mafort TT, Rufino R, Costa CH, Lopes AJ. Obesity: systemic and pulmonary complications, biochemical abnormalities, and impairment of lung function. Multidiscip Respir Med. 2016; 11: 28. doi: 10.1186/s40248-016-0066-z.

[7] Van Eyck A, Van Hoorenbeeck K, De Winter BY, Van Gaal L, De Backer W, Verhulst SL. Sleep-disordered breathing and pulmonary function in obese children and adolescents. Sleep Med. 2014; 15(8): 929-33. doi: 10.1016/j.sleep.2014.03.024.

[8] Pratanaphon S, Sonsuwan N, Chaimano S, Chandee S, Autkhruea K, Sa-nguanmoo P, et al. Obstructive sleep apnea effects on pulmonary and respiratory muscles function of obese children and adolescents: a preliminary study. Turk Thorac J. 2022; 23(2): 104-8. doi: 10.5152/TurkThoracJ.2021.0115.

[9] Dubern B, Tounian P, Medjadhi N, Maingot L, Girardet JP, Boulé M. Pulmonary function and sleep-related breathing disorders in severely obese children. Clin Nutr. 2006; 25(5): 803-9. doi: 10.1016/j.clnu.2005.12.001.

[10] Hulzebos E, Takken T, Reijneveld EA, Mulder MMG, Bongers BC. Reference values for respiratory muscle strength in children and adolescents. Respiration. 2018; 95(4): 235-43. doi: 10.1159/000485464.

[11] Calik MW. Treatments for obstructive sleep apnea. J Clin Outcomes Manag. 2016; 23(4): 181-92.

[12] Nóbrega-Júnior JCN, Dornelas de Andrade A, de Andrade EAM, Andrade MDA, Ribeiro ASV, Pedrosa RP, et al. Inspiratory muscle training in the severity of obstructive sleep apnea, sleep quality and excessive daytime sleepiness: a placebo-controlled, randomized trial. Nat Sci Sleep. 2020; 12: 1105-13. doi: 10.2147/NSS.S269360.

[13] Kaditis AG, Alonso Alvarez ML, Boudewyns A, Alexopoulos EI, Ersu R, Joosten K, et al. Obstructive sleep disordered breathing in 2- to 18-year-old children: diagnosis and management. Eur Respir J. 2016; 47(1): 69-94. doi: 10.1183/13993003.00385-2015.

[14] Cole TJ, Bellizzi MC, Flegal KM, Dietz WH. Establishing a standard definition for child overweight and obesity worldwide: international survey. BMJ. 2000; 320(7244): 1240-3. doi: 10.1136/bmj.320.7244.1240.

[15] Miller M, Hankinson J, Brusasco V, Burgos F, Casaburi R, Coates A, et al. Standardisation of spirometry. Eur Respir J. 2005; 26: 319-38. doi: 10.1183/09031936.05.00034805.

[16] American Thoracic Society/European Respiratory Society. ATS/ERS statement on respiratory muscle testing. Am J Respir Crit Care Med. 2002; 166(4): 518-624. doi: 10.1164/rccm.166.4.518.

[17] Longlalerng K, Sonsuwan N, Uthaikhup S, Kumsaiyai W, Sitilertpisan P, Traisathit P, et al. Translation, cross-cultural adaptation and psychometric properties of the Sleep-Related Breathing Disordered -Pediatric Sleep Questionnaire for obese Thai children with obstructive sleep apnea. Sleep Med. 2019; 53: 45-50. doi: 10.1016/j.sleep.2018.08.033.

[18] Pratanaphon S, Longlalerng K, Jitmana J, Chaikla K, Nankanya T, Pirunsarn U, et al. Content validity and psychometric characteristics of the Thai translated version of the physical activity questionnaire for children (PAQ-C) and adolescents (PAQ-A). J Assoc Med Sci. 2020; 53(3): 84-91.

[19] Silva JC, Carvalho IE, Dal Corso S, Lanza FC. Reference equation for maximal voluntary ventilation in children and adolescents. Pediatr Pulmonol. 2020; 55(2): 426-32. doi: 10.1002/ppul.24576.

[20] Labeix P, Berger M, Hayet I, Roche F, Hupin D. Impact of inspiratory muscle training on obstructive sleep apnea in coronary patients. the RICAOS study: preliminary results. Eur Respir J. 2018; 52(suppl 62): PA4350. doi: 10.1183/13993003.congress-2018.PA4350.

[21] Hill K, Cecins NM, Eastwood PR, Jenkins SC. Inspiratory muscle training for patients with chronic obstructive pulmonary disease: a practical guide for clinicians. Arch Phys Med Rehabil. 2010; 91(9): 1466-70. doi: 10.1016/j.apmr.2010.06.010.

[22] Romer LM, McConnell AK. Specificity and reversibility of inspiratory muscle training. Med Sci Sports Exerc. 2003; 35: 237-44. doi: 10.1249/01.MSS.0000048642.58419.1E

Journal of Associated Medical Sciences 2022; 55 (3): 26-35

JAMS
Journal of Associated Medical Sciences

Thai-Journal Citation Index Centre (TCI) & ASEAN Citation Index (ACI)

Journal of Associated Medical Sciences

Journal homepage: https://www.tci-thaijo.org/index.php/bulletinAMS/index

Evaluation of the Varian TrueBeam™ 6 MV phase-space files for the Monte Carlo simulation in small field dosimetry

Mananchaya Vimolnoch[1,2*] Isra Israngkul Na Ayuthaya[2] Sakda Kingkaew[2] Sornjarod Oonsiri[1,2]

[1]Medical Physics Program, Department of Radiology, Faculty of Medicine, Chulalongkorn University, Bangkok, Thailand.
[2]Division of Radiation Oncology, Department of Radiology, King Chulalongkorn Memorial Hospital, Bangkok, Thailand.

ARTICLE INFO

Article history:
Received 22 February 2022
Accepted as revised 16 June 2022
Available online 5 July 2022

Keywords:
Small field, phase-space file, Monte Carlo simulation

ABSTRACT

Background: The Monte Carlo (MC) simulation is an effective tool for determining the absorbed dose in small field sizes. To calculate accurate results, the MC simulation requires precise geometric and material descriptions of the linear accelerator head. Due to proprietary information issues, the description of the Varian TrueBeam™ linear accelerator (Varian Medical Systems, Palo Alto, CA) head geometry and material information are not available. Instead, the manufacturer provided a phase-space file just above the jaw for each photon energy level. Although several studies have validated the accuracy of this phase-space file, to the best of our knowledge, there are no reported data for a small field size (<2x2 cm^2) of 6 MV photon beams.

Objectives: The purpose of this study was to evaluate the Varian TrueBeam™ phase-space file of the 6 MV photon beam provided by the manufacturer for the Monte Carlo (MC) simulation in small field dosimetry.

Materials and methods: The TrueBeam™ linear accelerator was simulated using an EGSnrc MC code with a Varian phase-space file as the input. The simulation was compared with the measurement using percent depth dose (PDD) and beam profile, and the field output factor (FOF) for the 0.6x0.6, 1x1, 2x2, 3x3, 4x4, 6x6, and 10x10 cm^2 field sizes.

Results: The agreement between the measurements and simulated PDD data was under 2.2% beyond the buildup region. The distance to agreement (DTA) in the buildup region was within 1.0 mm. The simulation data presented identical profiles with the measurement within 1.0% of the dose difference or 1.2 mm of the DTA. The mean dose difference in the radiation field was ≤1.5% for the ≥1x1 cm^2 field size. The largest deviation was observed in the 0.6x0.6 cm^2 inline beam profile. The deviation of the penumbra and full width at half maximum (FWHM) between simulation and measurement was <2 mm. The agreement of the simulated and measured FOF was within 1.0%, except for the 0.6x0.6 cm^2 field size.

Conclusion: Overall, the MC simulation demonstrates data that is consistent with the measurement for the ≥1x1 cm^2 field sizes. These data assure that the 6 MV Varian phase-space file can be used as a radiation source for accurate MC dose calculation in a small field. However, a large discrepancy in beam profiles was observed at the 0.6x0.6 cm^2 field size due to the different primary source sizes among Truebeam™ machines.

* **Corresponding author.**
Author's Address: *Medical Physics Program, Department of Radiology, Faculty of Medicine, Chulalongkorn University, Bangkok, Thailand.*
** **E-mail address:** vmananchaya@gmail.com
doi: 10.12982/JAMS.2022.021
E-ISSN: 2539-6056

Introduction

Recent advanced techniques in photon beam radiotherapy have been developed to improve the accuracy of radiation delivery while still allowing for shorter treatment times. These advances have led to an increased use of small fields over the past decades.[1] However, accurate dose measurement in small fields is challenging due to its three conditions. The first condition is the lack of lateral electronic equilibrium (LCPE) that occurs when the size of the field becomes smaller than the range of the lateral charged particle equilibrium (r_{LCPE}). Source occlusion also occurs in small fields as a second condition, resulting in an overlapping of the penumbra. Both conditions are responsible for a sharp drop in beam output. The third condition is associated with the detector for a given field size. These detector aspects include the volume averaging around high-gradient dose distributions and the fluence/dose perturbations due to the different physical densities between the detector and medium.

In 2017, the International Atomic Energy Agency (IAEA) along with the American Association of Physicists in Medicine (AAPM) published Technical Reports Series #483 (TRS 483)[1] that provides a code of practice (CoP) for small field dosimetry. The CoP defines the field output factor $(\Omega_{Q_{clin},Q_{msr}}^{f_{clin},f_{msr}})$ as the ratio of absorbed dose to water in the clinical field $(D_{Q_{clin}}^{f_{clin}})$ and the absorbed dose to water in the machine-specific reference field $(D_{Q_{msr}}^{f_{msr}})$. The equation for field output factor is:

$$\Omega_{Q_{clin},Q_{msr}}^{f_{clin},f_{msr}} = \frac{D_{Q_{clin}}^{f_{clin}}}{D_{Q_{msr}}^{f_{msr}}} \quad \text{Eq.1}$$

In large clinical fields, the field output factor has commonly been approximated by the ratio between detector readings in the clinical field $(M_{Q_{clin}}^{f_{clin}})$ and reference field $(M_{Q_{msr}}^{f_{msr}})$ because the stopping-power ratios and perturbation correction factors are normally constant with field size. For small fields, this condition no longer holds. TRS 483 has recommended the field output correction factor $(k_{Q_{clin},Q_{msr}}^{f_{clin},f_{msr}})$ to account for the differences in the response of a detector in the clinical and reference fields. The equation then becomes

$$\Omega_{Q_{clin},Q_{msr}}^{f_{clin},f_{msr}} = \left(\frac{M_{Q_{clin}}^{f_{clin}}}{M_{Q_{msr}}^{f_{msr}}}\right) \times k_{Q_{clin},Q_{msr}}^{f_{clin},f_{msr}} \quad \text{Eq.2}$$

Another approach to determine the absorbed dose is the Monte Carlo (MC) method, which has been found to be an effective tool in overcoming the challenges of small field dosimetry. The MC can simulate the scenario of the radiation transport to calculate the accurate deposited dose when measurement is not possible.[2] Many recent studies have used the MC simulation to examine the field output correction factors of small field sizes.[3-5] To calculate accurate results, the MC simulation requires precise geometric and material descriptions of the linear accelerator head. Due to proprietary information issues, the description of the Varian TrueBeam™ linear accelerator (Varian Medical Systems, Palo Alto, CA) head geometry and material information upstream of the jaw are not available. Instead, the Varian MC research team provided a phase-space file just above the jaw for each photon energy level. This phase-space file can be used as source to transport particles through the geometry of the jaws, and other beam modifiers, for calculating the absorbed dose. The Varian phase-space file was generated using GEANT4 MC code with the Varian TrueBeam™ head schematics imported from the computer-aided design as the input.[6] The first version of the phase-space file was stored in a cylindrical space that cannot be used by the BEAMnrc MC code that requires the planar format. Varian subsequently released the second version of the phase-space file that was stored on a flat surface.

Although several studies have validated the accuracy of this phase-space file, to the best of our knowledge, there are no reported data for the 6 MV photon beam field sizes smaller than 2x2 cm^2.[6-11] The primary photon source width strongly affects the beam profiles of small fields due to the source occlusion effect. The source size of the TrueBeam™ machine varies between 1.0-1.5 mm.[12] Thus, It cannot be assumed that this universal phase-space file will produce an accurate dose distribution for small fields.

This study compares the dosimetric characteristics of the measured Varian TrueBeam™ 6 MV small photon beams with the MC simulation using the version 2 phase-space data available from the manufacturer. The simulation was compared with the measurement using percent depth dose (PDD), beam profile, and field output factor (FOF) as a function of jaw setting.

Materials and methods

All simulations and measurements were performed on a Varian TrueBeam™ linear accelerator using 6 MV photon beam energy.

Monte Carlo simulation

The EGSnrc code system,[13] user codes BEAMnrc,[14] and DOSXYZnrc[15] were used for the MC simulations. Each simulation consisted of three steps. First, BEAMnrc was used to simulate the particle transport through the components of the linear accelerator treatment head. Second, DOSXYZnrc was used to compute the dose deposited within the water phantom. Finally, the obtained results were compared with the measured data.

The Varian TrueBeam™ version 2 phase-space file of the 6 MV photon beam energy was adopted from the MyVarian website (https://www.myvarian.com).[6] This phase-space file contains information about the radiation interactions within the linear accelerator treatment head, such as the position, energy, directionality, and type of each particle. The phase-space file was then used as the radiation source in BEAMnrc. The data for the material and geometry of the linear accelerator components below the phase-space plane were taken from the Varian TrueBeam™ Monte Carlo package version 1.1 available on the MyVarian website. Figure 1 presents the schematics of the linear accelerator model simulations by BEAMnrc. The Varian phase-space file was located above the Y jaw at 26.7 cm from the source. Only the X and Y jaws were modeled using JAWS CM. The slab of air

was created after the X jaw using SLABS CM at a distance of 100 cm from the source. The particles that reached the end of the air slab were stored in the second phase-space file. These field size-specific phase-space files were used as an input source for the subsequent water phantom simulation in DOSXYZnrc. The number of histories ranging from $1x10^9$-$4x10^{10}$ was simulated with BEAMnrc transporting the particles from the location of the Varian phase-space file. The global ECUT and PCUT was 0.521 MeV and 0.01 MeV, respectively. The particles with total energies below these values were terminated with the energy deposited in the current voxel. No variance reduction techniques were used. The default EGSnrc transport parameters were applied in the simulation.

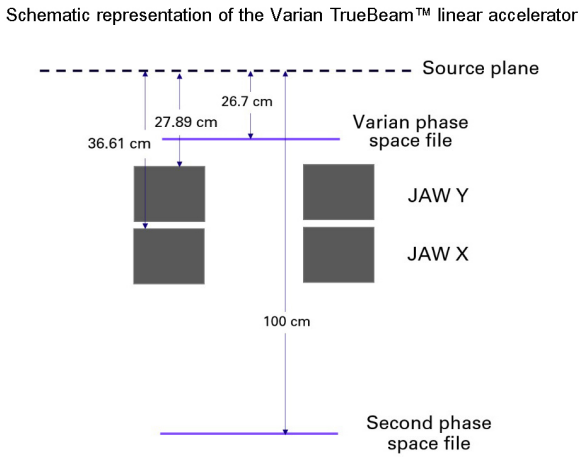

Figure 1. *Schematic representation of the Varian TrueBeam™ linear accelerator model.*

The MC methodology was evaluated by comparing the simulated PDD, beam profile, and FOF with the measurements. This process used nominal field sizes of 0.6x0.6, 1x1, 2x2, 3x3, 4x4, 6x6, and 10×10 cm^2 for the jaw-collimated fields.

To calculate the three-dimensional dose distributions in a virtual water phantom, a 30x30x30 cm^3 water phantom was generated using DOSXYZnrc. The voxel sizes were between 0.1 x 0.1 x 0.5 cm^3 and 0.5x0.5x0.5 cm^3. The voxel resolution varied according to the field size to obtain accurate penumbra data. A large enough number of histories were selected for each simulation to keep the statistical uncertainty less than 0.5% at the maximum dose voxel and 0.7% for all the voxels inside the radiation field.

The output files that contain the dose deposited in each voxel per number of particles and the associated statistical uncertainty were created using the DOSXYZnrc code. These files were exported to MATLAB (The MathWorks, Natick, MA) to calculate the dosimetric quantities. The PDDs and beam profiles were normalized so that a comparison between the MC simulation and the measurements could be done. To calculate the PDD, the dose scoring in voxels along the central beam axis was normalized to the dose at d_{max}. The simulated beam profile was determined by normalizing the voxel dose at 10 cm depth to the dose on the central axis.

Measurements

Percentage depth doses and beam profiles

The PDDs, crossline profiles, inline profiles, and FOFs were acquired in a 3D water scanning system (Blue Phantom2, IBA Dosimetry, Memphis, TN) with OmniPro-Accept software. The experiments were set at 100 cm SSD. The PDDs for the 6x6 and 10x10 cm^2 fields were measured using IBA CC13 (IBA Dosimetry, Schwarzen-Bruck, Germany). For field sizes smaller than 6x6 cm^2, the Sun Nuclear EDGE detector (Sun Nuclear Corporation, Melbourne, FL) was used. The measured crossline and inline beam profiles were obtained using the Sun Nuclear EDGE detector scanning across the field area at a depth of 10 cm. Similar to the MC simulation, the depth-dose curves were normalized to the maximum dose depth to calculate the PDD of each field size. The beam profiles were normalized to 100% at the central axis to their corresponding field size.

Field output factors

The FOFs at the 10 cm depth were measured using the IBA CC01, Sun Nuclear EDGE, and PTW 60003 natural diamond (PTW, Freiburg, Germany) detectors. These detectors were recommended by TRS 483 for small field dosimetry. The characteristics and description of the detectors used in this study are presented in Table 1. The IBA CC01 and Sun Nuclear EDGE detectors were set perpendicular to the central beam axis. Both detectors were positioned at the center of the radiation beam using crossline and inline scans to find the position of the maximum signal according to the TRS 483 guidelines. The natural diamond detector was vertically positioned and aligned at the center of the light field crosshair of the 1x1 cm^2 field. The IBA DOSE-1 electrometer was connected to each detector to measure the collected charge.

Table 1 Resistive load and training volume for inspiratory muscle traning of each participant.

Type	Model	Active volume	Active volume dimensions	Application
Cylindrical Ionization chamber	IBA CC01	10 mm^3	Ø 2 mm x l 3.6 mm	Field output factors
	IBA CC13	130 mm^3	Ø 6 mm x l 5.8 mm	PDDs≥6x6 cm^2
Shielded diode	Sun Nuclear Edge	0.019 mm^3	Square 0.8 mm x 0.8 mm thickness 0.03 mm	PDDs<6x6 cm^2 Beam profiles Field output factors
Natural diamond	PTW 60003 natural diamond	1.2 mm^3	Disk, Ø 2.3 mm thickness 0.28 mm	Field output factors

The FOFs in this study are defined in Eq.3. The ratio of the detector reading normalized to the 10x10 cm^2 reference field was multiplied by the field output correction factors (k). These k factors were taken from Table 26 of TRS 483 except for that for the Sun Nuclear Edge detector at the 0.6x0.6 cm^2 field size. This is because the protocol provides the k factor of Sun Nuclear Edge only for field sizes ≥0.8x0.8 cm^2.

$$FOF = \frac{\text{Chamber reading at any field size}}{\text{Chamber reading at 10×10 cm}^2} \times k \text{ (TRS 483)} \quad \text{Eq.3}$$

The S_{clin} was determined for selecting the k factors. The S_{clin} is defined by the full width at half maximum (FWHM) of the beam profile and given by

$$S_{clin} = \sqrt{A.B} \quad \text{Eq.4}$$

where A and B is the crossline and inline FWHM, respectively, at the 10 cm depth, determined from the beam profile measured with the Sun Nuclear EDGE detector.

Results

Percentage depth doses

To compare the simulated and measured PDD data, two different evaluation parameters were considered: the dose difference in the region beyond d_{max} and the distance to agreement (DTA) in the buildup region. The dose difference was defined as the percentage difference of the simulated to the measured dose. The DTA is the distance between a measurement and the MC calculation point with the same absorbed dose[16]. The percentage depth dose curves of the 6 MV photon beam are plotted in Figure 2 for the 10x10, 6x6, 4x4, 3x3, 2x2, 1x1, and 0.6x0.6 cm^2 field sizes delivered at 100 cm SSD. The differences between the simulation and measurement are described below.

In a region deeper than the maximum dose (>1.5 cm), the measurement and MC simulation data closely agreed with a dose difference of less than 2.2%, while the mean dose differences were less than 1.0% for all field sizes. The mean dose difference ± standard deviation between the simulated and measured PDDs beyond the buildup region are reported in Table 2. The absolute value of the dose difference was taken before finding the mean value. In the buildup region, the maximum deviation was found up to 8%. Because the buildup region is a high dose gradient region, small spatial shifts between the measurement and MC dose distribution can result in a high dose difference. When the DTA was analyzed in the buildup region, we found a 1.0 mm agreement between the MC produced PDD and the measurement. Further comparison of the PDD at a 10 cm depth (PDD_{10}) and PDD at a 20 cm depth (PDD_{20}) for simulation and measurement is also presented in Table 2. The maximum difference was ~1.0% for PDD_{10} and PDD_{20}.

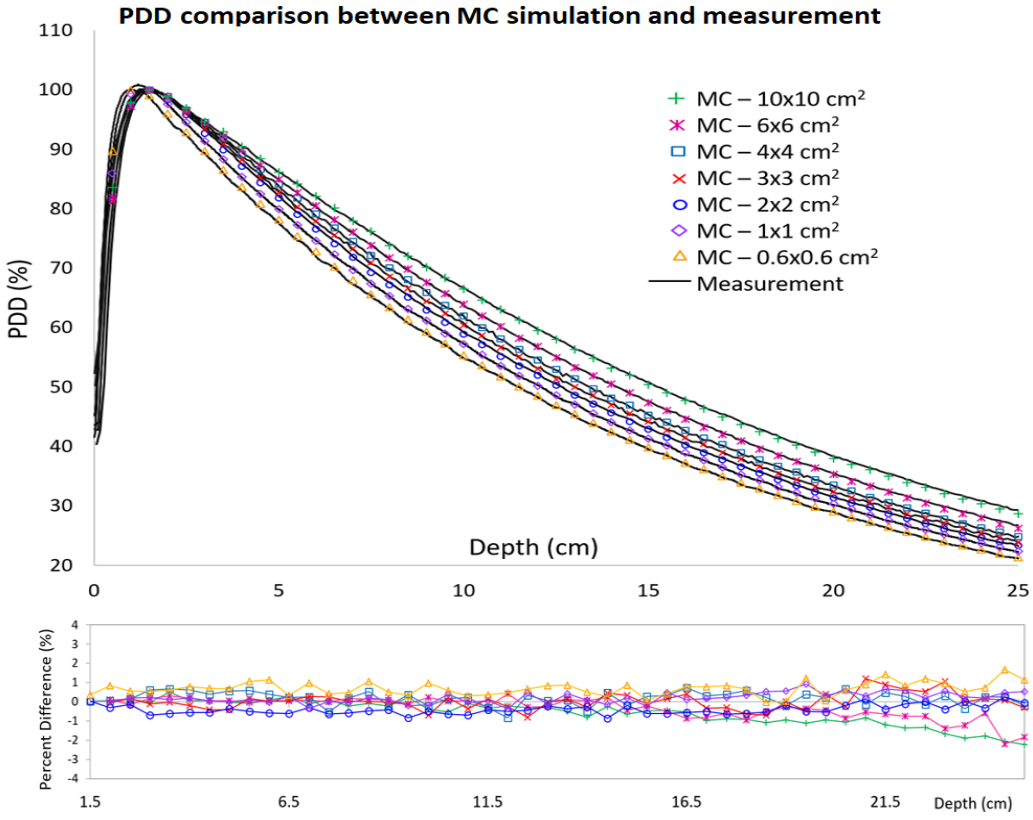

Figure 2. *Percent depth dose curves for all field sizes. Measurements are plotted as solid lines, and the Monte Carlo data are plotted as points. Percent differences between the simulation and measurement are presented in the lower panels.*

Table 2 The mean dose difference and standard deviation of PDDs between simulation and measurement beyond the buildup region. The comparison of PDD at 10 cm and PDD at 20 cm are reported.

Field size (cm^2)	Mean dose difference (%) ±SD	PDD_{10}			PDD_{20}		
		MC	Measured	%diff	MC	Measured	%diff
10x10	0.6±0.6	66.4	66.2	-0.4%	38.0	38.3	0.9%
6x6	0.4±0.5	63.9	63.8	-0.2%	35.3	35.4	0.4%
4x4	0.4±0.2	62.0	62.1	0.2%	33.5	33.4	-0.2%
3x3	0.3±0.3	60.3	60.7	0.7%	32.4	32.3	-0.4%
2x2	0.4±0.2	58.9	59.2	0.5%	31.3	31.5	0.5%
1x1	0.3±0.2	57.2	57.3	-0.2%	30.3	30.3	0.3%
0.6x0.6	0.7±0.4	55.3	54.8	-1.0%	29.0	29.0	-0.1%

Beam profiles

For the dose profiles, the crossline and inline directions were considered. Figure 3 presents the normalized measured and simulated half-profiles for all field sizes at the 10 cm depth. To evaluate the beam profile, the dose difference was analyzed in the radiation field region (within 80% of the normalized dose). The agreement between the simulation and measurement in the shoulder and penumbra region (beyond the in-field region) was evaluated by determining the DTA. Table 3 demonstrates the dose differences inside the radiation field between the measurement and simulation. The mean dose difference was less than or equal to 1.5% for field sizes ≥1x1 cm^2. For field sizes ≥4x4 cm^2, the deviation was within 1.5% for more than 97% of the points in the radiation field region. For field sizes ≤3x3 cm^2, a large deviation was observed. The mean dose differences were found up to 5.0% for the 0.6x0.6 cm^2 field size. The pass rate (the point displaying a percent difference of ≤1.5%) in the radiation field region was 78%, 75%, and 67% for the crossline profile of the 2x2, 1x1, and 0.6x0.6 cm^2 field, respectively. For the inline profile, the pass rate was 81%, 75%, and 17% for the 2x2, 1x1, and 0.6x0.6 cm^2 field, respectively. The discrepancy between the simulation and measurement was also found in the profile shoulders. In the small field, the profile exhibited a very steep dose gradient, and the flattened region was less than 80% of the normalized dose. Therefore, the DTA was applied to evaluate every point of the 0.6x0.6, 1x1, and 2x2 cm^2 fields. The DTA of the region where the dose difference exceeded 1.0% was less than 1.0 mm and 1.2 mm for all crossline and inline profiles, respectively.

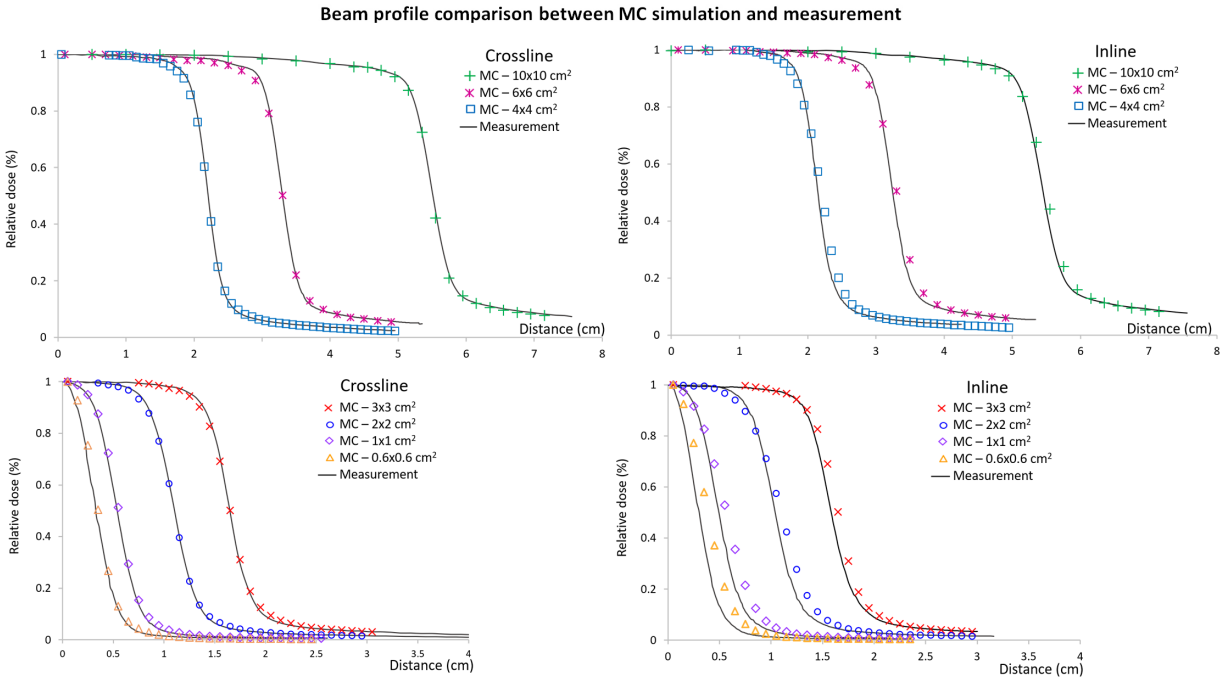

Figure 3. *Crossline (left) and inline (right) half profiles for the 10x10, 6x6, 4x4, 3x3, 2x2, 1x1, and 0.6x0.6 cm^2 field sizes. Measurements are plotted as continuous lines, and the Monte Carlo data are plotted as points.*

Table 3 Percent difference of the beam profiles between Sun Nuclear Edge measurement and MC simulation inside radiation field. The DTA of the region where the dose difference exceeds±1% is shown.

Field size (cm^2)	Crossline profile		Inline profile	
	Mean dose differences (%)±SD	DTA (mm)	Mean dose differences (%)±SD	DTA (mm)
10x10	0.2±0.2	<1.0	0.3±0.2	<1.0
6x6	0.7±0.4	<1.0	0.4±0.3	<1.0
4x4	0.5±0.4	<1.0	0.4±0.4	<1.0
3x3	0.5±0.5	<1.0	0.3±0.2	<1.0
2x2	0.7±0.7	<1.0	0.9±0.9	<1.2
1x1	0.6±0.7	<1.0	1.5±1.4	<1.1
0.6x0.6	4.9±3.6	<1.0	5.4±3.6	<1.2

Other profile characteristics, the FWHM and penumbra, were evaluated. The results are summarized in Table 4. The FWHM was determined from a distance of 50% relative dose and the penumbra was defined as the region between 20% and 80% of the central axis dose. As seen in Table 4, the simulated FWHM agrees with the measurement within 1.5 mm for the field sizes >0.6x0.6 cm^2. The deviation of the penumbra was also within 1.5 mm for all field sizes. Overall, the FWHM and penumbra widths tended to be larger than the measurement in the inline direction, with the differences increasing with the decreasing field size. However, the differences did not exceed 2.0 mm.

Field output factors

The comparison of the FOFs between the MC simulation and measurement for field sizes ranging from 0.6×0.6 cm^2-10×10 cm^2 are given in Table 5. Excellent agreement between the MC simulation and measurement was found within 1.0%, except for the 0.6x0.6 cm^2 field, where the maximum difference was 2.2% obtained by the IBA CC01 detector. The FOF of the 0.6x0.6 cm^2 field measured by the Sun nuclear EDGE detector was omitted because no correction factor was provided by TRS 483.

Table 4 Comparison of simulated and measured FWHM (distance between 50% isodose level) and penumbra width (distance between 20% and 80% isodose level) for all field sizes.

Field size (cm^2)	Crossline (mm)						Inline (mm)					
	FWHM width			Penumbra width			FWHM width			Penumbra width		
	MC	Measured	Deviation	MC	Measure	Deviation	MC	Measured	Deviation	MC	Measure	Deviation
10x10	110.0	110.1	0.1	5.3	5.5	-0.2	110.0	108.9	1.1	6.5	5.6	1.0
6x6	66.0	66.0	0.0	4.6	4.3	0.3	66.1	64.9	1.2	6.0	4.6	1.4
4x4	44.1	43.9	0.2	4.0	3.6	0.4	44.1	42.9	1.2	5.0	3.8	1.2
3x3	33.0	32.9	0.1	3.7	3.4	0.3	33.1	31.7	1.4	4.9	3.8	1.1
2x2	22.0	22.0	0.0	3.6	3.5	0.1	22.0	20.8	1.2	4.6	3.5	1.1
1x1	11.1	10.8	0.3	3.2	3.2	0.0	11.3	9.9	1.4	4.0	3.1	0.9
0.6x0.6	7.0	6.6	0.4	2.8	2.9	-0.1	7.7	6.0	1.7	3.3	2.7	0.6

Table 5 Field output factors of 6 MV using IBA CC01, Sun Nuclear EDGE, and PTW natural diamond compare with simulated FOF. The corrections were based on TRS 483 except for 0.6x0.6 cm^2 field size measured with Sun Nuclear EDGE where the correction factor is not provided by TRS 483.

Field Size (cm^2)	Field output factors						
	Simulation	EDGE	%Diff	Diamond	%Diff	CC01	%Diff
6x6	0.923	0.919	-0.4	0.918	-0.5	0.919	-0.4
4x4	0.867	0.862	-0.6	0.862	-0.6	0.864	-0.4
3x3	0.833	0.829	-0.5	0.829	-0.5	0.831	-0.3
2x2	0.795	0.791	0.5	0.790	-0.6	0.790	-0.6
1x1	0.683	0.690	0.9	0.683	0.0	0.679	-0.6
0.6x0.6	0.490	-	-	0.485	-1.0	0.479	-2.2

Discussion

The present study evaluated the MC simulation using the Varian phase-space file version 2 of the 6 MV photon beam for small field dosimetry. The MC simulation and measurement PDDs, beam profiles, and FOFs were compared. Overall, the MC simulation provided data that was consistent with the measurement. The agreement between all measured and MC simulated PDDs data in this study was under 2.2% beyond the buildup region. Large differences were found in the deeper depths (>25 cm) of the PDD where the MC simulation overestimated the dose compared with the measurement data. Our results agree with those of Bergman *et al.*,[9] who simulated the dose distribution of the 6 MV photon beam using a Varian phase-space file. In their study, a maximum deviation of 2% between the simulated and measured PDD for field sizes 2 × 2 cm^2-40 × 40 cm^2 was reported. In another study by Cheng *et al.*,[17] they reported a maximum dose difference of 1.5% for the PDD of a 10x10 cm^2 field. These studies, as well as ours, found that the maximum deviation was in the distal region of the PDD. In addition, an increasing discrepancy between the measured and simulated PDD with depth was observed in many reports[7-10, 18] that evaluated the Varian phase space file. A possible explanation for the discrepancy in the deeper depth region might be the differences in the primary beam energy of the phase-space file and the Varian TrueBeam™ machine in the experiment.[7,19]

The comparison of our simulated PDD_{10} and PDD_{20} with other Varian TrueBeam™ data[20-23] is summarized in Table 6. Our MC results agree within 1.0% for all the compared linear accelerators for the 3x3–10x10 cm^2 field sizes. In addition, the simulated PDD_{10} values fall within the range of those reported by Mamesa[23] who measured the PDDs of small fields using several detectors.

Table 6 Summary of the PDD parameters of 6 MV photon beam from MC simulation (this study) and measured data from previous studies. Measured PDD10 from Mamesa *et al*. were estimated from Figure 1. reported in their paper.

Field sizes (cm^2)	PDD_{10}					PDD_{20}	
	MC (this study)	Glide-Hurst *et al.*[20]	Bayer *et al.*[21]	Chang *et al.*[22]	Mamesa *et al.*[23]	MC (this study)	Chang *et al.*[22]
10x10	66.4	66.2	66.1	66.3	-	38.0	38.1
6x6	63.9	-	-	63.5	63.2 - 64.4	35.3	35.1
4x4	62.0	-	61.4	61.4	61.0 - 62.0	33.5	33.3
3x3	60.3	-	-	60.3	59.6 - 60.8	32.4	32.4
2x2	58.9	-	-	-	58.0 - 59.6	31.3	-
1x1	57.2	-	-	-	56.0 - 58.4	30.3	-
0.6x0.6	55.3	-	-	-	-	29.0	-

For the dose profile, small differences were observed between the measurement and simulation in the in-field dose area for field sizes ≥3x3 cm^2. The DTA of the region where the absolute difference exceeds 1.0% was less than 1.2 mm. Therefore, the simulated data demonstrated identical profiles with the measurement within 1.0% of the dose difference or 1.2 mm of DTA. The FWHM of the 10×10 cm^2 field at the 10 cm depth was similar to that described by Chang[22] with a difference of 0.7 mm. However, our simulated FWHM was 2.0 mm smaller than that reported by Glide-Hurst *et al.*[20] and Beyer *et al.*[21]. These differences were due to the volume averaging effect of the detector used for the beam profile scanning. The Glide-Hurst and Bayer studies used an IBA CC13 detector to measure the profile data, whereas the beam profiles were measured with an IBA SFD diode detector in Chang's study. The large active volume of the detector can lead to inaccurate field edge measurements where a steep dose gradient exists. The previous literature also reported that the FWHM measured using the IBA CC13 detector was 1.8 mm larger than that measured by the Sun Nuclear EDGE detector for the 10x10 cm^2 field.[24] Besoli *et al.*,[7] who validated the Varian phase-space file of the 6FFF MV beam, found that the simulated penumbra was more similar to the diode measurement. Our study used a Sun Nuclear Edge detector to measure the beam profile. Thus, the measured and simulated penumbra and FWHM results agreed within 2.0 mm for all field sizes. The profile data of the field sizes ranging from 1x1 cm^2-6x6 cm^2 were reported by Mamesa *et al.*[23] and the difference in FWHM was less than 2.0 mm compared with our MC results.

The discrepancy between the measurement and simulation in the inline profile was higher than the crossline profile. The widening of the simulated inline profile was observed as the field sizes decreased. Beam profile deviations were also observed for field sizes ≤3x3 cm^2 in other studies.[8, 9, 18] A possible reason for the discrepancy might be partly ascribed to the difference in the primary photon source width among the Varian TrueBeam™ linear accelerators, which were in the range of 1.0-1.5 mm.[12, 25] Pervious studies have found that the dose profile of a small field (<1x1 cm^2) was strongly dependent on the primary photon source size. Cranmer-Sargison *et al.*[25] reported that the dosimetric field widths increased as the source size increased. This is due to the partial source occlusion by the collimated jaw and is markedly affected by the upper jaws because it is closer to the source than the lower one. The slight deviation in the profile shoulder region between the MC and measurement is also explained by the difference in the source size. Because the Varian phase-space

file was scored above the collimator jaw, the user cannot change the primary photon source parameters, such as the energy, angular spread, and diameter. Therefore, it is not possible to fine tune the beam model to better match a specific linear accelerator. This could be crucial issue in a very small field (<1x1 cm^2) when the beam profile is highly dependent on the primary source size and source occlusion effect.

It should be noted that no corrections were made for the PDD and beam profile measurements in this study. The accuracy of the small field measurement by the Si-based diode detector was reported by Francescon *et al*.[26] The variation of the field output correction factor of the diode detector as a function of depth and distance from the central axis for PDD and beam profile measurements was reported in the literature. The beam profile in water measured with the diode detector yielded accurate results up to the penumbra region, but meaningfully underestimated the dose in the tail region where the field output correction factor was increased. Similar results were found by Papaconstadopoulos *et al*.[27] where the diode detector demonstrated minimal deviations within the radiation field. In contrast, significant corrections were observed at the gradient and the low-dose region of the profile. However, the error in the gradient and tail region of the beam profile is not clinically meaningful, because it is considered a very low dose area.[26] Dwivedi[28] reported that the variation of the beam profile measured by the Sun Nuclear Edge detector for field sizes ranging from 0.6x0.6 cm^2-6x6 cm^2 was less than 0.5 mm in FWHM compared with EBT3 radiochromic films (Ashland Inc., Wayne, NJ, USA). Although the Sun Nuclear Edge detector exhibits the correction factor >5% at all depths as reported by Francescon *et al*., other studies[28, 29] demonstrated that the PDD at the fall-off region measured by the Sun Nuclear Edge detector for field size ≤1x1 cm^2 was comparable with other detectors that have been recommended to avoid the need to correct the PDD, such as EBT3 film and the PTW microdiamond detector.[30]

For the FOF measurements, the Sun Nuclear Edge detector exhibits the overresponse FOFs for field size smaller than 2x2 cm^2 due to the scatter from the high density encapsulating material of the detector.[31-33] In contrast, the IBA CC01 and PTW natural diamond detectors were influenced by volume averaging effects that underestimated the FOFs.[10, 34] However, this effect becomes less critical for the PTW natural diamond detector due to the smaller size of the active volume. In addition, the PTW natural diamond detector measurement values were very consistent with the MC values, only deviating ≤1.0%. The difference in FOFs between the measurement and the 6 MV Varian phase-space file in the present study agrees well with previous studies by Constantin *et al*.[6] and Bergman *et al*.[9] However, the smallest field sizes in these studies were limited to 4x4 cm^2 and 2x2 cm^2. The data for comparison obtained using the 6 MV Varian phase space file for field sizes <2x2 cm^2 are scarce, only Gete *et al*.[8], who evaluated the 6FFF phase-space file, have reported the FOF for the 1x1 cm^2 field. In our study, the simulated FOF fell within 2.2% of the measured FOF for all field sizes. This is better than that reported by Gete *et al*.[8] where a deviation of 2.9% was found between the IBA CC01 detector and the simulated output factor of the 1x1 cm^2 field, whereas the deviation was less than 1.0% in our study. However, no correction factor was applied in Gete *et al*.,[8] because the TRS 483 was not published at the time of their study. The output factors of small fields cannot be accurately approximated as the ratio of the detector readings as it is usually done for broad beams. Many studies have reported that the deviation of the field output factors reduced significantly when the field output correction factors based on TRS 483 were implemented.[23, 35, 36] A further comparison with previous studies is presented in Table 7. The agreement was within 1.0% compared with Mamesa *et al*.[23] for the 1x1 cm^2-10x10 cm^2 field sizes. The FOFs taken from Mamesa's study were averaged between the IBA CC01, IBA EFD, and IBA PFD detectors. Casar *et al*.[37] also reported the FOFs that were determine by fitting the signal of the EBT3 radiochromic films and the W1 plastic scintillator (Standard Imaging, Middleton, WI, USA) using an analytical function. A 90 cm SSD was used in their study, making a direct comparison with our results difficult. However, the difference was ~1.6% compared with our MC results.

Table 7 Comparison of field output factors between our MC simulation and measured data from previous studies.

Field size (cm^2)	MC (this study)	Mamesa *et al*.[23]	%Diff	Casar *et al*.[37]	%Diff
6x6	0.923	0.921	-0.2	0.915	-0.9
4x4	0.867	0.865	-0.2	0.866	-0.1
3x3	0.833	0.832	-0.2	0.834	0.1
2x2	0.795	0.791	-0.6	0.793	-0.3
1x1	0.683	0.688	0.7	0.694	1.6

Many studies have found that the intermachine variability of the Varian TrueBeam™ machine is very small among different institutes.[20-22] Tanaka *et al*. [38] found a small difference of 1.0% and 1.5% when comparing the PDDs and beam profiles, respectively, between 21 TrueBeam™ machines and average data. They also reported that the deviation of the output factor of each data set from the average value was within 1.0% for the 3x3 cm^2- 30x30 cm^2 fields. These data support that the Varian phase-space file approach is feasible for MC simulation for large field because the TrueBeam™ linear accelerator data is very consistent. However, for small field, the dosimetric parameters is vary due to the difference in source size and detector selection. Akino *et al*.[36] found that the differences of the FOFs were

within ±5% for 0.5x0.5 cm^2 among 12 TrueBeam™ machines. The variation of PDD at 0.5x0.5 cm^2 was >1%. Whereas the variability <1% for 1x1 cm^2 was reported in their study. In this work, the MC results using the Varian phase-space file were compared with the published measured data from many institutions. The results revealed that our simulation agreed with other TrueBeam™ machines published data, including PDDs, beam profiles, and FOFs. Although a few studies have reported the commissioning data of Varian TrueBeam™ for small field sizes, the consistence between the MC simulation and measurement in this study indicates the excellent performance of the phase-space file for field sizes down to 1x1 cm^2. For very small field sizes (<1x1 cm^2), it is recommended that the phase-space file should be evaluated with measurement data from a given TrueBeam™ machines.

Conclusion

The Varian TrueBeam™ 6MV phase-space file version 2 released by Varian Medical System was evaluated against the measurement for small field sizes down to 0.6x0.6 cm^2. The MC simulation demonstrates good agreement with the PDDs. Although discrepancies in the inline profile were observed for field sizes ≤3x3 cm^2, it did not affect the PDD or the output factor, except for the 0.6x0.6 cm^2 field where the difference in the output factor was up to 2%. The Varian phase-space file can be used as a radiation source for accurate MC dose calculation with existing TrueBeam™ models for field sizes ≥1x1 cm^2. For very small field sizes (<1x1 cm^2) where the beam profile is strongly influenced by the source size, we recommend that the user verifies the phase-space with a specific TrueBeam™machine.

Conflicting interests

The authors declare no conflict of interest.

References

[1] PalmansH, Andreo P,Huq MS, et al. Dosimetry of small static fields used in external beam radiotherapy: an IAEA-AAPM International Code of Practice for reference and relative dose determination, Technical Report Series No. 483. International Atomic Energy Agency: Vienna, Austria, 2017.

[2] Chetty IJ, Curran B, Cygler JE, et al. Report of the AAPM Task Group No. 105: Issues associated with clinical implementation of Monte Carlo-based photon and electron external beam treatment planning. Med Phys. 2007; 34(12): 4818-53. doi: 10.1118/1.2795842.

[3] Benmakhlouf H, Sempau J, Andreo P. Output correction factors for nine small field detectors in 6 MV radiation therapy photon beams: a PENELOPE Monte Carlo study. Med Phys. 2014; 41(4): 041711. doi: 10.1118/1.4868695.

[4] Francescon P, Cora S, Satariano N. Calculation of k(Q(clin),Q(msr)) (f(clin),f(msr)) for several small detectors and for two linear accelerators using Monte Carlo simulations. Med Phys. 2011; 38(12): 6513-27. doi: 10.1118/1.3660770.

[5] Cranmer-Sargison G, Weston S, Sidhu NP, et al. Experimental small field 6MV output ratio analysis for various diode detector and accelerator combinations. Radiother Oncol. 2011; 100(3): 429-35. doi: 10.1016/j.radonc.2011.09.002.

[6] Constantin M, Perl J, LoSasso T, et al. Modeling the truebeam linac using a CAD to Geant4 geometry implementation: dose and IAEA-compliant phase space calculations. Med Phys. 2011; 38(7): 4018-24. doi: 10.1118/1.3598439.

[7] Belosi MF, Rodriguez M, Fogliata A, et al. Monte Carlo simulation of TrueBeam flattening-filter-free beams using Varian phase-space files: Comparison with experimental data. Med Phys. 2014; 41(5): 051707. doi: 10.1118/1.4871041.

[8] Gete E, Duzenli C, Milette M-P, et al. A Monte Carlo approach to validation of FFF VMAT treatment plans for the TrueBeam linac. Med Phys. 2013; 40(2): 021707. doi: 10.1118/1.4773883.

[9] Bergman AM, Gete E, Duzenli C, et al. Monte Carlo modeling of HD120 multileaf collimator on Varian TrueBeam linear accelerator for verification of 6X and 6X FFF VMAT SABR treatment plans. J Appl Clin Med Phys. 2014; 15(3): 4686. doi: 10.1120/jacmp.v15i3.4686.

[10] Qin Y, Zhong H, Wen N, et al. Deriving detector-specific correction factors for rectangular small fields using a scintillator detector. J Appl Clin Med Phys. 2016; 17(6): 379-91. doi: 10.1120/jacmp.v17i6.6433.

[11] Feng Z, Yue H, Zhang Y, et al. Monte Carlo simulation of beam characteristics from small fields based on TrueBeam flattening-filter-free mode. Radiat Oncol. 2016; 11(1): 30. doi: 10.1186/s13014-016-0601-2.

[12] Papaconstadopoulos P, Levesque IR, Aldelaijan S, et al. Modeling the primary source intensity distribution: reconstruction and inter-comparison of six Varian TrueBeam sources. Phys Med Biol. 2019; 64: 135005. doi.org/10.1088/1361-6560/ab1ccc.

[13] Kawrakow I. The EGSnrc Code System, Monte Carlo Simulation of Electron and photon Transport. NRCC Report PIRS-701. 2001.

[14] Rogers D, Walters B, Kawrakow I. BEAMnrc users manual. Nrc Report Pirs. 2009; 509: 12.

[15] Walters B, Kawrakow I, Rogers D. DOSXYZnrc users manual. Nrc Report Pirs. 2005; 794: 57-8.

[16] Low DA, Dempsey JF. Evaluation of the gamma dose distribution comparison method. Med Phys. 2003; 30(9): 2455-64. doi: 10.1118/1.1598711.

[17] Cheng JY, Ning H, Arora BC, et al. Output factor comparison of Monte Carlo and measurement for Varian TrueBeam 6 MV and 10 MV flattening filter-free stereotactic radiosurgery system. J Appl Clin Med Phys. 2016; 17(3): 100-10. doi: 10.1120/jacmp.v17i3.5956.

[18] Teke T, Duzenli C, Bergman A, et al. Monte Carlo validation of the TrueBeam 10XFFF phase–space files for applications in lung SABR. Med Phys. 2015; 42(12): 6863-74. doi: 10.1118/1.4935144.

[19] Tzedakis A, Damilakis JE, Mazonakis M, et al. Influence of initial electron beam parameters on Monte Carlo calculated absorbed dose distributions for radiotherapy photon beams. Med Phys. 2004; 31(4): 907-13. doi: 10.1118/1.1668551.

[20] Glide-Hurst C, Bellon M, Foster R, et al. Commissioning of the Varian TrueBeam linear accelerator: A multi-institutional study. Med Phys. 2013; 40(3): 031719. doi: 10.1118/1.4790563.

[21] Beyer GP. Commissioning measurements for photon beam data on three TrueBeam linear accelerators, and comparison with Trilogy and Clinac 2100 linear accelerators. J Appl Clin Med Phys. 2013; 14(1): 4077. doi: 10.1120/jacmp.v14i1.4077.

[22] Chang Z, Wu Q, Adamson J, Ren L, et al. Commissioning and dosimetric characteristics of TrueBeam system: composite data of three TrueBeam machines. Med Phys. 2012; 39(11): 6981-7018. doi: 10.1118/1.4762682.

[23] Mamesa S, Oonsiri S, Sanghangthum T, et al. The impact of corrected field output factors based on IAEA/AAPM code of practice on small-field dosimetry to the calculated monitor unit in eclipse™ treatment planning system. J Appl Clin Med Phys. 2020; 21(5): 65-75. doi: 10.1002/acm2.12855.

[24] Chang K-H, Lee B-R, Kim Y-H, et al. Dosimetric Characteristics of Edge Detector(TM) in Small Beam Dosimetry. Korean J Med Phys. 2009; 20: 191-8.

[25] Cranmer-Sargison G, Charles PH, Trapp JV,et al. A methodological approach to reporting corrected small field relative outputs. Radiother Oncol. 2013; 109(3): 350-5. doi.org/10.1016/j.radonc.2013.10.002.

[26] Francescon P, Beddar S, Satariano N, et al. Variation of kQclin,Qmsrfclin,fmsr for the small-field dosimetric parameters percentage depth dose, tissue-maximum ratio, and off-axis ratio. Med Phys. 2014; 41(10): 101708. doi: 10.1118/1.4895978.

[27] Papaconstadopoulos P, Tessier F, Seuntjens J. On the correction, perturbation and modification of small field detectors in relative dosimetry. Phys Med Biol. 2014; 59(19): 5937. doi: 10.1088/0031-9155/59/19/5937.

[28] Dwivedi S, Kansal S, Dangwal VK, et al. Dosimetry of a 6 MV flattening filter-free small photon beam using various detectors. Biomed Phys Eng. 2021; 7(4): 045004. doi: 10.1088/2057-1976/abfd80.

[29] Akino Y, Fujiwara M, Okamura K, et al. Characterization of a microSilicon diode detector for small-field photon beam dosimetry. J Radiat Res. 2020; 61(3): 410-8. doi.org/10.1093/jrr/rraa010.

[30] Das IJ, Francescon P, Moran JM, et al. Report of AAPM Task Group 155: Megavoltage photon beam dosimetry in small fields and non-equilibrium conditions. Med Phys. 2021. doi.org/10.1002/mp.15030.

[31] Kairn T, Charles PH, Cranmer-Sargison G, et al. Clinical use of diodes and micro-chambers to obtain accurate small field output factor measurements. Australas Phys Eng Sci Med. 2015; 38(2): 357-67. doi: 10.1007/s13246-015-0334-9.

[32] Azangwe G, Grochowska P, Georg D, et al. Detector to detector corrections: a comprehensive experimental study of detector specific correction factors for beam output measurements for small radiotherapy beams. Med Phys. 2014; 41(7): 072103. doi: 10.1118/1.4883795.

[33] Liu PZ, Suchowerska N, McKenzie DR. Can small field diode correction factors be applied universally? Radiother Oncol. 2014; 112(3): 442-6. doi: 10.1016/j.radonc.2014.08.009.

[34] Lechner W, Palmans H, Sölkner L, et al. Detector comparison for small field output factor measurements in flattening filter free photon beams. Radiother Oncol. 2013; 109(3): 356-60.

[35] Smith CL, Montesari A, Oliver CP, et al. Evaluation of the IAEA-TRS 483 protocol for the dosimetry of small fields (square and stereotactic cones) using multiple detectors. J Appl Clin Med Phys. 2020; 21(2): 98-110. doi.org/10.1002/acm2.12792.

[36] Akino Y, Mizuno H, Isono M, et al. Small-field dosimetry of TrueBeam(TM) flattened and flattening filter-free beams: A multi-institutional analysis. J Appl Clin Med Phys. 2020; 21(1): 78-87. doi: 10.1002/acm2.12791.

[37] Casar B, Gershkevitsh E, Mendez I, et al. A novel method for the determination of field output factors and output correction factors for small static fields for six diodes and a microdiamond detector in megavoltage photon beams. Med Phys. 2019; 46(2): 944-63. doi: 10.1002/mp.13318.

[38] Tanaka Y, Mizuno H, Akino Y, et al. Do the representative beam data for TrueBeam(™) linear accelerators represent average data? J Appl Clin Med Phys. 2019; 20(2): 51-62. doi: 10.1002/acm2.12518.

Journal of Associated Medical Sciences 2022; 55 (3): 36-43

JAMS
Journal of Associated Medical Sciences

Thai-Journal Citation Index Centre (TCI) & ASEAN Citation Index (ACI)

Journal of Associated Medical Sciences

Journal homepage: https://www.tci-thaijo.org/index.php/bulletinAMS/index

Comparative active compounds and antioxidant activity between the sweet- and sour-type star fruit (*Averrhoa carambola* L.) *In Vitro*

Jynwara Kaju[1] Jirakrit Leelarungrayub[2*] Surapol Natakankitkul[3] Supawatchara Singhatong[4] Chanchai Dechthummarong[5] James J Laskin[6]

[1]Biomedical Science Program. Faculty of Associated Medical Sciences, Chiang Mai University, Chiang Mai Province, Thailand.
[2]Department of Physical Therapy, Faculty of Associated Medical Sciences, Chiang Mai University, Chiang Mai Province, Thailand.
[3]Pharmaceutical Sciences, Faculty of Pharmacology. Chiang Mai University, Chiang Mai Province, Thailand.
[4]Department of Medical Technology, Faculty of Associated Medical Sciences, Chiang Mai University, Chiang Mai Province, Thailand.
[5]High Voltage Engineering Laboratory, Department of Electrical Engineering, Faculty of Engineering, Rajamangala University of Technology Lanna, Chiang Mai Province, Thailand.
[6]School of Physical Therapy and Rehabilitation Sciences, University of Montana, Missoula, Montana, USA.

ARTICLE INFO

Article history:
Received 25 April 2022
Accepted as revised 14 June 2022
Available online 5 July 2022

Keywords:
Antioxidant, active compound, sour-type and sweet-type star fruit

ABSTRACT

Background: Star fruit (*Averrhoa carambola L.*) is seasonal and originates from many Southeast Asia countries, including Thailand. Previous evidence claimed that it has various antioxidative compounds such as phenolics, saponins, flavonoid C-glycosides, tannin and L-ascorbic acid. In Thailand, the sweet-type of star fruit (SF) is cultivated and marketed more than the sour-type, but their different antioxidant and active compounds between both types have not been investigated.

Objectives: This study aimed to compare the active compounds and anti-oxidant activity between sweet- and sour-type SF *in vitro*.

Materials and methods: Active compounds such as total phenolic compound, total flavonoids and L-ascorbic acid in extracts were evaluated between sweet- and sour-type SF crude extracts by using Folin-Ciocalteau reagent, aluminum chloride colorimetric assay and high-performance liquid chromatography, respectively. Antioxidant activity on scavenging radicals such as the 2,2'-azino-bis (3-ethylbenzthiazoline-6-sulphonic acid) ($ABTS^{\bullet+}$) cation and 1,1-diphenyl-2-picrylhydrazyl (DPPH) cation and nitric oxide (NO) was analyzed. Moreover, the protective activity of glutathione (GSH) oxidation from free radicals generated by high voltage (HV)-stimulation in a mixture of plasma micro/nanobubble water; the same as that of protein oxidation in bovine serum albumin (BSA) and malondialdehyde (MDA) from 2,2'-Azobic (2-amidinopropane) dihydrochloride (AAPH), was evaluated *in vitro*.

Results: Sour-type SF extract at 1 gm showed higher total phenolics (1,625±2.3 µg equivalent gallic acid [GAE]), total flavonoid (245±3.6 µg equivalent quercetin), and ascorbic acid (Vit C) (565±4.5 µg) than sweet-type (520±3.5 µg GAE, 187±2.5 µg, and 513±2.6 µg). In addition, sour-type SF showed a lower dose of inhibitory concentration of 50% (IC50) than sweet-type on scavenging DPPH (32.32±2.3 & 58.9±2.4 mg) and NO (23.1 ± 1.1 mg & undetected). However, IC50 on $ABTS^{\bullet+}$ scavenging of sweet-type was lower than that of sour-type (348.8±2.5 & 511.9±2.6 mg). Sweet-type showed protective effects with a dose response at 0.25-1.0 mg of extract, 125-500 µg of protein carbonyl and 62.5-500 µg of lipid peroxidation. However, sour-type at high doses showed pro-oxidant activity on increased GSH oxidation, protein carbonyl and MDA formation.

Conclusion: Sour-type SF showed higher active antioxidants, such as total phenolics, total flavonoids and Vit C as well as radical scavenging of DPPH and NO, than sweet-type SF. However, high concentrations aggravated GSH, protein and lipid oxidation. Whereas, sweet-type SF showed beneficial protective effects.

* **Corresponding author.**
Author's Address: *Department of Physical Therapy, Faculty of Associated Medical Sciences, Chiang Mai University, Chiang Mai Province, Thailand.*
** **E-mail address:** donrawee.leela@cmu.ac.th
doi: 10.12982/JAMS.2022.022
E-ISSN: 2539-6056

Introduction

Many fruits contain various multi-vitamins and polyphenolic compounds, and have antioxidant activity that benefits human health.[1] Star fruit (SF) or Carambola is seasonal with the scientific name of *Averrhoa carambola* Less and has been cultivated in many countries of Southeast Asia, including Thailand. Nowadays, SF has many species or varieties such as Taiwan (big size with a green edge and sweet taste), Malaysia (big size with a sweet taste, and a lot of juice), and Guangdong, China (big size and white with a sweet taste).[2] However, two distinct classes of carambola can be found in Thailand; small size with a sour taste and big size with a sweet taste. They generally have typical characteristics of a five-pointed star-like cross section and green to yellowish skin, and has a very sour-slightly-sweet flavor.[3] Previous reports showed that the chemical constituents of SF are flavonoid C-glycosides, saponins, tannin,[4,5] L-ascorbic acid, (-) epicatechin and gallic acid (GAE).[6,7] In addition, its pharmaceutical values as a traditional medicine are anti- pyretic, appetite stimulation, laxation, diuretics and digestives.[2,7] In 2016, a study of SF juice supplement sour-type folk variety in Chiang Mai province showed L-ascorbic acid (16-17 mg in 100 g of extract) and retinoic acid (0.1-0.2 µg in 100 g of extract).[8] Furthermore, supplementation of fresh ripe sour-type SF juice at 100 g for one month, could increase high density lipoprotein (HDL) and decrease low density lipoprotein (LDL) as well as reduce inflammatory status by decreasing tumor necrosis factor (TNF)-α, interleukin-23 (IL-23) and nitric oxide (NO) levels in aging people. However, other types of star fruit; e.g., bigger size and sweeter taste, are available in Malaysia and India and distributed in many Thai markets. Updated data in 2020 showed that the sweet-type had antioxidant and anti-inflammatory activity in *in vitro* study, active compounds composed of total phenolic, total flavonoids and L-ascorbic acid.[9] In addition, it could improve total antioxidant capacity (TAC) and ascorbic acid (Vit C), and reduced lipid peroxide, as well as TNF-α in the plasma of people suffering from chronic obstructive pulmonary disease (COPD), after taking one-month of a prototype supplement containing sweet-type star fruit and honey.[10] Thus, both types of SF showed antioxidant compounds and effectiveness in people.

Unfortunately, the comparative activity between both types of SF had not been confirmed. Therefore, this study aimed to confirm their active compounds, especially total phenolic compound, total flavonoids, L-ascorbic acid, and scavenging activity on radicals such as organic cation radicals, 2,2'-azino-bis (3-ethylbenzthiazoline-6-sulphonic acid) $(ABTS)^{\bullet+}$ and NO. Moreover, the effect of protective activity on glutathione (GSH), protein and lipid peroxide formation from oxidative stress *in vitro* model is very challenging.

Materials and methods

Star fruit preparation

Raw sweet-type SF from the Malaysian variety was cultivated at organic gardens in Pathum Tani province and purchased for this study, whereas, the sour-type SF was purchased from a local farm in Chiang Mai province. Both types were baked in sealed boxes for 2 weeks until ripe (Figure 1), and then cleaned by soaking in clean water five times before blending in a fine homogenizer. The fibers and seeds were removed by filtering with a clean filter cloth and the SF juice was kept in a clean bottle before producing it in dry powder form or crude extract by the freeze-drying technique at the MANOSE RERSEARCH CENTER, Suthep sub-district, Mung district, Chiang Mai, Thailand. The final yield of crude extracts from fresh SF juice (5.0 %/*w:w*) was collected in a dark bottle and refrigerated before future analysis.

Figure 1. *Star fruit; sweet-type (left) and sour-type (right).*

Active compound analysis

Total phenolics

The total content of phenolics in crude extracts of sweet- and sour-types of SF were evaluated by following the Singleton and Rossi's protocol,[11] in which 50 µL of extracts (6.25-25 mg/mL) was mixed with 1.8 mL of diluted Folin-Ciocalteau reagent (10% v/v) (Merck KGaA, Germany), and kept in the dark for 5 min before adding 1,200 µL of (7.5%) sodium carbonate (Merck, Darmstadt). After that, the tubes were incubated for 60 min, and the pellets removed by centrifuging at a short high speed of 10,000 rpm, and the supernatant was read at 765 nm by spectrophotometry (Drawell Scientific, Shanghai). The total phenolic content at 1 gm of crude extract was calculated by comparing with standard GAE (0.008-1.0 mg/mL) (Fluka, Switzerland).

Total flavonoid content

Total flavonoid content in crude extracts of sour- and sweet-types was determined using the aluminum chloride colorimetric assay, adapted from a previous protocol.[12] Crude extracts at 25, 50 and 100 mg/mL, or different dilutions of standard quercetin (0.078-2.5 mg/mL) (Aldrich, Germany) at 500 µL, were added in 100 µL of 10% AlCl3 (Fischer Scientific, UK) solution. Then, 100 µL of sodium acetate solution (1.0 mol/L) (Fischer Scientific, UK) was added to 2.8 mL of deionized water. After 30 min incubation in the dark at room temperature, absorbance was measured by spectrophotometry (Drawell Scientific, Shanghai) at 415 nm. Total flavonoid content of both extracts at 1 gm was expressed as the mg of quercetin (Sigma-Aldrich, Germany).

L-ascorbic acid assay

The protocol for evaluating Vit C content in SF crude extracts from the sour- and sweet-types was performed by high-liquid chromatography (HPLC).[13] Before analysis, each extract at 20 mg was dissolved in 1.0 mL of deionized water, with the pellets being removed by short high-speed centrifugation at 10,000 rpm. Supernatant was filtered through a micro-filter (0.22 µm) before being analyzed in the HPLC system. The

specific peak and concentration of L-ascorbic acid in extracts were identified with a C18 reverse phase column (Eclipse Plus C18: 5 µm, 4.6 x 250 mm; Agilent, USA) under formic acid (0.1% *v/v*) (Sigma-Aldrich, Germany) as a mobile phase (pH 2.5) at a flow rate of 0.8 mL/min. Specific retention time for Vit C peak within 3.90-4.01 min was presented by a diode array detector (DAD) (SPD-MZOA, SHIMADZU, JAPAN) at 244 nm. The concentration of L-ascorbic acid in each extract was compared to standard Vit C (Fisher Scientific, UK).

Antioxidant activity assays

DPPH scavenging assay

Scavenging activity of the sour- and sweet type SF extracts that bleached the 1,1-diphenyl-2-picrylhydrazyl (DPPH) radical was evaluated as in the previous protocol.[14] $DPPH^{\bullet+}$ was generated by mixing the DPPH (CALBIOCHEM, Darmstadt, Germany) in Ethanol (Merck KGaA, Darmstadt, Germany). Different concentrations of both types of SF extracts were added at 12.5-100 mg to DPPH solution in the dark for 30 min before reading the absorbance with a spectrophotometer (Drawell Scientific, Shanghai) at 515 nm. The percentage of scavenging or inhibitory concentration of 50% (IC_{50}) of sweet- or sour-type SF extract from a global curve fitted the equation in the SigmaPlot progm for Windows (version 11.0).

$ABTS^{\bullet+}$ scavenging assay

Scavenging activity of sour- and sweet-type SF extracts that bleached the 2,2-Azino-bis (3-ethylbenzo thiazoline-6-sulfonic acid) ($ABTS^{\bullet+}$) cation was evaluated by following the previous protocol.[15] Stock $ABTS^{\bullet+}$ solution was generated by mixing ABTS (CALBIOCHEM, Darmstadt, Germany) solution (14 mmol/L) with 14 mmol/L of potassium persulfate (Merck KGaA, Darmstadt, Germany) in deionized water for 12 h in the dark before diluting in deionized water for starting absorbance of 0.70±0.02 at 734 nm by spectrophotometry (Drawell Scientific, Shanghai). Ten µL of sour- or sweet-type SF extract (100-800 µmg/mL) was added to 990 µL of working $ABTS^{\bullet+}$ solution in a plastic cuvette (size 1.5 mL), and gently alternated inversely 3 times before absorbance was read. The concentration of extracts (mg) at 50 percent of scavenging or reduced $ABTS^{\bullet+}$ between sour- and sweet-type SF was calculated by the global curve fit equation in the SigmaPlot program for Windows (version 11.0).

Nitric oxide (NO) scavenging assay

NO scavenging protocol was adapted from a previous report.[16] NO was generated by dissolving sodium nitroprusside (AnalaR NORMAPUR, VWR, Prolabo, Belgium) in deionized water (10 mmol/L), and kept in light at room temperature for 3 h before evaluation. The reaction mixture (3 mL) containing 2 mL of (10 mmol/L) sodium nitroprusside (SNP), 0.5 ml of saline phosphate buffer containing KH_2PO_4, Na_2HPO_4, NaCl and KCl (Merck, USA) (pH.7.4) and 0.5 mL of standard GAE (Fluka, Switzerland) solution or aqueous sour- or sweet-type SF extracts (6.25-100 mg/ml) was incubated at 25°C for 150 min. A 0.5 mL of the reaction mixture was taken to mix with 1.0 mL of sulfanilamide (Fluka, China) (1% in 2.5% of H_3PO_4, Merck, USA) and allowed to stand for 5 min in the dark at room temperature before a further 1 mL of napthyl ethylene diamine dihydrochloride (0.1% in water) (VWR, Prolabo, Belgium) was finally added. When the mixed solution was allowed to stand for 20 min at 25°C, absorbance at 537 nm was read by spectrophotometry (Drawell Scientific, Shanghai). The concentration of extracts (mg), at 50 percent of scavenging or reduced $ABTS^{\bullet+}$ between the sour- and sweet-type SF, was calculated by the global curve fit equation in the SigmaPlot program for Windows (version 11.0).

Protective activity of star fruit extracts

Glutathione (GSH) oxidation from high-voltage (HV) stimulation

The protective activity of GSH from free radicals was performed as in a previous study by stimulating HV in micro/nano-bubble (mnb) water mixture or using the Plasma-nano bubble technique at the High Voltage Engineering Laboratory, Department of Electrical Engineering, Faculty of Engineering, Rajamangala University of Technology Lanna, Chaing Mai, Thailand (Figure 2).[17] Previous reports demonstrated that discharged plasma in ionized water is able to dissociate water molecules and produce many reactive species such as radicals (hydroxyl radicals, OH°; superoxide radical, O°), hydrogen peroxide (H_2O_2), etc.[18] Then, GSH can be oxidized directly by those radicals in the system.[19] The laboratory-made plasma generator in this model study consisted of an HV power supply and a discharged plasma electrode. Micro/nano-air bubble water was generated in deionized water by a micro-bubble generator (AURA Tec Co., Ltd., model OM4-MDG-045) before preparing stock GSH (Sigma, St. Louis, Co, USA) at 100 mg/mL. One hundred mL of stock GSH solution was prepared in a 150-mL beaker before standing in a plastic box. The HV power supply used a high voltage transformer and direct current (DC) half wave circuit to convert input current at 1.5-2.0 amps, 100 volts and 50 Hz into an HV of up to 6 kVp and 1 Ap of discharged current. The discharged plasma electrodes had a ground electrode placed at the bottom of the beaker, and an anode electrode of tungsten (1.5 mm diameter) was dipped into the solution to produce the electrical plasma discharged in it. The protective effects between sweet- and sour-type SF extract at 0.25-1.0 mg was evaluated at 5-min incubation, designed at the same standard as Vit C (Fischer Scientific, UK) at 0.2 mg/mL, and confirmed in the system. Residual GSH concentration was determined using the 5, 5'-dithio-bis (2-nitrobenzoic acid) (DTNB) protocol.[20] Two hundred µL of mixed solution was taken to mix with 500 µL of DTNB (Sigma-Aldrich, Germany) and 500 µL of phosphate buffer (pH 8.0) solution. After incubating at room temperature for 5 min, a clear yellow supernatant solution was read by spectrophotometry at 412 nm (Drawell Scientific, Shanghai). The percentage of GSH was presented by comparing with non-HV stimulation.

Protein carbonyl formation in AAPH oxidized BSA

Protein oxidation was modified in bovine serum albumin (BSA) (20%) (Plasma Fractionation Center, The Thai Red Cross Society, Thailand) from 2-2' azo-bis-(2-methyl-propionamidine) HCl (AAPH) oxidation as in a previous protocol.[21] A mixture

of 200 µL of BSA (5 mg/mL), 400 µL of AAPH (200 mmol/L), and 100 µL of extract or GAE solutions (125-500 µg/mL) was incubated for 2 hours at room temperature. Protein carbonyl in the mixture was identified from a previous protocol.[22] A protein pellet in 400 µL of mixture was separated after precipitating with tricarboxylic acid (TCA) (10%), washed three times with ethanol-ethyl acetate (1:1, *v/v*) (1 mL) and centrifuged at 3,000 rpm for 3 min. The protein pellet was redissolved in 500 µL of guanidine hydrochloride (6 mol/L) and 500 µL of 2,4-Dinitrophenylhydrazine (DNPH) (10 mmol/L). After incubation for 10 min, absorbance was read by spectrophotometry at 370 nm (Drawell Scientific, Shanghai). The protein carbonyl was calculated by using a molar efficiency of $2.2x10^4$ cm^{-1} M^{-1}.

Figure 2. *High-voltage stimulation in the micro/nano-bubble water system. (Figure was modified with copyright permitted from a previous publication[9]).*

Lipid oxidation in erythrocytes from AAPH oxidation.

The last model of protective effect on lipid peroxidation of SF extracts was studied in healthy whole blood from AAPH oxidation.[23,24] Blood samples (10 mL each) were obtained by venipuncture from elderly healthy volunteers, who were aware of the study design and gave informed consent under the Ethic Human Committee at the Faculty of Associated Medical Sciences, Chiang Mai University, Thailand (AMSEC-62FB-001). Blood of 1.0 mL treated with AAPH in the presence or absence of the SF extracts at 62.5-500 µg/mL was incubated for up to 4 hours at 37°C. A negative control that ran together with an equivalent volume of isotonic buffer solution did not change the contents of thobarbituic acid-reactive substances (TBARs) significantly in red blood cells (RBCs) within 6 hours. After incubation for 4 hr and centrifugation at 3,000 rpm for 5 min, malondialdehyde (MDA) in plasma was detected with the reaction of TBARs.[25] A 250 µL of H_3PO_4 (0.4 mol/L) and 250 µL (0.6%) of thobarbituic acid (TBA) were added to 1 mL of reaction mixture before incubating at 95°C for 60 min. After stopping the reaction by cooling in an ice bath, the pink color of the supernatant obtained was read by spectrophotometry (Drawell Scientific, Shanghai) at 532 nm. Tetramethoxypropane was used as standard. The protective effect on MDA formation of extracts was confirmed by standard Vit C.

Statistical analysis

All data were represented with the mean and standard error of mean (SEM). Non-parametric Kruskal-Wallis and Mann-Whitney U tests were used for statistical analysis between standard antioxidants and different doses of extracts.

Results

The results of active compounds

The active compounds are represented in Table 1. Sour-type SF extract at 1 gm showed the higher total phenolics (1,625±2.3 µg of equivalent GAE) and total flavonoids (245±3.6 µg of equivalent quercetin) when compared to sweet-type SF extract (520±3.5 mg GAE & 187±2.5 µg). In addition, the results of Vit C content in both extracts were higher in sour-type (565±4.5 µg/g extract) than in sweet-type (513±2.6 µg/g extract), which confirmed the specific retention time of standard Vit C (Figure 3).

Table 1 Active compounds of star fruit extract (1 gm).

Active compounds	Sweet-type SF	Sour-type SF
Total phenolics (µg GAE)	520±3.5	1,625±2.3*
Total flavonoids (µg QE)	187±2.5	245±3.6*
Vit C (µg)	513±2.6	565±4.5*

Note: ** p<0.05 from Two-Independent-Samples Tests) (Mann-Whitney U test).*

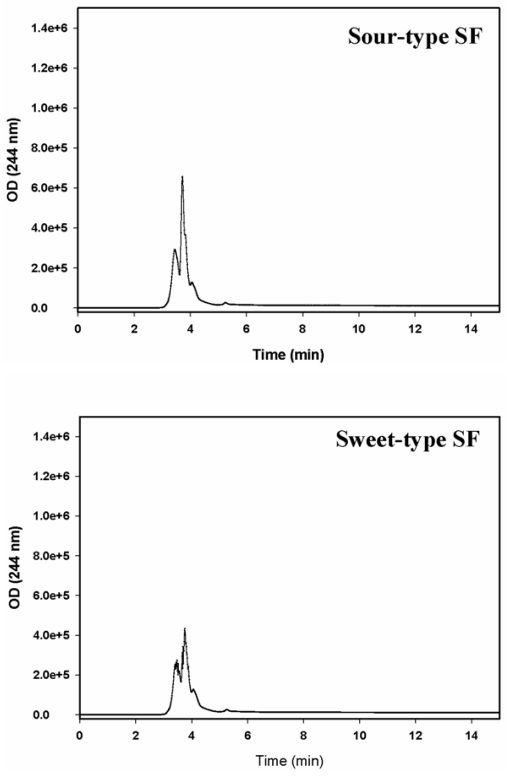

Figure 3. *HPLC peak of Vit C in both sour- and sweet-type SF extracts at 20 mg/mL and standard Vit C at 45 µg/mL.*

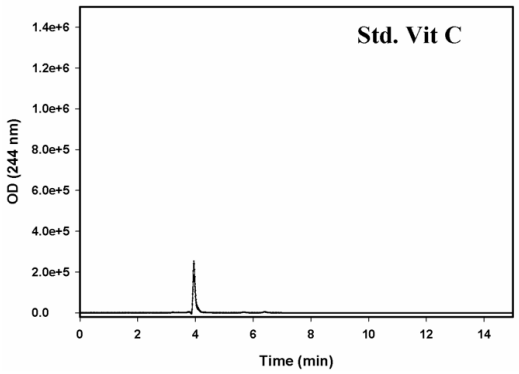

Figure 3. *HPLC peak of Vit C in both sour- and sweet-type SF extracts at 20 mg/mL and standard Vit C at 45 µg/mL.*

Radical scavenging activity

The results of three scavenging models on three radicals: DPPH cation, NO and $ABTS^{\bullet+}$ is presented in Figure 4. Sour-type SF showed higher activity with a lower concentration on scavenging DPPH (32.32±2.3 mg) and NO (23.10±1.1 mg), when compared to sweet-type SF (58.90±2.4 mg and non-detected) (Figure 4.A & C). However, sweet-type SF showed the higher activity on scavenging $ABTS^{\bullet+}$ (348.80±2.5 mg), when compared to sour-type SF (511.90±2.6 mg) (Fig. 4.B).

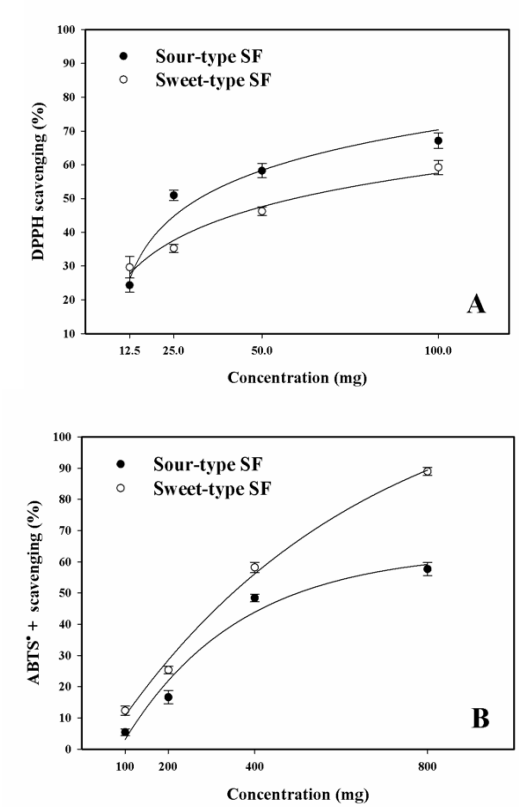

Figure 4. *Radical scavenging activity of sour- and sweet-type SF extracts. A: DPPH, B: ABTS, and C: NO.*

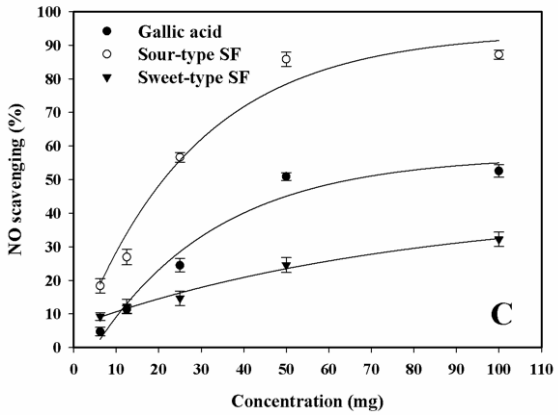

Figure 4. *Radical scavenging activity of sour- and sweet-type SF extracts. A: DPPH, B: ABTS, and C: NO.*

Protective activity of star fruit

The results of protective activity between sour- and sweet-type SF extracts were represented by three models: protective effects on GSH from high-voltage stimulation, protein carbonyl formation from AAPH-oxidized BSA, and protective activity of lipid peroxide formation in AAPH-oxidized whole blood.

In the system of oxidation, the GSH by HV was confirmed as in the previous study.[9] The GSH was oxidized and significantly reduced from 100±0.08 to 20.80±0.04 % after high-voltage stimulation for 5-15 min. Protective effect in the system was confirmed by standard Vit C (0.2 mg) with time-dependence (100±0.2, 94.5±0.16, 80.43±0.21, and 73.11±0.12%). Sweet-type SF extract showed protective effect on GSH oxidation (88.45±2.12, 84.19±2.10, and 77.29±1.5 %) with dose responses from 1.0-0.25 mg. Although, the sour-type SF extract showed protective effect on GSH oxidation from HV, high doses (1.0 and 0.5 mg/mL) showed pro-oxidative effects (79.81±1.28 and 82.92±0.38 %) when compared to lower concentrations (85.42±0.25%) (Figure 5A).

The results showed the protective effect of SF extract on BSA from AAPH oxidation. Protein carbonyl at 4.2±0.08 mmol/g protein was produced in the system after AAPH-oxidation, and significantly reduced to 2.06±0.04, 1.47±0.11, and 1.28 mmol/mg protein when GAE co-incubated with dose-response. The sweet-type SF extracts showed significant reduction of protein carbonyl to 2.41±0.08, 1.4±0.07 and 0.95±0.04 mmol/g protein, with a dose response of 125-500 µg when compared to non-treated AAPH oxidized BSA. Whereas, sour-type SF extract showed slightly inhibitory activity at 125 µg (3.89±0.21 mmol/g protein). However, it presented the pro-oxidative effect by significantly increasing the protein carbonyl content depending on the concentration being at 250 (5.06±0.10 mmol/g protein) and 500 µg (5.5±0.27 mmol/g protein) when compared to non-treated AAPH oxidized BSA (4.22±0.08 mmol/g protein) (Figure 5B).

The last protective model of SF extracts is presented in Figure 5C. The MDA formation in RBCs was increased after oxidation from AAPH (3.94±0.21 µmol/L) without any

treatment (first bar), when compared to that in those not oxidated (1.34±0.11 µmol/L) (data did not shown). The protective effect was confirmed by comparing with standard Vit C at 62.5-500 µg/mL (2.57±0.123 to 0.95 µmol/L). Sweet-type SF extract showed a protective effect on MDA formation with dose responses from 62.5 µg (2.95±0.23 mmol/L), 125 µg (2.81±0.12 mmol/L), 250 µg (2.72±0.15 mmol/L, and 200 µg (2.45 mmol/L). Data showed similarity to the sour-type SF extract at 62.5 µg (2.94±0.21 mmol/L), 125 µg (2.74±0.17 mmol/L) and 250 µg (2.75±0.15 mmol/L), but the pro-oxidative effect from high dose extract at 500 µg showed higher MDA formation (4.52±0.12 µmol/L), when compared to non-treated RBCs from AAPH oxidation and all of them treated with SF extracts (Figure 5C).

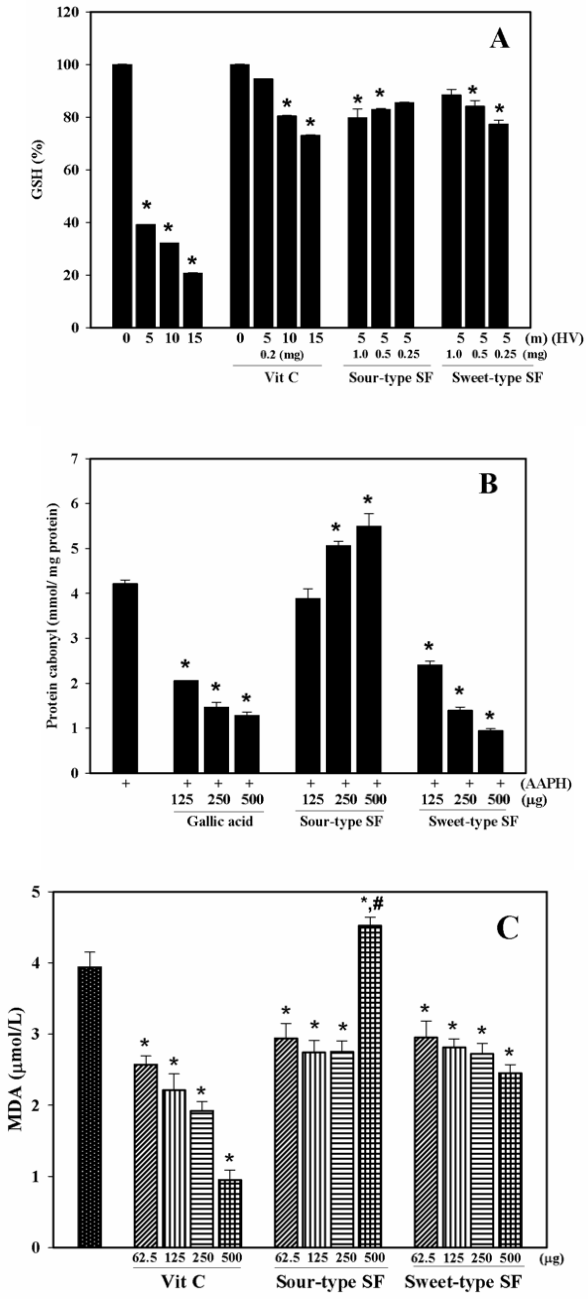

Figure 5. *Protective effects of SF extracts; sour- and sweet-types compared to standard Vit C or GAE, and control (first bar). GSH: glutathione, MDA: malondialdehyde, *,# p<0.05 from Kruskal-Wallis H test.*

Discussion

This study was an updated and a confirmed work of SF distributed in Thailand,[9,10] and it also supports a previous study on elderly people.[8,20] The results in this study represented active compounds such as phenolics and Vit C is the same as in the previous evidence from the data.[4,5,6,7] In particular, the sour-type in Chiang Mai province, Thailand, contained approximately 16-17 mg of L-ascorbic acid in 100 g of extract.[8] Whereas, the yield of L-ascorbic acid in sweet-type SF was lower at approximately 5-6 mg in 100 g of extract.[9] The results in this study also presented more L-ascorbic acid in the sour-type when compared to the sweet-type as well as total phenolics and total flavonoid contents.

Moreover, this study proved the activity of extract on scavenging radicals in different modes; DPPH, $ABTS^{\bullet+}$ and NO, which is all important in the basic knowledge of the antioxidant activity. These three models are based on the different activities of active compounds, be they hydrophilic or lipophilic compound in either type of SF extract. DPPH can be applied slowly to the antioxidant activity of various types of antioxidant compounds, and even with weak antioxidants[26] that are utilized in aqueous and non-polar organic solvents or both hydrophilic and lipophilic antioxidants.[27] Whereas, ABTS cation radicals represented TAC.[28,29] Furthermore, NO scavenging also was shown in elderly people, in which plasma NO was reduced after consumption of SF juice for 4 weeks.[20] NO scavenging of SF extract was evaluated following the previous protocol, which was generated from SNP in deionized water.[12] Thus, hydrolipic compound, such as L-ascorbic acid, was found in both types of SF extract as expected. In addition, the results on NO scavenging was confirmed with standard GAE, which is a versatile scavenger that rapidly deactivates a wide variety of reactive oxygen species (ROS) and reactive nitrogen species (RNS).[30] $ABTS^{\bullet+}$ is the last model in the scavenging assay, and its scavenging[5] is prepared in deionized water. The results in this study showed that sour-type SF had a lower dose of IC50 or higher scavenging activity of DPPH and NO when compared to sweet-type. However, the IC50 on $ABTS^{\bullet+}$ scavenging of sweet-type had lower and higher activity than in sour-type. Therefore, a higher content of L-ascorbic acid, total phenolics and total flavonoids in sweet-type may not reflect the results because a previous report claimed that total phenolic and flavonoid compounds directly affect antioxidant capacity.[31] Unfortunately, other non-phenol compounds in sweet-type SF have been preferred such as diglucosides, carambolasides and phenylpropanoids; (+)-isolariciresinol 9-*O*-β-D-glucoside, (+)-lyoniresinol 9-*O*-β-D-glucoside, (–)-lyoniresinol 9-*O*-β-D-glucoside and 1-*O*-feruloyl-β-D-glucose, three benzoic acids, protocatechuic acid, and 1-*O*-vanilloyl-β-D-glucose.[32] Therefore, some analytical results should be confirmed in the future. However, the results confirmed that both sweet- and sour-type of SF showed antioxidant compounds, which affect scavenging free radicals and are important in the physiological function of humans.

Moreover, results of the protective effect of SF extract on main antioxidant GSH were confirmed in an *in vitro* model. GSH with HV stimulation was studied previously in

the oxidation model.[9] Surprising results of sour-type SF in that study compared previous evidence of sweet-type having higher concentration and reduced protective activity in the protection of GSH. GSH was oxidized in the system with timely response from 5 to 15 min of stimulation, similar to a previous study.[9] When using standard L-ascorbic acid, the protective effect was presented in comparison to the non-treated system. The results showed that sour-type extract acted with pro-oxidant activity. Previous potentially relevant articles showed that Vit C was used to produce pro-oxidant by free radical formation; H_2O_2 generation.[33] Free radical formation in the micro/nano-bubble water system was recognized as the plasma-nano bubble technique,[17] in which gas bubbles were produced into any liquid.[34] After the electrical current is released in micro/nano water bubbles in a short time, many reactive species such as radicals, hydroxyl radicals, OH°; superoxide radical (O_2-), H_2O_2, etc. are generated,[35,36] which could be rechecked by optical emission spectroscopy (OES).[17] Therefore, those free radicals could be oxidized by GSH in this study.[19] The results of provoked activity on GSH oxidation in sour-type SF may be the high content of Vit C when compared to the sweet-type.

The results of SF sweet-type extract also showed the protective effect on protein and lipid peroxidation with the dose response. In contrast, the sour-type extract showed pro-oxidative effect on protein and lipid oxidation. It is possibly the higher concentration of Vit C that is referred to in previous evidence.[37] Similarly, previous evidence showed that storage of erythrocyte with Vit C increased protein sulhydryls (P-SH) levels and decreased superoxide dismutase (SOD), referring to the modulator of oxidative stress condition.[38] Moreover, a higher flavonoid in sour-type SF possibly may involve the pro-oxidant behavior in this study. Previous evidence reported that flavonoids contain multiple hydroxyl substitutions and important peroxyl radical activity.[39] Thus, the results in this study showed the pro-oxidation activity of SF sour-type and antioxidant activity of sweet-type in *in vitro* models. Thus, the results in this study supported previous studies in which participants who had chronic obstructive pulmonary disease (COPD)[10] stabilized with antioxidant activity in sweet-type SF. However, the benefits of sour-type SF must be considered and need to be studied further.

Conclusion

Sour-type SF showed higher active antioxidant compounds such as total phenolics, total flavonoids and Vit C as well as radical scavenging activity of DPPH and NO than sweet-type. However, its high concentration aggravated GSH, protein and lipid oxidation. On the other hand, sweet-type SF showed higher activity on scavenging ABTs radicals and beneficial protective effects in in vitro models.

Acknowledgements

This study was supported by a grant from the Royal Golden Jubilee PhD (RJPHD), Thailand Research Fund (TRF), Thailand (contract number- PHD/0117/2561). Furthermore, grateful thanks go to the High Voltage Engineering Laboratory, Department of Electrical Engineering, Faculty of Engineering, Rajamangala University of Technology Lanna, Chiang Mai, Thailand, for providing this study with research equipment.

Conflicting interests

The authors report no conflicts of interests in this study.

References

[1] Lim Y, Lim TT, Tee JJ. Antioxidant properties of several tropical fruits: A comparative study. Food Chem. 2007; 103(3): 1003-8.

[2] Manda H, Vyas K, Pandya A, Singhal G. A complete review on: Averrhoa carambola. World J Pharm Pharmaceu Sci. 2012; 1(1): 17-33.

[3] O'Hare TJ. Postharvest physiology and storage of carambola (star fruit): a review. Postharvest Biol Technol. 1993; 2(4): 257-67.

[4] Thomas S, Patil DA, Patil AG, Chandra N. Pharmacognostic evaluation and physiochemical analysis of Averrhoa carambola L. fruit. J Herb Med Toxicol. 2008; 2: 51-4.

[5] Yang D, Xie H, Jia X, Wei X. Flavonoid C-glycosides from star fruit and their antioxidant activity. J Funct Foods. 2015; 16: 204-10.

[6] Shui G, Leong LP. Analysis of polyphenolic antioxidants in star fruit using liquid chromatography and mass spectrometry. J Chromatogr A. 2004; 1022(1-2): 67-75.

[7] Dasgupta P, Chakraborty P, Bala NN. Averrhoa Carambola: An Updated Review. Inter J Phar Resear Rev. 2013; 2(7): 54-63.

[8] Leelarungrayub J, Yankai A, Pinkaew D, Puntumetakul R, Laskin JJ, Bloomer RJ. A preliminary study on the effects of star fruit consumption on antioxidant and lipid status in elderly Thai individuals. Clin Interv Aging. 2016; 11: 1183-92.

[9] Pothasak Y, Singhatong S, Natakankitkul S, Dechusupa N, Wanachantararak P, Dechthummarong C, et al. Active compounds, free radical scavenging and tumor-necrosis factor (TNF-α) inhibitory activities of star fruit-sweet type (Averrhoa carambola L.) in vitro. JAMS. 2020; 53(1): 19-23.

[10] Pothasak Y, Leelarungrayub J, Natakankitkul S, Singhatong S. Prototype Star Fruit-Honey Product and Effectiveness on Antioxidants, Inflammation and Walking Distance in Participants with Stable Chronic Obstructive Pulmonary Disease (COPD). Pharmacogn J. 2020; 12(5): 1121-34.

[11] Singleton VL, Rossi JA Jr. Colorimetry of total phenolics with phosphomolybdic-Phosphotungstic acid reagents. Am J Enol Vitic. 1965; 16: 144-58.

[12] Sembiring EN, Elya B, Sauriasari R. Phytochemical screening, total flavonoid and total phenolic content and antioxidant activity of different parts of Caesalpinia bonduc (L.) Roxb. Pharmacogn J. 2018; 10(1): 123-7.

[13] Chen P, Atkinson R, Wolf WR. Single-laboratory validation of a high-performance liquid chromatographic-diode array detector-fluorescence detector/mass spectrometric method for simultaneous determination of water-solution vitamins in multivitamin dietary tables. J AOAC Int. 2009; 92(2): 680-7.

[14] Thitilertdecha N, Teerawutgulraq A, Kilburn JD, Rakariyatham N. Identification of major phenolic compounds from Nephelium lappaceum L. and their antioxidant activities. Molecules. 2010; 15(3): 1453-65.

[15] Miller NJ, Rice-Evans C, Davies MJ, Gopinathan V, Milner A. A novel method for measuring antioxidant capacity and its application to monitoring the antioxidant status in premature neonates. Clin Sci. 1993; 84(4): 407-12.

[16] Chakraborthy GS. Free radical scavenging activity of Costus speciosus leaves. Indian J Pharm Educ Res. 2009; 43: 96-8.

[17] Dechthummarong C. Characterizations of electrical discharge plasma in air micro/nano-bubbles water mixture. Inter J Plasm Environ Sci Technol. 2019; 12: 64-8.

[18] Wenjuan B, Xuehong S, Junwen S, Xiangli Y. Nitrogen fixation into water by pulsed high-voltage discharge. IEEE Trans on Plasma Sci. 2009; 37(1): 211-8.

[19] Lushchak VI. Glutathione homeostasis and functions: potential targets for medical interventions. J Amino Acids [Internet]. 2012 Feb [cited 2022 Jan 19];2012: Article ID 736837. Available from: https://www.hindawi.com/journals/jaa/2012/736837/ doi: 10.1155/2012/736837

[20] Leelarungrayub J, Laskin JJ, Bloomer RJ, Pinkaew D. Consumption of star fruit juice on pro-inflammatory markers and walking distance in the community dwelling elderly. Arch Gerontol Geriatr. 2016; 64: 6-12.

[21] Mayo JC, Tan DX, Sainz RM, Natarajan M, Lopez-Burillo S, Reiter RJ. Protection against oxidative protein damage induced by metal-catalyzed reaction or alkylperoxyl radicals: comparative effects of melatonin and other antioxidants. Biochim et Biophys Acta. 2003; 1620(1): 139-50.

[22] Reznick AZ, Packer L, Oxidative damage to proteins: spectrophotometric method for carbonyl assay. Methods Enzymol. 1994; 233: 357-63.

[23] Leelarungrayub N, Chanarat N, Rattanapanone V. Potential Activity of Thai Shallot (Allium ascalonicum L.) Extract on the Prevention of Hemolysis and Glutathione Depletion in Human Erythrocyte from Oxidative Stress. CMU Journal. 2004; 3(3): 225-34.

[24] Yang HL, Korivi M, Lin MK, Chang HCW, Wu CR, Lee MS, et al. Antihemolytic and antioxidant properties of pearl powder against-2,2'-azobis(2-amidinopropane) dihydrochloride-induced hemolysis and oxidative damage to erythrocyte membrane lipids and proteins. J Food Drug Anal. 2017; 25(4): 898-907.

[25] Chirico S. HPLC determination of malondialdehyde (MDA) in plasma samples. Methods Enzymol. 1994; 233: 314-8.

[26] Prakash A. Antioxidant activity. Med Lab Anal Prog. 2001; 19(2): 1-6.

[27] Prior RL, Wu X, Schaich K. Standardized methods for the determination of antioxidant capacity and phenolics in foods and dietary supplements. J Agric Food Chem. 2005;53(10): 4290-302.

[28] Re R, Pellegrini N, Proteggente A, Pannala A, Yang M, Rice-Evans C. Antioxidant activity applying an improved ABTS radical cation decolorization assay. Free Radic Bio Med. 1999; 26(9-12): 1231-7.

[29] Dong JW, Cai L, Xing Y, Yu J, Ding ZT. Re-evaluation of ABTS˚+ assay for total antioxidant capacity of natural products. Nat Prod Commun. 2015; 10(12): 2169-72.

[30] Marino T, Galano A, Russo N. Radical scavenging ability of gallic acid toward OH and OOH radicals, reaction mechanism and rate constants from the density functional theory. J Phys Chem. 2014; 118(35): 10380-9.

[31] Mustafa RA, Hamid AA, Mohamed S, Bakar FA. Total phenolic compounds, flavonoids, and radical scavenging activity of 21 selected tropical plants. J Food Sci. 2010; 75(1): C28-35.

[32] Jia X, Yang D, Xie H, Jiang Y, Wei X. Non-flavonoid phenlics from Averrhoa carambola fresh fruit. J Func Food. 2017; 32: 419-25.

[33] Putchala MC, Ramani P, Sherlin HJ, Premkumar P, Natesan A. Ascorbic acid and its pro-oxidant activity as a therapy for tumor of oral cavity – a systematic review. Arch Oral Biol. 2013; 58(6): 563-74.

[34] Saeki R, Yasuoka K. Generation of hydrogen peroxide in gas bubbles using pulsed plasm for advanced oxidation processes. IEEE Trans on Plasma Sci. 2015; 43(10): 3440-4.

[35] Locke BR, Thagard SM. Analysis and review of chemical reactions and transport processes in pulsed electrical discharge plasma formed directly in liquid water. Plasma Chem Plasma Process. 2012; 32: 875-917.

[36] Locke BR, Shih KY. Review of the methods to form hydrogen peroxide in electrical discharge plasma with liquid water. Plasma Sources Sci Technol. 2011; 20: 034006.

[37] Pavlovic V, Cekic S, Rankovic G, Stoiljkovic N. Antioxidant and pro-oxidant effect of ascorbic acid. Acta Medica Medianae. 2005; 44(1): 65-8.

[38] Soumya R, Vani R. Vitamin C as a modulator of oxidative stress in erythrocytes of stored blood. Acta Haematol Polon. 2017; 48(4): 350-6.

[39] Cao G, Sofic E, Prior RL. Antioxidant and prooxidant behavior of flavonoids: structure-activity relationships. Free Radic Biol Med. 1997; 22(5): 749-60.

Journal of Associated Medical Sciences 2022; 55 (3): 44-50

JAMS
Journal of Associated Medical Sciences

Thai-Journal Citation Index Centre (TCI) & ASEAN Citation Index (ACI)

Journal of Associated Medical Sciences

Journal homepage: https://www.tci-thaijo.org/index.php/bulletinAMS/index

Species characterization and antifungal susceptibility profile of yeast isolates from blood cultures of fungemic patients in Thammasat University Hospital, Thailand

Pradchama Khumdee[1] Panarat Hematulin[2] Jiraporn Yansombat[1] Narissara Mungkornkaew[2]
S. M. Lutful Kabir[3] Worada Samosornsuk[4] Seksun Samosornsuk[4*]

[1]Graduate Program in Medical Technology, Faculty of Allied Health Sciences, Thammasat University, Pathumthani Province, Thailand
[2]Microbiology Laboratory Unit, Thammasat University Hospital, Pathumthani Province, Thailand
[3]Department of Microbiology and Hygiene, Bangladesh Agricultural University, Mymensingh 2202, Bangladesh
[4]Department of Medical Technology, Faculty of Allied Health Sciences, Thammasat University, Pathumthani Province, Thailand

ARTICLE INFO

Article history:
Received 20 April 2022
Accepted as revised 23 June 2022
Available online 18 July 2022

Keywords:
Yeast, MALDI-TOF MS, Sensititre YeastOne

ABSTRACT

Background: *Candida albicans* is the most isolated fungal agent in a worldwide health system. Species distribution of *Candida* infection is different according to geographical regions. However, a shift in favor of non-albicans *Candid*a species with antifungals resistance have increased as an important cause of candidemia.

Objectives: This study aimed to identify the species of yeasts isolated from the blood samples of patients at the university hospital and to determine in vitro susceptibilities of three most common isolates against nine antifungal agents.

Materials and methods:In total, 130 yeast isolates from 130 patients were defined the species using matrix-assisted laser desorption/ionization-time of flight mass spectrometry (MALDI-TOF MS). Antifungal susceptibility testing was carried out using broth dilution Sensititre YeastOne panels included amphotericin B, 5-fucytosine, fluconazole, itraconazole, voriconazole, posaconazole, anidulafungin, micafungin, and caspofungin.

Results: The most common species in all age groups was *C. tropicalis* (n=48, 36.9%), followed by *C. albicans* (n=38, 29.2%). *C. glabrata* (n=23, 17.7%) was more common among elderly patients, while *C. parapsilosis* (n=9, 6.9%) was more frequently isolated from younger patients. Antifungal susceptibility testing in *Candida* species expressed MIC in the low level of almost antifungal drug except for reduced fluconazole susceptibility against *C. glabrata and C. tropicalis* isolates.

Conclusion: *C. tropicalis* is the most common infection in candidemic patients. Fluconazole resistance strains were found in *C. glabrata* and *C. tropicalis*, respectively. In addition, voriconazole resistance strains were found in *C. tropicalis*.

Introduction

Bloodstream yeast infection (BYI) especially the genus *Candida* has increased worldwide in healthcare system because of the rising number of immunosuppressed patients leading to high disencouragement and fatality in the range of 40% to 60%.[1] From the ARTEMIS DISK Surveillance Program between 1997 and 2007, *Candida albicans* is the major species reported just before *C. glabrata*, *C. tropicalis*, *C. parapsilosis* and *C. krusei* (*Pichia kudriavzevi*i), respectively.[2] Species spreading of Candida infection is different according to geographical regions. However, a change of species distribution to non-albicans Candida (NAC) may be increasingly resistant to common antimicrobial agents.[3] Recently, 52 candidemic patients in a University Hospital Thailand have been identified as NAC (64%) and *Candida albicans* (36%). From 35 % of *C. tropicalis* isolates, 68.7% were high-level fluconazole

* **Corresponding author.**
Author's Address: *Department of Medical Technology, Faculty of Allied Health Sciences, Thammasat University, Pathumthani Province, Thailand*
** **E-mail address:** seksun@hotmail.com
doi: 10.12982/JAMS.2022.023
E-ISSN: 2539-6056

resistance.[4] Therefore, rapid and curate species identification have become important, especially in cases involving invasive infection.

The situation of non-*albicans Candida* was increasingly resistant to commonly used antimicrobial agents especially in azole agents.[5-6] Recently, fluconazole resistance in *C. glabrata* strains has been reported in Asia-Pacific region including Thailand.[7-8] Increasing resistance rates of fluconazole, voriconazole, micafungin, caspofungin and anidulafungin in non-albicans candidemia isolates especially *C. tropicalis* and *C. glabrata* isolates were reported in 5 tertiary hospitals of Taiwan.[9] In Thailand, *C. glabrata* and *C. tropicalis* isolates were increasingly resistant to azole agents and *C. glabrata* isolates were decreasingly susceptible to echinocandins especially caspofungin.[8, 10]

These research objectives were to identify yeasts in the species level and investigate their antifungal susceptibility patterns. All strains were isolated from blood samples of suspected yeast septicemic patients in 3.25 years period at a Thai University Hospital. In vitro antifungal susceptibility testing of three most common yeasts isolated from blood was conducted using nine antifungal agents in the SYO panel included amphotericin B, 5-fucytosine, fluconazole, itraconazole, voriconazole, posaconazole, anidulafungin, micafungin, and caspofungin.

Materials and methods

Sample collection

A total of 130 yeast isolates obtained from blood culture from January 2013 to March 2016 (3.25 years) in Microbiology Laboratory, Thammasat University Hospital located at the central region of Thailand were tested for identification and antifungal susceptibility test. The isolates were collected in sequential order without selection criteria. Duplicate isolates from the same patient were excluded. Reference strains of *Candida parapsilosis* ATCC 22019 and *C. krusei* ATCC 6258 were used as quality control. The study was approved by the Ethics Sub-Committee Board for Human Research Involving, Thammasat University, No.3, Thailand, Protocol code 132/2562.

Yeast identification using Matrix-assisted laser desorption/ ionization-time of flight mass spectrometry (MALDI-TOF MS)

Yeast isolates were subcultured on Sabouraud dextrose agar (SDA) at 37°C for 24 to 48 hours and fresh growth was extracted using formic acid extraction method described, briefly, fresh cells were suspended in a 1.5 mL sterile tube and mix thoroughly in 300 µL of sterile distilled water. Then, Yeast suspension was added with 900 µL of absolute ethanol and centrifuged at 13,000 rpm for 2 min and discarded the supernatant. The air-dried pellet at room temperature was resuspended in 50 µL of 70% formic acid and mix thoroughly before the addition of 50 µL of acetonitrile. After 2-min centrifugation at 13,000 rpm, 1 µL of the supernatant was placed onto a single spot of the polished steel target plate and air-dried prior to MALDI-TOF analysis.[10] Each spot was covered by 1 µL of α–cyano-4-hydroxycinnamic acid (HCCA) in 50% acetonitrile and 2.5% trifluoroacetric acid (TFA) (Sigma-Aldrich, France) matrix. Identification was performed on an Autoflex III MALDI-TOF/TOF mass spectrometer (Bruker Daltonics, Bremen, Germany). Instrument calibration using the Bruker Bacterial Standard Escherichia coli (#8255343) was performed with Flex control program. Ionized spectra for each spot were acquired on linear mode at a laser frequency of 20 Hz within a mass range from 2000 to 20000 Da. MBT Compass software was automatically smoothing, normalization, baseline subtraction and peak selection of different mass spectra. Mass spectra of each sample were selected to create sample profiles that were compared with those of MBT 8468 MSP Library using pattern-matching algorithms. Identification was provided with accompanying scores as per the manufacturer's schemes: a score <1.7 indicated no reliable identity; a score between 1.7 and 1.9 indicated identity at genus level; a score ≥2.0 indicated identity at species level.

Antifungal Susceptibility testing with Sensititer YeastOne

Susceptibility testing, reading, and interpretations of the results using Sensititer YeastOne (SYO) was followed according to the manufacturer's instructions (Thermo Fisher Scientific, Cleveland, OH, USA). All yeast isolates were subcultured on SDA at 35°C for 24 hr to 48 hr to confirm their purity and viability. After that, standard 0.5 McFarland yeast suspensions were adjusted in sterile distilled water with Sensititre nephelometer, and the reference method was performed simultaneously. The plates contained serial two fold dilutions of amphotericin B (0.12 to 8 mg/L), 5-flucytosine (0.06 to 64 mg/L), fluconazole (0.12 to 256 mg/L), itraconazole (0.015 to 16 mg/L), voriconazole (0.008 to 8 mg/L), posaconazole (0.008 to 8 mg/L), anidulafungin (0.015 to 8mg/L), micafungin (0.008 to 8mg/L), and caspofungin (0.008 to 8mg/L) and MICs endpoints were read after 24 hr of incubation (72 hr for *C. neoformans*) by the color changed from blue indicating no growth to magenta indicating growth.[8]

MIC results interpretation

Interpretation of susceptibility was performed by applying the clinical break points (CBPs) defined by the European Committee on Antimicrobial Susceptibility Testing (EUCAST) and Clinical & Laboratory Standards Institute (CLSI).[11-13] In the results that CBPs absence of EUCAST and CLSI , isolates were defined as having a wild-type or a non-wild-type drug susceptibility phenotype including amphotericin, 5-fucytosine, itraconazole, posaconazole and voriconazole (only *C. glabrata*) according to the epidemiological cutoff values (ECV) determined by SYO,[14-15] as shown in Table 3.

Statistical analysis

Analytical data between age group and yeast species were explained as a mean with standard deviation and a 95% confidence interval. The level of significance was set at 0.05. The data were analyzed using the Kruskal-Wallis test to avoid random significance when comparing several groups. The statistical tests were conducted with the aid of SPSS Statistical software version 27.

Results

Species identification

Overall, 130 isolates were collected from blood samples of 130 patients (75 males and 55 females) from January 2013 to March 2016 (3.25 years). The mean and median ages were 57 and 63 years, respectively, with an age range of 1-92 years.

The yeast species suspected fungemia was as follows. *C. tropicalis*, 48 (36.9%); *C. albicans*, 38 (29.2%); *C. glabrata*, 23 (17.7%); *C. parapsilosis*, 9 (6.9%); other NAC [*C. krusei* (*Pichia kudriavzevii*), *C. rugose* (*Diutina rugosa*), *C. intermedia*, *C. haemulonii* and *C. nivariensis*, 5 (3.8%); *Cryptococcus neoformans*, 5 (3.8%); and others (*Loderomyces elongisporus* and *Trichospron asahii*), 2 (1.5%) (Table 1).

Table 1 Yeast species classification among 130 patients with positive blood cultures.

Yeast species	Patients or Isolates N (%)	Gender		Age Mean±SD
		Males (N)	Female (N)	
Candida albicans	38 (29.2)	21	17	58±25
Non-albicans Candida (NAC)				
Candida tropicalis	48 (36.9)	27	21	58±25
Candida glabrata	23 (17.7)	16	7	64±23
Candida parapsilosis	9 (6.9)	4	5	42±32
Candida krusei (Pichia kudriavzevii)	1 (0.8)	1	0	73
Candida rugosa (Diutina rugosa)	1 (0.8)	0	1	49
Candida intermedia	1 (0.8)	1	0	70
Candida haemulonii	1 (0.8)	0	1	92
Candida nivaniensis	1 (0.8)	0	1	31
Other yeasts species				
Cryptococcus neoformans	5 (3.8)	3	2	41±22
Lodderomyces elongisporus	1 (0.8)	1	0	40
Trichosporon asahii	1 (0.8)	1	0	14
Total	**130 (100)**	**75**	**55**	**57±25**

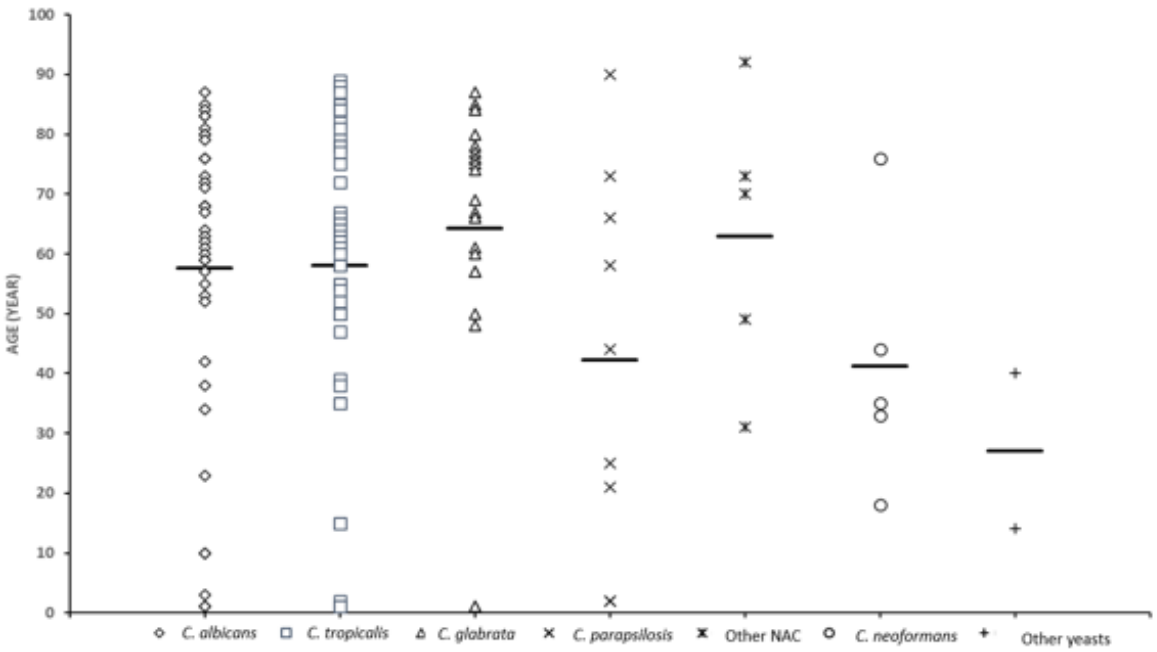

Figure 1. *Yeast species and an average patient's age (year) during the infection.*

From figure 1, *C. albicans*, *C. tropicalis*, *C. glabrata* and other NAC were more common among elderly patients (mean age >50 years), while *C. parapsilosis*, *C. neoformans* and other yeasts were more frequently isolated from younger patients (mean age<50 years). Notwithstanding, no statistically significant difference was found between yeast species and age groups.

The blood cultures were collected from patients who were admitted in different wards. Altogether, there were 43 patients (33.1%) at ICUs, 50 patients (38.5%) at medicine wards, 13 patients (10%) at surgical wards, 6 patients (4.6%) at pediatric wards, and 18 patients (13.8%) at other wards. Table 2 shows the yeast species distribution in relation to the hospitalized unit of the patient. Fungemia caused by yeasts were found in patients mostly admitted to medicine units (38.5%) and ICU (33.1%). However, yeast septicemia was uncommonly found in the pediatric units.

Table 2 Number of yeast species identified from patients in hospital wards.

Yeast species	Hospital Wards					
	ICU	Medicine	Surgery	Pediatric	Other	Total
C. albicans	*15*	*8*	7	1	6	38
C. tropicalis	*15*	*24*	1	1	7	48
C. glabrata	*8*	*8*	3	2	2	23
C. parapsilosis	*3*	*3*	1	1	1	9
Other NAC	*1*	*3*	1	0	0	5
C. neoformans	*0*	*2*	0	0	3	5
Other yeasts	*1*	*0*	0	1	0	2
Total N (%)	43 (33.1%)	50 (38.5%)	13 (10%)	6 (4.6%)	18 (13.8%)	130 (100%)

Antifungal susceptibility patterns

MICs were used to evaluate the efficacy of nine antifungal agents among *C. albicans, C. tropicalis and C. glabrata* from the blood samples summarized in Table 3. Following the EUCAST and CLSI clinical breakpoints (CBPs), we found that all *C. albicans* isolates were susceptible to fluconazole and voriconazole. Overall, 21(91.3%) of all *C. glabrata* isolates showed reduced susceptibility to fluconazole (MIC_{90}=32 µg/mL). Interestingly, 32 (66.7%) and 10 (20.8%) of *C. tropicalis* isolates showed susceptible and intermediate/SDD to fluconazole, whereas MIC_{90} indicated resistant level (MIC_{90}=16 µg/mL). The MIC values for posaconazole were overall low in *C. albicans*, but rather high in *C. tropicalis* when applying the EUCAST CBPs. The MIC values foranidulafungin, micafungin and caspofungin were overall low in all isolates when the CLSI CBPs were applied. However, 21 (55.3%) of *C. albicans* isolates were susceptible to andulafungin when applying EUCAST CBPs. Applying the epidemiological cutoff values (ECVs), all the isolates had wild type phenotype drug susceptibility to amphotericin, 5-flucytosine, micafungin and caspofungin. For triazole agents, all *C. albicans* isolates had wild type phenotype drug susceptibility to itraconazole and posaconazole, whereas 2 (4.2%) *C. tropicalis* isolates exhibited non-wild type phenotypes to itraconazole and only one isolate (4.4%) of *C. glabrata* exhibited non-wild type phenotypes to itraconazole, voriconazole and posaconazole.

Table 3 Antifungal susceptibility testing against Candida spp. isolated from blood samples.

					Susceptible isolates N (%)		ECV	Isolates N (%)	
		Range	MIC50	MIC90	EUCAST	CLSI	SYO	Wild type	Non-wild type
C. albicans (n=38)	Amphotericin B	0.12-0.5	0.5	0.5	38 (100)	ND	2	38 (100)	0 (0)
	5-Flucytosine	0.06-0.25	0.12	0.25	ND	ND	0.5	38 (100)	0 (0)
	Fluconazole	0.25-1	0.5	1	38 (100)	38 (100)			
	Itraconazole	0.015-0.12	0.12	0.12	16 (42.1)	ND	0.12	38 (100)	0 (0)
	Voriconazole	0.008-0.03	0.008	0.015	38 (100)	38 (100)			
	Posaconazole	0.008-0.06	0.03	0.06	38 (100	ND	0.06	38 (100)	0 (0)
	Anidulafungin	0.015-0.12	0.03	0.12	21 (55.3)	38 (100)			
	Micafungin	0.008-0.015	0.008	0.015	38 (100)	38 (100)			
	Caspofungin	0.015-0.25	0.03	0.06	ND	38 (100)	0.25	38 (100)	0 (0)

MIC50: minimal inhibitory concentration value at which ≥50% of the isolates in a test, MIC_{90}: maximum inhibitory concentration of an antibiotic, at which 90% of the isolates, ECV: epidemiological cutoff value, ND: not determined, S: susceptible, I: intermediate, SDD: susceptible dose-dependent.

Table 3 Antifungal susceptibility testing against Candida spp. isolated from blood samples. (continues)

					Susceptible isolates N (%)		ECV	Isolates N (%)	
		Range	MIC50	MIC90	EUCAST	CLSI	SYO	Wild type	Non-wild type
C. tropicalis (n=48)	Amphotericin B	0.12-1	0.5	1	48 (100)	ND	2	48 (100)	0 (0)
	5-Flucytosine	0.06-0.12	0.06	0.12	ND	ND	0.5	48 (100)	0 (0)
	Fluconazole	1-256	2	16	32 (66.7, S)	32 (66.7, S)			
					10 (20.8, I)	10 (20.8, SDD)			
	Itraconazole	0.12-1	0.25	0.5	7 (14.6)	ND	0.5	46 (95.8)	2 (4.2)
	Voriconazole	0.12-8	0.25	1	7 (14.6, S)	7 (14.6, S)			
					35 (72.9, I)	35 (72.9, I)			
	Posaconazole	0.12-1	0.25	0.5	0 (0)	ND	1	48 (100)	0 (0)
	Anidulafungin	0.015-0.25	0.12	0.25	18 (37.5)	48 (100)			
	Micafungin	0.015-0.06	0.03	0.03	ND	48 (100)	0.12	48 (100)	0 (0)
	Caspofungin	0.03-0.12	0.03	0.06	ND	48 (100)	0.25	48 (100)	0 (0)
C. glabrata (n=23)	Amphotericin B	0.25-1	0.5	1	23 (100)	ND	2	23 (100)	0 (0)
	5-Flucytosine	0.006-0.12	0.06	0.06	ND	ND	0.25	23 (100)	0 (0)
	Fluconazole	16-256	32	32	21 (91.3, I)	21 (91.3, SDD)			
	Itraconazole	0.12-16	1	2	ND	ND	2	22 (95.6)	1 (4.4)
	Voriconazole	0.06-8	1	2	ND	ND	2	22 (95.6)	1 (4.4)
	Posaconazole	0.12-8	2	2	ND	ND	4	22 (95.6)	1 (4.4)
	Anidulafungin	0.015-0.06	0.015	0.03	23 (100)	23 (100)			
	Micafungin	0.008-0.015	0.015	0.015	23 (100)	23 (100)			
	Caspofungin	0.03-0.12	0.06	0.12	ND	23 (100)	0.25	23 (100)	0 (0)

MIC50: minimal inhibitory concentration value at which ≥50% of the isolates in a test, MIC_{90}: maximum inhibitory concentration of an antibiotic, at which 90% of the isolates, ECV: epidemiological cutoff value, ND: not determined, S: susceptible, I: intermediate, SDD: susceptible dose-dependent.

Discussion

Hitherto, we reported that over 90%of yeast septicemic cases in the Thammasat University Hospital occurred from three *Candida* species including *C. tropicalis*, *C. albicans* and *C. glabrata*, respectively. This similar result from blood culture was conducted in the same geophysical area of Thailand during 2016 to 2017.[16] Likewise, the previous study in Pakistan and India found *C. tropicalis* was the most isolated candida in blood culture.[17] On the contrary, *C. albicans* isolates (46%) were reported as the most common cause of invasive fungal infection in a study in Srinagarind University Hospital, the Northeast Thailand between 2006 and 2011 and other countries in Asia-Pacific region including Australia, Japan, Korea, Hong Kong (China), Taiwan, Malaysia, Saudi Arabia and Singapore.[17-18] A predominance of *C. tropicalis* may cause from its pathogenic mechanism reported as a very strong biofilm producer,[19-20] the owner of various virulence factors such as hemolysin, proteinase activity and the ability to survive to high salt concentration.[19, 21] Besides, geographic variance especially in tropical countries including Thailand.[16-17, 22] Although no statistically significant difference between species of *Candida* and age group was seen, *C. glabrata* seem to be the most frequent detection among aged patients (mean age = 64±23 years) and *C. parapsilosis* seem to be more frequently isolated from younger patients (mean age = 42+32 years). Simultaneously, *C. glabrata* and *C. parapsilosis* were described in previous as common isolates in relation to different age groups studies.[23] The colonization of NAC including *C. glabrata* in the oral cavities of aged patients[24] lower urinary tract[23] or gastrointestinal tract[25] may support the opinion that NAC is more common midst aged patients. *C. tropicalis* and *C. albicans* were found in all age groups with the same mean age (58+25 years). Our study found that candidemia from *C. tropicalis* mostly occurred in medicine ward that was related to reported risk factors including the insertion of inherent urinary catheters, period of stay in hospitalized unit, diabetes mellitus, lengthened antibiotic therapy, immunosuppressive treatment, surgeries, and aging.[26]

In current work, we reported MIC values using the EUCAST and CLSI CBPs because no standard CBPs were determined by commercial antifungal susceptibility testing including the SYO method.[11] Reduced fluconazole susceptibility was perceived in *C. glabrata* and *C. tropicalis* isolates, 91.3% and 20.8%, respectively. This indicated that the use of fluconazole for treatment should be avoided in candidemic patients from non-albicans *Candida*. Our study found that *C. glabrata* is the second most common NAC in blood cultures. Fluconazole resistance in *C. glabrata* was reviewed in previous study.[27] Prolonged fluconazole exposure of this strain brought to develop its resistance[28] by upregulating *CgCDr1* and *CgCDR2* efflux pump expression significantly.[29] *ErG11* and *UPC2* overexpression level were related to the reduction of fluconazole susceptibility in *C. tropicalis* fungemia.[30] When applying the EUCAST CBPs, 21 (55.3%) of the *C. albicans* isolates and 18 (37.5%) of the *C. tropicalis* isolates were

categorized as intermediate anidulafungin susceptibility. However, according to the CLSI CBPs, these isolates were reported as anidulafungin susceptibility result. Anidulafungin intermediate susceptible result of *Candida* strains should be confirmed *FKS* mutation by *FKS* genes sequencing.[31] Resistance to all echinocandins including caspofungin anidulafungin or micafungin of *Candida* isolates possessed distinctive *FKS* hot spot mutations.[31]

Conclusion

In summary, *C. tropicalis* was the major species identified from the blood samples of patients with candidemia. Reduced susceptibility to antifungal drugs was not seen in *Candida albicans* isolated from blood, while triazole resistance was perceived in NAC including *C. glabrata and C. tropicalis.*

Conflicting interests

Authors declare that there are no commercial, personal, political any other potentially conflicting interests related to the submitted manuscript.

Funding Statement

We would like to thank National Research Council of Thailand (NRCT), 2019 and Thammasat University Hospital, 2018 for research fund.

References

[1]. Schroeder M, Weber T, Denker T, Winterland S, Wichmann D, Rohde H, et al. Epidemiology, clinical characteristics, and outcome of candidemia in critically ill patients in Germany: a single-center retrospective 10-year analysis. Ann Intensive Care. 2020; 10: 142.

[2]. Pfaller MA, Diekema DJ, Gibbs DL, Newell VA, Ellis D, Tullio V, et al. Results from the ARTEMIS DISK Global Antifungal Surveillance Study, 1997 to 2007: a 10.5-year analysis of susceptibilities of Candida species to fluconazole and voriconazole as determined by CLSI standardized disk diffusion. J Clin Microbiol. 2010; 48(4): 1366-77.

[3]. Perlin DS, Shor E, Zhao Y. Update on antifungal drug resistance. Curr Clin Micro Rpt. 2015; 2: 84-95.

[4]. Naranong C, Anunnatsiri S, Srigulbutr S. Epidemiology and antifungal susceptibility in patients with candidemia in a University Hospital, Thailand. J Med Assoc Thai. 2020; 103(10): 1048-56.

[5]. Awad L, Tamim H, Abdallah D, Salameh M, Mugharbil A, Jisr T, et al. Correlation between antifungal consumption and the distribution of Candida species in different hospital departments of a Lebanese medical Centre. BMC Infect Dis. 2018 20; 18(1): 589.

[6]. Liu F, Zhong L, Zhou F, Zheng C, Zhang K, Cai J, et al. Clinical Features, Strain Distribution, Antifungal Resistance and Prognosis of Patients with Non-albicans Candidemia: A Retrospective Observational Study. Infect Drug Resist. 2021; 14: 3233-46.

[7]. Wang H, Xu YC, Hsueh PR. Epidemiology of candidemia and antifungal susceptibility in invasive Candida species in the Asia-Pacific region. Future Microbiol. 2016; 11: 1461-77.

[8]. Boonsilp S, Homkaew A, Phumisantiphong U, Nutalai D, Wongsuk T. Species Distribution, Antifungal Susceptibility, and Molecular Epidemiology of Candida Species Causing Candidemia in a Tertiary Care Hospital in Bangkok, Thailand. J. Fungi. 2021; 7(7): 577.

[9]. Hii IM, Liu CE, Lee YL, Liu WL, Wu PF, Hsieh MH, et al. Resistance rates of non-albicans Candida infections in Taiwan after the revision of 2012 Clinical and Laboratory Standards Institute breakpoints. Infect Drug Resist. 2019; 12: 235-40.

[10]. Linberg E, HammarstrÖm H, Ataollahy N, Kondori N. Species distribution and antifungal drug susceptibilities of yeasts isolated from the blood samples of patients with candidemia. Scientific Reports. 2019; 9: 3838.

[11]. Berkow EL, Lockhart SR, Ostrosky-Zeichner L. Antifungal Susceptibility Testing: current approaches. Clin Microbiol Rev. 2020; 30: 33: e00069-19. doi.org/10.1128/CMR.00069-19.

[12]. Wayne PA, Clinical and Laboratory Standards Institute. Performance standards for antifungal susceptibility testing of yeasts, 1st edition, CLSI document M60-Ed1. Clinical and Laboratory Standards Institute. 2017.

[13]. Subcommittee on Antifungal Susceptibility Testing (AFST) of the ESCMID European Committee for Antimicrobial Susceptibility Testing (EUCAST), EUCAST definitive document EDef 7.1: method for the determination of broth dilution MICs of antifungal agents for fermentative yeasts. Clin Microbiol Infect. 2008; 14: 398-405.

[14]. Espinel-Ingroff A, Turnidge J, Alastruey-Izquierdo A, Botterel F, Canton E, Castro C, et al. Method dependent epidemiological cutoff values for detection of triazole resistance in Candida and Aspergillus species for the Sensititre YeastOne colorimetric broth and Etest agar diffusion methods. Antimicrob Agents Chemother. 2019; 63(1):e01651-18. doi.org/10.1128/AAC .01651-18.

[15]. Canton E, Pemán J, Hervás D, Iñiguez C, Navarro D, Echeverría J, et al. Comparison of three statistical methods for establishing tentative wild-type population and epidemiological cut off values for echinocandins, amphotericin B, flucytosine, and six Candida species as determined by the colorimetric Sensititre YeastOne method. J Clin Microbiol, 2012; 50: 3921-6.

[16]. Ngamchokwathana C, Chongtrakool P, Waesamaae A. Risk Factors and Outcomes of Non-albicans Candida Bloodstream Infection in Patients with Candidemia at Siriraj Hospital— Thailand's Largest National Tertiary Referral Hospital. J Fungi. 2021; 7: 269. doi.org/10.3390/jof7040269.

[17]. Wang H, Xu YC, Hsyeh PR. Epidemiology of candidemia and antifungal susceptibility in invasive Candida species in the Asia-Pacific region. Future Microbiol. 2016; 11(11): 1461-77.

[18]. Faksri K, Kaekes W, Chaicumpar K, Chaimanee P, Wongwajana S. Epidemiology and identification of potential fungal pathogens causing invasive fungal infections in a tertiary care hospital in northeast Thailand. Med Mycol. 2014; 52(8): 810-8.

[19]. El-Kholy MA, Helaly GF, El Ghazzawi EF, El-Sawaf G, Shawky SM. Virulence factors and antifungal susceptibility profile of C. tropicalis isolated from various clinical specimens in Alexandria, Egypt. J Fungi. 2021; 7(351): 1-11.

[20]. Tulasidas S, Rao P, Bhat S, Manipura R. A study on biofilm production and antifungal drug resistance among Candida species from vulvovaginal and bloodstream infections. Infect Drug Resist. 2018; 1(11): 2443-8.

[21]. Zuza-Alves DL, Silva-Rocha WP, Chaves GM. An update on Candida tropicalis based on basic and clinical approaches. Front Microbiol. 2017; 8(1927). doi.org/ 10.3389/ fmicb.2017.01927.

[22]. Tan BH, Chakrabarti A, Li RY, Patel AK, Watcharananan SP, Liu Z, et al. Asia Fungal Working Group (AFWG). Incidence and species distribution of candidaemia in Asia: A laboratory-based surveillance study. Clin Microbiol Infect. 2015; 21(10): 946-53.

[23]. Gupta A, Varma A. Candida glabrata candidemia: An emerging threat in critically ill patients. Indian J Crit Care Med. 2015; 19(3): 151-4.

[24]. Buranarom N, Komin O, Matangkasombut O. Hyposalivation, oral health, and Candida colonization in independent dentate elders. Plos One. 2020; 15(11). doi: 10.1371/journal.pone.0242832.

[25]. Charlet R, Pruvost Y, Tumba G, Istel F, Poulain D, Kuchler K, et al. Remodeling of the Candida glabrata cell wall in the gastrointestinal tract affects the gut microbiota and the immune response. Sci Rep. 2018; 8(3316).

[26]. Alenazy H, Alghamdi A, Pinto R, Daneman N. Candida colonization as a predictor of invasive candidiasis innon-neutropenic ICU patients with sepsis: A systematic review and meta-analysis. Inter J Infect Dis. 2021; 102: 357-62.

[27]. Hassan Y, Chew SY, Than LTL. Candida glabrata: Pathogenicity and resistance mechanisms for adaptation and survival. J Fungi. 2021; 7(8). doi: 10.3390/jof7080667.

[28]. Goemaere B, Lagrou K, Spriet I, Hendrickx M, Becker P. Clonal spread of Candida glabrata bloodstream isolates and fluconazole resistance affected by prolonged exposure: a 12-year single-center study in Belgium. Antimicrobial Agents Chemother. 2018; 62(8). doi: 10.1128/AAC.00591-18.

[29]. Yao D, Chen J, Chen W, Hu X. Mechanism of azole resistance in clinical isolates of Candida glabrata from two hospitals in China. Infect Drug Resist. 2019; 12: 771-81.

[30]. Wang, An N, Yang Y, Yang X, Fan Y, Feng J. Candida tropicalis distribution and drug resistance is correlated with ERG11 and UPC2 expression. Antimicrob Resist Infect Control. 2021. 10(1). doi: 10.1186/ s13756-021-00890-2.

[31]. Kritikos A, Neofytos D, Khanna N, Schreiber PW, Boggian K, Bille J, et al. Fungal Infection Network of Switzerland (FUNGINOS). Accuracy of Sensititre YeastOne echinocandins epidemiological cut-off values for identification of FKS mutant Candida albicans and Candida glabrata: a ten-year national survey of the Fungal Infection Network of Switzerland (FUNGINOS). Clin Microbiol Infect. 2018; 24(1). doi: 10.1016/ j.cmi.2018.05.012.

Journal of Associated Medical Sciences 2022; 55 (3): 51-59

JAMS
Journal of Associated Medical Sciences

Thai-Journal Citation Index Centre (TCI) & ASEAN Citation Index (ACI)

Journal of Associated Medical Sciences

Journal homepage: https://www.tci-thaijo.org/index.php/bulletinAMS/index

In Vitro anti-metastasis of *Perilla frutescens* leaf water extract on aggressive human breast cancer cells

Chakkrit Khanaree[1] Wanisa Punfa[1] Payungsak Tantipaiboonwong[2] Piyawan Nuntaboon[2] Maitree Suttajit[2] Supachai Topanurak[3] Nahathai Dukaew[4, 5] May Thuu Mon[6] Rentong Hu[7] Komsak Pintha[2*]

[1]School of Traditional and Alternative Medicine, Chiang Rai Rajabhat University, Chiang Rai Province, Thailand
[2]Division of Biochemistry, School of Medical Sciences, University of Phayao, Phayao Province, Thailand
[3]Department of Molecular Tropical Medicine and Genetics, Faculty of Tropical Medicine, Mahidol University, Bangkok, Thailand
[4]Department of Pharmacology, Faculty of Medicine, Chiang Mai University, Chiang Mai Province, Thailand
[5]Clinical Research Center for Food and Herbal Product Trials and Development (CR-FAH), Faculty of Medicine, Chiang Mai University, Chiang Mai Province, Thailand
[6]Department of Biochemistry, University of Medicine 1, Yangon, Myanmar
[7]Department of Laboratory Medicine, The Affiliated Hospital of Youjiang Medical University for Nationalities, Baise, Guangxi, China

ARTICLE INFO

Article history:
Received 21 January 2022
Accepted as revised 23 June 2022
Available online 5 July 2022

Keywords:
Perilla frutescens, anti-metastasis, anti-invasion, anti-migration, breast cancer

ABSTRACT

Background: *Perilla frutescens* is a long-established plant that is often used in foods and traditional medicines in Asian countries. The perilla leaf contains a considerable number of bioactive substances, such as phenolics and flavonoids, which have been demonstrated to possess anticancer activity *in vitro* and *in vivo*.

Objectives: We aimed to study anti-metastatic activity, anti-invasion activity, and anti-migration activity of perilla leaf water extract (PLW) at 90°C for 1-5 min in MDA-MB-231 aggressive human breast cancer cells.

Materials and methods:Dry perilla leaves were extracted using hot water for 1-5 min to obtain crude extract and then lyophilized for PLW powder. PLW was evaluated for total phenolic, total flavonoid, and rosmarinic acid (RA) contents by Folin-Ciocalteau reagent, aluminum chloride colorimetric assay, and ultra-high-pressure liquid chromatography, respectively. Antioxidant activity of PLW was determined by DPPH and ABTS assays. MTT assay was performed to evaluate the cytotoxicity of PLW on MDA-MB-231 cells. Effective PLW was further determined its inhibitory effect on human breast cancer cell metastasis by a Boyden chamber-based transmembrane assay, the MMP-9 activity, and the proteolytic type IV collagenase activity.

Results: PLW by 5-min infusion showed the highest amount of total phenolic and flavonoid contents, as well as RA. Moreover, by the 5-min infusion, PLW had the highest antioxidant capacity when compared to PLW by infusions for 1-4 min. Following that, cytotoxicity testing revealed that the PLW is not toxic to MDA-MB-231 cells after a 24-hr exposure. The PLW at non-toxic doses (12.5-100 µg/mL) intensely presents an inhibitory effect on cell invasion and migration. The gelatinolytic activity showed that the PLW at concentrations of 12.5-100 µg/mL decreases MMP-9 activity in a dose-related manner. Furthermore, after treatment with the PLW, the proteolytic type IV collagenase activity was reduced considerably in a dose-related manner.

Conclusion: Our findings further showed that the PLW samples inhibit proteolytic enzymes involved in basement membrane breakdown, which might explain the anti-invasion and anti-migration properties of breast cancer cells. From the result, the application of perilla leaf might be developed as an herbal tea and used as an anti-metastatic agent for breast cancer prevention and treatment.

* **Corresponding author.**
Author's Address: *Division of Biochemistry, School of Medical Sciences, University of Phayao, Phayao Province, Thailand.*
E-mail address: komsakjo@gmail.com
** **doi:** 10.12982/JAMS.2022.024
E-ISSN: 2539-6056

Introduction

Female breast cancer is the most commonly diagnosed cancer and was the fifth leading cause of cancer death globally, in 2020.[1] In Thailand, breast cancer is the third most commonly occurring cancer and the third leading cause of cancer death.[2] Importantly, metastasis of breast cancer cells remains the primary cause of death in the majority of breast cancer patients.[3] The breast cancer cell metastasis occurs as the common metastatic process seen in a variety of solid tumors, which is promoted by the crucial steps including detachment from the primary tumor, migration, invasion, and travel to other sites through blood and lymphatic vessels, then adhesion and growth at a site other than the primary tumor.[4] The crucial step that promotes cancer cell metastasis happens through the activity of proteolytic enzymes, particularly matrix metalloproteinases (MMPs) and collagenase, on the extracellular matrix (ECM). Especially, the type IV collagen-specific collagenases and MMP-9, show an important role in the degradation of ECM components.[5,6] Inhibiting ECM-degrading enzymes is thus an attempt to prevent the metastasis of the cancer cells.

Recently, various investigations have provided support for the use of plant phytochemicals and derivatives in cancer metastasis prevention. Interestingly, several studies suggested that plant polyphenols, such as epigallocatechin gallate, resveratrol, curcumin, and rosmarinic acid can inhibit breast cancer cell metastasis by suppressing MMPs and collagenases activity.[7-10] Thus, plant polyphenols may offer a new source of anti-metastasis agents against breast cancer cells.

Perilla frutescens is used as functional foods and traditional medicines for the treatment of several conditions and diseases in Asian counties.[11] It is an aromatic plant of the mint family (Lamiaceae) that grows up to 4–6 feet tall with square and branching stems. Its dark green and hairy leaf is large (7x12 cm) with an oval shape and pointy end (Figure 1). Many studies have revealed that the Thai perilla leaf contains a variety of bioactive polyphenol substances such as rosmarinic acid, luteolin, and apigenin, which have a wide range of biological activities including anti-mutagenicity, anti-inflammation, anti-oxidant activities, and inhibition of carcinogenesis.[12] Moreover, our previous study showed that perilla leaf ethanolic extract (PLE) could inhibit migration and invasion of aggressive breast cancer cell line, MDA-MB-231.[13] Thus, perilla leaf has the potential to be developed as a herbal supplement for anti-metastasis agents against breast cancer.

However, ethanol, the most commonly effective solvent used for extracting bioactive compounds, is more toxic and regarded as an environmental pollutant. Unlike ethanol and organic solvents, water is an environmentally friendly solvent. It is a nontoxic, nonflammable, and simple solvent.[14] Using the different solvents and extraction processes might be different in bioactive substances and their activities. A study in 2018 by Pintha *et al*. showed that PLE by means of maceration has anti-metastatic properties *in vitro*.[13] In the current study, we explored the anti-metastatic activities including anti-invasion and anti-migration of perilla leaf water extract (PLW), which was prepared by means of infusion and compared with PLE.

Materials and methods

Plant material and extraction

Thai perilla leaf samples were collected from Phayao, Thailand. The voucher number was deposited at Queen Sirikit Botanic Garden Herbarium, Chiang Mai, Thailand (Code: QBG-93756). For the preparation of PLW, the dried leaves of perilla were firstly finely crushed and infused in hot water (90°C) for 1-5 min. Then, the extracts were filtered through filter paper (Whatman No.1), lyophilized, and powdered. For the preparation of PLE, the dried leaves of perilla were extracted with 70% ethanol at a 1:10 ratio for 12 hrs with constant stirring and then left overnight. The ethanolic solution was then filtered using filter paper (Whatman No.1). The PLE was evaporated and lyophilized to powder, respectively. PLW and PLE were kept at -20°C until used for further experiments.

Quantification of total phenolic content (TPC)

Briefly, 20 µL of the different concentrations of PLW or PLE dissolving in DMSO (RCI Labscan limited, Bangkok, Thailand) was added to 100 µL of Folin-Ciocalteu reagent (10% v/v) (Merck, Darmstadt, Germany) into 96-well plate and incubated in the dark standing at room temperature. After 3 min, 80 µL of sodium carbonate (7.5% w/v) (VWR Chemicals BDH®, Leicestershire, UK) was added. The reaction was incubated for 30 min at room temperature in the dark, the absorbance was measured at 765 nm using a Synergy™ HT Multi-Detection Microplate Reader (BioTek Instruments, Inc., VT, USA). TPC was expressed in milligram of gallic acid equivalents (GAE) per gram dry weight of extract (mg GAE/gm extract) using a calibration gallic standard curve.[15]

Quantification of total flavonoid content (TFC)

Concisely, 25 µL of the assigned concentrations of PLW or PLE in DMSO (RCI Labscan limited, Bangkok, Thailand) was mixed with 125 µL of deionized water and 7.5 µL of 5% $NaNO_2$ (VWR Chemicals BDH®, Leicestershire, UK) in a 96-well plate. Following 6 min, 15 µL of 10% (w/v) aluminum chloride (VWR Chemicals BDH®, Leicestershire, UK) was added to the mixture at room temperature in the dark for another 6 min. After that, 50 µL of 1 M NaOH (VWR Chemicals BDH®, Leicestershire, UK) was added and the volume was made up to 250 µL with deionized water. The reaction was incubated at room temperature in the dark for 15 min and the absorbance of sample was measured at 532 nm using a Synergy™ HT Multi-Detection Microplate Reader (BioTek Instruments Inc., VT, USA). TFC was expressed in milligrams of catechin equivalents (CE) per gram dry weight of extract (mg CE/gm extract) using a calibration catechin standard curve.[15]

Detection of rosmarinic acid (RA) in PLW and PLE

The ultra-high-pressure liquid chromatography (UHPLC) condition was performed using reverse-phase ZORBAX Eclipse plus C18 column (4.6 mm x 150 mm, 5 µm particle diameters) (Agilent Technologies Inc., CA, USA). The assay was performed using two solvents, including 0.1% trifluoroacetic acid (VWR Chemicals BDH®, Leicestershire, UK) in acetonitrile and 100% methanol. Samples (10 µL) were injected into the column with a flow rate of 1.0 mL/min. The RA peaks were detected at 280 nm. The peak area and retention time of each fraction were compared with a calibration curve of

various concentrations of RA standard and calculated and expressed as mg/gm extract.[16]

Determination of antioxidant activity by DPPH radical scavenging assay

In brief, the mixture of 20 µL of assigned concentrations PLW or PLE and 180 µL of 0.2 mM DPPH reagent (Sigma-Aldrich, MA, USA) were added to a 96-well plate. After incubation at room temperature in the dark for 30 min, absorbance of the reaction mixture was detected at 517 nm against blank as methanol using a Synergy™ HT Multi-Detection Microplate Reader (BioTek Instruments Inc., VT, USA). The percentage of scavenging inhibition was calculated, and the antioxidant activity was expressed as scavenged free radicals by 50% (SC_{50}).[17]

Determination of antioxidant activity by ABTS radical scavenging assay

Briefly, the mixture (10 µL) of the PLW or PLE assigned concentrations and 990 µL of working ABTS solution (Sigma-Aldrich, MA, USA) were incubated for 6 min at room temperature in the dark. The absorbance of the reaction sample was detected at 734 nm against with distilled water as blank reference, using the UV-visible spectrophotometer (Shimadzu, Kyoto, Japan). The percentage of scavenging inhibition was calculated and the antioxidant activity was expressed as scavenged free radicals by 50% (SC_{50}).[17]

Cell lines and culture condition

MDA-MB-231 human breast carcinoma cells and NIH3T3 fibroblast cells were obtained from the American Type Culture Collection (ATCC, DC, USA). MDA-MB-231 and NIH3T3 cell lines were cultured and maintained in Dulbecco's Modified Eagle Medium (DMEM) (Thermo Fisher Scientific Inc., MA, USA) supplemented with 10% (v/v) fetal bovine serum (Thermo Fisher Scientific Inc., MA, USA), penicillin (100 U/mL) and streptomycin (100 µg/mL) (Thermo Fisher Scientific Inc., MA, USA) in 5% CO_2 with humidified incubator at 37°C.

Determination of cytotoxicity by MTT assay

The MDA-MB-231 cells were seeded in a 96-well plate for 24 hrs prior treatment with PLW or PLE (0-200 µg/mL) for 24 hrs. Next, 15 µL of MTT dye (5 mg/mL) (AppliChem, Darmstadt, Germany) was added and incubated at 37°C for 4 hrs. After 4 hrs, all solutions were removed. Then, DMSO (100 µL) (RCI Labscan limited, Bangkok, Thailand) was added to dissolve the formazan crystal. The formazan crystal product measured the absorbance at 540/630 nm using a Synergy™ HT Multi-Detection Microplate Reader (BioTek Instruments Inc., VT, USA). The percentage of cell viability was calculated and non-cytotoxic concentrations ($\leq IC_{20}$) were used for the further experiments.[15]

Determination of cell migration and invasion

Cell migration was tested using polyvinylpyrrolidone-free polycarbonate filters (Merck, Darmstadt, Germany) coated with 0.01% (w/v) gelatin (Sigma-Aldrich, MA, USA), whereas cell invasion was tested with a filter coated with Matrigel (Corning, NY, USA) (15 gm per filter). The NIH3T3 fibroblast cell culture media was added to the lower chamber to function as a chemoattractant. The top inserts were then seeded with 1.5×10^5 MDA-MB-231 cells in DMEM containing various doses of PLW or PLE (0-100 µg/mL). After that, the chambers were incubated at 37°C with 5% CO_2. Cells that migrated or invaded through the bottom surface of the membrane were preserved with methanol and stained with toluidine blue (VWR Chemicals BDH®, Leicestershire, UK) after an 18 hrs incubation period. Migrating or invading cells in 20% acetic acid were detected at the 570 nm absorbance with a Synergy™ HT Multi-Detection Microplate Reader (BioTek Instruments Inc., VT, USA). The cell migration or invasion were calculated as follows: $(OD_{treated}/OD_{control})\times100\%$.[18]

Determination of MMP-9 activity

The culture supernatant of MDA-MB-231 cells after treatment with PLW or PLE (0-100 µg/mL) was subjected to gel electrophoresis. Equal quantities of total protein of each treatment were loaded on 10% polyacrylamide gels (Bio-Rad, CA, USA) containing 0.1% (w/v) gelatin (Bio-Rad, CA, USA). The electrophoretic gels were sliced into single-lane strips after being washed twice with Triton X-100 (AppliChem, Darmstadt, Germany). Each gel strip was re-incubated in activation buffer for 24 hrs with PLW or PLE (0–100 µg/mL) and then stained with 0.1% (w/v) Coomassie Brilliant Blue R (Bio-Rad, CA, USA). The proteolytic activity of MMP-9 was thought to be displayed as clear bars on a blue backdrop, signifying digested bands. The digested bands were quantified using Bio 1D software (Viber Lourmat).[16]

Determination of type IV collagenase activity

An EnzChek collagenase assay kit (Thermo Fisher Scientific Inc., MA, USA) was used to determine the proteolytic activity of type IV collagenase (Molecular Probe). In a 96-well microplate, 1 U/mL collagenase was combined with 10 µg/mL fluorescein-conjugated gelatin (DQ gelatin) with different doses of PLW or PLE suspended in reaction buffer. The rate of proteolysis was measured by using a fluorometer to measure fluorescence intensity at 3 min intervals for 30 min. At an excitation wavelength of 485 nm and an emission wavelength of 528 nm, the fluorescence levels were measured. The activity of enzyme inhibitors was calculated using linear regression of the fluorescence intensity obtained at the time.[16]

Statistical analysis

The results were presented as mean±standard deviation of three independent experiments using one-way ANOVA with Dunnett's test. For all assessed multiple comparisons, Prism version 6.0 software was utilized, and $p<0.05$, $p<0.01$, and $p<0.001$ were measured to be significant.

Results

Phenolic and flavonoid contents of PLW compared with PLE

Table 1 shows the total phenolic and flavonoid contents of PLW at different times of infusion (1–5 min) compared to PLE. The TPC of the PLW (infusion for 1-5 min) ranged from 195-222 mg GAE/gm extract, whilst the TFC of the PLW (infusion for 1-5 min) ranged from 107-120 mg CE/gm extract. PLW by 5-min infusion exhibited greater TPC (222±2.73 mg GAE/gm extract) and TFC (120±4.41 mg CE/gm extract) as compared to PLW by infusion for 1-4 min. However, the greatest amounts of TPC (260±15.24 mg GAE/gm extract) and TFC (136±6.59 mg CE/gm extract) were found in PLE.

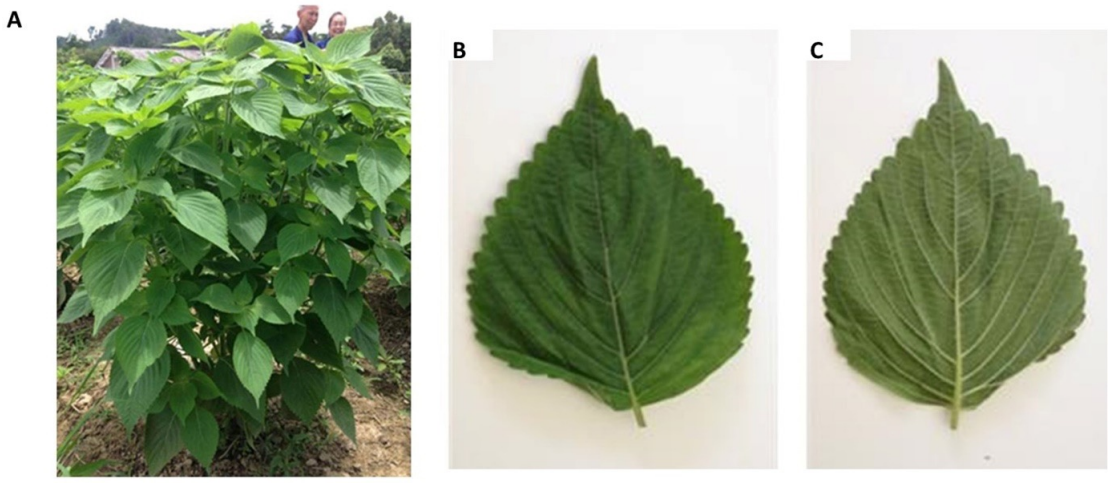

Figure 1. *Perilla frutescens plant (A), front side (B), and backside (C) of its leaves (Photos taken at University of Phayao, Thailand).*

Table 1 Total phenolic and flavonoid contents of PLW and PLE.

Extracts	%Yield	Total phenolic content (mg GAE/gm extract)	Total flavonoid content (mg CE/gm extract)
PLW by 1-min infusion	14.7	195.00±4.03	107.00±4.98
PLW by 2-mininfusion	15.6	204.00±1.86	112.00±7.80
PLW by 3-min infusion	14.5	205.00±0.89	115.00±6.26
PLW by 4-min infusion	15.3	206.00±4.73	116.00±6.28
PLW by 5-min infusion	15.4	222.00±2.73	120.00±4.41
PLE	12.3	260.00±15.24*	136.00±6.59*

**p<0.05 vs PLW by infusion for 1-5 min.*

RA content in PLW compared to PLE

The main peak in the RA standard was observed at a retention time of 5.483 min (Figure 2G). The RA content in PLE was 167.54±0.92 mg/gm extract (Figure 2F). The RA contents in PLW by infusion for 1-5 min were 104.26±3.28, 105.60±0.69, 106.77±1.69, 108.56±0.10, and 110.23±1.66 mg/gm extract, respectively (Figures 2A-E). As shown in Figure 2, the PLW by 5-min infusion had the greatest amount of RA, when compared to the PLW by infusion for 1-4 min.

Antioxidant capacities of PLW and PLE

Table 2 showed the SC_{50} values of DPPH and the $ABTS^{\bullet+}$ scavenging radicals of PLW and PLE. For the DPPH method, SC_{50} values of PLW by infusion for 1-5 min ranged from 23.99-24.79 µg/mL. PLW by 5-min infusion showed the highest activity with the SC_{50} values of 23.99±0.31 µg/mL but did not show a significant difference when compared to PLE (23.26±0.76 µg/mL). Similarly, PLW by infusion for 1-5 min could inhibit the stable $ABTS^{\bullet+}$ radicals with SC_{50} values of 7.70-8.26 µg/mL, with the greatest activity as shown in PLW by 5-min infusion (7.70±0.14 µg/mL). On the other hand, PLE revealed the most $ABTS^{\bullet+}$ radicals' inhibitory activity with the SC_{50} values of 6.90±0.11 µg/mL that showed a statistical significance when compared to PLW by infusion for 1-5 min.

Cytotoxicity of PLW to MDA-MB-231 cells

MDA-MB-231 cells were treated with varying concentrations of the extracts (12.5-200 µg/mL) for 24 hrs and compared to non-treated cells to assess the cytotoxic impact of PLW by 5-min infusion and PLE. As demonstrated in Figures 3A-B, PLW by 5-min infusion and PLE at concentrations of 12.5-200 µg/mL did not cause substantial toxicity in MDA-MB-231 cells, when compared to untreated control cells. As a result, subsequent tests utilized PLW by 5-min infusion or PLE concentrations of up to 200 µg/mL. From the UHPLC results of this study, 1 gm of PLW by 5-min infusion yielded RA about 110 mg. Therefore, PLW by 5-min infusion at doses of 12.5-200 µg/mL was RA about 1.38-22 µg/mL. Thus, the effect of RA (1-20 µg/mL) on the viability of MDA-MB-231 cells was determined. There was no significant effect on cell viability after RA treatment for 24 hrs as shown in Figure 3C.

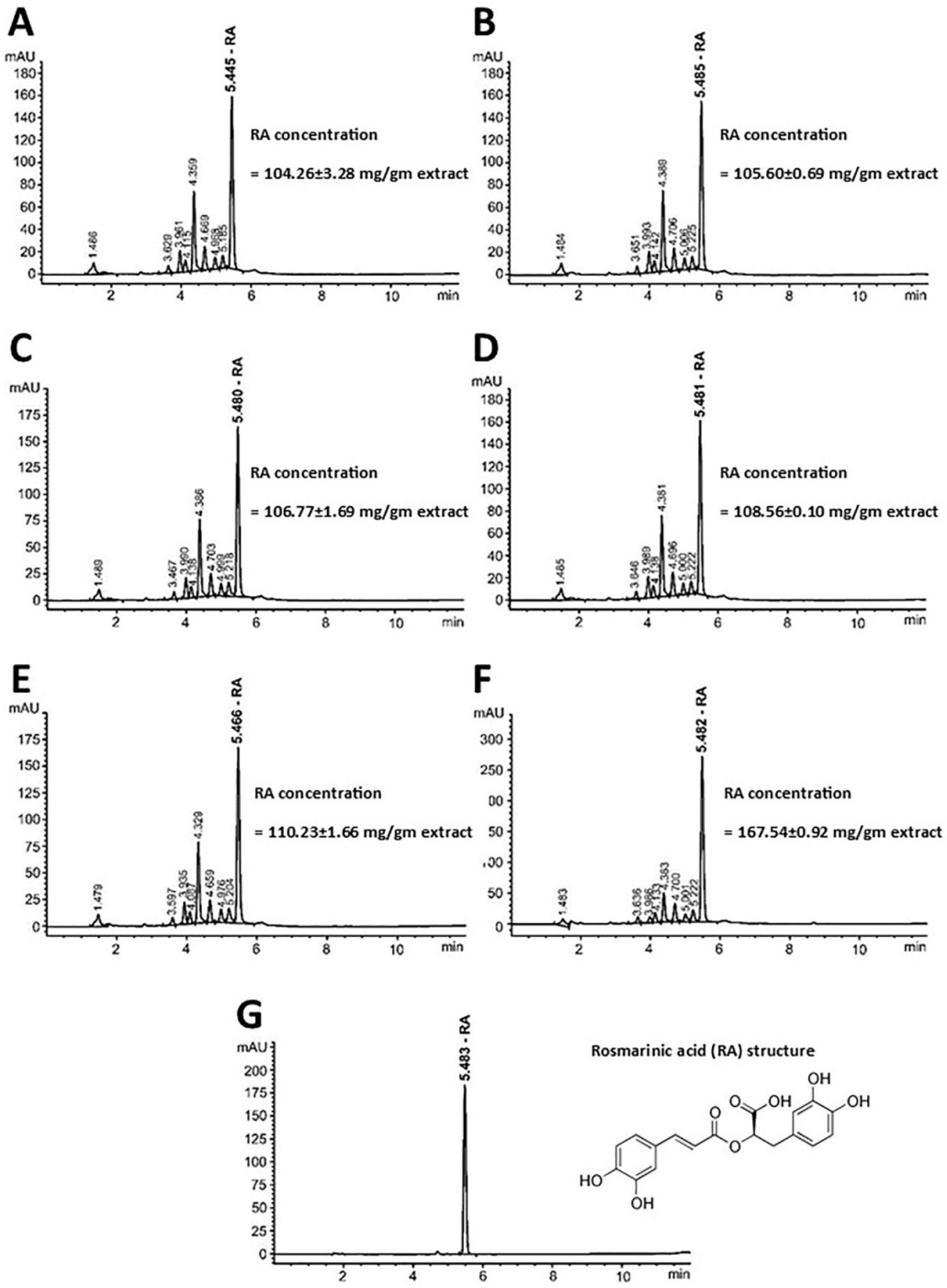

Figure 2. *The UHPLC chromatogram of PLW by 1-min (A), 2-min (B), 3-min (C), 4-min (D), and 5-min (E) infusion comparison with PLE (F) and RA standard (G).*

Table 2 The scavenge DPPH and ABTS$^{\bullet+}$ radicals of PLW and PLE.

Extracts	SC_{50} values of DPPH scavenging (µg/mL)	SC_{50} values of ABTS$^{\bullet+}$ scavenging (µg/mL)
PLW by 1-min infusion	24.57±0.37	8.19±0.32
PLW by 2-min infusion	24.48±0.63	8.26±0.25
PLW by 3-min infusion	24.79±0.38	7.75±0.20
PLW by 4-min infusion	24.72±0.21	7.79±0.12
PLW by 5-min infusion	23.99±0.31	7.70±0.14
PLE	23.26±0.76	6.90±0.11*

**p<0.05 vs PLW by infusion for 1-5 min.*

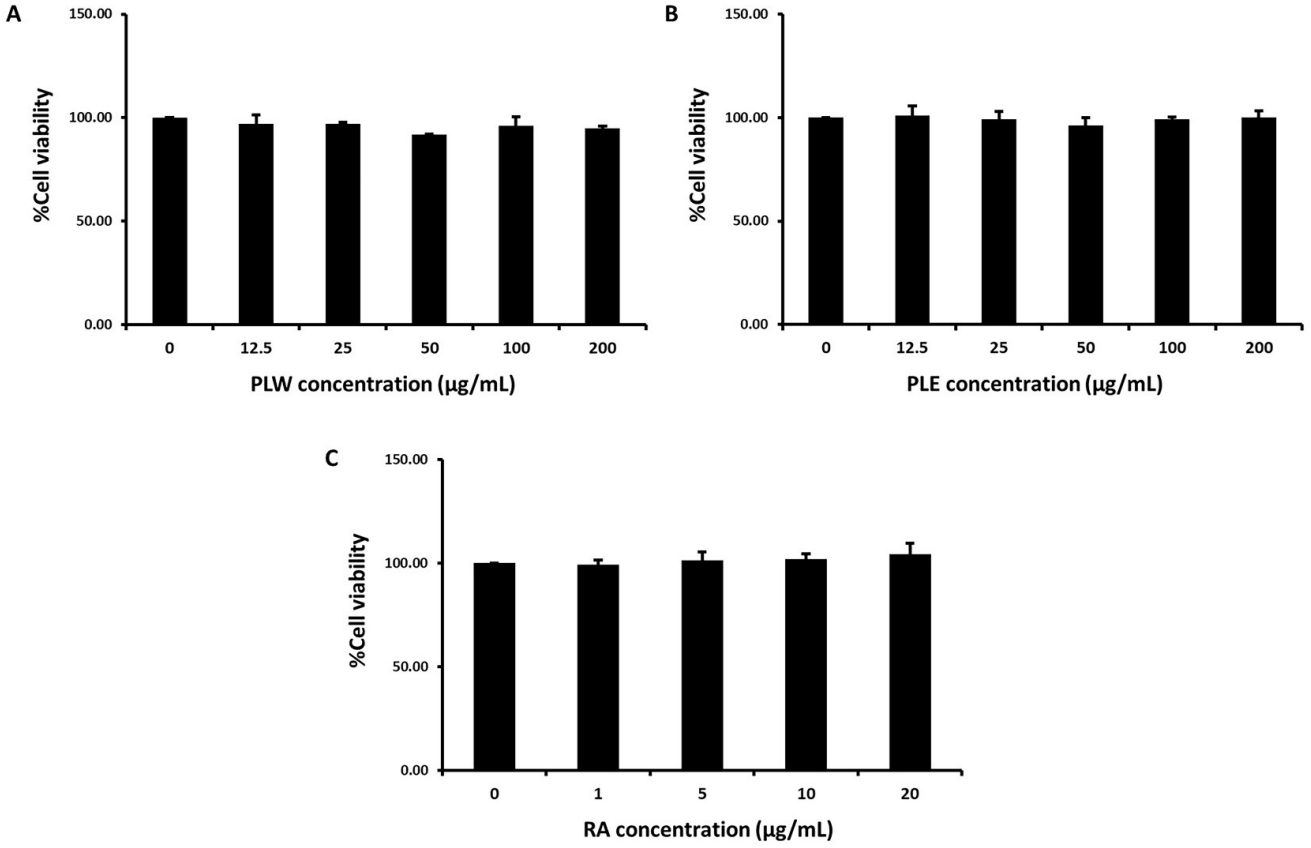

Figure 3. *The cytotoxic effect of PLW by 5-min infusion (A), PLE (B), and RA (C) on MDA-MB-231 cells. Data were represented as a percentage of viable cells compared to the untreated control cells.*

Inhibition effect of MDA-MB-231 on cell migration and invasion by PLW

MDA-MB-231 cells were shown to have considerably less invasion and migration when exposed to PLE at a concentration of 100 µg/mL (Figure 4). As shown in Figure 4A, PLW by 5-min infusion concentrations of 12.5-100 µg/mL decreased cell invasion of MDA-MB-231 cells passing through the Matrigel in a dose-related manner with IC_{50} values at 71.03±2.82 µg/mL. On the other hand, PLW considerably reduced cell migration when tested on the gelatin-coated filters (Figure 4B) as well as PLE (100 µg/mL). In addition, MDA-MB-231 cells were treated with RA at a non-toxic dose of 10 µg/mL. At this concentration, RA remarkably decreased the cell migration and invasion by approximately 50% and 30%, respectively when compared with the untreated cells. Our results confirmed that RA in PLW can evidently reduce MDA-MB-231 cell invasion and migration.

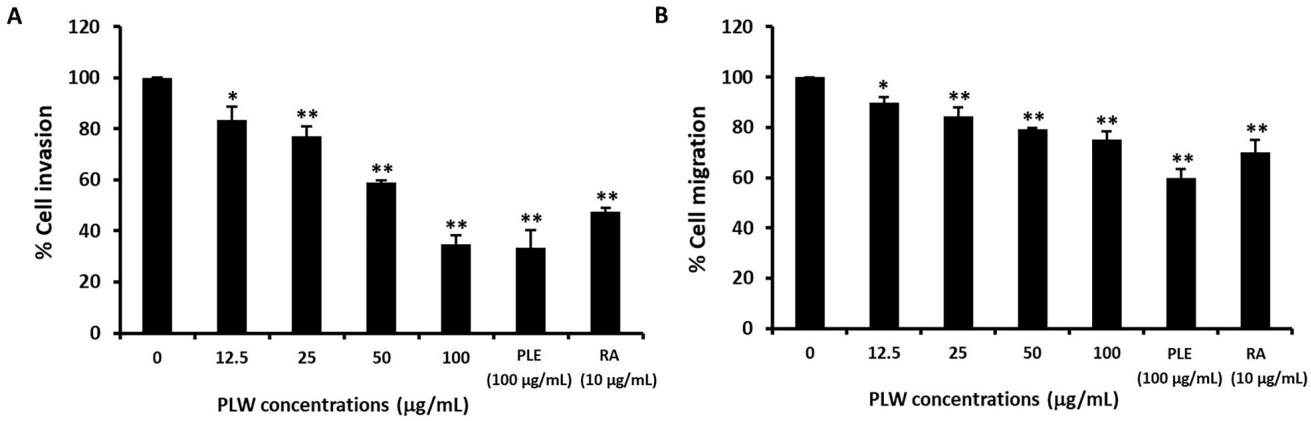

Figure 4. *Effect of PLW by 5-min infusion, PLE, and RA on cell invasion and cell migration in MDA-MB-231 cells. Cell invasion (A) and cell migration (B) were expressed as a percentage compared to the untreated control cells. (*p<0.01, **p<0.001 when compared to untreated control cells).*

Reduction of activity of MMP-9 by PLW

The different doses of PLW by 5-min infusion (0-100 µg/mL) or PLE (100 µg/mL) or RA (100 µg/mL) were added to the culture supernatant of MDA-MB-231 cells to determine whether the extracts might decrease MMP-9 activity. The results demonstrated that the administration of PLW by 5-min infusion (25-100 µg/mL) dramatically reduces the activity of MMP-9 in a dose-related manner (Figure 5A). Moreover, MMP-9 activity is substantially reduced by treatment with PLE (100 µg/mL) or RA (100 µg/mL).

Inhibition activity of type IV collagenase by PLW

Collagenase was incubated with varied concentrations (0-100 µg/mL) of PLW by 5-min infusion to assess the inhibitory effect of the PLW on the activity of type IV collagenase. The results demonstrate that PLW by 5-min infusion, as well as PLE (100 µg/mL) and RA (100 µg/mL), dramatically decrease type IV collagenase activity in a dose-related manner (Figure 5B).

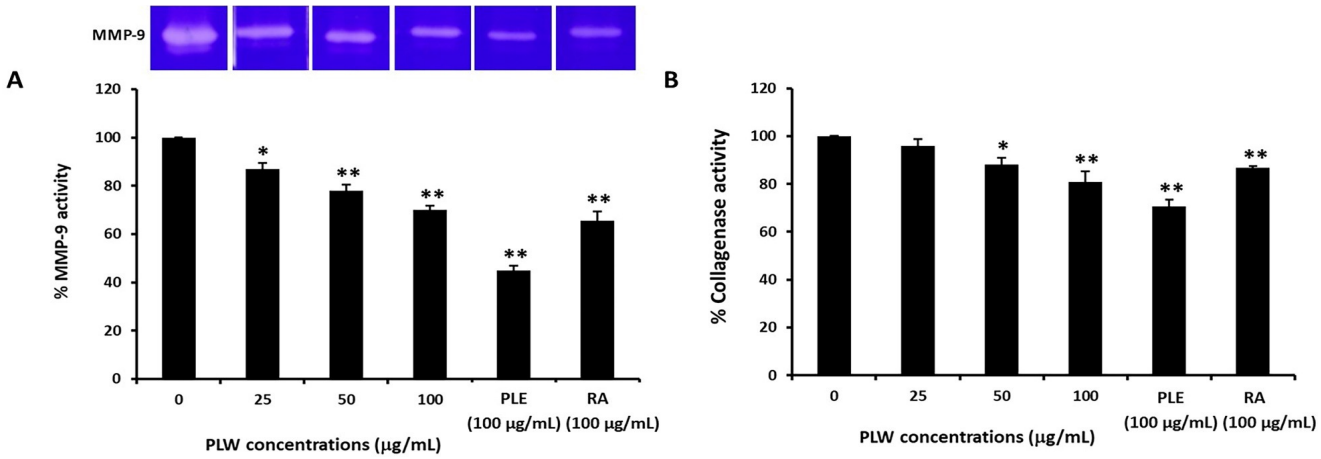

Figure 5. *Effects of PLW by 5-min infusion, PLE, and RA on MMP-9 and type IV collagenase activities. (*p<0.01, **p<0.001 when compared to untreated control cells).*

Discussion

The therapeutic options to prevent metastasis in breast cancer patients are currently limited. Standard chemotherapeutics mainly exert anti-cancer effects by mechanisms such as inhibiting DNA/RNA synthesis, inducing apoptosis or suppressing cell proliferation, although they do not prevent cell motility. As a result, cancer cells that survive or resist chemotherapy can undergo migration and invasion, resulting in metastases.[19] The search for new anticancer agents with anti-metastatic effects is still therefore required.

Perilla frutescens is an herbal medicine regularly used and cultivated in nations throughout South-East Asia.[11] It has been demonstrated to contain polyphenol compounds such as rosmarinic acid, apigenin, and luteolin, which have a wide range of biological activities. Our previous study showed that PLE by mean of maceration has antimetastatic properties *in vitro*.[13] However, ethanol might be regarded as environmental pollutant. In certain processes, water can be replaced ethanol for food and pharmaceutical manufacturing, resulting to reducing costs and eliminating the environmental problems.[14] Thus, this study aimed to investigate the development of perilla leaf extract used as herbal tea supplement for anti-metastasis of breast cancer. To extract bioactive compounds from perilla leaf, this study utilized hot water infusion and ethanol maceration. The results showed that different extraction methods, solvents, and times caused different contents of bioactive compounds in the extracts. Moreover, PLE has been shown to contain both polar and non-polar compounds, whereas PLW contains only polar compounds. However, this study found that RA was the main component and bioactive ingredient in PLW and PLE. RA is a phenolic compound which has been used as a natural food supplement. There are many reports about the beneficial activities on health, including antioxidant, anti-microbial, anthelmintic, anti-inflammatory agents, anti-allergy, anti-diabetic, and neuroprotective functions.[20] For anti-cancer effects, RA could suppress the development of cancers in several organs including the colon, breast, liver, stomach, as well as leukemia cells.[21]

Extraction solvents and time have an impact on bioactive components, which, in turn, have a main effect on the extract's biological activity.[22, 23] The antioxidant activity of extracts was investigated in this study utilizing the DPPH and $ABTS^{\bullet+}$ scavenging radical activity assays. The results suggested that PLW still had antioxidant activity as well as PLE, with the maximum activity being PLW by 5-min infusion. Consequently, PLW by 5-min infusion was utilized in the subsequent studies and further characterization of its anti-metastasis activity was compared to PLE.

Invasion and migration of cancer cells are crucial components of cancer metastasis, which is the major cause of cancer recurrence and death in cancer patients. Even though breast cancer therapies have advanced to unprecedented levels in recent years, many patients continue to face the problem that their cancer's proliferation and metastasis cannot be managed, partially due to inadequate therapy or therapeutic resistance.[3] The results represent the inhibitory efficiency of PLW against migration and invasion of breast

cancer cells. Similarly, the previous reports of Cho-Long Kim revealed that PLE could decrease cell migration and invasion in breast cancer cells.[24] Moreover, RA, the major compound presented in PLW, inhibited the migration of derived breast cancer stem-like cells, and inhibited the invasion of MDA-MB-231.[13, 25] Thus, the RA in PLW supports the anti-migration and anti-invasion effects, which reflect the anti-metastatic activity against breast cancer.

To better understand its anti-metastatic characteristics, the inhibitory effects of PLW on the proteolytic enzymes involved in ECM breakdown were investigated. ECM degradation by MMPs is a crucial stage in tumor invasion.[26] The deregulation of MMP expression stimulates invasion and metastasis in breast cancer.[27] Many studies have suggested that MMP-9 is involved in the development of invasive breast cancer through the metastatic cascade, as well as being a potential prognostic factor.[5] In addition, Type IV collagenase, one of the most significant members of the MMPs family, has been shown to be intimately connected with many tumor systems and linked to tumor cell invasive potential.[6, 28] Type IV collagenase overexpression has been detected in a number of malignancies, including colorectal cancer, gastric cancer, and breast cancer.[29] This demonstrates the ability of the PLW and PLE to inhibit MMP-9 and type IV collagenase activities. According to RA, a key component of PLW, was shown to reduce MMP-9 production in an animal model by activating AMPK and inhibiting its directly and competitively.[30]

The new findings of this study showed that perilla leaf can be extracted by water. Furthermore, PLW has an anti-metastatic activity in breast cancer cells. However, the effects of PLW have not been previously studied and reported. Most experiments used ethanol or methanol as the solvent for extraction. These toxic solvents must be eliminated before consumption or use in humans. The solvent-free extracts are important and necessary for the development of herbal supplements or herbal drugs. Therefore, the Thai perilla leaf has a vital potential for establishment as an instant drink, functional tea, and herbal tea for cancer metastasis prevention and treatment.

Conclusion

In this study, we demonstrated that PLW can suppress the migration and invasion in aggressive breast cancer cells. PLW works by reducing the space available for cell movement through inhibiting MMP-9 and type IV collagenase activities, which is a crucial step of metastasis. These findings indicated that perilla leaf extract, infused by hot water, inhibits proteolytic enzymes involved in ECM breakdown, reducing the process of breast cancer cell migration and invasion. Therefore, the applications of perilla leaf might also be developed as an instant drink, functional tea, and herbal tea for anti-metastatic breast cancer treatment.

Acknowledgements

This study was supported by Unit of Excellence (FF65-UoE009) University of Phayao, and Program Management Unit "Area-based": PMU "A", Office of National Higher Education Science Research and Innovation Policy Council (RSC64015). The authors wish to acknowledge the School of Traditional and Alternative Medicine, Chiang Rai Rajabhat University, the School of Medical Sciences, University of Phayao, and the Faculty of Tropical Medicine, Mahidol University for the use of their facilitates and support.

Conflicts of interest

There are no conflicts of interest.

References

[1] Sung H, Ferlay J, Siegel RL, Laversanne M, Soerjomataram I, Jemal A, et al. Global cancer statistics 2020: GLOBOCAN estimates of incidence and mortality worldwide for 36 cancers in 185 countries. CA Cancer J Clin. 2021; 71(3): 209-49. doi: 10.3322/caac.21660.

[2] Globocan. Thailand - Global Cancer Observatory 2020. 2020 [cited 2021 Aug 29]. Available from: https://gco.iarc.fr/today/data/factsheets/populations/764-thailand-fact-sheets.pdf.

[3] Redig AJ, McAllister SS. Breast cancer as a systemic disease: a view of metastasis. J Intern Med. 2013; 274(2): 113-26. doi: 10.1111/joim.12084.

[4] Tungsukruthai S, Petpiroon N, Chanvorachote P. Molecular mechanisms of breast cancer metastasis and potential anti-metastatic compounds. Anticancer Res. 2018; 38(5): 2607-18. doi: 10.21873/anticanres.12502.

[5] Daniele A, Abbate I, Oakley C, Casamassima P, Savino E, Casamassima A, et al. Clinical and prognostic role of matrix metalloproteinase-2, -9 and their inhibitors in breast cancer and liver diseases: A review. Int J Biochem Cell Biol. 2016; 77: 91-101.

[6] Tryggvason K, Höyhtyä M, Pyke C. Type IV collagenases in invasive tumors. Breast Cancer Res Treat. 1993; 24: 209-18. doi: 10.1007/BF01833261.

[7] Deb G, Thakur VS, Limaye AM, Gupta S. Epigenetic induction of tissue inhibitor of matrix metalloproteinase-3 by green tea polyphenols in breast cancer cells. Mol Carcinog. 2015; 54: 485-99. doi: 10.1002/mc.22121.

[8] Tang FY, Su YC, Chen NC, Hsieh HS, Chen KS. Resveratrol inhibits migration and invasion of human breast-cancer cells. Mol Nutr Food Res. 2008; 52(6): 683-91. doi: 10.1002/mnfr.200700325.

[9] Bachmeier B, Nerlich AG, Iancu CM, Cilli M, Schleicher E, Vené R, et al. The chemopreventive polyphenol curcumin prevents hematogenous breast cancer metastases in immunodeficient mice. Cell Physiol Biochem. 2007; 19: 137-52. doi: 10.1159/000099202.

[10] Xu Y, Jiang Z, Ji G, Liu J. Inhibition of bone metastasis from breast carcinoma by rosmarinic acid. Planta Med. 2010; 76(10): 956-62. doi: 10.1055/s-0029-1240893.

[11] Asif M. Phytochemical study of polyphenols in *Perilla Frutescens* as an antioxidant. Avicenna J Phytomed. 2012; 2(4): 169-78.

[12] Khanaree C, Pintha K, Tantipaiboonwong P, Suttajit M, Chewonarin T. The effect of *Perilla Frutescens* leaf on 1, 2-dimethylhydrazine-induced initiation of colon carcinogenesis in rats. J Food Biochem. 2018; 42: e12493.

[13] Pintha K, Tantipaiboonwong P, Yodkeeree S, Chaiwangyen W, Chumphukam O, Khantamat O, et al. Thai perilla (*Perilla Frutescens*) leaf extract inhibits human breast cancer invasion and migration. Maejo Int J Sci Technol. 2018; 12(2): 112-23.

[14] Bergeron C, Gafner S, Clausen E, Carrier DJ. Comparison of the chemical composition of extracts from *Scutellaria lateriflora* using accelerated solvent extraction and supercritical fluid extraction versus standard hot water or 70% ethanol extraction. J Agric Food Chem. 2005; 53(8): 3076-80. doi: 10.1021/jf048408t.

[15] Chumphukam O, Pintha K, Khanaree C, Chewonarin T, Chaiwangyen W, Tantipaiboonwong P, et al. Potential anti-mutagenicity, antioxidant, and antiinflammatory capacities of the extract from perilla seed meal. J Food Biochem. 2018; 42(11): e12556.

[16] Pintha K, Yodkeeree S, Pitchakarn P, Limtrakul P. Anti-invasive activity against cancer cells of phytochemicals in red jasmine rice (*Oryza sativa* L.). Asian Pac J Cancer Pre. 2014; 15(11): 4601-7. doi: 10.7314/apjcp.2014.15.11.4601.

[17] Wu Q, Er-Bu A, Liang X, Luan S, He C, Yin L, et al. Determination of the main naphthoquinones in *Onosma hookeri* Clarke. var. longiforum Duthie and its optimization of the ultrasound-assisted extraction using response surface methodology. J Food Sci. 2020; 86(2): 357-65. doi: 10.1111/1750-3841.15460.

[18] Pintha K, Yodkeeree S, Limtrakul P. Proanthocyanidin in red rice inhibits MDA-MB231 breast cancer cell invasion via the expression control of invasive proteins. Biol Pharm Bull. 2015; 38: 571-81. doi: 10.1248/bpb.b14-00719.

[19] Bagnyukova TV, Serebriiskii IG, Zhou Y, Hopper-Borge EA, Golemis EA, Astsaturov I. Chemotherapy and signaling: How can targeted therapies supercharge cytotoxic agents?. Cancer Biol Ther. 2010; 10(9): 839-53.

[20] Alagawany M, Abd El-Hack ME, Farag MR, Gopi M, Karthik K, Malik YS, et al. Rosmarinic acid: modes of action, medicinal values and health benefits. Anim Health Res Rev. 2017: 1-10. doi: 10.1017/S1466252317000081.

[21] Hossan MS, Rahman S, Bashar ABMA, Jahan R, Al-Nahain A, Rahmatullah M. Rosmarinic acid: A review of its anticancer action. WJPPS. 2014; 3(9): 57-70.

[22] Turkmen N, Sari F, Velioglu YS. Effects of extraction solvents on concentration and antioxidant activity of black and black mate tea polyphenols determined by ferrous tartrate and Folin-Ciocalteu methods. Food Chem. 2006; 99(4): 835-41.

[23] Ngo TV, Scarlett CJ, Bowyer MC, Ngo PD, Vuong QV. Impact of different extraction solvents on bioactive compounds and antioxidant capacity from the root of Salacia chinensis L. J Food Qual. 2017; 2017(1): 1-8.

[24] Kim CL, Shin YS, Choi SH, Oh S, Kim K, Jeong HS, et al. Extracts of *Perilla Frutescens* var. acuta (Odash.) kudo leaves have antitumor effects on breast cancer cells by suppressing YAP activity. Evid Based Complement Alternat Med. 2021; 2021: e5619761.

[25] Li H, Zhang Y, Chen HH, Huang E, Zhuang H, Li D, et al. Rosmarinic acid inhibits stem-like breast cancer through hedgehog and Bcl-2/Bax signaling pathways. Phcog Mag. 2019; 15: 600-6.

[26] Deryugina EI, Quigley JP. Matrix metalloproteinases and tumor metastasis. Cancer Metastasis Rev. 2006; 25(1): 9-34. doi: 10.1007/s10555-006-7886-9.

[27] Merdad A, Karim S, Schulten HJ, Dallol A, Buhmeida A, Al-Thubaity F, et al. Expression of matrix metalloproteinases (MMPs) in primary human breast cancer: MMP-9 as a potential biomarker for cancer invasion and metastasis. Anticancer Res. 2014; 34(3): 1355-66.

[28] Wang ZN, Xu HM. Relationship between collagen IV expression and biological behavior of gastric cancer. World J Gastroenterol. 2000; 6: 438-39. doi: 10.3748/wjg.v6.i3.438.

[29] Sun XM, Dong WG, Yu BP, Luo HS, Yu JP. Detection of type IV collagenase activity in malignant ascites. World J Gastroenterol. 2003; 9(11): 2592-95. doi: 10.3748/wjg.v9.i11.2592.

[30] Han YH, Kee JY, Hong SH. Rosmarinic acid activates AMPK to inhibit metastasis of colorectal cancer. Front Pharmacol. 2018; 5(9): 68. doi: 10.3389/fphar.2018.00068.

Journal of Associated Medical Sciences 2022; 55 (3): 60-67

JAMS
Journal of Associated Medical Sciences

Thai-Journal Citation Index Centre (TCI) & ASEAN Citation Index (ACI)

Journal of Associated Medical Sciences

Journal homepage: https://www.tci-thaijo.org/index.php/bulletinAMS/index

The increases of cognitive impairment, depression level, and physical inactivity in Thai adolescents with obese type 2

Savitree Thummasorn* **Akleema Ingding** **Phornpawi Tripheri** **Sarita Janwarn** **Atthaphon Jaimuk**

Department of Occupational Therapy, Faculty of Associated Medical Sciences, Chiang Mai University, Chiang Mai Province, Thailand

ARTICLE INFO

Article history:
Received 7 April 2022
Accepted as revised 26 June 2022
Available online 5 July 2022

Keywords:
Physical activity components, cognitive performance, depression severity

ABSTRACT

Background: Overweight and obesity are major public health concerns worldwide, as they increase cognitive dysfunction and depression among diabetic and obese individuals. Studies have shown that increased physical activity decreased cognitive impairment and depression in such persons. However, a comparison of physical activity, cognitive function and depression among Thai adolescences who are underweight, normal weight, overweight, and obese has never been investigated. In addition, it is known that physical activity was associated with cognitive and brain function in people of all ages. Moreover, physical activity can be used as tool for the treatment and prevention of psychiatric diseases. However, the associations of physical activity with cognition and mental health problem such as depression in Thai adolescents with underweight, overweight, and obese have never been investigated.

Objectives: This study compared the levels of physical activity, cognitive function and depression among Thai adolescents who were underweight, overweight and obese. In addition, the associations of physical activity with cognitive impairment and depression were also studied.

Materials and methods: 212 adolescents were divided into five groups depending on their body mass index (BMI) classifications as followed as: 1) normal weight group (n=66), 2) underweight group (n=41), 3) overweight group (n=38), 4) obesity type 1 group (n=37), and 5) obesity type 2 group (n=30). After that, assessments of physical activity, cognitive function and level of depression were conducted for all the participants. The measurement outcomes of this study including physical activity components, cognitive performance, and depression severity were measured in all groups. In this study, multi-factor ANOVA was used to compare the difference between physical activity, depression, and TMT scores among the groups. The multiple correlation analysis was used to analyze the correlation between physical activity and its associated factor in each group. P value <0.05 was statistically significant.

Results: Levels of total physical activity and depression were decreased in adolescents who were underweight, obese type 1 and obese type 2. In contrast, cognitive level was decreased in adolescents with only obesity type 2. It was interesting that level of total physical activity in adolescents with obese type 2 was significantly decreased when compared with overweight adolescents, while the total physical activity between obesity type 1 and 2 adolescents showed no significant difference. It is possible that severity of obesity type 2 was higher than that for overweight persons, while the level of severity between obese type 1 and 2 individuals may have little difference in this study. Moreover, our results showed that the level of physical activity only in leisure time in adolescents with obesity type 2 was lower than that in those overweight. It is possible that physical activity during leisure time may be a major factor in inducing a difference in the level of total physical activity between adolescents with obesity type 2 and those overweight.

Conclusion: Level of total physical activity in Thai adolescents with obesity type 2 was decreased via decreased physical activity during leisure time. It is possible that the decrease of physical activity during leisure time may be a major factor in the decrease of total physical activity in Thai adolescents with obesity type 2.

* **Corresponding author.**
Author's Address: *Department of Occupational Therapy, Faculty of Associated Medical Sciences, Chiang Mai University, Chiang Mai Province, Thailand*
** **E-mail address:** savi_ps@hotmail.com
doi: 10.12982/JAMS.2022.025
E-ISSN: 2539-6056

Introduction

Overweight and obesity are major public health concerns worldwide and their prevalence has increased over the last twenty years.[1] It has been established that overweight and obesity are associated with several problems such as cardiovascular and neurological disease and diabetes.[2,3] Moreover, studies have demonstrated that the level of excessive blood sugar increased the impairment of brain structures that led to cognitive dysfunction in diabetic and obese individuals.[4] This is consistent to other studies that reported obesity associated with cognitive impairment, especially in perception, learning and memory.[5] In addition, studies have shown that obesity also increases the risk of depression in these individuals.[6] It is interesting that a study demonstrated that obesity increased the risk of cognitive impairment in individuals with depression.[7] Furthermore, the cognitive level of obese individuals with depression was significantly decreased when compared to those without.[8] Therefore, it is necessary for researchers to try and reduce cognitive impairment and depression for obese individuals in order to maintain good quality of life by doing physical exercises and nutritional consumption. Recent study found that physical activity (PA) can decrease body fat in diabetic and obese individuals.[9] Moreover, physical activity can also decrease cognitive impairment in children and adolescents who are obese or overweight.[10] Interestingly, the recent study reported that the physical activities such as strength exercise, flexibility exercise (range-of-motion exercises or stretching), and walking can reduce stress level in individual with depressive disorder.[11] However, the comparison of physical activity, cognitive function, and depression among Thai adolescents who were overweight and obese has never been investigated. In addition, it was established that the prevalence of underweight adolescents has increased worldwide.[12, 13] Study reported that older adults with underweight was associated with the low levels of physical activity, cognition, and quality of life.[14, 15] Moreover, the study reported that psychological problems was also increased in underweight adolescents.[16] Thus, this study compared the levels of physical activity, cognitive function and depression among Thai adolescences who were underweight, normal weight, overweight and obese. In this study, the measurement outcomes including physical activity components, cognitive performance, and depression severity were measured in all groups. In addition, the associations of physical activity with cognitive impairment and depression were also studied. It is known that physical activity was associated with cognitive and brain function in people of all ages.[17, 18] However, the associations of physical activity with cognition in Thai adolescents with underweight, overweight, and obese have never been investigated. Additionally, it is established that physical activity can be used as public health tool for the treatment and prevention of psychiatric diseases.[19] However, the associations of physical activity with mental health problem such as depression in Thai adolescents with underweight, overweight, and obese have never been investigated. Thus, the associations of physical activity with cognition, and depression in Thai adolescents with normal weight, underweight, overweight, and obese were also studied in this study. This study hypothesized that levels of physical activity and cognition were decreased in Thai adolescents with obesity and underweight when compared with normal weight. Moreover, we hypothesized that level of depression was increased in Thai adolescents with obesity and underweight when compared with normal weight. This information can provide understanding on the levels of physical activity, cognition and depression severity in Thai adolescents who are underweight, normal weight, overweight, and obese. Moreover, this information can provide understanding on the associations of physical activity with cognitive impairment and depression in Thai adolescents with underweight, normal weight, overweight, and obese.

Materials and methods

Study design and participants

Study design

A cross-sectional design was employed to compare the levels of physical activity, cognitive function and depression among Thai adolescents who were underweight, normal weight, overweight, and obese. In addition, the associations of physical activity with cognitive impairment and depression in underweight, normal weight, overweight, and obese Thai adolescents were also studied.

Setting

Adolescents with underweight, normal weight, overweight, and obese studying in Chiang Mai University, Chiang Mai province, Thailand was invited to participate in the study. The periods of recruitment, exposure, and data collection in this study were conducted from November 2020 to April 2021.

Participants

Study protocol was reviewed and approved by the Institutional Ethics Committee of the Faculty of Associated Medical Sciences, Chiang Mai University, Chiang Mai, Thailand. All the participants gave their written informed consent. All methods were performed in accordance with the relevant guidelines and regulations (Ethic number: AMSEC-63EX-066). The population consisted of 1st year health science students at Chiang Mai University, Chiang Mai province, Thailand (N=1064). The sample size (n=212) was calculated using Power Analysis and Sample Size (PASS) software based on the following assumptions: 95% confidence interval, a 5% margin of error and a population proportion of 78%. The number of participants (n=212) was selected considering equal sex and age ratio of the population. Each member of the population has an equal chance of being selected by the random sampling method. After that, 212 participants were divided into five groups depending on the World health organization Asian body mass index (BMI) classifications[20]: BMI ≤18.5 kg/m^2 as underweight, between 18.5 and 22.9 kg/m^2 as normal weight, between 23 and 24.9 kg/m^2 as overweight and BMI between 25 and 29.9 kg/m^2 as obesity type 1, and BMI ≥30 kg/m^2 as obesity type 2. Thus, 212 participants were divided into five groups as followed as: 1) normal weight group (n=66), 2) underweight group (n=41), 3) overweight group (n=38), 4) obesity type 1 group (n=37), and 5) obesity type 2 group (n=30). Assessments of physical activity, cognitive

function and level of depression were conducted for all the participants on the same day. The measurement outcomes of this study including physical activity components, cognitive performance, and depression severity were measured in all groups. The exclusion criteria used in this study were the inability to complete all questionnaires assessments, the physical disability, and participant's underlying diseases (depression, diabetes and eating disorders). In this study, the physical disability, which refers to a limitation on a person's physical functioning and mobility, was evaluated by interviewing the participants' illness history. Participants, who have a one of seven types of physical disabilities (cerebral palsy, stroke, spina bifida, arthritis, spinal cord injury, epilepsy, and muscular dystrophy), were excluded from this study.

Assessment of physical activity

The Global Physical Activity Questionnaire (GPAQ) is a self-administered questionnaire that assesses physical activity and was designed originally by the World Health Organization (WHO).[21, 22] The reporting duration (min) and frequency (time/week) of physical activity for the participants were divided into three domains: work, transportation, and leisure. The total scores of physical activity were calculated by the sum of total metabolic equivalent of task (MET)-minutes of the activity computed for each domain.[23] Next, the total scores of physical activities were classified into two groups: sufficiently active (at least 600 MET-minutes per week) and inactivity (less than 600 MET-minutes per week). For the examples of questions in each domain of physical activity (work, transportation, and leisure) were shown below:[21, 22]

- Work domain: Does your work involve vigorous-intensity activity that causes large increases in breathing or heart rate like carrying or lifting heavy loads, digging or construction work for at least 10 minutes continuously?
- Transportation domain: Do you walk or use a bicycle (pedal cycle) for at least 10 minutes continuously to get to and from places?
- Leisure domain: Do you do any moderate-intensity sports, fitness or recreational (leisure) activities that cause a small increase in breathing or heart rate such as brisk walking, (cycling, swimming, volleyball) for at least 10 minutes continuously?

Assessment of cognition

In this study, the Trail Making Test (TMT) was used to evaluate neuropsychological function. The TMT consists of two parts: Part A (TMT-A) and B (TMT-B). Both parts can provide information about visual scanning ability, motor speed and dexterity, and speeded processing, while Part B provides information about cognitive flexibility, alternating attention, and ability to inhibit a dominant but incorrect response.[24] Performance of the TMT was calculated by taking the completion time of the TMT-B minus that of the TMT-A (delta TMT). TMT performance provided information about cognitive flexibility and working memory.[25]

Assessment of depression

The Patient Health Questionnaire modified for Adolescents (PHQ-A) is a check list questionnaire that consists of 9 questions related to symptoms occurring in adolescents. Total scores ranging from 0 to 27 are used to self-screen for primary depression during the previous 2 weeks. The PHQ-A scores can be classified as minimal (PHQ-A scores ≤4), mild (PHQ-A scores 5-9), moderate (PHQ-A scores 10–14), moderately severe (PHQ-A scores 15-19) and severe depression (PHQ-A scores 20-27).[26]

Data analysis

All data were presented as mean values±SD. Multi-factor ANOVA was used to compare the difference between physical activity, depression, and TMT scores among the groups. In addition, the associations of physical activity with cognitive impairment and depression were also studied. It is known that physical activity was associated with cognitive and brain function in people of all ages.[17, 18] However, the associations of physical activity with cognition in Thai adolescents with underweight, overweight, and obese have never been investigated. Additionally, it is established that physical activity can be used as public health tool for the treatment and prevention of some psychiatric diseases.[19] However, the associations of physical activity with depression in Thai adolescents with underweight, overweight, and obese have also never been investigated. Thus, the associations of physical activity with cognitive impairment and depression in Thai adolescents with normal weight, underweight, overweight, and obese were studied in this study. In this study, the multiple correlation analysis was used to analyze the correlation between physical activity and associated factor. A $p<0.05$ was statistically significant.

Results

Participant characteristics

General characteristics of all the participations are shown in Table 1. In this study, the analyzed sample included 66 participants with normal weight, 38 with overweight, 37 with obesity type 1, and 30 with obesity type 2. The mean BMI of each type of participant was 20.36±0.16 of those with normal weight, 17.51±0.13 of those underweight, 23.85±0.11 of those overweight, 27.37±0.24 of those with obesity type 1 and 33.53±0.68 of those with obesity type 2. In this study, the passive and active leisure activities were interviewed. It is known that the passive leisure activities involved using little or no physical or mental activity such as watching television, reading books, etc. In contrast, active leisure activities involved using physical or mental energy such as exercise, dancing, swimming, etc. Our results showed that the frequency of adolescents who performed active leisure activities was not significantly different among the five groups. Moreover, the underlying diseases, such as hyperlipidemia and hypertension, had no significant differences among the five groups at the time of this study. Also, the socioeconomic status, physical disability, and history of head injury, had no significant differences among groups. Thus, these findings suggested that the personal factors including socioeconomic status, physical disability, underlying disease, and history of head injury were not significantly different in Thai adolescents with normal weight, underweight, overweight, and obese type 1 and 2 in this study. (Table 1)

Table 1 General characteristics of the participants in each group.

General characteristics	Groups				
	Normal weight (n=66)	Underweight (n=41)	Overweight (n=38)	Obese 1 (n=37)	Obese 2 (n=30)
Gender (frequency) Male/Female	25/41	5/36	10/28	13/24	7/23
Age(years) Average (SD)	18.86±0.65	18.76±0.62	18.84±0.49	18.81±0.52	19±0.69
BMI (kg/m^2) Average (SD)	20.36±1.29	17.51±0.8	23.85±0.66	27.37±1.48	33.53±2.74
Leisure (frequency) Passive/Active	50/16	39/2	29/9	30/7	23/7
Socioeconomic status (frequency) Low/Middle/High	2/62/2	0/37/4	0/33/5	1/33/3	1/29/0
Underlying disease (frequency) Yes/No	5/61	6/35	7/31	4/33	7/23
History of head injury (frequency) Yes/No	0/66	1/40	2/36	1/36	7/23
Physical disability (frequency) Yes/No	0/66	0/41	0/38	0/37	0/30

BMI: body mass index.

The average score of physical activity among the groups

The ability of young adults to perform physical activity is shown in Figure 1. In this study, the total physical activity score was investigated and is shown in Figure 1A. The results showed that the total physical activity scores of individuals who were underweight, overweight, and obese type 1 and 2 were significantly lower than normal weight individuals (Figure 1A). Moreover, the total physical activity scores of obesity type 2 individuals were also significantly lower than overweight persons (this result showed the increase of total physical inactivity in Thai adolescents with obese type 2). The ability of adolescents to perform physical activity in each domain (work, transportation, and leisure) is shown in Figure 1B-D. The results demonstrated that the average scores of works, transportation, and leisure activities in underweight, overweight, and obese type 1 and 2 individuals were significantly decreased when compared with normal weight persons. Interestingly, the average scores of leisure activities in obese type 2 individuals were significantly decreased when compared with overweight persons (this result showed the increase of leisure inactivity in Thai adolescents with obese type 2) (Figure 1B-D).

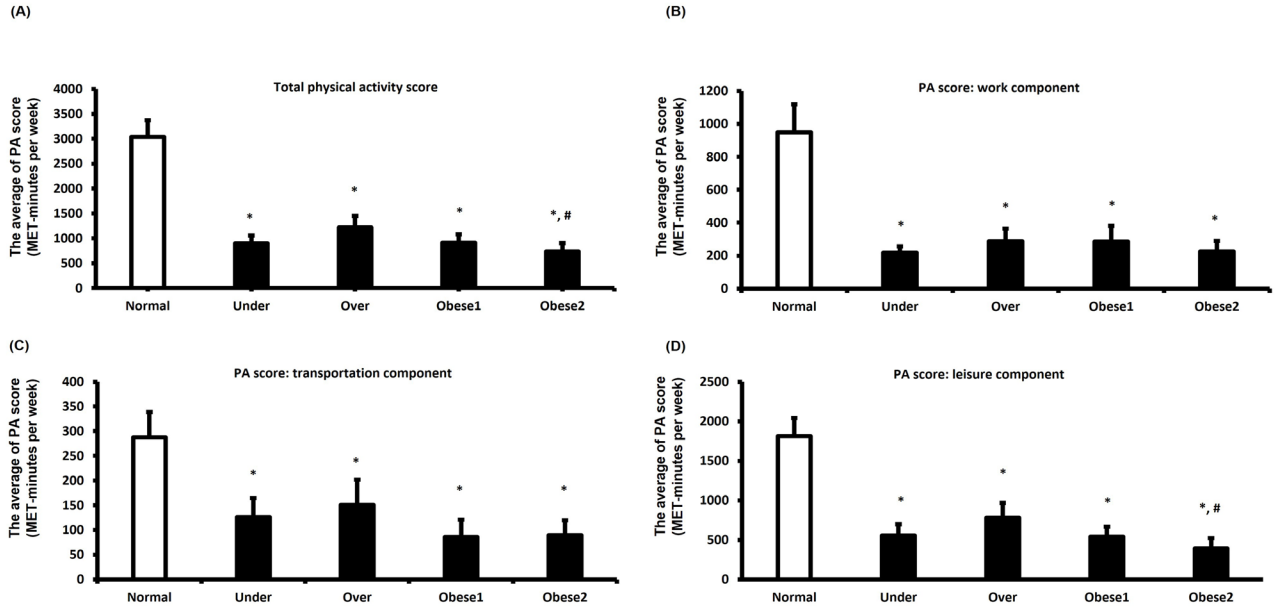

Figure 1. *Total score of physical activity, (A): average scores of work activity, (B): average scores of transportation activity, (C): average scores of leisure activity, (D): in normal weight, underweight, overweight, and obese adolescences, *p<0.05 vs. normal weight, #p<0.05 vs. overweight, PA: physical activity.*

Average score of depression among the groups

Results of depression, using the PHQ-A, are presented in Figure 2. The increase in PHQ-A scores represented the increase of depression level. The results of this study showed that depression levels in the underweight, obesity type 1 and obesity type 2 groups were significantly increased when compared with the normal weight group. In addition, the average score of depression in obese type 2 individuals was significantly increased when compared with overweight persons (Figure 2). Thus, these findings suggested that the depression severity was increased in Thai adolescents with obese type 2.

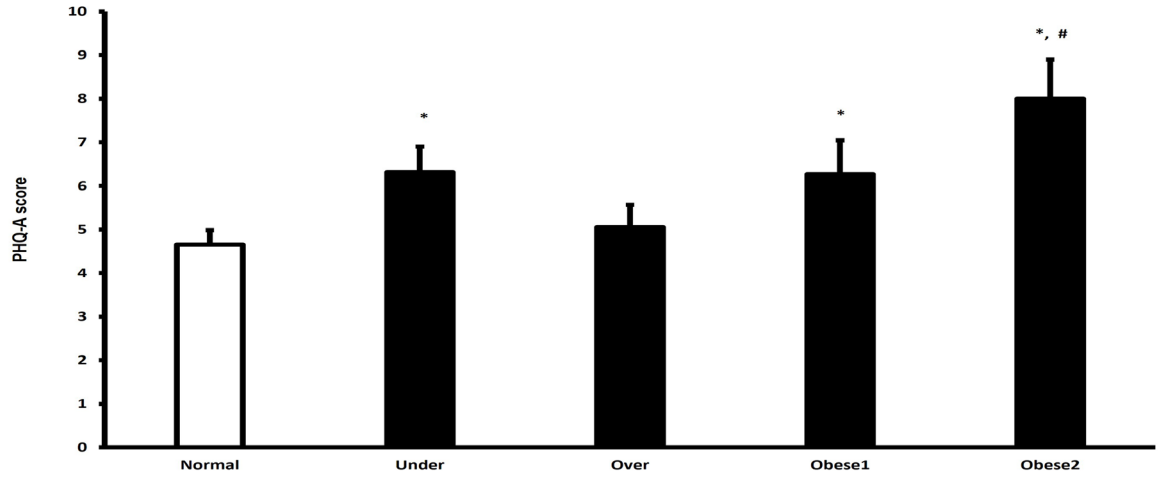

Figure 2. *Depression score of normal weight, underweight, overweight, and obese adolescences, *p<0.05 vs. normal weight, #p<0.05 vs. overweight, PHQ-A: patient health questionnaire-adolescent.*

Average score of cognition among the groups

The results of cognitive function by using the TMT average score are presented in Figure 3. There were significant differences in the TMT-A between obese type 1 and 2 individuals and normal weight persons (Figure 3A). The average cognition score in individuals with obesity type 2 was significantly different in the TMT-B when compared to normal weight, underweight, overweight, and obese type 1 persons (Figure 3B). TMT performance was presented by delta TMT scores (TMT-B minus TMT-A) as shown in Figure 3C. The results showed that TMT performance in individuals with obesity type 2 was significantly decreased when compared to those with normal weight, overweight and obesity type 1 (Figure 3C). Thus, these findings suggested that the cognitive impairment was increased in Thai adolescents with obese type 2.

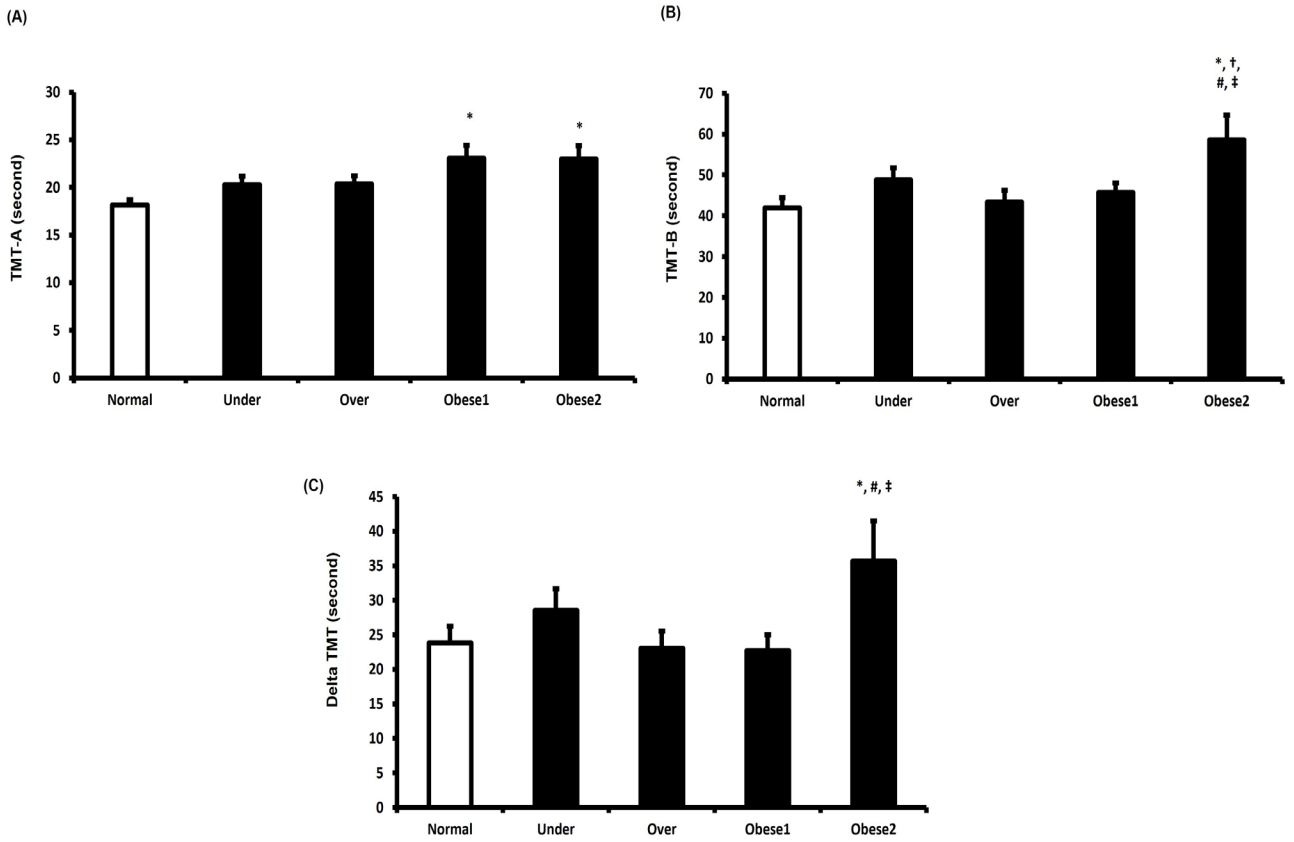

Figure 3. *Number of seconds in the TMT-A, (A): TMT-B, (B): delta TMT (TMT performance), (C): in normal weight, underweight, overweight, and obese adolescences, *p<0.05 vs. normal weight, †p<0.05 vs. underweight, #p<0.05 vs. overweight, ‡p<0.05 vs. obese type 1, TMT: Trail making test.*

Correlations between physical activity and associated factors

Correlation analysis between physical activity and associated factors in each group is shown in Table 2. The results showed that cognitive function (TMT performance) was associated negatively with physical activity in adolescents with obesity type 2 (r= -0.507, *p*=0.011). Furthermore, the results in this study demonstrated that depression (PHQ-A score) was associated negatively with physical activity in adolescents who were underweight (r= -0.621, *p*=0.008), obese type 1 (r= -0.406, *p*=0.014), and obesity type 2 (r= -0.742, *p*=0.005) (Table 2).

Table 2 Correlations between the physical activity and associated factors.

Parameters	Normal weight (n=66)	Underweight (n=41)	Overweight (n=38)	Obese 1 (n=37)	Obese 2 (n=30)
Correlation between the physical activity and delta TMT (s)	r=-0.162	r=-0.083	r=-0.205	r=-0.013	r=-0.507(*)
	p=0.195	*p*=0.604	*p*=0.216	*p*=0.089	*p*=0.011
Correlation between the physical activity and PHQ-A	r=0.07	r=-0.621(*)	r=-0.119	r=-0.406(*)	r=-0.742(*)
	p=0.578	*p*=0.008	*p*=0.477	*p*=0.014	*p*=0.005

*Cognition was defined as the TMT performance (delta TMT: TMT-B minus TMT-A). * p<0.05, TMT: Tail making test.*

Discussion

This study compared the levels of physical activity, cognitive function and depression among adolescents who were underweight, normal weight, overweight, and obese. Moreover, it reported the correlation between physical activity and associated factors in Thai adolescents with underweight, normal weight, overweight, and obese type 1 and 2. In this study, the data of socioeconomic status, underlying disease, head injury, and physical disability was investigated by interviewing in all participants. It is established that the socioeconomic status, underlying disease, head injury, and physical disability can affect the levels of cognition, depression, and physical activity in the healthy people.[27-30] However, our results showed that the socioeconomic status, physical disability, and history of head injury, had no significant differences among groups. Thus, these findings suggested that the personal factors including socioeconomic status, physical disability, underlying disease, and history of head injury were not influence on levels of cognition, depression, and physical activity in all participants of this study. In the results of physical activity levels, it was observed that the levels of total physical activity in Thai adolescents, who were underweight, overweight, and obese type 1 and 2, were decreased significantly when compared to those with normal weight. This finding is consistent with previous study, which showed that physical activity was decreased significantly in underweight, overweight and obese individuals.[9] It was interesting that results in this study demonstrated the level of total physical activity in adolescents with obese type 2 as significantly decreased when compared with overweight ones, while the total physical activity between obese type 1 and 2 individuals showed no significant difference. It is possible that severity of obesity type 2 was higher than that for overweight peoples, while the level of severity between obese type 1 and 2 individuals may have little difference in this study. This hypothesis is consistent to World health organization Asian BMI classification used in this study: BMI ≤18.5 kg/m^2 as underweight, between 18.5 and 22.9 kg/m^2 as normal weight, between 23 and 24.9 kg/m^2 as overweight and BMI between 25 and 29.9 kg/m^2 as obese 1, and BMI ≥30 kg/m^2 as obese 2.[20] Therefore, this study reported that the level of total physical activity in adolescents with obesity type 2 was lower than that in overweight individuals only. Moreover, our result showed that level of physical activity during leisure time in adolescents with obesity type 2 was lower than that in those overweight. This finding is consistent to the result of total physical activity showed that the level of total physical activity in adolescents with obesity type 2 was lower than that in overweight individuals. It is possible that physical activity during leisure time may be a major factor in inducing a difference in the level of total physical activity between adolescents with obesity type 2 and those overweight. Moreover, it is consistent with results of this study in that physical activity in other domains showed no significant difference in level of work and transportation of physical activities between adolescents with obesity type 2 and those overweight. In the future, this hypothesis needs to investigate that the mechanism of decreased total physical activity in Thai adolescents with obesity type 2 was induced via reducing the physical activity during leisure time or not.

Furthermore, this study observed that the depression level was increased significantly in Thai adolescents who were underweight, and obese type 1 and 2. These findings are consistent with previous studies, which found that the prevalence of depression was higher among underweight and obese individuals.[31] It is interesting that results in this study demonstrated the depression level in adolescents with obesity type 2 as increased significantly, when compared with those overweight. It is possible that increased BMI may increase the severity of depressive symptoms. This hypothesis is consistent with a study showing that BMI was associated with severity of depressive symptoms in overweight and obese individuals.[32] However, this hypothesis needs to be clarified in the future. Additionally, it is interesting that our result showed the difference of depression level between adolescents with obesity type 2 and those overweight. Moreover, our results showed that cognitive flexibility and working memory were decreased significantly in adolescents with obesity type 2 only. According to previous study, the results indicated that increased BMI

showed significantly increased episodic memory deficit in adolescents.[33] Therefore, the findings in this study demonstrated that the cognitive impairment, depression level, and physical inactivity were increased in adolescents with obese type 2.

In addition, this study investigated the correlation between physical activity and associated factors. Results demonstrated that cognitive function was associated negatively with physical activity in adolescents with obesity type 2. This finding is consistent with a study showing that physical activity associated with cognitive function in obesity.[34] Furthermore, the results of this study showed that depression associated negatively with physical activity in adolescents who were underweight, and obese type 1 and 2. These findings are consistent with studies reporting that depression was associated with physical activity in obese and underweight individuals.[6] In the future, these findings need to investigate that the physical activity can be used as a predictor for severity of depressive symptoms and cognitive impairment in Thai adolescents with obesity type 2 or not.

Conclusion

In conclusion, this study showed that level of total physical activity in Thai adolescents with obesity type 2 was decreased via decreased physical activity during leisure time. It is possible that the decrease of physical activity during leisure time may be a major factor in the decrease of total physical activity in Thai adolescents with obesity type 2. Moreover, we suggested that cognitive function was associated negatively with physical activity in Thai adolescents with obesity type 2, while depression was associated negatively with physical activity in Thai adolescents who were underweight, and obese type 1 and 2.

Study limitation

The results of our study are valid only for the Thai adolescents and may not extent to other countries. In the future, the levels of physical activity, cognitive function, and depression in the population living other countries as well as confounding factors in this study need to be investigated.

Conflicts of interest

The authors declare no conflict of interest.

References

[1] Midthjell K, Lee CM, Langhammer A, Krokstad S, Holmen TL, Hveem K, et al. Trends in overweight and obesity over 22 years in a large adult population: the HUNT Study, Norway. Clin Obes. 2013; 3(1-2): 12-20.

[2] Jensen MD, Ryan DH, Apovian CM, Ard JD, Comuzzie AG, Donato KA, et al. 2013 AHA/ACC/TOS guideline for the management of overweight and obesity in adults: a report of the American College of Cardiology/American Heart Association task force on practice guidelines and the obesity society. Circulation. 2014; 129(25 Suppl 2): S102-38.

[3] Clinical guidelines on the identification, evaluation, and treatment of overweight and obesity in adults--the evidence report. National Institutes of Health. Obes Res. 1998; 6 Suppl 2: 51S-209S.

[4] Yoon S, Cho H, Kim J, Lee DW, Kim GH, Hong YS, et al. Brain changes in overweight/obese and normal-weight adults with type 2 diabetes mellitus. Diabetologia. 2017; 60(7): 1207-17.

[5] Gunstad J, Paul RH, Cohen RA, Tate DF, Gordon E. Obesity is associated with memory deficits in young and middle-aged adults. Eat Weight Disord. 2006; 11(1): e15-19.

[6] Polanka BM, Vrany EA, Patel J, Stewart JC. Depressive disorder subtypes as predictors of incident obesity in US adults: moderation by race/ethnicity. Am J Epidemiol. 2017; 185(9): 734-42.

[7] Restivo MR, McKinnon MC, Frey BN, Hall GB, Taylor VH. Effect of obesity on cognition in adults with and without a mood disorder: study design and methods. BMJ Open. 2016; 6(2): e009347.

[8] Restivo MR, McKinnon MC, Frey BN, Hall GB, Syed W, Taylor VH. The impact of obesity on neuropsychological functioning in adults with and without major depressive disorder. PLoS One. 2017; 12(5): e0176898.

[9] Donnelly JE, Blair SN, Jakicic JM, Manore MM, Rankin JW, Smith BK, et al. American College of Sports Medicine position stand. Appropriate physical activity intervention strategies for weight loss and prevention of weight regain for adults. Med Sci Sports Exerc. 2009; 41(2): 459-71.

[10] Martin A, Booth JN, Laird Y, Sproule J, Reilly JJ, Saunders DH. Physical activity, diet and other behavioural interventions for improving cognition and school achievement in children and adolescents with obesity or overweight. Cochrane Database Syst Rev. 2018; 3: CD009728.

[11] Koo KM, Kim K. Effects of physical activity on the stress and suicidal ideation in Korean adult women with depressive disorder. Int J Environ Res Public Health. 2020; 17(10).

[12] Dong Y, Zou Z, Yang Z, Wang Z, Yang Y, Ma J, et al. Prevalence of excess body weight and underweight among 26 Chinese ethnic minority children and adolescents in 2014: a cross-sectional observational study. BMC Public Health. 2018; 18(1): 562.

[13] Singh JK, Acharya D, Rani D, Gautam S, Thapa Bajgain K, Bajgain BB, et al. Underweight and associated factors among teenage adolescent girls in resource-poor settings: a cross-sectional study. Risk Manag Healthc Policy. 2021; 14: 9-19.

[14] Selvamani Y, Singh P. Socioeconomic patterns of underweight and its association with self-rated health, cognition and quality of life among older adults in India. PLoS One. 2018; 13(3): e0193979.

[15] Kantanista A, Osinski W. Underweight in 14 to 16 year-old girls and boys: prevalence and associations with physical activity and sedentary activities. Ann Agric Environ Med. 2014; 21(1): 114-19.

[16] Zeiler M, Philipp J, Truttmann S, Waldherr K, Wagner G, Karwautz A. Psychopathological symptoms and well-being in overweight and underweight adolescents: a network analysis. Nutrients. 2021; 13(11).

[17] Erickson KI, Hillman C, Stillman CM, Ballard RM, Bloodgood B, Conroy DE, et al. Physical Activity, cognition, and brain outcomes: a review of the 2018 physical activity guidelines. Med Sci Sports Exerc. 2019; 51(6): 1242-51.

[18] Haapala EA, Eloranta AM, Venalainen T, Schwab U, Lindi V, Lakka TA. Associations of diet quality with cognition in children - the physical activity and nutrition in children study. Br J Nutr. 2015; 114(7): 1080-87.

[19] Biddle SJ, Asare M. Physical activity and mental health in children and adolescents: a review of reviews. Br J Sports Med. 2011; 45(11): 886-95.

[20] Girdhar S, Sharma S, Chaudhary A, Bansal P, Satija M. An epidemiological study of overweight and obesity among women in an urban area of north India. Indian J Community Med. 2016; 41(2): 154-57.

[21] Cleland CL, Hunter RF, Kee F, Cupples ME, Sallis JF, Tully MA. Validity of the global physical activity questionnaire (GPAQ) in assessing levels and change in moderate-vigorous physical activity and sedentary behaviour. BMC Public Health. 2014; 14: 1255.

[22] Chu AH, Ng SH, Koh D, Muller-Riemenschneider F. Reliability and validity of the self- and interviewer-administered versions of the global physical activity questionnaire (GPAQ). PLoS One. 2015; 10(9): e0136944.

[23] Sitthipornvorakul E, Janwantanakul P, van der Beek AJ. Correlation between pedometer and the global physical activity questionnaire on physical activity measurement in office workers. BMC Res Notes. 2014; 7: 280.

[24] Barry D, Petry NM. Predictors of decision-making on the Iowa gambling task: independent effects of lifetime history of substance use disorders and performance on the Trail Making Test. Brain Cogn. 2008; 66(3): 243-52.

[25] Hobert MA, Niebler R, Meyer SI, Brockmann K, Becker C, Huber H, et al. Poor trail making test performance is directly associated with altered dual task prioritization in the elderly--baseline results from the TREND study. PLoS One. 2011; 6(11): e27831.

[26] Mansour M, Krishnaprasadh D, Lichtenberger J, Teitelbaum J. Implementing the patient health questionnaire modified for adolescents to improve screening for depression among adolescents in a Federally Qualified Health Centre. BMJ Open Qual. 2020; 9(4).

[27] Ahmed S, Venigalla H, Mekala HM, Dar S, Hassan M, Ayub S. Traumatic brain injury and neuropsychiatric complications. Indian J Psychol Med. 2017; 39(2): 114-21.

[28] Ferraro OE, Guaita A, Villani S. Cognitive, physical and disability trajectories in community-dwelling elderly people. Aging Clin Exp Res. 2021; 33(10): 2671-77.

[29] Groessl EJ, Kaplan RM, Rejeski WJ, Katula JA, Glynn NW, King AC, et al. Physical activity and performance impact long-term quality of life in older adults at risk for major mobility disability. Am J Prev Med. 2019; 56(1): 141-46.

[30] Li W, Ruan W, Peng Y, Lu Z, Wang D. Associations of socioeconomic status and sleep disorder with depression among US adults. J Affect Disord. 2021; 295: 21-27.

[31] Carey M, Small H, Yoong SL, Boyes A, Bisquera A, Sanson-Fisher R. Prevalence of comorbid depression and obesity in general practice: a cross-sectional survey. Br J Gen Pract. 2014; 64(620): e122-27.

[32] Iodice S, Ceresa A, Esposito CM, Mucci F, Conti DM, Pergoli L, et al. The independent role of body mass index (BMI) and severity of depressive symptoms on biological changes of women affected by overweight/obesity. Int J Environ Res Public Health. 2021; 18(6): 2923. doi: 10.3390/ijerph18062923.

[33] Cheke LG, Simons JS, Clayton NS. Higher body mass index is associated with episodic memory deficits in young adults. Q J Exp Psychol (Hove). 2016; 69(11): 2305-16.

[34] Wang C, Chan JS, Ren L, Yan JH. Obesity reduces cognitive and motor functions across the lifespan. Neural Plast. 2016; 2016: 2473081.

Journal of Associated Medical Sciences 2022; 55 (3): 68-75

JAMS
Journal of Associated Medical Sciences

Thai-Journal Citation Index Centre (TCI) & ASEAN Citation Index (ACI)

Journal of Associated Medical Sciences

Journal homepage: https://www.tci-thaijo.org/index.php/bulletinAMS/index

Prospective study of early onset coagulopathy as a predictor of outcome in septicaemic patients admitted to a tertiary care centre in eastern India

Sohail[1] **Samir Sahu**[1] **Priyanka Samal**[2] **Siba Prasad Dalai**[1*] **Subhashree Ray**[3] **Anuhya Parasa**[1]

[1]*PG Department of Medicine, Institute of Medical Sciences & SUM Hospital, Siksha O Anusandhan (deemed to be) University, 8-Kalinga Nagar, Bhubaneswar, Odisha, India*

[2]*Department of Hematology, Institute of Medical Sciences & SUM Hospital, Siksha O Anusandhan (deemed to be) University, 8-Kalinga Nagar, Bhubaneswar, Odisha, India*

[3]*Department of Biochemistry, Institute of Medical Sciences & SUM Hospital, Siksha O Anusandhan (deemed to be) University, 8-Kalinga Nagar, Bhubaneswar, Odisha, India*

ARTICLE INFO

Article history:
Received 14 March 2022
Accepted as revised 4 July 2022
Available online 18 July 2022

Keywords:
Early onset coagulopathy, sepsis, mortality, SIRS, APACHE II

ABSTRACT

Background: Severe sepsis and septic shock are among the leading causes of morbidity and mortality in intensive care units worldwide despite rapid advances in treatment protocols. Even with all advances, determining the prognosis of sepsis continues to remain tricky.

Objectives: This study was planned to assess early onset coagulopathy as a predictor of outcome and mortality in septicemic patients and to study the underlying risk factors associated with mortality in septicemic patients with underlying coagulopathy.

Materials and methods: 240 patients fulfilling the criteria of SIRS and sepsis were included in the study. Coagulation parameters including platelet count, prothrombin time – international normalized ratio (PT-INR), activated partial thromboplastin time (aPTT) were evaluated within 48 hours of admission and 28-day mortality was evaluated. Independent predictors of 28-day mortality were evaluated using logistic regression model.

Results:Twenty-eight-day mortality rate was 77.77% (98/126) in patients with coagulopathy and a meagre 1.7% (2/114) in patients without coagulopathy which was statistically significant (p<0.05). Log Odd's ratio calculated using chi-square test was found to be 5.2781, 95% CI (1.633-17.321), which was highly significant. Univariate logistic regression for mortality showed PT-INR, aPTT and APACHE II scores to be independent variables. Multivariate logistic regression revealed severe increase in PT-INR [adjusted OR=1.622 (0.841, 3.092)], moderate increase in aPTT [adjusted OR=4.537 (0.989, 7.326)], and severe increases in aPTT [adjusted OR=3.851 (2.438, 4.996)], and APACHE II scores [adjusted OR=5.381 (1.925, 11.01)], were independently associated with 28-day mortality whereas age, sex, any severity of thrombocytopenia, mild to moderate increase in PT-INR, and mild increase in aPTT were not.

Conclusion: Early onset coagulopathy was found to be significantly associated with increased mortality risk in septicemic patients. Septicemic patients should be screened for coagulopathy within 24-48 hours of admission in appropriate clinical scenario to predict mortality outcome and take necessary action at the earliest.

* **Corresponding author.**
Author's Address: *PG Department of Medicine, Institute of Medical Sciences & SUM Hospital, Siksha O Anusandhan (deemed to be) University, 8-Kalinga Nagar, Bhubaneswar, Odisha, India*
** **E-mail address:** drsibadalai@gmail.com
doi: 10.12982/JAMS.2022.026
E-ISSN: 2539-6056

Introduction

Sepsis is a well-known clinical syndrome that results from an overly aggressive systemic host response to infection.[1] Severe sepsis is characterized by hypotension, coagulopathy, and multisystem organ dysfunction, which are primarily caused by dysregulation of host-derived inflammatory mediators.[2] Coagulopathy is a condition in which the blood's ability to clot the blood is impaired.[3] Derangement of coagulation parameters is one of the common laboratory findings in septicemic patients.

The complex triad of infection, inflammation and ensuing coagulopathy have been variably implicated in the pathophysiology of severe sepsis. In sepsis, the inflammatory response of the host to an invading organism develops a procoagulant state. The relationship between tissue factor (TF) and inflammatory cytokine release is crucial to this process of initiating the coagulation cascade.[4] Tissue factor is responsible for binding and activating Factor VII on cell surfaces, resulting in the formation of the enzyme-cofactor complex that stimulates the formation of Factor Xa. TF are also expressed by endothelial cells, mononuclear phagocytes such as monocytes and macrophages in various organs like lung, kidney, and brain astrocytes. After TF expression, proinflammatory cytokines including TNF, IL-8, and IL-6 are upregulated and they play a significant role in natural anticoagulant suppression and endothelial damage.[5] Next, platelet-activating factor (PAF) is released directly as a result of inflammation which accelerates the process of thrombosis by expression of platelet p-selectin which in turn increases monocyte TF expression and platelet adhesion to leukocytes and endothelium. When platelets are attached to leukocytes and endothelium, they serve as a surface for thrombin production and cellular signalling of other coagulation factors.[6] In severe sepsis, the disruption of three intrinsic anticoagulants (tissue factor pathway inhibitor, activated protein C, and thrombomodulin) lead to the onset of hyper-coagulopathy.

Severe sepsis and septic shock remain among the leading causes of morbidity and mortality in intensive care units worldwide despite rapid advances in treatment protocols.[7,8] Several trials and protocols have focused on developing better methods for detecting sepsis early, managing it effectively, and preventing complications. Even with all advances, determining the prognosis of sepsis continues to remain tricky. This study was planned to assess early onset coagulopathy as a predictor of outcome and mortality in septicemic patients and to study the underlying risk factors associated with mortality in septicemic patients with underlying coagulopathy.

Materials and methods

This was a hospital based prospective observational study carried out from November 2018 to October 2020 in IMS and SUM Hospital, Bhubaneswar after approval from institutional ethics committee. Based on previous literature, prevalence of coagulopathy in sepsis being around 48%, the sample size was calculated to be around 240 with 8% allowable error at 5% level of significance and 80% power of test. Patients with suspected or documented infection (via culture reports), fulfilling the criteria of Systemic inflammatory response syndrome (SIRS) were included in the study. Patients less than 16 years of age, patients admitted with trauma, surgical patients, pregnant women, and unwilling patients were excluded from the study. Detailed history regarding onset of symptoms and comorbidities was obtained. Risk factors included diabetes mellitus, hypertension, chronic kidney disease (CKD), chronic liver disease (CLD), malignancy (on treatment with either chemotherapy/ radiotherapy except palliative care), HIV infection, and ischemic heart disease (IHD). Coagulation parameters were obtained within 48 hours of admission which included platelet count, prothrombin time – international normalized ratio (PT-INR), activated partial thromboplastin time (aPTT), and other tests e.g. procalcitonin (PCT) (done as per Clinician discretion). Acute physiology and chronic health evaluation score (APACHE II) was calculated based on clinical and laboratory parameters and interpreted accordingly.[9] Patients were followed up over a period of 28 days, and 28-day mortality was noted, if any. Data obtained was categorized as mentioned in Table 1. Patient was considered to have coagulopathy even if any one of these parameters were deranged which include platelet count <1,50,000, PT-INR>1.5 times the upper limit of normal (ULN) and aPTT>1.5 times ULN.3,10 Patients admitted with septicemia having coagulation parameters deranged within 48 hours of admission were considered to have early-onset coagulopathy in our study.[11]

Table 1 Categorization of data.

Platelet count (cells/mm^3)	
>1,50,000	No thrombocytopenia
1, 50,000-75,000	Mild thrombocytopenia
75,000-50,000	Moderate thrombocytopenia
50,000-25,000	Severe thrombocytopenia
<25,000	Life-threatening thrombocytopenia
International Normalized Ratio (INR)	
Normal	
more than 1-1.5 times ULN	Grade 1 (mild derangement)
more than 1.5-2 times ULN	Grade 2 (moderate derangement)
more than 2 times ULN	Grade 3 (severe derangement)
Serum procalcitonin	
PCT<0.5 ng/mL	Local bacterial infection possible, systemic infection (sepsis) unlikely.
PCT>0.5 & <2 ng/mL	Suggests systemic infection (sepsis).
PCT>2 & <10 ng/mL	Suggests severe sepsis.
PCT>10 ng/mL	Suggests exclusively septic shock

Statistical analysis was carried out with the help of SPSS (version 20) for Windows package (SPSS Science, Chicago, IL, USA) and appropriate statistical methods were used to analyse the data. The description of the data was done in form of mean±SD for quantitative data while in the form of frequency and proportion for qualitative (categorical) data. The p values of $p<0.05$ were considered significant. For quantitative data, Student's t-test was used

to test statistical significance of difference between two independent group means. Chi square test (or Fisher's exact test in case of small frequencies in cell) was used to examine the association between patients with diabetes, chronic liver disease or chronic kidney disease and patients with and without thrombocytopenia. To determine the independent variables among various parameters like age, sex, thrombocytopenia, elevated PT-INR, aPTT and APACHE II scores on 28-day mortality, a univariate logistic regression analysis was performed, and then multivariate logistic regression was calculated to calculate the independent predictors of mortality using the 28-day mortality as the dependent factor. When appropriate, the odds ratio (OR) was calculated.

Observation and discussion

The study was conducted on 240 subjects fulfilling the inclusion and exclusion criteria. Mean age of the patients was 56.27 years (19-101, SD=15.05) in our study. Maximum number of patients (32.9%) were in 61-70 years age group followed by 23.3% patients in 71-80 years age group. There was a male preponderance (53% vs 43%). Diabetes mellitus was observed to be the most common underlying illness present in 32.5% cases followed by hypertension (HTN) in 19.6%, chronic liver disease (CLD) in 15.0%, ischemic heart disease (IHD) in 12.5% and malignancy in 11.7%. Chronic kidney disease (CKD) was present in 6.7% cases and human immunodeficiency virus (HIV) infection in 4.6% cases.

In our study we observed that 55.8% (134/240) of septicemic patients did not have thrombocytopenia whereas 20% (48/240) patients had mild thrombocytopenia, 5.8% had moderate (14/240), 12.1% (29/240) had severe and 6.3% (15/240) had life threatening thrombocytopenia within 48 hours of admission which was in concurrence with a retrospective analysis by Venkata C *et al*. in 2013, where thrombocytopenia occurred in 47.6% of the sepsis-related 304 cases admitted in ICU.[12] Most critically ill patients with a systemic inflammatory response have coagulation disorders and thrombocytopenia is often the most frequent finding.[10]

Sepsis leads to deranged coagulation, ranging from mild alterations up to severe disseminated intravascular coagulation (DIC). PT-INR levels were normal in 33% (80/240) study subjects whereas 29.6% (71/240) had mild derangement, 15% (36/240) moderate and 22.1% (53/240) had severe derangement in PT-INR value. The aPTT values were normal in 37.1% (89/240) study subjects whereas 35.4% (85/240), 19% (46/240), 8.3% (20/240) of study subjects had mild, moderate, and severe aPTT derangements respectively. Similar findings were seen in a study of 235 patients by Chakraverty *et al*. wherein INR was deranged in 66% cases.[13]

Coagulopathy was seen in 52.5% (126/240) study subjects and was absent in the rest of the study subjects. Thrombocytopenia related coagulopathy was seen in 44.1% (106/240) patients; PT-INR derangement related coagulopathy was seen in 37.08% (89/240) patients and aPTT derangement related coagulopathy was observed in 27.5% (66/240) patients.

Lower 28-day mortality, 14.1% (19/134) was observed in with patients having normal platelet counts whereas 54.16% (26/48) mortality was seen in mild thrombocytopenia, 92.85% (13/14) in moderate thrombocytopenia, 93.1% (27/29) in severe thrombocytopenia and 100% (15/15) mortality in life threatening thrombocytopenia (Figure 1). This was found to be statistically significant by using Fisher's exact test ($p<0.05$). Sharma *et al*. in their study of 69 patients with septic shock in 2007, observed that incidence of thrombocytopenia in their study was 55% and platelet count was found to be predictor of increased mortality.[14]

Patients with normal PT-INR had 3.7% (3/80) mortality whereas mortality was 22.53% (16/71) in mild PT-INR derangement, 88.8% (32/36) in moderate and 92.4% (49/53) in severe PT-INR derangement respectively, which was found to be statistically significant with Fisher's exact test ($p<0.05$) (Figure 2). Chakraverty *et al*. observed that PT-INR derangement was associated with poorer outcome in critically ill patients.[13]

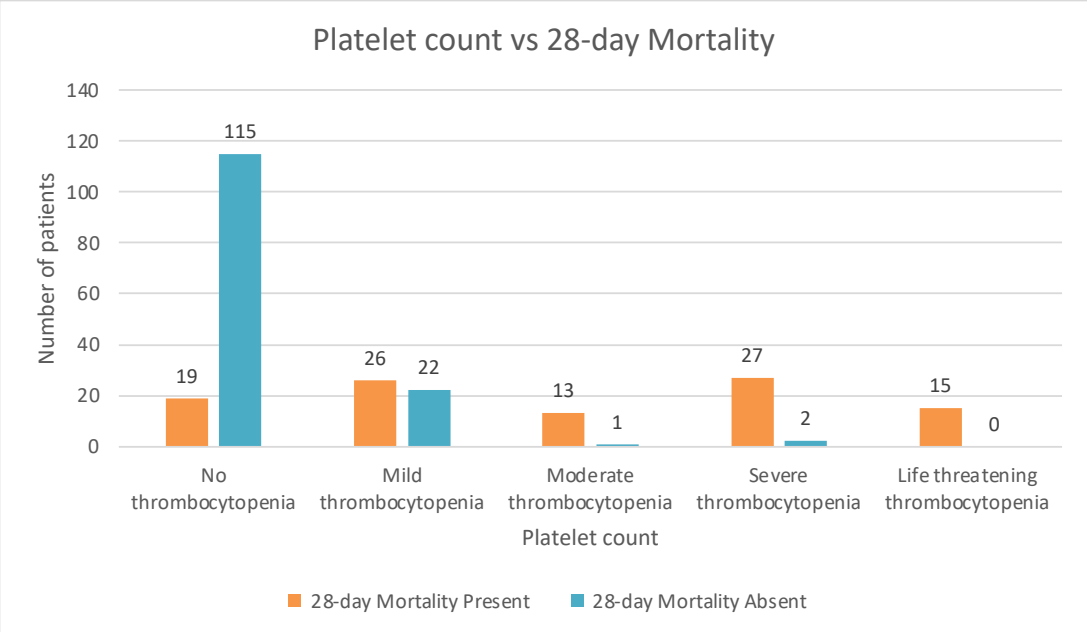

Figure 1. *Analysis of 28-day mortality with thrombocytopenia in study subjects (p<0.001).*

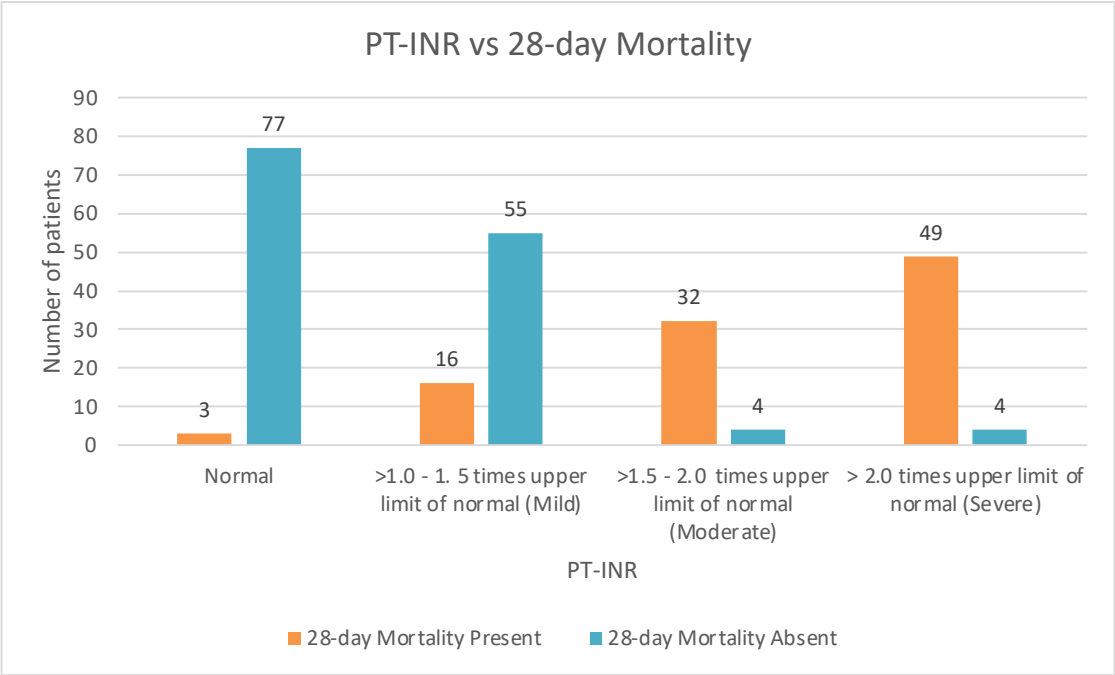

Figure 2. *Analysis of 28-day mortality with PT-INR in study subjects (p<0.001).*

Mortality was 10.1% (9/89) in patients with normal aPTT values; 34.1% (29/85) in mild aPTT derangement, 95.6% (44/46) in moderate and 90% (18/20) in severe aPTT derangement which was again statistically significant (p<0.05) (Figure 3).

28-day mortality rate was 77.77% (98/126) in patients with coagulopathy and a meagre 1.7% (2/114) in patients without coagulopathy which was statistically significant (p<0.05). Log Odd's ratio calculated using chi-square test was found to be 5.2781, 95% CI (1.633-17.321), which was highly significant.

Mortality in patients having thrombocytopenia related coagulopathy was 76.41% (81/106), and amongst non-thrombocytopenic patients was 14.1% (19/134) (Figure 4). This finding contrasted with the observation made by Venkata *et al*. in a retrospective analysis in 2013, which included 304 patients where no significant mortality difference was seen in thrombocytopenic (32.4%) and non-thrombocytopenic patients (24.5%).[11] This apparent difference could partly be explained by the presence of other coexistent abnormal coagulation parameters in our patients, however adjusted Odd's ratio was not found to be significant.

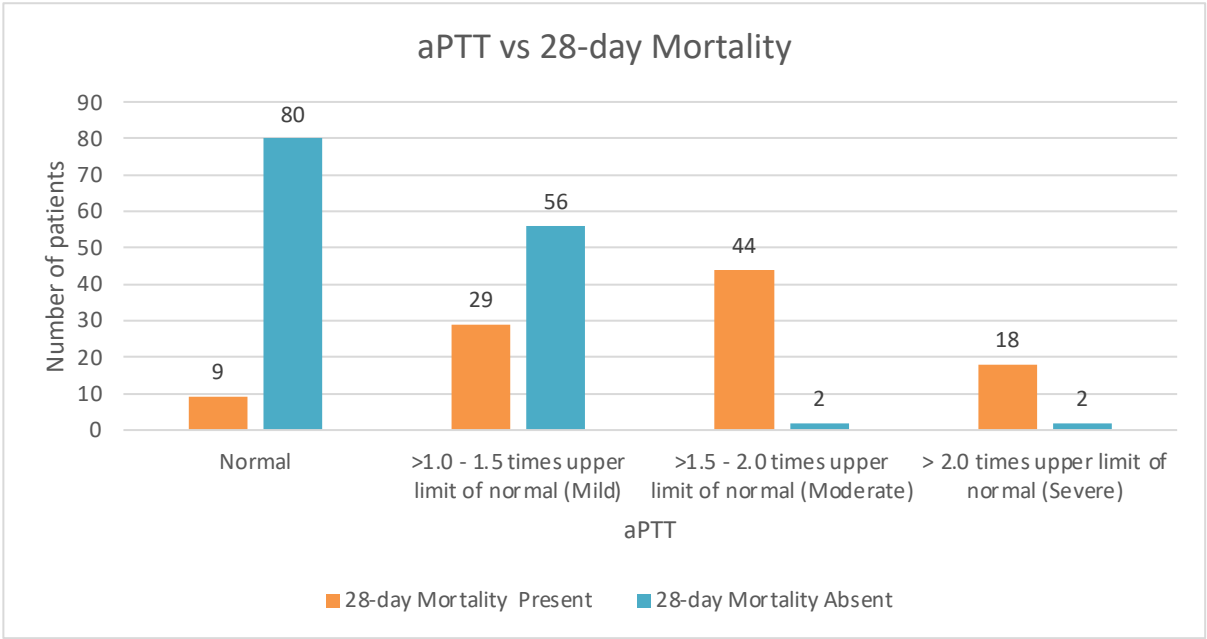

Figure 3. *Analysis of 28-day mortality with aPTT in study subjects (p<0.001).*

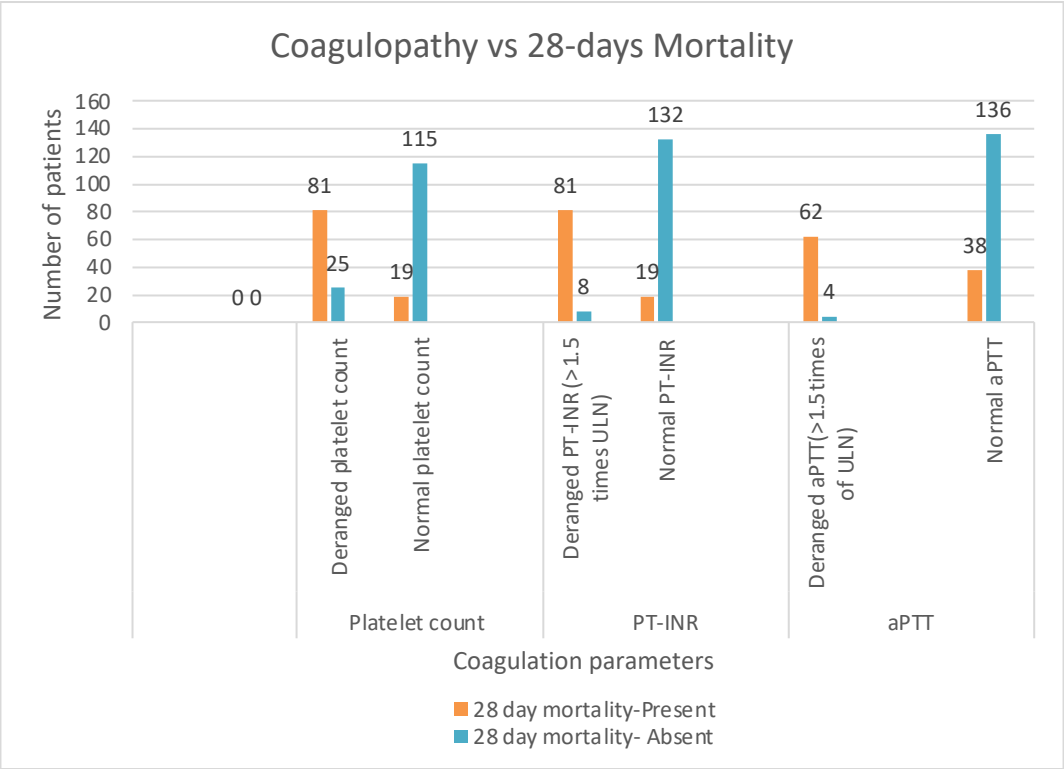

Figure 4. *Analysis of 28-day mortality with coagulopathy in relation to individual coagulation parameters in study subjects (p<0.001).*

Twenty-eigth-day mortality in patients with coagulopathy associated with PT-INR derangement was 91% (81/89) and in patients with coagulopathy associated with aPTT derangement was 93.9% (62/66) (Figure 4). Significant statistical association was observed by using Fisher's exact test (p<0.05) between 28-day mortality and coagulopathy.

In our study, 28-day mortality was seen in overall 41.7% (100/240) study subjects and remainder 58.3% (140/240) subjects survived during the 28-day follow up. Todi *et al*. in a multicentric prospective observational study conducted in India in 2010, which included 5,478 admissions, observed that the mortality rate among admissions related to sepsis was 59.26%[15]. Mortality rates seen in our study was considerably higher as compared to western literature. This difference was possibly due to sample size bias.

Measurement of procalcitonin (PCT) can be used as a marker of severe sepsis caused by bacteria and generally grades well with the degree of sepsis[16]. In our study, PCT was done in 42 subjects, at clinician's discretion, wherein 26.2% (11/42) had normal PCT levels, 9.5% had levels between 0.51-2.0 ng/ml (suggestive of sepsis), 21.4% had levels between 2.01-9.99 ng/mL (suggestive of severe sepsis) and 42.9% had levels >10 ng/mL (suggesting septic shock).[16,17] Observed mortality rate increased with higher PCT values such that no mortality 0% (0/29) was seen in subjects with normal PCT values and 100% (18/18) mortality was seen in subjects with values >10 ng/mL. Thus, high PCT level was associated with increased mortality risk. Relationship between 28-day mortality and PCT level was found to be statistically significant by Fisher's exact test (p<0.05). Similar findings were observed in 2015 by Li *et al*. in a retrospective analysis of 115 patients admitted in ICU with ventilator associated pneumonia where serum procalcitonin was found to be an independent prognostic biomarker of mortality in critically ill patients.[17] Also, relationship between PCT and coagulopathy was assessed in our study. Coagulopathy was absent i.e., 0% (0/11) in subjects with normal PCT levels; however, prevalence of coagulopathy increased to 100 % (18/18) in subjects having PCT>10.0 ng/mL. This association was also shown to be statistically significant with Fisher's exact test (p<0.05).

Mortality was also seen to increase with an increase in APACHE II score. In our study, 0 % (0/110) mortality was seen with APACHE II score 5-14 whereas 100% (91/91) mortality was seen with APACHE II score >25 (Figure 5). This association was shown to statistically significant with Fisher's exact test (p<0.05). This was in concurrence with a study conducted by Naved *et al*. which included all patients admitted to ICU wherein 84.6% deaths had APACHE II score between 31-40.[18] Desai *et al*. in a prospective study in rural ICU setting observed mortality rate of 87.5% (i.e., 21 out of 24 non-survivors) having APACHE II score >21.[19]

Presence of coagulopathy was seen to increase with an increase in APACHE II score. Coagulopathy was present in 18.18% (20/110) patients with APACHE II score 5-14, 30% (9/30) patients with APACHE II score 15-19, 66.66% (6/9) in patients with APACHE II score 20-24 and 100 % (91/91) in patients with APACHE II score >25 (Figure 5). This was found to be statistically significant using Fisher's exact test (p<0.05). This was in concurrence with a prospective multi-national clinical trial study in 2005, conducted by Dhainaut *et al*., where alteration in coagulation parameters was

associated with increased 28-day mortality rate and integrating composite coagulopathy with the APACHE II score improved the ability to predict which patients would develop multiple organ failure and die.[20]

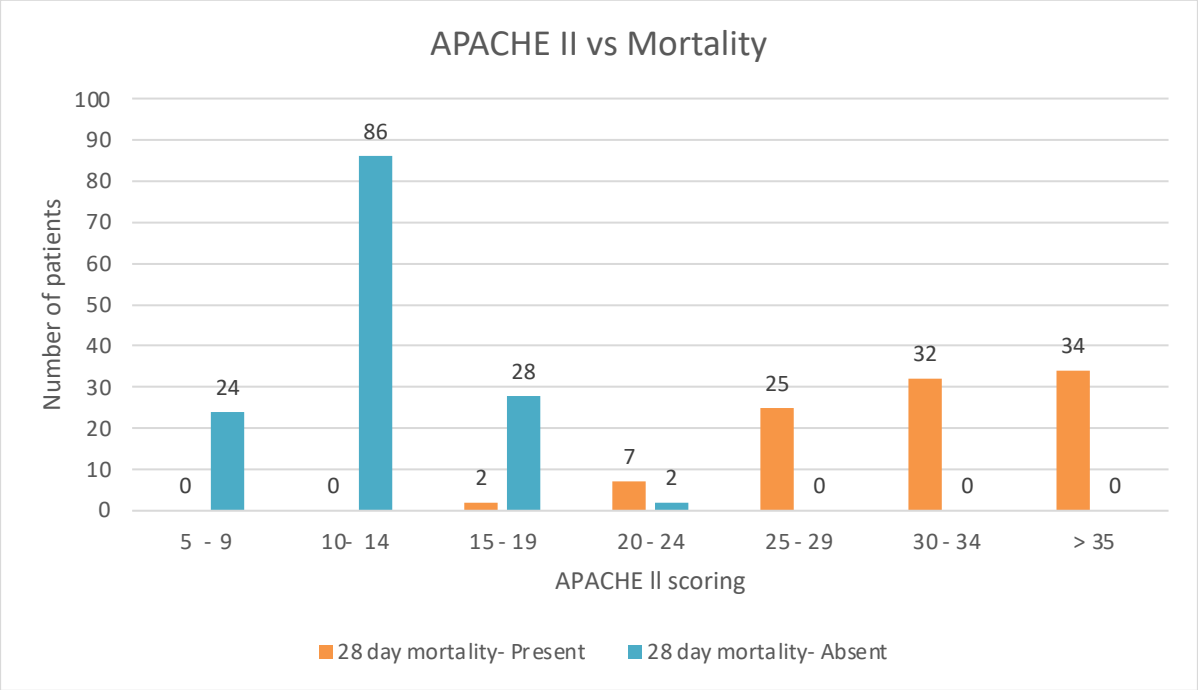

Figure 5. *Analysis of 28-day mortality with APACHE II scoring in study subjects.*

In our study, out of 126 subjects who were found to have coagulopathy, maximum mortality was seen in <40 years age group and with >60 years age group. 100% mortality was seen in age group <40 years (9/9) and 81-90 years age group (13/13), whereas 82.7% (72/87) mortality was seen in age group above 60 years. Relationship between age group and 28-day mortality was seen to be statistically significant using Fisher's exact test (p<0.05). Higher mortality rates (50-60%) was seen in elderly age group admitted with sepsis in studies conducted by Nasa *et al*. in 2012 and Martin *et al*. in 2006.[21,22] Because of its association with comorbidities, impaired immunological responses, malnutrition, greater exposure to presumably resistant strains in healthcare facilities, and increased use of medical devices such as indwelling catheters and central venous lines, the elderly age group is most likely a risk factor for mortality.[23] However, when age group less than 40 years were considered, out of 18 patient in-toto enrolled in our study, 50% (9/18) had coagulopathy, out of which 100% (9/9) died. Contrasting results were obtained by Martin *et al*. in their longitudinal observational study in 2006, involving 10,422,301 adult septicemic patients over 24 years wherein younger septicemic patients had decreased mortality rate. This difference could be due to the different sample size. Also, in our study, septicemic patients were having additional coagulopathy element were taken into consideration unlike Martin *et al* study which included only septicemic patients[21]. Younger age group patients admitted with septicemia and having additional element of coagulopathy had significantly increased mortality rate. However, we could not find any major study in previous literature to compare our findings.

In our study, 58.2% (57/98) mortality was observed in male population and 41.8% (41/98) was observed in female population. This relationship of gender with 28-day mortality was observed to be statistically significant using Fisher's exact test (p<0.05). Gender related differences in mortality rate was also seen by Adrie *et al*. and women were found to have much lower mortality rates as compared to male population.[24] The higher immune system activation, sex hormone profile and sex-related gene polymorphisms in females could probably explain this variation.[24]

The mortality rate amongst patients with coagulopathy and comorbidities were also assessed. Malignancy (28/28) and HIV (11/11) were associated with 100% mortality whereas diabetes, hypertension, CKD, IHD, CLD were found to be 89.74% (35/39), 93.75% (30/32), 91.6% (11/12), 90.9% (10/11) and 52.7% (19/36) respectively. In our study, significant proportion of patients with underlying medical illnesses developed coagulopathy followed by mortality. However, coagulopathy observed in patients with CLD was possibly related to the underlying CLD itself and hence observed mortality amongst CLD was on lower side as compared to other illnesses. Wang *et al*. in 2012 in their longitudinal study observed association between baseline chronic medical conditions and sepsis and hence they inferred that patient's comorbidities and functional health status were also important determinants of outcomes in sepsis.[25]

Univariate logistic regression for mortality showed PT-INR, aPTT and APACHE II scores to be independent variables. Multivariate logistic regression revealed severe increase in PT-INR [adjusted OR=1.622 (0.841, 3.092)], moderate increase in aPTT [adjusted OR=4.537 (0.989, 7.326)], and severe increases in aPTT [adjusted OR=3.851 (2.438,

4.996)], and APACHE II scores [adjusted OR=5.381 (1.925, 11.01)], were independently associated with 28-day mortality whereas age, sex, any severity of thrombocytopenia, mild to moderate increase in PT-INR, and mild increase in aPTT were not.

Conclusion

Early onset coagulopathy is significantly associated with increased mortality risk in septicemic patients. Septicemic patients should be screened for coagulopathy within 24-48 hours of admission in appropriate clinical scenario to predict mortality outcome and take necessary action at the earliest. Significant correlation exists between APACHE II scoring and coagulopathy. Role of PCT in septicemic patients with coagulopathy might have considerable prognostic significance. Underlying medical illnesses, age and gender are of important consideration while treating septicemic patients and hence should be carefully assessed. Younger age group patients admitted with septicemia having additional coagulopathy element may have increased mortality risk. However larger studies are required to confirm this observation on wider scale.

Limitations

Sample size was small. This being a tertiary care hospital-based study, it may induce bias by selecting more seriously ill patients which are referred from peripheral hospitals and therefore may be associated with increased mortality rate. Pregnant females and trauma related sepsis were excluded from our study. Also, differences in treatment protocols between clinicians could affect outcome and we would require large multicentric trials for reducing the bias.

References

[1] Annane D, Bellissant E, Cavaillon J-M. Septic shock. Lancet [Internet]. 2005; 365(9453): 63-78. doi.org/10.1016/S0140-6736(04)17667-8.

[2] Cohen J. The immunopathogenesis of sepsis. Nature [Internet]. 2002; 420(6917): 885-91. doi.org/10.1038/nature01326.

[3] Hunt BJ. Bleeding and coagulopathies in critical care. N Engl J Med [Internet]. 2014; 370(22): 2153. doi.org/10.1056/NEJMc1403768.

[4] Schouten M, Wiersinga WJ, Levi M, van der Poll T. Inflammation, endothelium, and coagulation in sepsis. J Leukoc Biol [Internet]. 2008; 83(3): 536–45. doi.org/10.1189/jlb.0607373.

[5] Pawlinski R, Mackman N. Cellular sources of tissue factor in endotoxemia and sepsis. Thromb Res [Internet]. 2010;125 Suppl 1:S70-3. doi.org/10.1016/j.thromres.2010.01.042.

[6] Mosad E, Elsayh KI, Eltayeb AA. Tissue factor pathway inhibitor and P-selectin as markers of sepsis-induced non-overt disseminated intravascular coagulopathy. Clin Appl Thromb Hemost [Internet]. 2011; 17(1): 80-7. doi.org/10.1177/1076029609344981.

[7] Alberti C, Brun-Buisson C, Burchardi H, Martin C, Goodman S, Artigas A, et al. Epidemiology of sepsis and infection in ICU patients from an international multicentre cohort study. Intensive Care Med [Internet]. 2002; 28(2): 108-21. doi.org/10.1007/s00134-001-1143-z.

[8] Martin GS, Mannino DM, Eaton S, Moss M. The epidemiology of sepsis in the United States from 1979 through 2000. N Engl J Med [Internet]. 2003; 348(16): 1546-54. doi.org/10.1056/NEJMoa022139.

[9] Knaus WA, Draper EA, Wagner DP, Zimmerman JE. APACHE II: a severity of disease classification system. Crit Care Med. 1985; 13(10): 818-29.

[10] Levi M, Opal SM. Coagulation abnormalities in critically ill patients. In: Surgical Intensive Care Medicine. Cham: Springer International Publishing; 2016. p. 463-71.

[11] Guitton C, Gérard N, Sébille V, Bretonnière C, Zambon O, Villers D, et al. Early rise in circulating endothelial protein C receptor correlates with poor outcome in severe sepsis. Intensive Care Med [Internet]. 2011; 37(6): 950-6. doi.org/10.1007/s00134-011-2171-y.

[12] Venkata C, Kashyap R, Farmer JC, Afessa B. Thrombocytopenia in adult patients with sepsis: incidence, risk factors, and its association with clinical outcome. J Intensive Care [Internet]. 2013; 1(1): 9. doi.org/10.1186/2052-0492-1-9.

[13] Chakraverty R, Davidson S, Peggs K, Stross P, Garrard C, Littlewood TJ. The incidence and cause of coagulopathies in an intensive care population. Br J Haematol [Internet]. 1996; 93(2): 460-3. doi.org/10.1046/j.13652141.1996.5101050.x.

[14] Sharma B, Sharma M, Majumder M, Steier W, Sangal A, Kalawar M. Thrombocytopenia in septic shock patients--a prospective observational study of incidence, risk factors and correlation with clinical outcome. Anaesth Intensive Care [Internet]. 2007; 35(6): 874-80. doi.org/10.1177/0310057-X0703500604.

[15] Todi S, Chatterjee S, Sahu S, Bhattacharyya M. Epidemiology of severe sepsis in India: an update. Crit Care [Internet]. 2010; 14(Suppl 1): P382. doi.org/10.1186/cc8614.

[16] Pfister R, Kochanek M, Leygeber T, Brun-Buisson C, Cuquemelle E, Machado MB, et al. Procalcitonin for diagnosis of bacterial pneumonia in critically ill patients during 2009 H1N1 influenza pandemic: a prospective cohort study, systematic review and individual patient data meta-analysis. Crit Care [Internet]. 2014; 18(2): R44. doi.org/10.1186/cc13760.

[17] Li B, Zhao X, Li S. Serum procalcitonin level and mortality risk in critically ill patients with ventilator-associated pneumonia. Cell Physiol Biochem [Internet]. 2015; 37(5): 1967-72. doi.org/10.1159/000438557.

[18] Naved SA, Siddiqui S, Khan FH. APACHE-II score correlation with mortality and length of stay in an intensive care unit. J Coll Physicians Surg Pak [Internet]. 2011; 21(1): 4-8. doi.org/01.2011/JCPSP.0408.

[19] Desai S, Lakhani JD. Utility of SOFA and APACHE II score in sepsis in rural set up MICU. J Assoc Physicians India. 2013; 61(9): 608-11.

[20] Dhainaut J-F, Shorr AF, Macias WL, Kollef MJ, Levi M, Reinhart K, et al. Dynamic evolution of coagulopathy in the first day of severe sepsis: relationship with mortality and organ failure. Crit Care Med [Internet]. 2005; 33(2): 341-8. doi.org/10.1097/01.ccm.0000153520.31562.48.

[21] Martin GS, Mannino DM, Moss M. The effect of age on the development and outcome of adult sepsis. Crit Care Med [Internet]. 2006; 34(1): 15-21. doi.org/10.1097/01.ccm.0000194535.82812.ba.

[22] Nasa P, Juneja D, Singh O, Dang R, Arora V. Severe sepsis and its impact on outcome in elderly and very elderly patients admitted in intensive care unit. J Intensive Care Med [Internet]. 2012; 27(3): 179-83. doi.org/10.1177/08850666-10397116.

[23] Angus DC, Linde-Zwirble WT, Lidicker J, Clermont G, Carcillo J, Pinsky MR. Epidemiology of severe sepsis in the United States: analysis of incidence, outcome, and associated costs of care. Crit Care Med [Internet]. 2001; 29(7): 1303-10. doi.org/10.1097/00003246200107000-00002.

[24] Adrie C, Azoulay E, Francais A, Clec'h C, Darques L, Schwebel C, et al. Influence of gender on the outcome of severe sepsis: a reappraisal. Chest [Internet]. 2007; 132(6): 1786-93. doi.org/10.1378/chest.07-0420.

[25] Wang HE, Shapiro NI, Griffin R, Safford MM, Judd S, Howard G. Chronic medical conditions and risk of sepsis. PLoS One [Internet]. 2012; 7(10): e48307. doi.org/10.1371/journal.pone.0048307.

Journal of Associated Medical Sciences 2022; 55 (3): 76-81

JAMS
Journal of Associated Medical Sciences

Thai-Journal Citation Index Centre (TCI) & ASEAN Citation Index (ACI)

Journal of Associated Medical Sciences

Journal homepage: https://www.tci-thaijo.org/index.php/bulletinAMS/index

Effects of aerobic dance exercise on oxidative stress and inflammatory status in abdominal obese women subjects

Suwadee Meemark[1] **Suthap Pongthaisong**[2] **Orathai Tangvarasittichai**[1*]

[1]*Chronic Diseases Research Unit, Department of Medical Technology, Faculty of Allied Health Sciences, Naresuan University, Phitsanulok Province, Thailand*

[2]*SaiNgam District Public Health Office, Ministry of Public Health, Kumpangphet Province, Thailand*

ARTICLE INFO

Article history:
Received 21 March 2022
Accepted as revised 4 July 2022
Available online 22 July 2022

Keywords:
Obese women, aerobic dance exercise, oxidative stress, hs-CRP, TNFα, IL-6

ABSTRACT

Background: Oxidative stress (OS) and inflammation have been suggested to play a pivotal role in the pathogenesis of chronic diseases. Oxidative stress and inflammatory markers (IM) may be change after regular physical exercise. However, physical activity affects the redox balance and inflammatory markers in abdominal obese (AO) women are still unclear.

Objectives: Aim of this study was to assess OS, total antioxidant and IM on before and after 2 months participation in aerobic dance exercise of 151 obese women.

Materials and methods: A total of 151 obese women [median aged=48.0 years] participated in aerobic dance exercise. All women were subjected to physical and medical examination. Venous blood samples were collected for all biochemical examination.

Results: At the end of the study, the median of glucose, triglyceride, insulin levels, Model assessment of insulin resistance, malondialdehyde, high sensitivity C-reactive protein, tumor necrosis factor α and interleukin-6 were significantly decreased (p<0.05) and high-density lipoprotein-cholesterol and total antioxidant capacity (TAC) were significantly increased (p<0.05) after participation in aerobic dance exercise. Oxidative stress, TAC and IM were involved into the adaptive metabolic changes and redox responses induced by physical exercise aerobic dance.

Conclusion: Exercise aerobic dance reduced the potential OS, IM and protects the higher risk for developing diseases in AO that pathophysiologically linked to OS and IM.

Introduction

Physical exercise is the performance of some activity induces metabolic changes including develop or maintain overall health and physical fitness. Regular exercise decreases the obesity, cardiovascular risk and chronic diseases. Exercise has been advocated as a major component in the medical management of T2DM patients to improve their health,[1] with consequent improvements in insulin sensitivity, glycemic control, lipid profile and blood pressure.[1,2] These may be caused by the most significant changes in the muscular tissue, in which the increasing energy demand and greater oxygen utilization by mitochondria.[3] Oxidative stress and inflammation have been suggested to play a central role in the pathogenesis of both diabetes and atherosclerosis.[4]

Lifestyle changes and physical exercise can reduce the risk of diabetes, cardiometabolic and many chronic diseases risk by changing in risk factors, including glucose, lipids, oxidative stress, and inflammation.[5-7] The responses to physical exercise interventions are assessed with anthropometric measurement, blood glucose, lipid profiles and inflammatory biomarkers, such as interleukin 6 (IL-6),

* **Corresponding author.**
Author's Address: *Chronic Diseases Research Unit, Department of Medical Technology, Faculty of Allied Health Sciences, Naresuan University, Phitsanulok Province, Thailand*
** **E-mail address:** orathait@hotmail.com
doi: 10.12982/JAMS.2022.027
E-ISSN: 2539-6056

tumor necrosis factor-α (TNF-α), and C-reactive protein (CRP).[8,9] In many cases, the most effective intervention to prevent or treat chronic disease is increasing physical exercise or active lifestyle; however, the molecular or cellular mechanisms by which physical exercise and activity of their effects remain poorly understood.

Herein, we assessed the blood glucose, insulin, lipid profiles, malondialdehyde, total antioxidant and inflammatory markers both at before and after an aerobic dance exercise participation in AO women subjects, to test whether different in responses after an aerobic dance exercise period may occur in these AO women subjects. We aimed to identify clinical markers that could be potentially useful for patients at risk for chronic diseases linked to oxidative stress and inflammation.

Materials and methods

Subjects:

One hundred and fifty-one women from the seven sub-districts of Sai Ngam district, Khampangpetch Province (February 2011-January 2013) were selected from the total of 428 AO subjects (waist circumference (WC) ≥80 cm) who participated in a Project of Health Survey for Protection of Hypertension and T2DM (age≥40 years).[10] All eligible participants were apparently healthy with no clinical signs of associated pathologies, no antihypertensive, antihyperglycemic medication, no history of coronary, cerebrovascular atherosclerotic disease, recurrent or a past history of psychiatric illness, end stage renal failure, cancer, infection and any life threatening diseases. They all agreed to participate a two month aerobic dance exercise (45-60 minutes) and agreed to donate blood sample both in before and after participation in the present study. All women were subjected to physical and medical examination. All participants gave written informed consent and they all agreed to participate and to provide blood sample for their health check before and after study period. The Ethics Committee of Naresuan University approved the study protocol.

Aerobic dance exercise

All 151 women were participated the aerobic dance exercise in each center of the seven sub-districts of Sai Ngam district, Khampangpetch Province. This aerobic dance exercise session proceeded for 45-60 minutes/day, 5 days/week on the 2 months study. This aerobic exercise was performed between 5:00 and 6:00 pm, participants were recommended to do 8-minute warm-up routine, which stretches and strengthens the muscles of the hips, thighs, and ankles before start into an aerobic dance exercise. After warm-up, participants will begin with a fast music (k-pop, hip-hop, pop) for bounce, bending the knees and moving the shoulders. Step one foot out to the right for a double bounce, bring it back in, and repeat to the left. Next step to the side for a single bounce and do the same on the other side. Keep the shoulders moving to this dance workout and pick up the rhythm with some quicker side steps. Move the arms even more for a total-body workout taken from the dance floor (field). Bounce the body as continue the dance workout with forward steps. Really pop those hips and raise the elbows. Follow along with this fun aerobic dance exercise workout to dance away the weight and shake out the stress.

Anthropometric and blood pressure measurement

Subjects' height, weight, and blood pressure (BP) were measured, and body mass index (BMI) was calculated. Waist circumference (WC) was measured at the midpoint between both of rib cage and the top of lateral border of iliac crest during minimal respiration. AO defined as WC≥80 cm or 31.5 inches (female).[11] Blood pressure (BP) was measured after the participants were seated and rested for 5 minutes as the mean value of at least two measurements of these participants on the same day with a Terumo digital BP monitor (ES-P110). Hypertension was defined as an average BP≥140/90 mmHg or if the participant was taking antihypertensive medications or had been diagnosed with HT.[12]

Blood sample collection and biochemical determination

Venous blood samples were collected without stasis after a 12 hr fast and a 30 min rest in a supine position. Blood specimens were processed and assayed on the central laboratory of Department of Medical Technology, Faculty of Allied Health Sciences on the same day. A serum sample from each subject was divided into four aliquots (2–3 mL each) one for automatic analyzer and other aliquots were frozen and stored at -20°C for later analysis of MDA, TAC, TNF-α and IL-6 both in before and after a study period. Fasting plasma glucose (Glu), total cholesterol (TC), triglycerides (TG), high density lipoprotein cholesterol (HDL-C) were determined by using HITACHI 912 auto-analyzer and low-density lipoprotein cholesterol (LDL-C) was calculated by Friedewald's equation, which is valid for TG values less than or equal to 400 mg/dL.

Insulin Assay

Fasting insulin levels were measured based on micro-particle enzyme immunoassay technology using Abbott reagents with Axsym system (Abbott laboratories, Illinois, USA). All participants underwent evaluation of Homeostasis model assessment (HOMA)-formula for insulin resistance index (HOMA-IR), HOMA-B (as beta cell function or insulin activity), and Quantitative Insulin Sensitivity Check Index (QUICKI; as insulin sensitivity).[13-15] HOMA-IR was defined using the following formula: fasting glucose (mmol/L) × fasting insulin (lU/mL)/22.5.

HOMA-B as formula: [20 × insulin (lU/mL)]/[glucose (mmol/L) - 3.5].

QUICKI as formula: 1/[LOG (insulin (lU/mL)] + LOG [glucose (mmol/L)].

Malondialdehyde (MDA) assay

The method is based on the formation of red (pink) chromophore following the reaction of thiobarbituric acid (TBA) with MDA and the other breakdown products of peroxidized lipids called thiobarbituric acid reactive substance. One molecule of MDA reacts with two molecules of TBA to yield a pink pigment with maximum absorption at 532 nm. This was measured by spectrophotometry using 1,1,3,3-tetraethoxypropane as standard as described previously.16 The results were expressed as µmol of MDA formed per liters of serum. Intra-assay and interassay imprecision were 3.24 and 5.78%,

respectively. The normal range of MDA was <3.5 µmol/L.

Total antioxidant (TAC) status

The method is based on formation of the $ABTS^{\bullet+}$ cation [2, 20-azinobis (3-ethylbenzothiazoline-6-sulfonic acid)] and its scavenging by antioxidant sample constituents (serum) measured by spectrophotometry at 600 nm decay of green/blue color absorption is inversely associated with antioxidant sample content and the control antioxidant is Trolox, a hydrophilic vitamin E analog.[17]

Systemic inflammation assays

The concentrations of IL-6, TNF-α determined using the ELISA assay kits purchased from Invitrogen (Carlsbad, CA). Standard curves were constructed for determination of each analyte concentration according to the manufacturers' instructions. In accordance with standard practice, a protocol provided by Invitrogen for custom assays was used with no modifications. High sensitivity CRP (hs-CRP) concentrations were determined by using latex-enhanced immunoneplelometric assay on the Hitachi 912 auto-analyzer (Roche Diagnostic, Switzerland) that has been standardized against the World Health Organization reference. The normal range of hs-CRP was <3.0 mg/L.

Statistical analysis:

The distributions of variables were expressed in median and interquartile range. Wilcoxon signed ranks tests (2-tailed non-parametric tests) were used to assess the differences between before and after of the study period. The *p* values less than 0.05 were considered statistically significant.

Results

General clinical characteristics at start and after participation of aerobic dance exercise study of these AO women are listed in Table 1. One hundred and fifty-one AO women were carried out the 2 months period of continuous aerobic dance exercise without any adverse events. During the aerobic dance exercise period, twenty-four participants dropped out from one hundred and seventy five participants of the aerobic dance exercise study. All clinical markers before and after aerobic dance exercise study are show in Table 1. After aerobic dance exercise period, we found that Glu, BUN, CT, UA, TC, TG, HDL-C, LDL-C, insulin levels, HOMA-IR, MDA, hs-CRP, TNF-α and IL-6 levels were significantly decreased ($p<0.05$), while HDL-C, TAC, HOMA-B (β-cell function) and QUICKI (insulin sense) were significantly increased ($p<0.05$), respectively as shown in Table 1.

Table 1 Categorization of data.

Variables	Before (n=151)	After (n=151)	*p* value
Age (yr)	48.0 (41.0-56.0)*	48.0 (41.0-56.0)*	
Systolic BP (mmHg)	126.0 (116.0-140.0)	126.0 (114.0-138.0)	0.336
Diatolic BP (mmHg)	80.0 (71.0-85.0)	79.0 (72.0-85.0)	0.450
BMI (kg/m^2)	26.2 (23.4-29.1)	25.7 (23.8-28.8)	0.054
WC (cm)	87.0 (80.0-94.0)	86.0 (81.0-94.0)	0.372
Glu(mmol/L)	5.28 (4.95-6.05)	4.95 (4.51-5.72)	<0.001
BUN (mmol/L)	4.64 (3.57-5.71)	3.92 (3.21-4.64)	<0.001
CT(µmmol/L)	79.56 (70.72-79.56)	79.56 (70.72-88.40)	<0.001
UA (mmol/L)	339.2 (261.8-428.4)	315.4 (267.8-392.7)	0.002
TC (mmol/L)	5.57 (2.97-6.27)	5.24 (4.64-6.19)	0.005
TG (mmol/L)	1.89 (1.29-2.98)	1.66 (1.13-2.31)	<0.001
HDL-C (mmol/L)	1.45 (1.25-1.79)	1.50 (1.32-1.75)	<0.001
LDL-C (mmol/L)	3.07 (2.42-2.68)	2.94 (2.29-3.56)	0.033
Insulin (µU/mL)	6.00 (4.00-9.50)	5.50 (3.70-8.30)	0.008
HOMA-IR	0.80 (0.50-1.30)	0.70 (0.50-1.10)	0.009
HOMA-B	69.2 (46.4-95.1)	75.0 (53.3-105.9)	0.006
QUICKI (insulin sensitivity)	123.8 (75.7-189.3)	143.4 (89.8-205.0)	0.002
MDA (µmol/L)	4.67 (3.82-5.78)	4.50 (3.66-5.50)	0.007
TAC (µmol TroloxEquiv/L)	564.0 (407.4-774.2)	547.0 (423.0-787.0)	0.006
hs-CRP (mg/L)	2.36 (0.95-5.84)	2.16 (0.97-4.26)	<0.001
TNF-α (pg/mL)	3.58 (2.21-4.98)	3.14 (2.13-4.58)	0.004
IL-6 (pg/mL)	2.78 (1.21-3.74)	2.01 (1.12-3.00)	<0.001

**Data are median (interquartile range) of variables with a skewed distribution.*

Discussion

AO is the one major risk factor of metabolic syndrome (MetS), which a cluster of cardiovascular risk factors characterized by visceral obesity, dyslipidemia (low levels of HDL-C and elevated TG levels), hypertension, glucose intolerance, and also demonstrated by insulin resistance and low-grade inflammation with increased adipokine production.[10] Our study demonstrated that AO women were elevated in BP, BMI, WC, Glu, TG and LDL-C, insulin, insulin resistance, MDA, TNF-α, IL-6, hs-CRP, and decreased in HDL-C, insulin sensitivity (QUICKI), β-cell function (HOMA-B) and TAC at the beginning time. MDA is a lipid peroxidation marker which results from increased oxidative stress in AO subjects.[10] More important of ROS elevation may cause damage of macromolecules and produce cytotoxic end products.[18,19] Vascular oxidative stress caused activation of systemic inflammatory pathways that play a major role in the pathogenesis of CVD. Total antioxidant status is a measurement of the net balance of the interactions between ROS and antioxidants in circulation, assessing the ability of the antioxidants to inhibit the specific radical formation.[20] This method provides an overall measure of antioxidant status and does not give information on the specific species of antioxidants. OS or increased free radical generation leads to inflammation, lipid peroxidation and macro-molecules damage, which are associated with the onset of various pathological conditions, such as cardiovascular disease (CVD), diabetes mellitus, cancer, and obstructive pulmonary disease.[21,22]

Adipose tissue produces numbers of adipokines and cytokines such as adiponectin, leptin, TNF-α and IL-6. IL-6 has been suggested to promote hs-CRP production from the liver as a biomarker of the sub-clinical inflammation related to obesity.[23] Hs-CRP is a sensitive marker of low-grade inflammation that is not only associated with insulin resistance, but also predicted the development of MetS, T2DM, hypertension and CVD.[24,25] Furthermore, cardiovascular morbidity and mortality is increased in patients with elevated CRP levels.[26] After 2 months participation in aerobic dance exercise, these AO women were demonstrated decreased in GLU, UA, TC, TG, LDL-C, MDA, TNF-α, IL-6, hs-CRP, insulin, insulin resistance while increased in HDL-C, insulin sensitivity (QUICKI), β-cell function (HOMA-B) and TAC without weight loss. Physical activity and exercise training increase energy expenditure and reduce body fat and visceral fat, even with/without weight loss,[27,28] and caused the reduction of IL-6 and TNF-α,[29-31] as in the same of present study (shown in Table 1). Moreover, exercise or physical activity also induces adiponectin production from adipose tissues.[32-34] It exerts antiapoptotic, anti-inflammatory, and antioxidative activities.[35,36]

On the other hand, many studies of the interventional studies and randomized controlled trials demonstrate did not significantly effect of regular aerobic exercise on the systemic inflammatory biomarkers in adults [37-39] and the regular aerobic exercise did not reduce CRP levels.[40] The effects of physical exercise may depend on the type of activity (aerobic/resistance), intensity (mild/moderate/intense/exhaustive), and frequency (sessions per day/week/month) of the physical exercise and may also on the individual's characteristic (age, endurance capacity, and health status).

In conclusion, our finding demonstrated the benefits of aerobic dance exercise on various physiological benefits, through its energy expenditure, Glu, lipid profiles, antioxidant and anti-inflammatory actions. The inflammatory actions of exercise are mainly exerted on adipose tissue of the AO women subjects. Then regular aerobic dance exercise exerts the most substantial anti-inflammatory, antioxidant, energy expenditure effects in individuals having high risk in these biomarkers, particularly AO subjects.

Acknowledgements

We sincerely thank National Health Security office (NHSO), Region 3's Blog (Nakornsawan) for financial support. We specially thank all co-workers of the Sai-Ngam Subdistrict Health Promotion Hospitals for their regulated aerobic dance exercise, blood collection and technical assistance in each sub-district. And also thank for those who participated and donated blood samples for this study. Finally, we sincerely thank Asst. Prof. Dr. Ronald A. Markwardt, Faculty of Public Health, Burapha University, for his critical reading and correcting of the manuscript.

Declaration of interest

none

References

[1] Stewart KJ. Role of exercise training on cardiovascular disease in persons who have type 2 diabetes and hypertension. Cardiol Clin. 2004; 22(4): 569-86.

[2] Hu G, Jousilahti P, Barengo NC, Qiao Q, Lakka TA, Tuomilehto J. Physical activity, cardiovascular risk factors, and mortality among Finnish adults with diabetes. Diabetes Care. 2005; 28: 799-805.

[3] Barbieri E, Sestili P. Reactive oxygen species in skeletal muscle signaling. J Signal Transduct. 2012; doi: 10.1155/2012/982794.

[4] Willerson JT, Ridker PM. Inflammation as a cardiovascular risk factor. Circulation. 2004; 109: II2-10.

[5] Bateman LA, Slentz CA, Willis LH, Shields AT, Piner LW, Bales CW, et al. Comparison of aerobic versus resistance exercise training effects on metabolic syndrome (from the Studies of a Targeted Risk Reduction Intervention Through Defined Exercise -STRRIDE-AT/RT). Am. J. Cardiol. 2011; 108(6): 838-44.

[6] Huffman KM, Slentz CA, Bateman LA, Thompson D, Muehlbauer MJ, Bain JR, et al. Exercise induced changes in metabolic intermediates, hormones, and inflammatory markers associated with improvements in insulin sensitivity. Diabetes Care. 2011; 34(1): 174-6.

[7] Slentz CA, Bateman LA, Willis LH, Granville EO, Piner LW, Samsa GP, et al. Effects of exercise training alone vs a combined exercise and nutritional lifestyle intervention on glucose homeostasis in prediabetic individuals: a randomised trial. Diabetiologia. 2016; 59 (10): 2088-98.

[8] Gleeson M, Bishop NC, Stensel DJ, Lindley MR, Mastana SS, Nimmo MA. The anti-inflammatory effects of exercise: mechanisms and implications for the prevention and treatment of disease. Nat Rev Immunol. 2011; 11(9): 607-15.

[9] Walsh NP, Gleeson M, Shephard RJ, Gleeson M, Woods JA, Bishop NC, et al. Position statement. Part one: Immune function and exercise. Exerc Immunol Rev. 2011; 17(17): 6-63.

[10] Tangvarasittichai S, Pongthaisong S, Tangvarasittichai O. Tumor Necrosis Factor-α, Interleukin-6, C-Reactive Protein Levels and Insulin Resistance Associated with Type 2 Diabetes in Abdominal Obesity Women. Ind J Clin Biochem. 2016; 31(1): 68-74.

[11] Alberti KG, Zimmet P, Shaw J. Metabolic syndrome-a new world-wide definition. A consensus statement from the International Diabetes Federation. Diabet Med. 2006; 23: 469-80.

[12] World Health Organization-International Society of Hypertension. World Health Organization-International Society of hypertension guidelines for the management of hypertension. Guidelines Subcommittee. J Hypertens. 1999; 17(2): 151-83.

[13] Duncan MH, Singh BM, Wise PH, Carter G, Alaghband-Zadeh J. A simple measure of insulin resistance. Lancet. 1995; 346: 120-1.

[14] Matthews DR, Hosker JP, Rudenski AS, Naylor BA, Treacher DF, Turner RC. Homeostasis model assessment: insulin resistance and beta-cell function from fasting plasma glucose and insulin concentrations in man. Diabetologia. 1985; 28: 412-9.

[15] Haffner SM, Kennedy E, Gonzalez C, Stern MP, Miettinen H. A prospective analysis of the HOMA model. The Mexico City Diabetes Study. Diabetes Care. 1996; 19: 1138-41.

[16] Tangvarasittichai S, Poonsub P, Tangvarasittichai O, Sirigulsatien V. Serum levels of malondialdehyde in type 2 diabetes mellitus Thai subjects. Siriraj Med J. 2009; 61: 20-3.

[17] Miller NJ, Rice-Evans C, Davies MJ, Gopinathan V, Milner A. A novel method for measuring antioxidant capacity and its application to monitoring the antioxidant status in premature neonates. Clin Sci (Lond). 1993; 84: 407-12.

[18] Dvora´kova´-Lorenzova´ A, Sucha´nek P, Havel PJ, Stavek P, Karasova L, Valenta Z, et al. The decrease in C-reactive protein concentration after diet and physical activity induced weight reduction is associated with changes in plasma lipids, but not interleukin-6 or adiponectin. Metabolism. 2006; 55: 359-65.

[19] Cai H, Harrison DG. Endothelial dysfunction in cardiovascular diseases: the role of oxidant stress. Circ Res. 2000; 87: 840-4.

[20] Morrell CN. Reactive oxygen species: finding the right balance. Circ Res. 2008; 103: 571-2.

[21] Mercken EM, Hageman GJ, Schols AM, Akkermans MA, Bast A, Wouters EF. Rehabilitation decreases exercise-induced oxidative stress in chronic obstructive pulmonary disease. Am J Respir Crit Care Med. 2005; 172: 994-1001.

[22] Cases N, Sureda A, Maestre I, Tauler P, AquiloÂ A, CoÂrdova A, et al. Response of antioxidant defences to oxidative stress induced by prolonged exercise: antioxidant enzyme gene expression in lymphocytes. Eur J Appl Physiol. 2006; 98: 263-9.

[23] Niskanen L, Laaksonen DE, Nyysso¨nen K, Punnonen K, Valkonen VP, Fuentes R, et al. Inflammation, abdominal obesity, and smoking as predictors of hypertension. Hypertension. 2004; 44: 859-65.

[24] Grundy SM, Cleeman JI, Daniels SR, Donato KA, Eckel RH, Franklin BA, et al. Diagnosis and management of the metabolic syndrome: An American Heart Association/ National Heart, Lung, and Blood Institute Scientific Statement. Circulation. 2005; 112: 2735-52.

[25] Laaksonen DE, Niskanen L, Nyysso¨nen K, Punnonen K, Tuomainen TP, Valkonen VP, et al. C-reactive protein and the development of the metabolic syndrome and diabetes in middleaged men. Diabetologia. 2004; 47: 1403-10.

[26] Ridker PM, Buring JE, Cook NR, Rifai N. C-reactive protein, the metabolic syndrome, and risk of incident cardiovascular events: an 8-year follow-up of 14 719 initially healthy American women. Circulation. 2003; 107: 391-7.

[27] Giannopoulou I, Ploutz-Snyder LL, Carhart R, Weinstock RS, Fernhall B, Goulopoulou S, et al. Exercise is required for visceral fat loss in postmenopausal women with type 2 diabetes. J Clin Endocrinol Metab. 2005; 90(3): 1511-8.

[28] Ross R, Bradshaw AJ. The future of obesity reduction: beyond weight loss. Nat Rev Endocrinol. 2009; 5(6): 319-26.

[29] Forsythe LK, Wallace JMW, Livingstone MBE. Obesity and inflammation: the effects of weight loss. Nutr Res Rev. 2008; 21(2): 117-33.

[30] Trøseid M, Lappegård KT, Claudi T, Damås JK, Mørkrid L, Brendberg R, et al. Exercise reduces plasma levels of the chemokines MCP-1 and IL-8 in subjects with the metabolic syndrome. Eur Heart J. 2004; 25(4): 349-55.

[31] Lambert CP, Wright NR, Finck BN, Villareal DT. Exercise but not diet-induced weight loss decreases skeletal muscle inflammatory gene expression in frail obese elderly persons. J Appl Physiol. 2008; 105(2): 473-78.

[32] Mujumdar PP, Duerksen-Hughes PJ, Firek AF, Hessinger DA. Long-term, progressive, aerobic training increases adiponectin in middle-aged, overweight, untrained males and females. Scand J Clin Lab Invest. 2011; 71(2): 101-7.

[33] Lee S, Park Y, Dellsperger KC, Zhang C. Exercise training improves endothelial function via adiponectin dependent and independent pathways in type 2 diabetic mice. Am. J. Physiol-Heart Circ Physiol. 2011; 301(2): H306-H314.

[34] Yu Z, Ye X, Wang J, Qi Q, Franco OH, Rennie KL, et al. Associations of physical activity with inflammatory factors, adipocytokines, and metabolic syndrome in middle-aged and older chinese people. Circulation. 2009; 119(23): 2969-77.

[35] Hui X, Lam KS, Vanhoutte PM, Xu A. Adiponectin and cardiovascular health: an update. Br J Pharmacol. 2012; 165(3): 574-90.

[36] Andrade-Oliveira V, Câmara NOS, Moraes-Vieira PM. Adipokines as drug targets in diabetes and underlying disturbances. J Diabetes Res. 2015; 681612: 11.

[37] Beavers KM, Brinkley TE, Nicklas BJ. Effect of exercise training on chronic inflammation. Clin Chim Acta. 2010; 411(11-12): 785-93.

[38] Rauramaa R, Halonen P, Väisänen SB, Lakka TA, Schmidt-Trucksäss A, Berg A, et al. Effects of aerobic physical exercise on inflammation and atherosclerosis in men: the DNASCO study: a six-year randomized, controlled trial. Ann. Intern. Med. 2004; 140(12): 1007-14.

[39] Marcell TJ, McAuley KA, Traustadóttir T, Reaven PD. Exercise training is not associated with improved levels of C-reactive protein or adiponectin. Metab Clin Exp. 2005; 54(4): 533-41.

[40] Kelley GA, Kelley KS. Effects of aerobic exercise on C-reactive protein, body composition, and maximum oxygen consumption in adults: a meta-analysis of randomized controlled trials. Metab Clin Exp. 2006; 55(11): 1500-7.

Journal of Associated Medical Sciences 2022; 55 (3): 82-90

JAMS
Journal of Associated Medical Sciences

Thai-Journal Citation Index Centre (TCI) & ASEAN Citation Index (ACI)

Journal of Associated Medical Sciences

Journal homepage: https://www.tci-thaijo.org/index.php/bulletinAMS/index

Efficacy of metacognitive strategy training on reducing disability of post-stroke survivor: A pilot study

Kshanaprava Mohakud[1] Samir Sahu[2] Sakti Prasad Das[3] Surjeet Sahoo[4*]

[1]Occupational Therapy, MOT (Rehabilitation), Department of Occupational Therapy, Swami Vivekanand National Institute Rehabilitation Training and Research, Cuttack-754010, Odisha, India.
[2]Department of Medicine, IMS & SUM Hospital, Siksha O Anusandhan (deemed to be) University, Bhubaneswar, Odisha, India.
[3]Swami Vivekanand National Institute Rehabilitation Training and Research, Cuttack, Odisha, India.
[4]Department of Psychiatry, IMS & SUM Hospital, Siksha O Anusandhan (deemed to be) University, Bhubaneswar, Odisha, India.

ARTICLE INFO

Article history:
Received 8 March 2022
Accepted as revised 14 July 2022
Available online 3 August 2022

Keywords:
Stroke, rehabilitation, metacognitive strategy training, independence, disability

ABSTRACT

Background: Post-stroke survivors experience significant challenges with their functional health. Despite advances in neuro-rehabilitation, they cannot participate in meaningful daily life activities, leading to disability. Many intervention approaches are applied in stroke rehabilitation to make them independent and lead a quality life.

Objectives: The objective of this pilot study was to investigate the effect of the Metacognitive Strategy Training (MCST) on Conventional Occupational Rehabilitation Therapy on improving independence and reducing the disability of post-stroke survivors.

Materials and methods: Thirty subjects with post-stroke syndrome participated in an exploratory, double-blind, randomized controlled trial with pre-post and follow-up studies. Subjects were randomized over two intervention groups. Group-1 received MCST with conventional therapy (n=15), and Group-2 conventional therapy only (n=15). The Functional Independence Measure (FIM) measures independence at baseline (Time1), post-intervention (Time2), and after six months (Time3).

Results: Changes in Functional Independence Measure scores for the two groups over six months showed significant effects of group ($F(1,24)=9.422$, $p<0.005$), time ($F(1.160, 27.848)=21.449$, $p<0.0001$) but time and group interaction was not significantly affected ($F(1.160, 27.848)=0.172$, $p=0.719$). Post hoc analysis with a Bonferroni adjustment revealed that FIM was statistically significantly increased from pre-intervention to post-intervention (22.597 (95% CI, 34.511 to 10.683), $p<0.0001$), and from pre-intervention to six month follow up. (24.203 (95% CI,37.554 to 10.853), $p=0.0001$), but not from post-intervention to six months (1.606 (95% CI, -5.988 to 2.776), $p=1.000$).

Conclusion: MCST has better efficiency in reducing disability and improving the independence of post-stroke survivors in the long term.

* **Corresponding author.**
Author's Address: *Department of Psychiatry, IMS & SUM Hospital, Siksha O Anusandhan (deemed to be) University, Bhubaneswar, Odisha, India.*
** **E-mail address:** surjeetsahoo@gmail.com
doi: 10.12982/JAMS.2022.028
E-ISSN: 2539-6056

Introduction

Stroke, the life-changing syndrome, causes sensorimotor, language, and cognitive impairment, which varies on the severity of damage.[1,2] Though there are many advances in neuro-rehabilitation, half of the post-stroke survivor depends on others for their activities of daily living (ADL) as they cannot achieve their functional goals.[3] The limitations in ADL and constraints for meaningful participation in social goals leads to disability of post-stroke individual.[4] It is the fourth leading cause of disability and the fourth-highest burden of disease worldwide (WHO).[5]

Many intervention strategies have been adopted to improve the ADL of post-stroke survivors. Evidence suggests that the conventional approach used for stroke rehabilitation is only confined to improving the particular task trained to the individual after repetitive practices.[6,7] Also, the retention effect of the learned skills is not consistently maintained in the long term.[8,9] The conventional approach lacks the scope for generalization and transferring learned skills to other tasks or contexts to improve the ADL.[10] To overcome this, the novel metacognitive strategy training is applied in stroke rehabilitation.

Metacognitive strategy training (MCST), or strategy training, is a top-down holistic approach that helps to improve ADL and occupational performance and maintains the post-stroke individual's independence. MCST does not focus on the participant's impairment, causing the performance limitation as in the conventional approach.[11] The approach uses meaningful activities as the basis of the end goal of the intervention.[12] It combines theory and evidence of motor, cognitive sciences, and learning principles in a client-centred framework. In this performance-based problem-solving approach, the client learns and acquiesces skills to maintain independence. This process incorporates the strategy of goal-plan-do-check through guided discovery.[13,14] In the MCST intervention process, the client identifies the challenging activities according to their importance. With the help of the therapist, the client sets realistic goals, plans the steps to achieve the goals, then performs the activities, and finally checks the mistakes and rectifies himself. Then the client practices the task in a correct pattern repetitively. During the intervention process, the therapist facilitates learning of the client through prompting, cueing, and questions rather than direct teaching, unlike the conventional approach. By this strategy, the participants go through a personalized assessment of ADL and social goals of real life problems and learn to use these techniques for other untrained new activities and situations through self-monitoring. Hence MCST improves independence in daily activities and promotes participation in meaningful activities leading to continued improvement rather than further deterioration in the long term.[15,16]

The concepts and theories underlying MCST are experience-dependent neuroplasticity which suggests that learning new skills leads to structural and functional changes in the brain.[17] For example, the experience-dependent neuroplasticity causes the enhanced growth of the hippocampal area in music learners. The sensorimotor network changes in dancers occur as they perform the activity repetitively.[18-20] As a result, the experience-dependent neuroplasticity helps the clients re-engage in occupation with the changes in the brain.[21,22] Therefore, the MCST intervention targets the improvement of performance and activity participation which will help for impairment reduction within specific cognitive domains of the participants. MCST approach directly affects the action of the frontoparietal network of our brain. The cognitive control network involves flexible moment-to-moment task control and reflects compositional coding to enable the transfer of knowledge to novel tasks.[23,24]

Previous reports suggest there are escalating pieces of evidence for MCST on the improvement of functional outcomes of post-stroke survivors.[11,15,25–29] Also, shreds of evidence suggest that MCST has more significant improvements in the vocational and community outcomes of the post-stroke individual.[10,11,13,14,24,27,28,30–32] Hence our study has hypothesized that "MCST has a significant effect in improving functional independence and reduction of disability of stroke survivors". The objective of our study is to investigate and compare the efficacy of MCST on conventional therapy on the functional independence and reduction of disability of the post-stroke survivors.

Materials and methods

The study design was an explorative, randomized; double-blind controlled pilot trial. The participants were selected from two centers; a tertiary care hospital and a tertiary care rehabilitation institute. After selection, for allocation of groups, participants were randomized to receive either the conventional occupational therapy or the MCST occupational therapy. The inclusion criteria of the participants for the study were based on the diagnosis of first onset subacute and chronic stroke age 18 to 60 years diagnosed by a neurologist. The client is medically stable (afebrile, with stable vital signs, without essential changes in medical conditions or required changes in treatments within 48 hours before assessment, with functional limitations, being able to take adequate nutrition orally), with sufficient language skills to understand and respond to primary interview and questionnaires.

The exclusion criteria were the followings:

1. Participants of acute post-stroke (less than 15 days), Stroke Patients with comorbidities and other neurological diagnoses like multiple sclerosis, motor neuron disease, and Parkinson's disease.
2. Patients having psychiatric diseases like dementia, current bipolar disorder, major depressive disorder, or psychotic disorder were excluded from this study. The patients having cognitive impairment (screened by MMSE, score <24), aphasia (both receptive and expressive), and vision abnormalities (e.g., diplopia).
3. Patients having alcoholic substances were not included in the study.
4. The participants participate less than 80% of the intervention program or did not follow up were excluded from the study.

To maintain and confirm the balanced group sizes blocked randomization of ratio 1:1 procedure was used

from each site. The random number function in Excel (Microsoft Corporation, Microsoft Excel 2010, Version 14.0.) was used to create a random sort order within each block. To ensure allocation concealment, we created sequentially numbered sealed opaque envelopes with the support of an external therapist who was not associated with the study. After reviewing all inclusion/exclusion criteria and getting consent from the patients, the treatment group allocation was completed. The treating therapist was blinded to the randomization procedure and block size. The ethical committee approved the study at the university.

Assessment and intervention procedures

After the recruitment of participants, the baseline assessment was conducted by one of the authors, who was blinded to group allocation. Before starting therapy, the occupational therapist conducted a goal-setting interview using the Canadian Occupational Performance Measure (COPM) for both groups. The participants spell out 4 to 6 meaningful functional activity goals prioritizing their importance. The experimental MCST intervention was based on CO-OP treatment guidelines.[33] The duration of the intervention MCST group was 45 minutes in each session for a minimum of 3 sessions and a maximum of 5 sessions in a week. Each participant was given a maximum of 10 sessions of MCST therapy. Among the selected goals, only three goals were trained, and the rest untrained activities were kept for the transfer of skills for the experimental group. The therapist trained participants on the global cognitive strategy goal-plan-do-check.

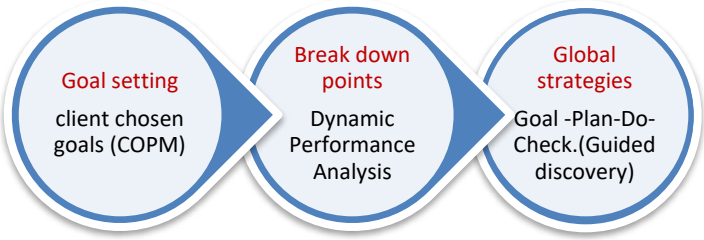

Figure 1. *Intervention process of MCST group.*

The MCST intervention procedure consists of the key principles such as goal setting, Dynamic Performance analysis and global strategies (Figure.1). The participants used this strategy during the treatment procedure as the fundamental concept of the problem-solving framework, which enabled identifying domain-specific strategies, acquiring skills, and achieving goals. The therapist guided the participants in discovering a plan to achieve the goals for their individualized prioritized tasks. The participants performed the activities as per the plan and then checked whether the plan had worked as expected. If the goal was not achieved, the therapist facilitated the participants to modify the plan or the alternative methods to reach the goal. In every new plan, the participant repeats the strategy Do-Check cycle till the achievement of the goal. The therapist regularly gives opportunities to participants and facilitates the generalization of skills and strategies in different contexts and environments. During this whole procedure, the participants were provided with a workbook and materials to note the critical points for achieving individualized goals. At the end of each session, the therapists prompted the participants to identify critical principles they learned and discuss methods for applying these principles in subsequent sessions. Then the participants checked whether the plan worked or required reviewing. The these steps were repeated iteratively until the goals were achieved.

The control group was given conventional therapy, a combination of component-based therapy, and task-specific training. The therapy is based on impairment-level or component-level treatment (e.g., ROM, muscle strength, muscle tone, synergy, etc.) and techniques with short-term goals evaluated by the therapist and managed by direct training and whole-activity treatments. In the control group, participants engaged in a facilitated discussion with the therapists, who used already transcribed, open-ended questions to encourage the participants' rehabilitation experiences.

Both the MCST and the control groups also received stroke rehabilitation with specific services as per the individual needs like physical therapy, speech-language therapy, or nursing.

Outcome measures

The measurement of the study was done through the functional independence measure (FIM) and the demographic characteristics of all the participants. Demographic (age, gender, education, occupation) were collected through personal interviews and medical information (stroke onset, sub-type, stroke-affected side, area of lesion) from the patients' medical records that were included in the study. One of our authors, who was blinded to group allocation, conducted a standardized assessment before the intervention at starting Time 1), after 2 weeks of discharge from occupational therapy at two months (Time 2), and six months after Time 1 (Time 3). As the number of intervention sessions varied among participants based on the severity of their stroke and their individual

rehabilitation needs, the therapists or the administrative staffs were asked to inform the authors when the participant was discharged from occupational therapy after the completion of 12 sessions or 6 weeks of therapy, whichever came first. Time 2 assessments were performed for 15 days or two weeks after intervention for both groups to give community exposure to the participants.

The functional Independence Measure (FIM) assesses and grades functional independence. It is an eighteen-items questionnaire, and it measures physical and cognitive function and the level of independence and disability of an individual. It is a Likert type of 7-point scale and graded in descending order as -7. Complete Independence (Safety and Timely), 6-Modified independence (with the help of device), 5-Helper-Modified Dependence with Supervision, 4- Minimal Assistance (subjects performs75% of task), 3-Moderate Assistance (subjects performs 75% of task), 2-Maximal Assistance (subjects performs50% of task), 1-Total Assistance or entirely dependent. The internal consistency in 96.9% of tests and item discriminant validity in 100% of tests. The validity and reliability of FIM are maintained for assessing independence in people with stroke, and the reliability coefficients for each impairment category for both subscales ranged from 0.86 to 0.97.[34,35]

Data Analysis

Data were analyzed by SPSS Version 17.0 (SPSS Inc., Chicago), and the significance level for all tests was set at $p<0.05$. The normality of data was confirmed using Shapiro-Wilk's test. To examine baseline between-group differences, independent sample t-tests were used for continuous data and x^2 (chi-square) for categorical data. Between-group baseline comparisons were made on age, gender, education, and FIM scores. Means and standard deviations were calculated for both groups for the primary outcome measure, FIM. We used repeated measure ANOVA to examine the participant's independence in daily activities (FIM scores) improved over time at three-time points (from baseline to three months and six months and three months to six months) with different intervention assignments (MCST & conventional). Wilk's lambda was calculated followed by appropriate Mauchly's test of sphericity, and pairwise comparison between time, group, and time group interaction was compared with a significance level less than 0.05. Post hoc analysis with a Bonferroni adjustment was done for multiple comparisons.

Results

From the flow of the study procedure, fifty-six participants enrolled in the study (Figure 2). Of these, 17 participants were excluded because they did not meet eligibility criteria, and 3 participants withdrew during the screening process before randomization. Thus, we randomized 36 participants to the intervention, 18 in each group. Six participants could not continue at least 80% of the intervention program. Hence only thirty participants are considered for the study (Figure 2).

Our study found 73.3% male and 26.7% female in the experimental group and 91% male and 9% female in the control group. The mean age is 46.42±9.88 and 44.81±11.25 for the experimental group & control group, respectively. The mean year of education is 13.46±3.99 and 13.23±3.93for the experimental group & control group, respectively. Mostly ischemic left side affection hemiplegia participated in both groups in our study. The mean stroke duration was 13.30±15.33& 12.74±14.81 for the experimental group & control group, respectively. All the participants were right-handed in the experimental group, and 91% were right-handed in the control group. Both groups did not differ in baseline criteria (Table 1). Table 2 represents FIM's mean and standard deviation between the groups at different time points.

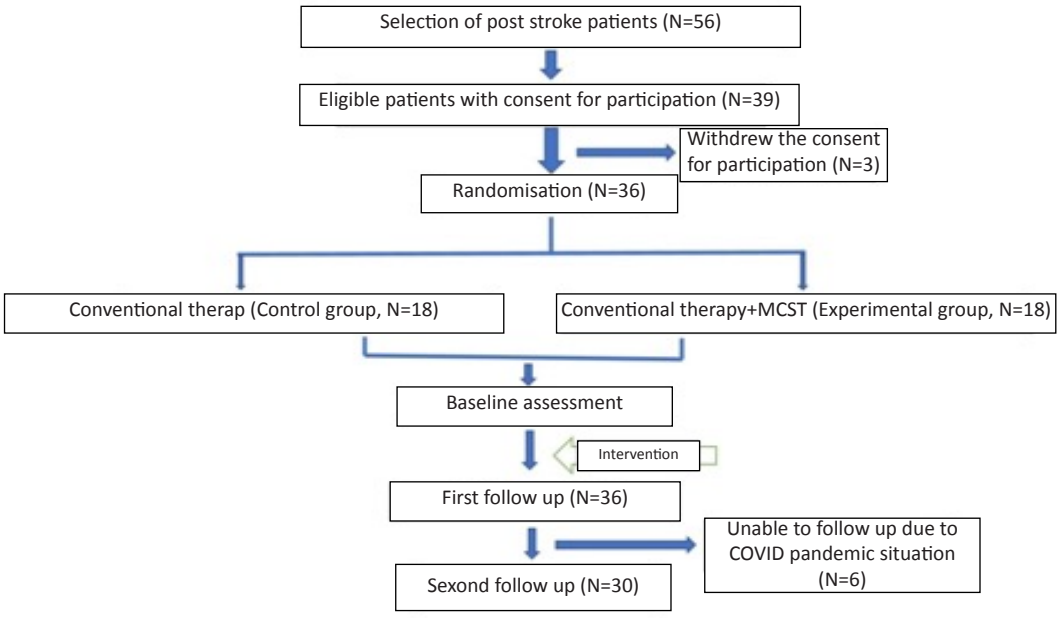

Figure 2. *Flow diagram of study procedure.*

Table 1 Socio demography data.

Variables	Experimental Group (n=15)	Control Group (n=15)	
Age			
Mean±SD	46.42±9.88	44.81±11.25	T=0.065, *p*=0.437
Gender			
Male	73.3%	91%	X^2=1.262, *p*=0.261
Female	26.7%	9%	
Year of education			
Mean±SD	13.33±4.065	12.55±3.04	T=0.508, *p*=0.616
Affection side			
Left. side	80%	55%	X^2=1.930, *p*=0.165
Right. Side	20%	45%	
Subtype stroke			
Hemorrhagic	27%	36%	X^2=0.280, *p*=0.597
Ischemic	73%	64%	
Stroke duration (month)			
Mean±SD	13.30±15.33	12.74±14.81	T=0.863, *p*=0.397
Type of stroke			
Acute	73%	73%	X^2=0.140, *p*=0.647
Chronic	27%	27%	
Dominance hand			
Rt. handed	100%	91%	X^2=.053, *p*=0.819
Lt. handed	0%	9%	

Table 2 Descriptive statistics with mean and SD for experimental and control group at three time points for FIM.

	Variable	Mean	SD
FIM 1	Experimental group	100.27	24.417
	Control group	75.91	31.316
FIM 2	Experimental group	120.73	7.43
	Control group	100.64	20.68
FIM 3	Experimental group	124.40	2.613
	Control group	100.18	30.717

From the repeated measures ANOVA for the FIM at 3-point time Sphericity assumption is violated (p<0.001). Since the sphericity assumption was violated “Greenhouse -Geisser" correction method was referred to as interpretation (Table 3).

As our data violated the assumption of sphericity, we look at the values in the "Greenhouse-Geisser" row. We can report that When only considering time as an independent variable, there is a significant difference between the scores of FIM of groups over three-time points with (F 1.160, 27.848)=21.449, p<0.0001).

Table 3 Mauchly's test of sphericity. Measure: FIM at different time points.

Within Subjects Effect	Mauchly's W	Approx. Chi-Square	df	Sig.	Epsilon		
					Greenhouse-Geisser	Huynh-Feldt	Lower-bound
FIM	0.276	29.581	2	0.000*	0.580	0.617	0.500

**Significant (p<0.001).*

Similarly, considering only one group, there is (F (1,24)=9.422, p<0.005) of two groups over six months of the period. When considered time and group interaction then there is no significant difference (F (1.160, 27.848)=0.172, p=0.719). From the result, we conclude that the changes in score from one-time point to another time point (baseline to post-intervention to follow up) between the groups. Similarly, the change or difference between groups averaged over each time point. But the difference between the group is not improved at different time points (Table 4 and 5).

Table 4 Tests of within-subjects effects. Measure: FIM at different time points.

		Type III Sum of Squares	df	Mean Square	F	Sig.	Partial Eta Squared
FIM	Sphericity Assumed	9299.139	2	4649.569	21.449	0.000*	0.472
	Greenhouse-Geisser	9299.139	1.160	8014.263	21.449	0.000*	0.472
	Huynh-Feldt	9299.139	1.233	7539.981	21.449	0.000*	0.472
	Lower-bound	9299.139	1.000	9299.139	21.449	0.000*	0.472
FIM * group	Sphericity Assumed	74.370	2	37.185	0.172	0.843	0.007
	Greenhouse-Geisser	74.370	1.160	64.094	0.172	0.719	0.007
	Huynh-Feldt	74.370	1.233	60.301	0.172	0.734	0.007
	Lower-bound	74.370	1.000	74.370	0.172	0.682	0.007
Error (FIM)	Sphericity Assumed	10405.297	48	216.777			
	Greenhouse-Geisser	10405.297	27.848	373.649			
	Huynh-Feldt	10405.297	29.599	351.537			
	Lower-bound	10405.297	24.000	433.554			

** Significant (p<0.0001).*

Table 5 Tests of between-subject effects.

Source	df	F	Sig.
Intercept	1	773.273	0.000
Group	1	9.422	0.005*
Error	24		

** Significant (p<0.0001).*

Post hoc analysis with a Bonferroni adjustment revealed that FIM was statistically significantly increased from FIM 1 to FIM 2 (MD -22.597 (95% CI, -34.511 to -10.683), p<0.001) and FIM 1 to FIM 3 (MD -24.203 (95% CI, -37.554 to -10.853), p<0.001) but not from FIM 2 to FIM 3 (MD -1.606 (95% CI, -5.988 to 2.776), p>0.001 (Table 6).

Table 6 Pairwise comparisons. Measure: theme.

(I) FIM	(J) FIM	Mean Difference (I-J)	SE	Sig.b	95% Confidence Interval for Difference	
					Lower Bound	Upper Bound
1	2	-22.597*	4.629	0.000*	-34.511	-10.683
	3	-24.203*	5.187	0.000*	-37.554	-10.853
2	1	22.597*	4.629	0.000*	10.683	34.511
	3	-1.606	1.703	1.000	-5.988	2.776
3	1	24.203*	5.187	0.000	10.853	37.554
	2	1.606	1.703	1.000	-2.776	5.988

** Significant (p<0.0001).*

Discussion

From the pilot study, we investigated the effect of MCST intervention on improving the functional independence of post-stroke survivors. We found there is a better improvement of functional independence in activities of daily living in the participants of MCST as compared to the participants of the conventional group after the completion of therapy. Also, after six months from baseline, that is, after the 3 moths follow-up period, this improvement is better in the MCST group than in a conventional therapy group. These findings are consonant with the previous study's findings.[10,11,15,33] These improvements may be because, in MCST, we used the global cognitive strategy with dynamic performance analysis, and the therapist acts as a moderator, not a direct trainer like in conventional therapy.[14,24,28] MCST improves goal-directed behaviour, planning, self-monitoring, and problem-solving skill of the participants. The goal-directed behaviour also creates interest, motivation, and control over participants' emotions. It improves the active participation and determination of the participants.[10,11,15] Hence, they do repeated practice in different environments in a different context, which improves experience dependant neuronal plasticity in the brain network, shaping the subsequent recovery trajectories.[36,37] It establishes patterns of behaviour or habits of the individual.[38] As a result, there is a more remarkable improvement in functional independence leading to a reduction in disability in the MCST treatment approach compared to conventional therapy. There is no significant improvement from post-intervention (3 month) to the follow-up (6 month) between the groups. However, the mean score of the MCST group is improved

where as in the conventional therapy group there is no such change in improvement in scores. This fact might pronounce there is steady improvement in the MCST intervention. This improvement may be because, the MCST intervention helps in generalization of learning and makes the participants confident [15,33] In our study the MCST group has more female participants than the conventional therapy which slowed down the rate of recovery of the MCST group.[39,40] Hence caused the statistical insignificance between 3 months & 6 months.

Limitation

The study is a pilot study with a Small sample size. Therefore, a large sample size is recommended to generalize the inference. The conventional therapy given to the control group was not standardized for the intervention based on impairment and components decided by the therapist. A standardize conventional intervention protocol may be used in future studies for better comparison of Experimental MCST intervention. This study had a relatively short follow-up period, three months after the post-intervention assessment and an average of 7 months following the baseline assessment. Hence a larger follow-up period, at least minimum of 1 year is recommended to infer a better retention effect of the MCST intervention.

Conclusion

MCST has greater efficacy in improving independence and reducing disability of post-stroke survivors than standard conventional therapy. So it can be applied as an intervention technique in the field of neurorehabilitation of post-stroke survivors for its long-term effect & better outcome. Many valuable lessons are learned while conducting this early phase of the clinical trial, which may be useful in designing the future confirmatory trials.

Funding Source

Nil.

Conflict of Interest

The authors declare no conflict of interest among them.

Acknowledgements

The authors are highly grateful to the Dean IMS & SUM Hospital and Director of Swami Vivekanand National Institute Rehabilitation Training and Research for their constant support throughout the study. The authors are also thankful to the staff and the patients of Occupational Therapy department for their help during the study.

References

[1] Gillen G, Nilsen DM, Attridge J, Banakos E, Morgan M, Winterbottom L, York W. Effectiveness of interventions to improve occupational performance of people with cognitive impairments after stroke: an evidence-based review. Am J Occup Ther. 2015; 69(1): 6901180040p1-9.

[2] Nilsen DM, Gillen G, Geller D, Hreha K, Osei E, Saleem GT. Effectiveness of interventions to improve occupational performance of people with motor impairments after stroke: An evidence-based review. Am J Occup Ther. 2015; 69(1): 6901180030p1-9.

[3] Appelros P, Samuelsson M, Karlsson-Tivenius S, Lokander M, Terént A. A national stroke quality register: 12 years experience from a participating hospital. Eur. J. Neurol. 2007; 14: 890-4.

[4] Wolf T.J, Baum C, Connor LT. Changing face of stroke: Implications for occupational therapy practice. Am. J. Occup. Ther. 2009; 63: 621-5.

[5] Shea N, Frith CD. The Global Workspace Needs Metacognition. Trends Cogn. Sci. 2019; 23: 560-71.

[6] Teasell RW, Foley NC, Salter KL, Jutai JW. A blueprint for transforming stroke rehabilitation care in Canada: the client for change. Arch. Phys. Med. Rehabil. 2008; 89: 575-8.

[7] Veerbeek JM, van Wegen E, van Peppen R, van der Wees PJ, Hendriks E, Rietberg M, Kwakkel G. What is the evidence for physical therapy poststroke? A systematic review and meta-analysis. PloS one. 2014; 9(2): e87987.

[8] French B, Leathley MJ, Sutton CJ, McAdam J, Thomas LH, Forster A, et al. A systematic review of repetitive task training with modelling of resource use, costs and effectiveness. Health Technol Asses. 2008; 12(30): 1-17.

[9] Polatajko HJ, McEwen SE, Ryan JD, Baum CM. Pilot randomized controlled trial investigating cognitive strategy use to improve goal performance after stroke. Am J Occup Ther. 2012; 66(1): 104-9.

[10] Skidmore ER, Swafford M, Juengst SB, Terhorst L. Self-awareness and recovery of independence with strategy training. Am. J. Occup. Ther. 2018; 7 2(1): 1-5.

[11] Skidmore ER, Butters M, Whyte E, Grattan E, Shen J, Terhorst L. Guided training relative to direct skill training for individuals with cognitive impairments after stroke: a pilot randomized trial. Arch. Phys. Med. Rehabil.2017; 98(4): 673-80.

[12] Christiansen CH, Baum CM, Bass JD. In: Christiansen CH, Baum CM, Bass JD, editor. Health, occupational performance, and occupational therapy. Occup. Ther. Perform. Particip. 4th Ed. Thorofare NJ SLACK: Year Book; 2015: 7-21.

[13] Boone AE, Morgan KA, Engsberg JR. A new combined motor and cognitive strategy training intervention for stroke: Stakeholder perceptions. Br. J. Occup. Ther. 2017; 80(12): 726-34.

[14] Wolf TJ, Doherty M, Boone A, Rios J, Polatajko H, Baum C, McEwen S. Cognitive oriented strategy training augmented rehabilitation (COSTAR) for ischemic stroke: a pilot exploratory randomized controlled study. Disabil. Rehabil. 2021; 43(2): 201-10.

[15] Skidmore ER, Dawson DR, Butters MA, Grattan ES, Juengst SB, Whyte EM, et al. Strategy training shows promise for addressing disability in the first 6 months after stroke. Neurorehabilitation and neural repair. 2015; 29(7): 668-76.

[16] Toglia JP. The dynamic interactional model of cognition in cognitive rehabilitation. In: Katz N, editor. Cognition, occupation, and participation across the life span: Neuroscience, neurorehabilitation, and models of intervention in occupational therapy. American Occupational Therapy Association; 2011: 161-201.

[17] May A. Experience-dependent structural plasticity in the adult human brain. Trends Cog Sci. 2011; 15(10): 475-82.

[18] Carey LM, Seitz RJ. Functional neuroimaging in stroke recovery and neurorehabilitation: conceptual issues and perspectives. Int J Stroke. 2007; 2(4): 245-64.

[19] Herdener M, Esposito F, di Salle F, Boller C, Hilti CC, Habermeyer B, Scheffler K, Wetzel S, Seifritz E, Cattapan-Ludewig K. Musical training induces functional plasticity in human hippocampus. J Neurosci. 2010; 30(4): 1377-84.

[20] Hänggi J, Koeneke S, Bezzola L, Jäncke L. Structural neuroplasticity in the sensorimotor network of professional female ballet dancers. Hum Brain Mapp. 2010; 31(8): 1196-206.

[21] Jones RN, Manly J, Glymour MM, Rentz DM, Jefferson AL, Stern Y. Conceptual and measurement challenges in research on cognitive reserve. J Int Neuropsychol Soc. 2011; 17(4): 593-601.

[22] Jefferson SC, Clayton ER, Donlan NA, Kozlowski DA, Jones TA, Adkins DL. Cortical stimulation concurrent with skilled motor training improves forelimb function and enhances motor cortical reorganization following controlled cortical impact. Neurorehabil neural repair. 2016; 30(2): 155-8.

[23] Cole MW, Reynolds JR, Power JD, Repovs G, Anticevic A, Braver TS. Multi-task connectivity reveals flexible hubs for adaptive task control. Nat neurosci. 2013; 16(9): 1348-55.

[24] Ito T. Cognitive Information Transformation in Functional Brain Networks (Doctoral dissertation, Rutgers The State University of New Jersey, Graduate School-Newark). [Thesis on the Internet]. [New Jersey (USA)]: The State University of New Jersey;2020 [cited 2022 April 27]. Available from: https://rucore.libraries.rutgers.edu/rutgers-lib/65797/PDF/1/play. [Oxford (England)]: University Oxford; 2015 [cited 2015 Jul 28]. Available from: http://ora.ox-.ac.uk/objects/uuid:6e7d952a-dc5b-4af0-b0bb-f2ae2184eed0.

[25] Polatajko HJ, McEwen SE, Ryan JD, Baum CM. Pilot randomized controlled trial investigating cognitive strategy use to improve goal performance after stroke. Am J Occup Ther. 2012; 66(1): 104-9.

[26] Kringle EA, Setiawan IM, Golias K, Parmanto B, Skidmore ER. Feasibility of an iterative rehabilitation intervention for stroke delivered remotely using mobile health technology.Disabil. Rehabil. Assist. Technol.2019; 15(8): 908-16.

[27] Chang FH, Chiu V, Ni P, Lin YN, Kang JH, Liou TH, Lu L, Han DS, Skidmore ER. Enhancing community participation for stroke survivors with cognitive impairment: study protocol for a randomised controlled trial in Taiwan. BMJ open. 2020; 10(12): e040241.

[28] Song CS, Lee ON, Woo HS. Cognitive strategy on upper extremity function for stroke: A randomized controlled trials. Restor. Neurol. Neurosci. 2019; 37(1): 61-70.

[29] Prescott S, Fleming J, Doig E. Goal setting approaches and principles used in rehabilitation for people with acquired brain injury: A systematic scoping review. Brain Inj. 2015; 29(13-14): 1515-29.

[30] Ahn SN, Yoo EY, Jung MY, Park HY, Lee JY, Choi YI. Comparison of Cognitive Orientation to daily Occupational Performance and conventional occupational therapy on occupational performance in individuals with stroke: A randomized controlled trial. NeuroRehabilitation. 2017; 40(3): 285-92.

[31] Araújo CR, Cardoso AA, Magalhães LD. Efficacy of CO-OP Approach With and Without Parental Coaching: RCT Study Protocol: Efficacité de l'approche CO-OP avec et sans coaching parental: protocole d'essai clinique randomisé. Can. J. Occup. Ther. 2021; 88(2): 182-94.

[32] Kersey J, Evans WS, Mullen K, Askren A, Cavanaugh R, Wallace SE, Hula WD, Walsh Dickey M, Terhorst L, Skidmore E. Metacognitive strategy training is feasible for people with aphasia. OTJR Occup. Particip. Health. 2021; 41(4): 309-18.

[33] Polatajko HJ, Mandich AD, Missiuna C, Miller LT, Macnab JJ, Malloy-Miller T, Kinsella EA. Cognitive orientation to daily occupational performance (CO-OP) part III-the protocol in brief. Physical & occupational therapy in pediatrics. 2001; 20(2-3): 107-23.

[34] Kidd D, Stewart G, Baldry J, Johnson J, Rossiter D, Petruckevitch A, Thompson AJ. The Functional Independence Measure: a comparative validity and reliability study. Disabil. Rehabil. 1995; 17(1): 10-4.

[35] Hsueh I-P, Lin J-H, Jeng JS, & Hsieh C-L. Comparison of the psychometric characteristics of the functional independence measure, 5 item Barthel index, and 10 item Barthel index in patients with stroke. J. Neurol. Neurosurg. Psychiatry. 2002; 73: 188-90.

[36] Kleim JA, Jones TA, Schallert T. Motor enrichment and the induction of plasticity before or after brain injury. Neurochem. Res. 2003; 28: 1757-69.

[37] Jones TA, Jefferson S C. Reflections of experience-expectant development in repair of the adult damaged brain. Dev. Psychobiol. 2011; 53: 466-75.

[38] Taub E, Uswatte G, Elbert T. New treatments in neurorehabilitation founded on basic research. Nat Rev Neurosci. 2002; 3: 228-36.

[39] Mohakud K, Sahu S, Das SP, Sahu S. Gender Differences in Functional Performance and Community Reintegration of Post Stroke Survivors in Eastern India. Turk J Phys Med Rehabil.2021; 32(2): 2612 -22.

[40] Petrea RE, Beiser AS, Seshadri S, Kelly-Hayes M, Kase CS, Wolf PA. Gender differences in stroke incidence and poststroke disability in the Framingham heart study. Stroke. 2009; 40(4): 1032-7.

Journal of Associated Medical Sciences 2022; 55 (3): 91-95

JAMS
Journal of Associated Medical Sciences

Thai-Journal Citation Index Centre (TCI) & ASEAN Citation Index (ACI)

Journal of Associated Medical Sciences

Journal homepage: https://www.tci-thaijo.org/index.php/bulletinAMS/index

Chronic deep venous thrombosis as the presenting manifestation of acute promyelocytic leukaemia : A case report

Prabodh Kumar Das[1] **Rajesh Kumar Bhola**[2*]

[1]*Department of Medical Oncology/Hematology, All India Institute of Medical Sciences, Bhubaneswar, Odisha, India.*
[2]*Laboratory Haematology Division, Department of Pathology, IMS & SUM Hospital, Siksha 'O' Anusandhan, Deemed to be University, Bhubaneswar, Odisha, India.*

ARTICLE INFO

Article history:
Received 17 May 2022
Accepted as revised 21 July 2022
Available online 26 July 2022

Keywords:
Acute promyelocytic leukaemia, chronic deep venous thrombosis, acute myeloid leukaemia, disseminated intravascular coagulation

ABSTRACT

Background: Acute promyelocytic leukaemia (APL) usually presents with disseminated intravascular coagulation or hyper-fibrinogenolysis followed by bleeding manifestation. But thrombosis as a presenting manifestation is less often reported in APL.

Objectives: We describe an uncommon case of chronic deep venous thrombosis (DVT) of lower limb with unsuspected APL.

Results: A 27 year old male presented with DVT and was treated with enoxaparin and later Dabigatran for 2 months without any improvement. A routine haematological assessment showed Leucopenia with few circulating abnormal promyelocytes. The bone marrow assessment with flow cytometry and molecular studies established the diagnosis of APL. Patient was never having any bleeding manifestation despite on anticoagulation too. A thrombophilia work up revealed presence of hyper-homocysteinemia and mild lupus anticoagulant in addition to APL as a prothrombotic event.

Conclusion: DVT with leukopenia warrants further investigation to rule out Acute Promyelocytic Leukaemia. It includes a thorough peripheral smear examination to look for few circulating abnormal promyelocytes, bone marrow studies and molecular /cytogenetics analysis.

Introduction

Acute promyelocytic leukaemia (APL) is one of the subtypes of acute myeloid leukaemia (AML) with high cure rate as well as high mortality. It commonly presents with bleeding manifestation and disseminated intravascular coagulation (DIC) which is responsible for early death. Comparatively thrombosis is not a very common manifestation and most commonly presents during recovery phase from chemotherapy. But, thrombosis especially chronic deep venous thrombosis (DVT) as an initial manifestation is still rare with few case reports in literature.[1] We report such a rare case of unprovoked chronic DVT in a young adult with APL. Additional prothrombotic risk factors like hyper-homocysteinemia and transient mild positive lupus anticoagulant were identified.

Case report

A 27 year old male evaluated outside for the complaint of sudden onset unprovoked pain and swelling of right calf for the past 10 days.Professionally being an academician he had relatively sedentary lifestyle with long hours of computer work. He was born of non-consanguineous marriage with no significant family history of thrombophilic risk factors. He was taking many ayurvedic medications. The

* **Corresponding author.**
Author's Address: *Laboratory Haematology Division, Department of Pathology, IMS & SUM Hospital, Siksha 'O' Anusandhan, Deemed to be University, Bhubaneswar, Odisha, India.*
** **E-mail address:** rajeshkumarbhola@soa.ac.in
doi: 10.12982/JAMS.2022.029
E-ISSN: 2539-6056

physical examination revealed swelling and tenderness of right calf. No hepatosplenomegaly or lymphadenopathy noted. The systemic examinations were within normal limits.The right lower limb venous system Doppler showed hypoechoic thrombus filling the lumen of vein extending from mid superficial femoral vein till distal posterior tibial vein distally extending through sapheno-popliteal junction in the small saphenous vein suggestive of DVT. The chest X-ray and abdominal ultrasound didn't elicit any abnormality. He was started on injection low molecular weight heparin (LMWH) enoxaparin 60 mg twice a day for 2 days followed by Dabigatran 150 mg twice a day for 2 months. But the DVT didn't resolve clinically with persistent leg swelling.

He was referred for haematology consultation after 2 months for non-resolving DVT despite on anticoagulants. He was haemodynamically stable with unremarkable physical examination. The laboratory investigations revealed following findings. The complete blood count revealed leukopenia with Hb 11.6 gm/dL, WBC count $1.62x10^3$/µL, platelet count $106x10^3$/µL, RBC count $3.5x10^6$/µl, PCV 32.2%, MCV 92 fL, MCH 33.1 pg, MCHC 36 gm/dL, RDW-SD 47.7 fL, RDW-CV 14.6%, reticulocyte count 0.92%. The peripheral smear showed normocytic normochromic blood picture with macrocytes, tear drop cells and few fragmented RBC. We reviewed the whole slide in search of abnormal cells. Interestingly it also elicited 3 % abnormal promyelocytes with occasional faggots (Figure 1A). The liver function tests were normal with total bilirubin 0.37 mg/dL, bilirubin (direct) 0.12 mg/dL, alkaline phosphatase 117.0 IU/L, SGOT 17.50 IU/L, SGPT 16.30 IU/L, total protein 8.45 gm/dL, albumin 4.95 gm/dL. The vitamin B12 levels were >2000 pg/mL. The renal function tests were also within normal limits with creatinine 1.19 mg/dL, urea 15 mg/dL. The uric acid levels were 5.30 mg/dL with no evidence of hyperuricemia. The screening for hepatitis B, hepatitis C and HIV were negative.

In view of leukopenia with few circulating abnormal promyelocytes, a possibility of acute promyelocytic leukaemia was considered with review of clinical history and physical examination for any specific bleeding manifestation. Still we couldn't elicit any features of active or past bleeding since presentation. A bone marrow aspiration was done which showed 66% abnormal promyelocytes with hyper-granular cytoplasm and faggots and strong myeloperoxidase stain positivity (Figure 1B and 1C). A flow cytometry assessment was performed. The gated population showed moderate CD45 positivity with intermediate side scatter (SSC) and were positive for cytoplasmic MPO, CD117, CD13, CD33, CD38 (subset 52%), CD58 while were negative for CD34, nuclear TdT, HLA DR, CD19, CD79a, membrane CD3, cytoplasmic CD3, CD7, CD64, CD11c, CD14, CD56, CD36, CD4, CD2, CD16, CD15, CD10 (Figure 2). A conventional cytogenetics showed t(15;17)(q22;12) and reverse transcriptase showed PML-RARA positivity with bcr1 transcript (Figure 1D). A diagnosis of acute promyelocytic leukaemia with PML-RARA was rendered.

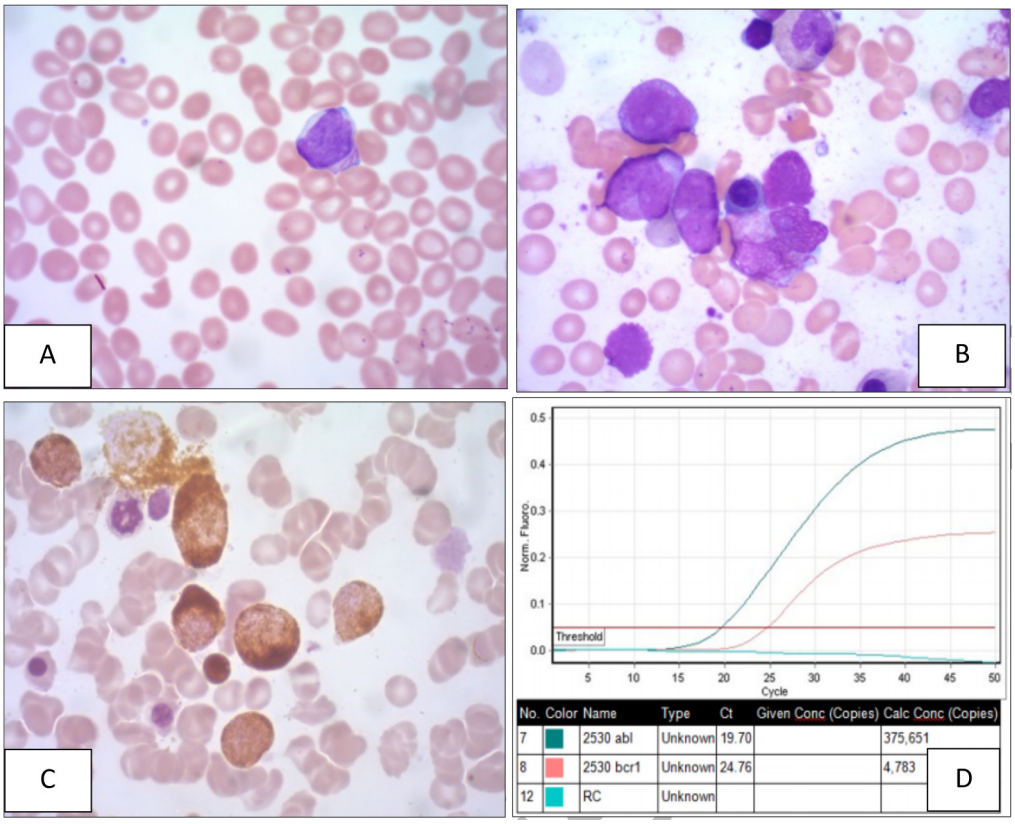

Figure 1. *Peripheral smear Shows a promyelocyte with faggot (Leishman Giemsa stain, oil immersion field 1000X)(A), Bone marrow aspiration smear shows abnormal promyelocytes with faggots (Leishman Giemsa stain, oil immersion field 1000X) (B). Promyelocytes are strong myeloperoxidase positive (MPO stain, oil immersion field 1000X) (C). RT PCR showing t(15;17) PML-RARA bcr-1 transcript (D).*

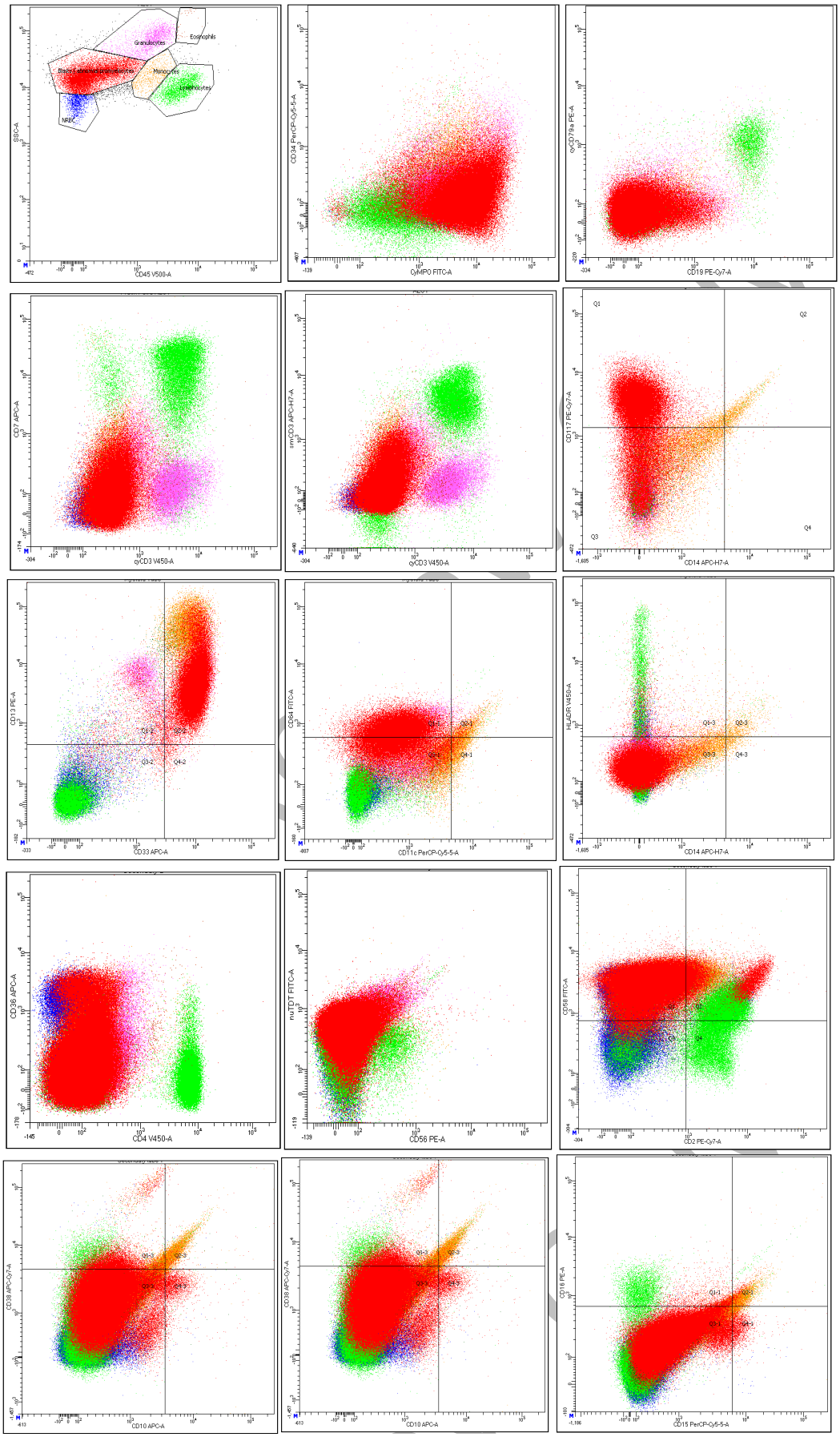

Figure 2. *Flow cytometry assessment on BD FACSCanto II 3 Laser 8 color flow cytometry and analyzed by FACSDiva 2.1 software shows the promyelocyte/ blasts gate on moderate CD45 with intermediate side scatter (SSC) population which is positive for cytoplasmic MPO, CD117, CD13, CD33, CD58, CD64 (dim) while negative for CD34, nuclear TdT, HLA DR, CD19, CD79a, membrane CD3, cytoplasmic CD3, CD7, CD64, CD11c, CD14, CD56, CD36, CD4, CD2 CD16, CD15, CD10, CD38.*

We further evaluated for prothrombotic or bleeding risk factors. The prothrombin time (PT) 12.2 seconds (Reference interval 9.4-11.4 sec), activated partial thromboplastin time (aPTT) 32.2 sec (RI 21.4-29.0 sec), thrombin time 23.9 sec (RI 14-21 s), Fibrinogen 246.8 mg/dL (200-400 mg/dL). D-dimer was elevated with 2.53 µg/L fibrinogen equivalent unit (FEU) (Reference cut off <0.5 µg/L FEU) which was indicative of ongoing thrombosis. The assessment for inherited thrombophilic risk factors showed mild hyperhomocys teinemia with Homocysteine levels 20.76 µmol/L (RI 5.46-16.20) with normal levels of protein C 65%, free protein S 77%, factor VIII 154%). Thesickling test was negative. The assessment for acquired thrombophilia showed mild positivity for lupus anticoagulant with a Dilute Russell's Viper Venom Time (DRVVT) screen by confirm ratio of 1.31 (RI<1.2).

Patient was started on chemotherapy with all-trans retinoic acid (ATRA) 45 mg/m^2 plus Arsenic trioxide (ATO) 0.15 mg/kg IV for 5 days a week in induction phase followed by consolidation with some modifications and injection dexamethasone 10 mg/m^2 12 hourly for prevention of differentiation syndrome until end of induction therapy. He didn't develop differentiation syndrome during the therapy. He achieved post induction morphological remission. DVT resolved completely. He is doing well with 2 years of follow up without any relapse of APL or recurrence of DVT.

Discussion

The acute promyelocytic leukaemia (APL) is classically known for bleeding issues, especially due to disseminated intravascular coagulation (DIC) or secondary hyperfibrinolysis. Paradoxically thrombotic events complicating APL is a rarely reported events. In one of the series, *M Breccia et al* have reported an incidence of 8.87% (n=11) of major thrombotic events in 124 APL cases.[2] One of the largest series of 94 cases of APL with thrombosis was reviewed by Rashidi *et al*. They found that 40.4 % (n=38) developed thrombosis before initiation of therapy, 43.6% (n=41) during induction therapy.[3] The common thrombotic events include DVT or pulmonary embolism (PE), myocardial infarction (MI), and stroke. Cerebral venous sinus thrombosis, hepatic vein thrombosis, acute limb ischemia, splenic infarction, portal vein thrombosis, renal artery thrombosis or more than one thrombotic events though rare but have also been reported in literature.[3-8] But a thorough literature survey didn't show any evidence of chronic DVT as a presenting manifestation of APL.

The ATRA therapy was also associated with an increased risk of thrombosis as high as 16%. It has been postulated that ATRA causes an imbalance between procoagulant and fibrinolytic forces which possibly induces a prothrombotic state. ATRA causes upregulation of cytokines production leading to persistent mild increased coagulation activation markers. Although in literature, there are several case reports of thrombosis and APL but the number of cases with thrombosis especially chronic DVT as presenting manifestation of APL are a few.

The risk factors for developing thrombosis in APL included a higher leukocyte count, immunophenotypic expression of CD2&CD15, prevalence of the bcr3 transcript type, and expression of FLT3-ITD. The order of frequency of sites is deep vein thrombosis, sub-endocardiac ischemia, and intraventricular thrombosis. A low fibrinogen <170 mg/dL; anaemia (haemoglobin>10 gm/dL), M3 variant subtype are the other risk factors of thrombosis. But contrary to it, our case showed Sanz low risk with low WBC count, normal platelet count, negative for CD2 and CD15 and PML-RARA *bcr1 transcript*.

In order to analyse the non-leukemic prothrombotic risk factors, we found hyperhomocysteinemia and mild positive lupus anticoagulant in our case. There are few reports of acute myeloid leukemia especially APL with hyperhomocysteinemia causing thrombosis.It has been observed in a murine model of APL that Methionine-induced hyperhomocysteinemia could revert the fibrinolytic pathway activation.[9] Hence we feel that hyperhomocystenemia in our case might be the cause of thrombosis and non-development of bleeding due to DIC or hyperfibrinolysis and remained undiagnosed for 2 months. But the cause of hyperhomosys-teinemia can be hereditary or due to disturbed metabolism of homocystein as seen in cancer as we couldn't do any molecular studies.[10] Similarly few case reports have been described about AML with coexisting antiphopholipid syndrome but specifically APML with lupus anticoagulant are scarce.[11-13]

Our case is rare in many aspects and provides major input regarding approach to cases with unprovoked DVT and leukopenia. It shows that an unprovoked DVT may mask and delay the diagnosis of APL especially low risk groups. The peripheral smear with unexplained leukopenia requires a thorough evaluation of the whole slide which may be lifesaving in a scenario of APL which is otherwise highly fatal. In addition all cases of thrombosis in APL should be searched for other additional inherited or acquired prothrombotic risk factors. Possibly we are describing the first case of chronic DVT as the presenting manifestation of APL with additional leukaemia associated hyperhomocysteinemia and mild lupus anticoagulant.

Sources of Financial Support

Nil.

References

[1] Ng CH, Chng WJ. Recent advances in acute promyelocytic leukaemia. F1000Res. 2017;6:1273. doi: 10.12688/f1000research.10736.1.

[2] Breccia M, Avvisati G, Latagliata R, Carmosino I, Guarini A, De Propris MS, Gentilini F, Petti MC, Cimino G, Mandelli F, Lo-Coco F. Occurrence of thrombotic events in acute promyelocytic leukemia correlates with consistent immuno-phenotypic and molecular features. Leukemia. 2007; 21(1): 79-83. doi: 10.1038/sj.leu.2404377.

[3] Rashidi A, Silverberg ML, Conkling PR, Fisher SI. Thrombosis in acute promyelocytic leukemia. Thromb Res. 2013; 131(4): 281-9. doi: 10.1016/j.thromres.2012.11.024.

[4] Mitrovic M, Suvajdzic N, Elezovic I, Bogdanovic A, Djordjevic V, Miljic P, Djunic I, Gvozdenov M, Colovic N, Virijevic M, Lekovic D, Vidovic A, Tomin D. Thrombotic events in acute promyelocytic leukemia. Thromb Res.2015; 135(4): 588-93. doi: 10.1016/j.thromres.2014.11.026.

[5] Trottier-Tellier F, Durand M, Kolan C, Wistaff R, Nguyen PV, Laskine M. Recurrent arterial and venous thromboemboli as initial presentation of acute promyelocytic leukemia. J Clin Med Res. 2014; 6(5): 388-91. doi: 10.14740/jocmr1864w.

[6] Kutiyal AS, Dharmshaktu P, Kataria B, Garg A. A Rare Occurrence of Simultaneous Venous and Arterial Thromboembolic Events - Lower Limb Deep Venous Thrombosis and Pulmonary Thromboembolism as Initial Presentation in Acute Promyelocytic Leukemia. Clin Med Insights Oncol. 2016 Feb 25; 10: 1-4. doi: 10.4137/CMO.S37866.

[7] Krill T, Baliss M, Zaibaq J, Abdulla HM, Parupudi S. Acute lymphoblastic leukemia presenting with mesenteric ischemia. Gastroenterol Hepatol Bed Bench. 2019 Fall; 12(4): 370-3.

[8] Sorà F, Chiusolo P, Laurenti L, Autore F, Giammarco S, Sica S. Massive Pulmonary Embolism at the Onset of Acute Promyelocytic Leukemia. Mediterr J Hematol Infect Dis. 2016; 8(1): e2016027. doi: 10.4084/MJHID.2016.027.

[9] Jácomo RH, Santana-Lemos BA, Lima AS, Assis PA, Lange AP, Figueiredo-Pontes LL, Oliveira LO, Bassi SC, Benício MT, Baggio MS, Garcia AB, Falcão RP, Rego EM. Methionine-induced hyperhomocysteinemia reverts fibrinolytic pathway activation in a murine model of acute promyelocytic leukemia. Blood. 2012; 120(1): 207-13. doi: 10.1182/blood-2011-04-347187.

[10] Hasan T, Arora R, Bansal AK, Bhattacharya R, Sharma GS, Singh LR. Disturbed homocysteine metabolism is associated with cancer. Exp Mol Med. 2019; 51(2): 1-13. doi: 10.1038/s12276-019-0216-4.

[11] Saxena SK, Bin Salih SA, Al-Jizeeri AH, Kheir OA. Acute myeloblastic leukemia in a patient with primary antiphospholipid syndrome. Saudi Med J. 2003; 24(9): 1013-5.

[12] Stasi R, Stipa E, Masi M, Oliva F, Sciarra A, Perrotti A, Zaccari G, Papa G. Antiphospholipid antibodies: prevalence, clinical significance and correlation to cytokine levels in acute myeloid leukemia and non-Hodgkin's lymphoma. ThrombHaemost. 1993; 70(4): 568-72.

[13] Lossos IS, Bogomolski-Yahalom V, Matzner Y. Anticardiolipin antibodies in acute myeloid leukemia: prevalence and clinical significance. Am J Hematol. 1998; 57(2): 139-43. doi: 10.1002/(sici)1096-8652(199802)57:2<139::aid-ajh8>3.0.co;2-x.

Journal of Associated Medical Sciences 2022; 55 (3): 96-104

JAMS
Journal of Associated Medical Sciences

Thai-Journal Citation Index Centre (TCI) & ASEAN Citation Index (ACI)

Journal of Associated Medical Sciences

Journal homepage: https://www.tci-thaijo.org/index.php/bulletinAMS/index

Identification and monitoring of *Mycobacterium tuberculosis* growth in liquid culture by Antigen 85 detection

Chanjuti Sriruan[1] Watchara Kasinrerk[2,3] Sorasak Intorasoot[1,4] Bordin Butr-Indr[1,4] Nathiprada Netirat[5] Jiaranai Khantipongse[5] Ponrut Phunpae[1,4*]

[1]*Division of Clinical Microbiology, Department of Medical Technology, Faculty of Associated Medical Sciences, Chiang Mai University, Chiang Mai Province, Thailand.*
[2]*Biomedical Technology Research Center, Department of Medical Technology, Faculty of Associated Medical Sciences, Chiang Mai University, Chiang Mai Province, Thailand.*
[3]*Division of Clinical Immunology, Department of Medical Technology, Faculty of Associated Medical Sciences, Chiang Mai University, Chiang Mai Province, Thailand.*
[4]*Infectious Diseases Research Unit (IDRU), Faculty of Associated Medical Sciences, Chiang Mai University, Chiang Mai Province, Thailand.*
[5]*Office of Disease Prevention and Control Region, 1 (ODPC 1) Chiang Mai, Department of Disease Control, the Ministry of Public Health, Muang District, Chiang Mai Province, Thailand.*

ARTICLE INFO

Article history:
Received 28 March 2022
Accepted as revised 7 July 2022
Available online 3 August 2022

Keywords:
Mycobacterium tuberculosis, Ag85B protein, ELISA assay

ABSTRACT

Background: *Mycobacterium tuberculosis* is the most common causative agent of tuberculosis. It releases secretory proteins, especially the Ag85 complex, from actively growing mycobacteria, which can be detected in mycobacterial liquid culture. Ag85B is the most abundant in the Ag85 complex and is an interesting target for the detection of tuberculosis. In addition, measuring Ag85 level is beneficial for comparing growing and non-growing mycobacteria in liquid culture.

Objectives: To detect Ag85B protein from active growing *M. tuberculosis* in liquid culture for the diagnosis of tuberculosis and compare the level of Ag85B between growing and non-growing mycobacteria.

Materials and methods: A sandwich ELISA assay using anti-Ag85B monoclonal antibody was performed to detect Ag85B protein. Drug-susceptible mycobacteria, *M. tuberculosis* H37Ra and *M. tuberculosis* H37Rv, as well as 12 other *M. tuberculosis* complex strains isolated from clinical specimens were cultured in liquid media. In addition, mycobacterial culture was separated into two conditions: untreated and treated with streptomycin. Then the liquid media were collected, filtered for sterility, and used for the detection of Ag85B. The levels of Ag85B between treated and untreated conditions were analyzed.

Results: In untreated mycobacterial culture, Ag85B protein was detected and continuously increased each day. However, Ag85B in treated mycobacterial culture increased slightly in the early days and then stabilized. These results demonstrate that the growth of mycobacteria was inhibited after culturing with streptomycin. Thus, the increase of Ag85B was not observed because this protein cannot be secreted by dead mycobacteria. On the other hand, living mycobacteria can secrete the Ag85B protein continuously. Moreover, Ag85B accumulated and increased with each passing day.

Conclusion: *M. tuberculosis* can produce and release Ag85B protein. In this study, detection of Ag85B in liquid culture by a sandwich ELISA assay was used to identify *M. tuberculosis*. When *M. tuberculosis* was suppressed or killed by anti-TB medications, it stopped growing and the increase in Ag85B proteins disappeared. As a result, the levels of Ag85B could be used to detect living mycobacteria. Furthermore, this knowledge can be further applied to monitor mycobacterial growth affected by testing mycobacteria with anti-TB drugs.

* **Corresponding author.**
Author's Address: *Division of Clinical Microbiology, Department of Medical Technology, Faculty of Associated Medical Sciences, Chiang Mai University, Chiang Mai Province, Thailand.*
** **E-mail address:** ponrut.p@cmu.ac.th
doi: 10.12982/JAMS.2022.030
E-ISSN: 2539-6056

Introduction

Tuberculosis (TB), which is caused by *Mycobacterium tuberculosis* complex (MTBC),[1] is still one of the top 10 causes of death in the world,[2] in part because TB is a disease that is transmitted through the respiratory system. However, TB is curable and preventable. In addition, multi-drug resistant TB (MDR-TB) is a major public health concern. Moreover, there is a delay in treatment or a lack of access to therapy, resulting in community spread. To be properly treated, patients with TB require rapid, accurate and consistent antibiotic medication.[3] However, there are numerous limitations to the diagnostic techniques and drug susceptibility tests generally available for diagnosing latent or active TB and monitoring therapy response. These limitations have a considerable impact on the transmission of tuberculosis. To overcome these issues, a new technique for detection is necessary. Currently, the standard method for mycobacterial drug susceptibility testing is based on mycobacterial culture on solid media, which takes approximately 4 to 6 weeks to provide results.[4] For rapid detection, a molecular assay and a liquid culture method were developed. However, a mismatch between phenotypic and molecular methods for drug susceptibility testing of drug-resistant tuberculosis was reported by Ahmad and colleagues in 2006.[5]

The antigen 85 (Ag85) complex, which consists of three related proteins, Ag85A (32 kDa), Ag85B (30 kDa), and Ag85C (32.5 kDa), was secreted by mycobacteria.[6, 7] Living mycobacteria secrete Ag85 proteins continuously throughout culture in broth media. Among the Ag85 complex, Ag85B is the most abundant protein produced by MTBC when grown in broth culture and discovered on the surface of the mycobacterial cell.[6,7] Furthermore, Ag85B detection has been employed as a rapid TB diagnosis method.[7] However, Ag85 could be found in both *M. tuberculosis* and non-tuberculosis mycobacteria (NTM) liquid culture.[8] Bacterial protein secretion (Ag85B) in target organ is dynamic and regulated, and quantification of secreted bacterial proteins can contribute to the understanding of pathogenesis and immunity in tuberculosis and other infections.[9]

Therefore, Ag85B proteins might be an interesting target for identifying or monitoring the active growth of mycobacteria. In this study, we propose to detect Ag85B from the active growth of mycobacteria in liquid culture, and to evaluate Ag85B levels from mycobacterial liquid culture, treated and untreated with streptomycin (SM).

Materials and methods

Mycobacterial strain

This study was performed with mycobacteria, including *M. tuberculosis* H37Ra, *M. tuberculosis* H37Rv, and *M. tuberculosis*, isolated from 12 clinical specimens. These mycobacteria were obtained from the Tuberculosis Laboratory, Office of Disease Prevention and Control Region 1, Chiang Mai, and the Division of Clinical Microbiology Laboratory, Department of Medical Technology, Faculty of Associated Medical Sciences, Chiang Mai University. All mycobacteria were cultured in Ogawa media for 3 to 6 weeks before use. In addition, the characteristics of drug-resistant mycobacteria were tested using a standard agar proportion method.

Preparation of mycobacterial and bacteria culture filtrate from liquid culture

Each mycobacterial suspension was prepared. The concentration of cells in the mycobacterial culture was adjusted to 10^6 CFU/mL based on turbidity using McFarland Standard No. 1. Streptomycin, an anti-TB drug, was used to treat each mycobacterial species at the standard drug susceptibility levels (2.0 µg/mL) in Middlebrook 7H9 supplemented with OADC. Then the liquid media were collected from each mycobacterial culture on days 0, 1, 3, 6, 9, 12, and 15. In addition, *Staphylococcus aureus* or *Escherichia coli* culture filtrate were also prepared. Individual bacterial culture in log phase in trypticase soy broth (0.5 McFarland, ~1.5×10^8 CFU/mL) were diluted 1:100 in Middlebrook 7H9 tubes. After that liquid media were collected from each bacterial culture on the same day as collect liquid media from *M. tuberculosis* culture. These bacteria were used as the controls for Ag85B detection. The collected liquid medium of *M. tuberculosis*, *S. aureus* and *E. coli* were transferred to a sterile microtube after being filtered through membranes with a pore size of 0.2 µm. One hundred microliters of *M. tuberculosis* culture filtrate were placed into 1% Ogawa medium and cultivated at 37°C for 6 weeks to check for sterility. The remaining filtered solution was stored at -20°C. If no mycobacteria grew on the medium after 6 weeks, the culture filtrate was tested for Ag85B by sandwich ELISA.

Sandwich ELISA for detection of Ag85B protein

This study performed sandwich ELISA assay for Ag85B detection using the protocol suggested by Phunpae and colleagues in 2014.[7] Briefly, the anti-Ag85B monoclonal antibody clone AM85B-8, kindly provided by Prof. Dr. Watchara Kasinrerk, Biomedical Technology Research Center, Department of Medical Technology, Faculty of Associated Medical Sciences, Chiang Mai University, was employed to establish an ELISA for detecting Ag85B. ELISA wells were coated with 50 µL (40 µg/mL) of anti-Ag85B mAb clone AM85B-8 as captured antibody. The wells were blocked with 2% skimmed milk in PBS pH 7.2, at 37°C for 1 hr. The culture filtrate samples were added into the antibody coated wells. The plate was subsequently incubated at 37°C for 1 hr and washed 3 times. Fifty microliters of rabbit anti-Ag85B polyclonal antibody at a concentration of 20 µg/mL was added and incubated at 37°C for 1 hr. The antigen-antibody complexes were detected by adding HRP-conjugated swine anti-rabbit immunoglobulin antibodies, which were purchased from Dako (Glostrup, Denmark), and the color was developed using TMB substrate (Invitrogen). The reaction was stopped by adding 1 N HCl and the absorbance was measured at 450 nm. The sandwich ELISA assay was usually tested each sample in triplicate on a particular day.

Detection of mycobacteria by fluorescent staining

Microscopic slides were prepared. Thirty microliters of *M. tuberculosis* cultures each day (on days 0, 1, 3, 6, 9, 12, and 15) were transferred to a glass slide and spread to a diameter of 1 cm. The slides were air dried and then heat fixed over the flame. The samples were stained with Auramine O stain. Auramine O was added to the slide and incubated at room temperature for 15 min. After rinsing

with water, the slide was decolorized with 0.5% acid-alcohol for a maximum of 2 min and then washed with water. The slide was then counterstained with potassium permanganate for 2 min. The slide was again washed with water and air dried. The slides were scanned using a fluorescence microscope at 400x magnification. Mycobacteria was graded by following the European Union/WHO scale.[10]

Results

Detection of Antigen 85B in the *M. tuberculosis* culture

As living *M. tuberculosis* can secrete Ag85B in liquid media, the detection of Ag85B is an interesting target for TB diagnosis. To study the release of Ag85B from *M. tuberculosis* in liquid culture, sandwich ELISA was performed for Ag85B detection. Culture filtrates of *M. tuberculosis* H37Ra and *M. tuberculosis* H37Rv, drug-susceptible mycobacteria, were collected on days 0, 1, 3, 6, 9, 12, and 15. All liquid culture media were filtered through a standard syringe filter, pore size 0.2 µm and then the culture supernatant were tested for sterility by culture in Ogawa medium for 4-6 weeks. The result showed that all samples, 100%, no bacterial contamination. Then samples were analyzed for the presence of Ag85B using a sandwich ELISA assay. In addition, the sensitivity of this sandwich ELISA assay for detecting Ag85B protein was 8 ng/mL and the cutoff value indicating a positive result is 0.500.[7] The results were performed by statistical t-test analysis with a 95% confidence interval.

The result showed that Ag85B could be detected from all studied *M. tuberculosis*. As a negative control, Ag85B was not detected from *S. aureus*, Gram-positive bacteria, and *E. coli*, Gram-negative bacteria, cultured in liquid media. Moreover, the amount of Ag85B secreted by *M. tuberculosis* in the liquid media was found to increase further each day as living mycobacteria could secrete the Ag85B protein continuously. Therefore, this study observed that longer *M. tuberculosis* cultivation was related to higher levels of Ag85B in liquid culture. When comparing the daily increase in Ag85B with day 0, Ag85B levels increased with a significant difference ($p \leq 0.05$) from day 3 onwards (Figure 1, Figure 2 and Table 1).

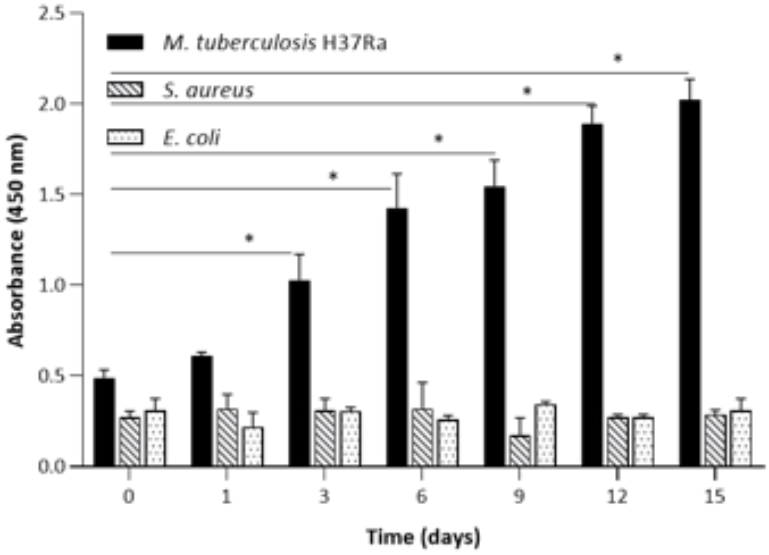

Figure 1. *Detection of Ag85B protein from M. tuberculosis H37Ra cultured in liquid media using sandwich ELISA method. S. aureus and E. coli were used as the negative controls for Ag85B detection. *: Statistically significant (p≤0.05, t-test).*

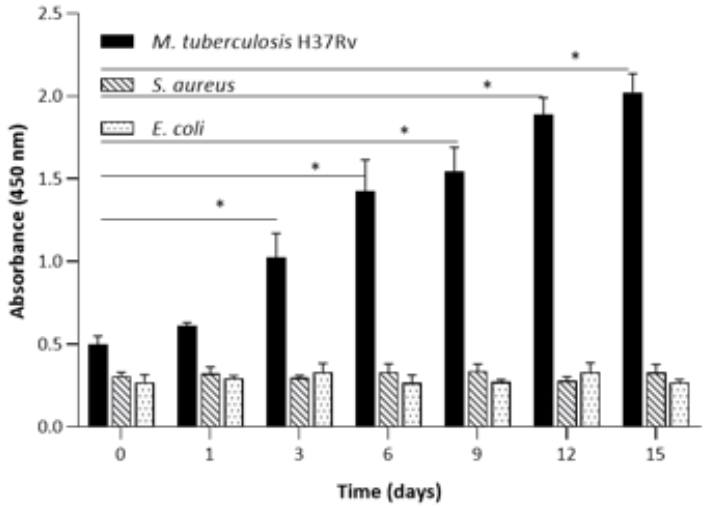

Figure 2. *Detection of Ag85B protein from M. tuberculosis H37Rv cultured in liquid media using sandwich ELISA method. S. aureus and E. coli were used as the negative controls for Ag85B detection. *: Statistically significant (p≤0.05, t-test).*

Table 1 Detection of Ag85B protein from *M. tuberculosis* sample cultured in liquid media using sandwich ELISA method.

Sample No.	Mycobacterial Samples	Treatment with Streptomycin	ELISA absorbance at 450 nm of M. tuberculosis culture filtrate (Mean±SD)					
			Day 1	Day 3	Day 6	Day 9	Day 12	Day 15
1	Drug-susceptible MTB	with	0.843±0.03	0.835±0.03	0.931±0.02	0.937±0.03	0.979±0.01	1.035±0.04
		without	0.848±0.02	1.063±0.03	1.577±0.01	1.942±0.04	2.007±0.01	2.378±0.03
2	Drug-susceptible MTB	with	0.379±0.04	0.439±0.01	0.539±0.04	0.541±0.02	0.534±0.01	0.673±0.04
		without	0.513±0.02	0.786±0.03	1.436±0.02	1.866±0.04	1.91±0.01	2.055±0.04
3	Drug-susceptible MTB	with	0.612±0.02	0.608±0.01	0.679±0.04	0.698±0.01	0.739±0.02	0.849±0.04
		without	0.606±0.04	0.805±0.03	1.451±0.03	2.247±0.03	2.357±0.04	2.409±0.03
4	Drug-susceptible MTB	with	0.385±0.04	0.471±0.01	0.508±0.01	0.512±0.04	0.544±0.04	0.577±0.01
		without	0.606±0.03	0.683±0.04	1.491±0.04	1.959±0.04	1.987±0.03	2.007±0.04
5	Drug-susceptible MTB	with	0.419±0.02	0.562±0.03	0.591±0.02	0.612±0.01	0.652±0.01	0.713±0.02
		without	0.463±0.01	0.703±0.02	1.436±0.02	1.927±0.02	1.951±0.02	2.355±0.01
6	Drug-susceptible MTB	with	0.535±0.02	0.608±0.02	0.641±0.03	0.647±0.02	0.58±0.03	0.779±0.03
		without	0.531±0.02	0.869±0.03	1.156±0.03	1.347±0.02	1.459±0.02	1.593±0.02
7	Drug-susceptible MTB	with	0.551±0.04	0.585±0.01	0.643±0.04	0.633±0.02	0.618±0.04	0.772±0.02
		without	0.511±0.02	0.577±0.03	0.752±0.04	1.905±0.02	2.43±0.04	2.841±0.01
8	Drug-susceptible MTB	with	0.559±0.04	0.585±0.01	0.666±0.01	0.701±0.04	0.824±0.04	0.842±0.03
		without	0.552±0.03	0.831±0.04	1.358±0.01	2.066±0.04	2.343±0.01	2.829±0.04
9	Drug-susceptible MTB	with	0.566±0.04	0.765±0.04	0.783±0.03	0.812±0.03	0.845±0.04	0.943±0.01
		without	0.511±0.04	0.761±0.01	0.822±0.01	1.257±0.04	1.786±0.03	1.997±0.02
10	Drug-susceptible MTB	with	0.894±0.04	0.946±0.04	0.964±0.04	1.059±0.02	1.155±0.04	1.158±0.04
		without	0.637±0.04	1.204±0.03	1.747±0.03	2.425±0.04	2.418±0.01	2.791±0.04
11	Streptomycin-resistant MTB	with	0.721±0.01	0.851±0.02	1.265±0.04	1.552±0.02	1.716±0.04	2.274±0.03
		without	0.778±0.03	0.799±0.04	1.173±0.03	1.377±0.04	1.768±0.01	2.353±0.04
12	Streptomycin-resistant MTB	with	0.826±0.01	1.027±0.02	1.328±0.04	1.485±0.01	1.921±0.04	2.121±0.02
		without	0.812±0.03	1.023±0.04	1.169±0.01	1.397±0.02	1.723±0.02	2.203±0.04

The sandwich ELISA assay was tested each sample in triplicate on a particular day.

Identification and monitoring of Antigen 85B in the mycobacterial culture treated with streptomycin

M. tuberculosis H37Ra, *M. tuberculosis* H37Rv, and 12 clinical isolates of *M. tuberculosis* were inoculated with SM in liquid media. All samples in this study were tested using standard methods to confirm *M. tuberculosis*. These mycobacteria were cultured in parallel with the untreated group without SM in liquid media to study the release of Ag85B when *M. tuberculosis* was treated with or without an antimicrobial drug. Culture filtrates were collected on days 0, 1, 3, 6, 9, 12, and 15. Then samples were analyzed for the presence of Ag85B using a sandwich ELISA assay. The results were obtained by statistical t-test analysis with a 95% confidence interval.

Ag85B was detected in 12 clinical isolates of *M. tuberculosis* cultured in liquid media. Moreover, Ag85B was found to increase further each day, the same as the increase of Ag85B from *M. tuberculosis* H37Ra and *M. tuberculosis* H37Rv.

The results of *M. tuberculosis* H37Ra, *M. tuberculosis* H37Rv and 10 clinical isolates of *M. tuberculosis* cultured in liquid culture containing SM showed that Ag85B levels were slightly increased on days 3-9 and then stable (Figure 3, Figure 4 and Table 1). In parallel, positive fluorescent AFB stains on days 0, 1, 3, 6, 9, 12, and 15 were quantified as 1+, 1+, 1+, 1+, 2+, 2+, and 2+ respectively. In addition, these 10 clinical isolated cultures were characterized as drug-susceptible mycobacteria by the standard proportion method. When these mycobacteria were cultured in liquid media containing SM, their growth was inhibited and unable to release Ag85B. As Ag85 cannot be secreted by dead mycobacteria, stable Ag85B accumulation in liquid culture was observed. There was no significant difference (p>0.05) in the Ag85B levels when comparing day 6 with days 9, 12, and 15.

In contrast, an increase in Ag85B levels was observed in 2 of 12 clinical isolates in liquid culture containing SM. The pattern of increase in Ag85B was also similar in both aforementioned samples (SM-resistant mycobacteria No. 1 and 2), as shown in Figure 5 and Table 1. In addition, these 2 clinical specimens were characterized as SM-resistant *M. tuberculosis* by standard proportion method. Moreover, to determine the number of SM-resistant *M. tuberculosis* by fluorescent AFB staining without and with SM on days 0, 1, 3, 6, 9, 12, and 15, specimens were graded as 1+/1+, 1+/1+, 1+/2+, 2+/2+, 3+/3+, 3+/3+, and 3+/3+, respectively. This indicated that over more days of SM-resistant mycobacterial culture, the accumulation of Ag85B increased continually in liquid media. This also indicated that mycobacteria were

still living and growing in liquid culture treated with SM. However, in 10 of 12 clinical isolates, drug-susceptible mycobacteria, *M. tuberculosis* H37Ra and *M. tuberculosis* H37Rv cultured with SM showed similar results in Ag85B levels. The Ag85B showed a slight increase and then stabilized, as shown in Figure 6. In parallel, the fluorescent AFB staining of mycobacteria culture without and with SM on days 0, 1, 3, 6, 9, 12, and 15 were graded as 1+/scanty, 1+/1+, 2+/1+, 3+/1+, 3+/1+, 3+/1+, and 3+/1+, respectively.

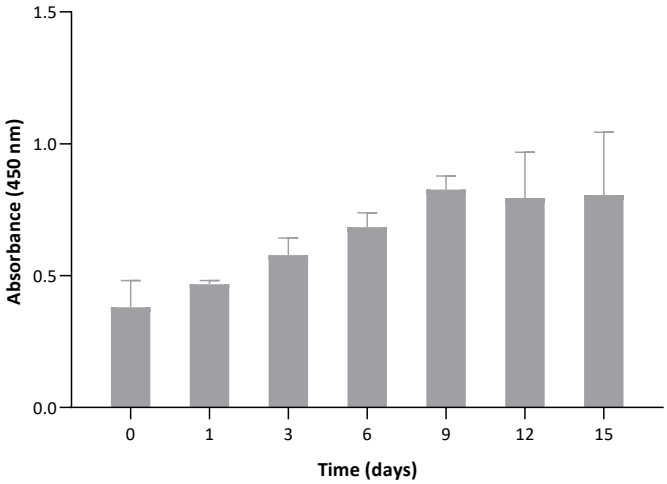

Figure 3. *Detection of Ag85B protein from M. tuberculosis H37Ra cultured in liquid media containing streptomycin using sandwich ELISA method.*

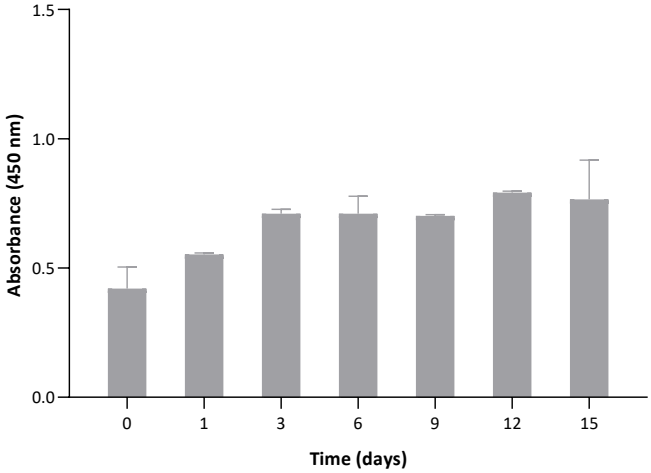

Figure 4. *Detection of Ag85B protein from M. tuberculosis H37Rv cultured in liquid media containing streptomycin using sandwich ELISA method.*

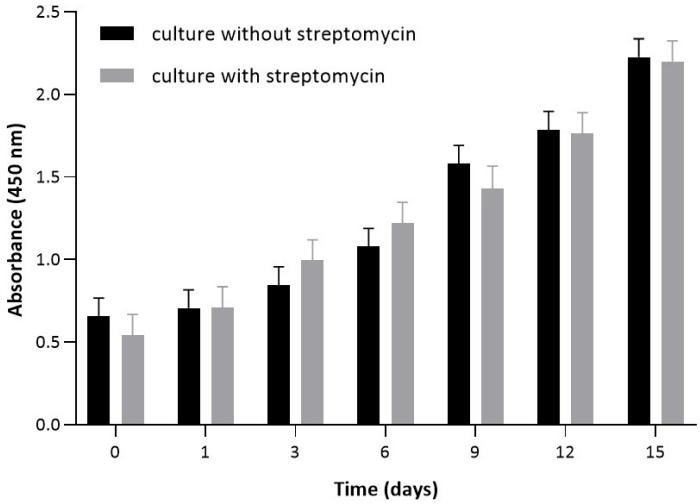

Fluorescent AFB stains	1+/1+	1+/1+	2+/2+	2+/2+	3+/3+	3+/3+	3+/3+

Figure 5. *The Ag85B protein detection from streptomycin-resistant M. tuberculosis (Sample No. 11) compares between culturing in liquid media with and without streptomycin using sandwich ELISA method.*

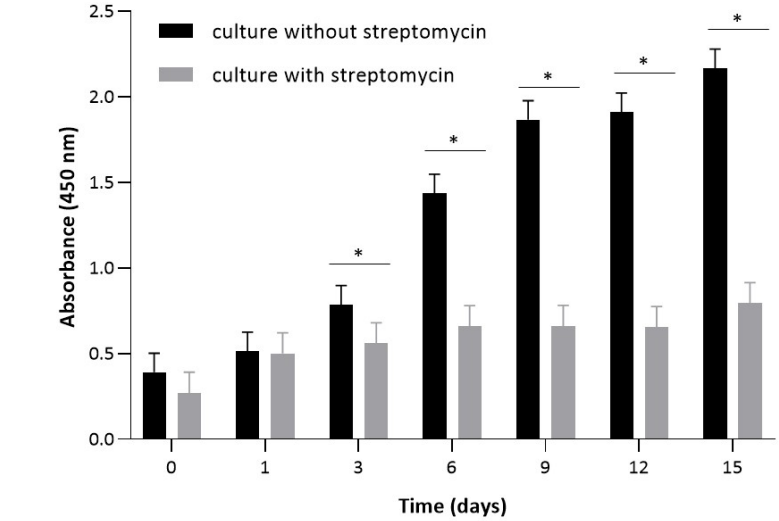

Figure 6. *Ag85B protein detection from drug-susceptible mycobacteria (Sample No. 5) compares between culturing in liquid media with and without streptomycin using sandwich ELISA method. *: Statistically significant (p≤0.05, t-test).*

Detection of mycobacteria by fluorescent staining

To define the number of *M. tuberculosis* according to the European Union/WHO scale, *M. tuberculosis* were inoculated in liquid culture with or without antimicrobial drug on days 0, 1, 3, 6, 9, 12, and 15. Fluorescent staining was performed to observe the number of mycobacteria on each day. In case of mycobacteria culture without SM, the number of mycobacteria increased and cord formation was also observed on smeared slide. Formation of cord factor occurred and grew to a large size over additional days in mycobacterial liquid culture in the same manner as using *M. tuberculosis* H37Rv as a model (Figure 7-A). Furthermore, 2 SM-resistant mycobacteria cultured with SM showed a similar number and cord formation to *M. tuberculosis* H37Rv in untreated condition. On the other hand, 10 isolates of drug-susceptible mycobacteria and *M. tuberculosis* H37Rv were cultured with SM, showing a small number of mycobacteria and no cord formation in liquid media, as shown in Figure 7-B.

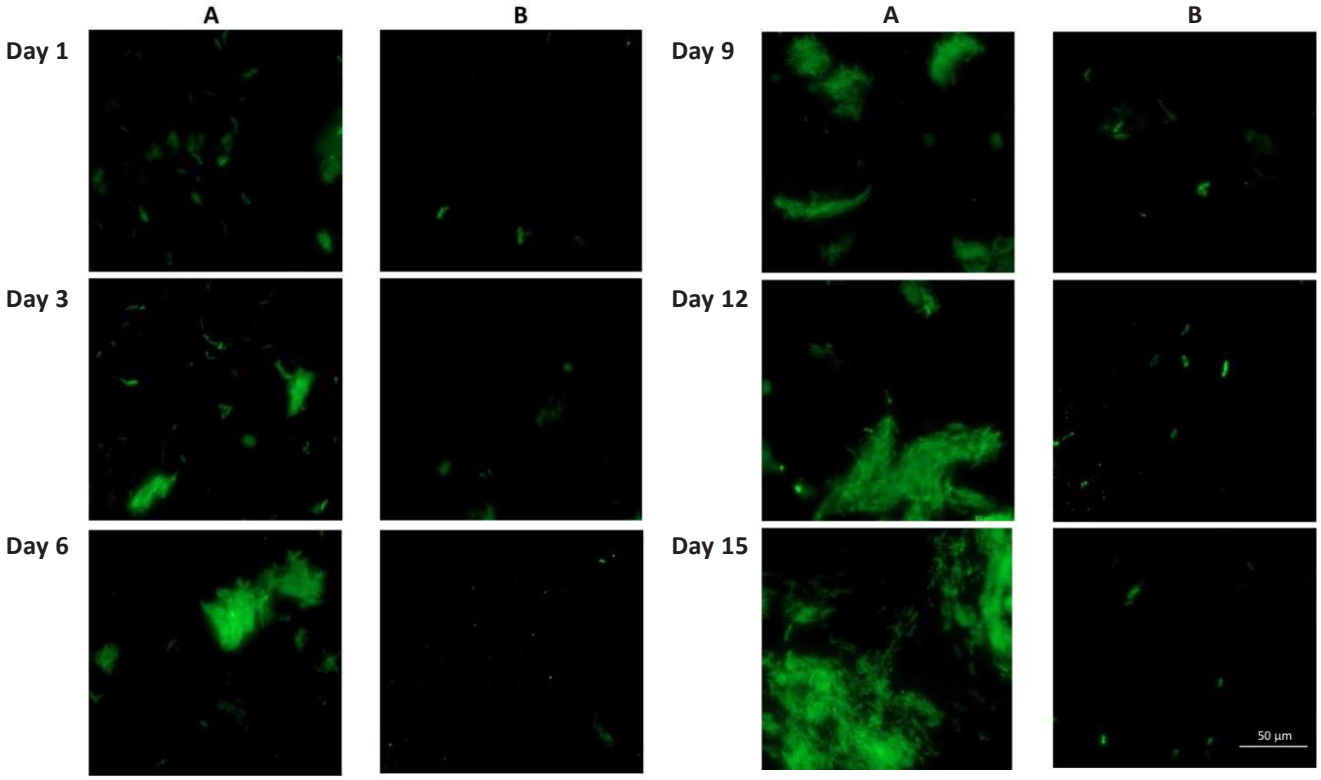

Figure 7. *Fluorescent acid fast stain of M. tuberculosis H37Rv in untreated liquid culture (A) and treated liquid culture with streptomycin (B), at 400x magnification.*

Discussion

TB is the most infectious mortal disease in the world, with an estimated 10 million new cases and 1.5 million deaths per year.[3,11] Therefore, TB patients need to receive proper and consistent antibiotic treatment as soon as possible in order to be adequately treated.[3] At present, several methods are performed for the diagnosis of TB, including AFB staining and mycobacterial culture. However, there are some limitations; for example, using microscopic examination for AFB staining has low sensitivity.[12] Mycobacterial culture is the gold standard method for TB diagnosis, although it takes a long time to complete, at about 4-6 weeks.[4,13] Rapid mycobacterial culture methods and molecular assays, which have a high specificity, should play a key role in TB diagnosis.[14] However, they are not possible in all clinical settings. However, serology-based TB tests have the potential to solve these issues. This is due to the fact that they may be completed rapidly at a low cost, especially in a low-resource clinical setting. Moreover, numerous studies have investigated proteins as potential candidates for TB immunodiagnostic tests. Antigen 85 complex is also being studied as a potential antigen for diagnosing or monitoring mycobacterial infection growth.

The Ag85 complex is the largest amount of protein secreted by actively replicating *M. tuberculosis*. In addition, Ag85 complex has 2 forms, soluble form and solid form, which are found on the surface of mycobacterial cell membranes.[15] The Ag85 complex is a *Mycobacterium*-specific 30-32 kDa family of three proteins (Ag85A, Ag85B, and Ag85C). Moreover, Ag85B was found to be the most abundant protein in liquid culture.[16] Therefore, Ag85B is an interesting target for diagnosis and monitoring of active TB.[17]

In this study, we aimed to detect Ag85B protein from the active growth of *M. tuberculosis* in liquid culture using a sandwich ELISA assay that was developed by Phunpae and colleagues in 2014. Anti-Ag85B mAb clone AM85B-8 was coated on the ELISA plate as capture antibody, and anti-Ag85 pAb was used as a secondary antibody to detect antigen-antibody complexes on the plate. The sensitivity of this ELISA for detecting Ag85B was 8 ng/mL.[7] Therefore, we have a specific and sensitive tool to detect Ag85B in *M. tuberculosis* culture filtrate. The drug susceptible-mycobacteria *M. tuberculosis* H37Ra and *M. tuberculosis* H37Rv have the ability to produce Ag85B since they are cultured in Middlebrook 7H9 broth. Consequently, Ag85B levels continuously increase over a longer period of culture. This means that *M. tuberculosis* are still growing and replicating, so they can release Ag85B and form cord factor.

The culture supernatant was filtered through a standard filter. The culture filtrate was sterile. Therefore, it is safe and can be used for testing. However, the use of culture filtrate that was filtered immediately when performing ELISA assay should be performed in a laboratory setting and operated with caution.

Moreover, to monitor Ag85B levels from liquid mycobacterial culture between untreated and treated *M. tuberculosis* culture, the number of *M. tuberculosis* and cord formation was observed on smeared slide. Mycobacterial cell and cord factor gradually formed in liquid culture as the days passed. SM was chosen to be a drug for treatment in mycobacterial liquid culture. SM is an aminoglycoside antibiotic derived from *Streptomyces griseus*. This drug is a common broad spectrum antibiotic used for TB infections and for susceptible Gram-negative infections.[18]

Ag85B levels were compared among 12 clinical isolates of *M. tuberculosis* in mycobacterial culture with and without SM. In this study, mycobacteria have been identified to be *M. tuberculosis* by standard culture method. *M. tuberculosis* in this study can be divided into 2 groups. In the first group, consisting of 10 drug-susceptible mycobacteria, Ag85B was found to increase slightly on days 3-9 and then remained stable when treated with SM in liquid media. In contrast to the second group, which consisted of 2 SM-resistant mycobacteria treated with SM, the increase in Ag85B was the same as in mycobacterial cultures without SM. This result is related to the results of Ag85 protein levels. The increase in Ag85B was also found in mycobacterial cultures with SM. This indicates that mycobacteria cannot be suppressed by SM. Therefore, they can grow and continue to release Ag85B. However, in case of drug-susceptible mycobacteria, the slight increase in Ag85B levels in the first period followed by stabilization, some mycobacteria might grow during treatment and release Ag85B in the initial phase before being suppressed by SM.

The number of days required for *M. tuberculosis* culture in liquid medium for collecting the culture filtrate should be 3 and 9. Then they were tested with a sandwich ELISA to compare the increase in Ag85B. On the third day of Ag85B detection, the difference between the alive and the dead mycobacteria was the same as using the drug culture. In the case of alive mycobacteria, Ag85B levels will continue to increase on day 9, but with dead mycobacteria, Ag85B levels will remain stable or no difference is observed even after longer incubation.

This study, microorganism identified as *M. tuberculosis* were used as samples for Ag85B detection. This protein was identified by establish sandwich ELISA using a monoclonal antibody that our researcher produces and develops. This is an alternative method to test for *M. tuberculosis*. However, further study should test this method with non-tuberculosis mycobacteria for obtaining additional information

The ELISA assay of this study is useful for preliminary detection whether *M. tuberculosis* is alive because active growth will release more Ag85B in the liquid culture medium over time. Therefore, this is an advantage for monitoring alive mycobacteria as well. This research is especially useful in laboratories without an automated instrument for TB culture. The standard culture method requires a period of 4-6 weeks for cultivation; therefore, this method would help reduce the time spent in laboratory. Moreover, it is particularly useful in laboratories that do not have special tools or molecular biology tools, for example, LPA or PCR techniques. In addition, the sandwich ELISA assay for the detection of Ag85B would provide the starting point for the development of new techniques and technologies in today's diagnostic tests. It also provides basic knowledge in applying other faster techniques such as the development of biosensor detection methods.

In this study, we presented knowledge about the different Ag85B levels between *M. tuberculosis* cultures with and without SM. This knowledge might have some advantages for further studies, including the study of the different Ag85B levels between mycobacterial cultures with and without anti-TB drugs and the development of new techniques for mycobacterial drug susceptibility testing by detecting Ag85B levels. This fundamental knowledge would be used in the further development and application of MTBC detection from clinical specimens, such as sputum or other respiratory samples. The clinical specimens might be pretreated with NaOH-NALC methods, and then cultured in liquid culture medium to monitor the level of Ag85B for tuberculosis detection. Therefore, in further study, it might be tested from clinical specimens.

Conclusion

M. tuberculosis can produce and secrete Ag85B protein. The Ag85B detection by sandwich ELISA assay can be used to identify *M. tuberculosis*. In addition, the growth of *M. tuberculosis* can be monitored by detecting an increase in Ag85B in liquid culture. When *M. tuberculosis* is suppressed or killed by anti-TB drugs, it stops growing and the increase in Ag85B proteins disappears. Consequently, the levels of Ag85B protein could be used to detect live mycobacteria and monitor the growth of mycobacteria affected by testing with anti-TB drugs.

Conflict of interest

The authors declare no conflict of interest.

Acknowledgements

This work was supported by CMU Junior Research Fellowship Program and grant scholarships for Teaching Assistants (TA's) and Research Assistants (RA's) from the Graduate School of Chiang Mai University. The authors wish to express their great appreciation to all staff members at the Division of Clinical Microbiology, Department of Medical Technology, and the Biomedical Technology Research Center, Faculty of Associated Medical Sciences at Chiang Mai University. The authors wish to express their gratitude to all staff members at the Tuberculosis Laboratory, Office of Disease Prevention and Control Region 1, Chiang Mai, for their support, kindness and great help in the experimental work.

References

[1] Furin J, Cox H, Pai *M. tuberculosis*. The Lancet 2019; 393(10181): 1642-56.

[2] World Health Organization. Global tuberculosis report 2020: executive summary. World Health Organization [Internet]. 2020 [cited 2020 Jun 15] Available from: https://apps.who.int/iris/handle/10665/337538/.

[3] World Health Organization. (2020). Global tuberculosis report 2020. World Health Organization [Internet]. 2020 [cited 2020 Jun 15] Available from: https://apps.who.int/iris/handle/10665/337539/.

[4] Adigun R, Singh R. Tuberculosis. In: StatPearls [Internet]. 2021 [cited 2021 Jan] Available from: https://www.ncbi.nlm.nih.gov/books/NBK441916/.

[5] Ahmad S, Mokaddas E, Al-Mutairi N, Eldeen HS, Mohammadi S. Discordance across phenotypic and molecular methods for drug susceptibility testing of drug-resistant *Mycobacterium tuberculosis* isolates in a low TB Incidence Country. PLoS One 2016; 11(4): e0153563.

[6] Karbalaei Zadeh Babaki M, Soleimanpour S, Rezaee SA. Antigen 85 complex as a powerful *Mycobacterium tuberculosis* immunogene: biology, immune-pathogenicity, applications in diagnosis, and vaccine design. Microb Pathog 2017; 112: 20-9.

[7] Phunpae P, Chanwong S, Tayapiwatana C, Apiratmateekul N, Makeudom A, Kasinrerk W. Rapid diagnosis of tuberculosis by identification of Antigen 85 in mycobacterial culture system. Diagn Microbiol Infect Dis 2014; 78(3): 242-8.

[8] Zhang W, Shu Q, Zhao Z, Fan J, Lyon C J, Zelazny A M, *et al*. Antigen 85B peptidomic analysis allows species-specific mycobacterial identification. Clinical Proteomics, 2018; 15(1). doi:10.1186/s12014-017-9177-6.

[9] Joel D Er, Amber C, Miriam B. Dynamics of *Mycobacterium tuberculosis* Ag85B revealed by a sensitive enzyme-linked immunosorbent assay. the mBio. 2019 Apr 23; 10(2): e00611-19. doi: 10.1128/mBio.00611-19.

[10] Imaz M, *et al*. Performance of LED fluorescence microscopy for the detection of acid-fast bacilli from respiratory samples in peripheral laboratories in Argentina. Biomedica 2017; 37(2): 164-174.

[11] World Health Organization. Global tuberculosis report 2019. World Health Organization [Internet]. 2019 [cited 2020 Jun 15] Available from: https://apps.who.int/iris/handle/10665/329368/.

[12] Ryu YJ. Diagnosis of pulmonary tuberculosis: recent advances and diagnostic algorithms. Tuberc Respir Dis (Seoul) 2015; 78(2): 64-71.

[13] Heemskerk D CM, Marais B, *et al*. Tuberculosis in adults and children [Internet]. 2015 [cited 2020 May 7] Available from: https://www.ncbi.nlm.nih.gov/books/NBK344406/.

[14] Amicosante M, D'Ambrosio L, Munoz M, Mello FCQ, Tebruegge M, Chegou NN, *et al*. Current use and acceptability of novel diagnostic tests for active tuberculosis: a worldwide survey. J Bras Pneumol 2017; 43(5): 380-92.

[15] Kuo CJ, Bell H, Hsieh CL, Ptak CP, Chang YF. Novel mycobacteria antigen 85 complex binding motif on fibronectin. J Biol Chem 2012; 287(3): 1892-902.

[16] Lee BY, Horwitz MA. Identification of macrophage and stress-induced proteins of *Mycobacterium tuberculosis*. J Clin Invest 1995; 96(1): 245-9.

[17] Goletti D, Lee MR, Wang JY, Walter N, Ottenhoff THM. Update on tuberculosis biomarkers: From correlates of risk, to correlates of active disease and of cure from disease. Respirology 2018; 23(5): 455-66.

[18] Chakraborty S, Rhee KY. Tuberculosis drug development: history and evolution of the mechanism-based paradigm. Cold Spring Harb Perspect Med 2015; 5(8): a021147.

Journal of Associated Medical Sciences 2022; 55 (3): 105-108

JAMS
Journal of Associated Medical Sciences

Thai-Journal Citation Index Centre (TCI) & ASEAN Citation Index (ACI)

Journal of Associated Medical Sciences

Journal homepage: https://www.tci-thaijo.org/index.php/bulletinAMS/index

Reinfection of SARS CoV-2 in patients with relapse of symptoms after clinical recovery: A Case Series

Tatikonda Chandramouli **Shakti Bedanta Mishra*** **Arun Rath**

Department of Critical Care Medicine, IMS and SUM Hospital, Siksha O Anusandhan (Deemed to be) University, K-8, Kalinga Nagar, Bhubaneswar-751003, Odisha, India.

ARTICLE INFO

Article history:
Received 26 February 2022
Accepted as revised 1 July 2022
Available online 1 August 2022

Keywords:
COVID-19 infection, SARS CoV-2 reinfection, health care workers

ABSTRACT

Background: It has been more than a year, and still, we are battling with a novel coronavirus (SARS-COV-2). Initially, the interim guidelines by the World health organization (WHO) stated that infection ranges from asymptomatic to critical life-threatening pneumonia with the symptomatology of fever, cough and breathing difficulty.

Objectives: To observe the reinfection of SARS CoV-2 in patients with relapse of symptoms after clinical recovery.

Materials and methods: Three cases were observed during the isolation period. Reverse transcription polymerase chain reaction (RT-PCR) and severity of similar symptoms in the fourth week from the onset was monitored.

Results: All the three patients had health care exposure, and which pointed us towards health care associated reinfection could be a possible cause of step-up in the symptom severity.

Conclusion: Reinfection by SARS CoV-2 can be considered in patients with relapse of symptoms after clinical recovery after natural infections.

Introduction

It has been more than a year, and still, we are battling with a Severe Acute Respiratory Syndrome Corona Virus-2 (SARS-COV-2). Initially, the interim guidelines by the World health organization (WHO) stated that infection ranges from asymptomatic to critical life-threatening pneumonia with the symptomatology of fever, cough and breathing difficulty.[1] Further, researchers contributed about extra-pulmonary manifestations for disease expression and potential sources of viral transmission.[2] The disease pattern never stopped surprising us with its atypical presentations like cerebral infarcts, rhabdomyolysis, acute coronary syndromes following full clinical recovery. As it is a novel disease with many faces, which mandates vigilant monitoring and regular follow-up by clinicians.[2] These rare cases are to be earmarked with patient-centric specific treatment strategies.

We observed the following three cases during the isolation period who tested positive for Reverse transcription polymerase chain reaction (RT-PCR), COVID test and developed increased severity of similar symptoms in the fourth week from the onset of desease symptoms. The basic idea to put present these cases is not only because of their atypical presentations but also because of paucity in the literature.

Case scenarios

Case 1: A 28-year-old male health care worker with no comorbidities presented with prodromal symptoms of fever, cough and tested positive for RT-PCR COVID test. The chest radiograph had normal lung fields and started on symptomatic treatment with favipiravir, levocetirizine, and

* **Corresponding author.**
Author's Address: *Department of Critical Care Medicine, IMS and SUM Hospital, Siksha O Anusandhan (Deemed to be) University, K-8, Kalinga Nagar, Bhubaneswar-751003, Odisha, India.*
** **E-mail address:** shakitimishra84@gmail.com
doi: 10.12982/JAMS.2022.031
E-ISSN: 2539-6056

oral vitamin C. Patient was asymptomatic during the treatment period and discharged home on the 14th day after the RT-PCR negative report. The patient developed respiratory distress with a respiratory rate of 36/min, and saturation measured on pocket pulse-oximeter at home was 90% on room air on the 22nd day after discharge. The patient was admitted and started on oxygen therapy with a nasal cannula; High Resolution Computerized Tomography (HRCT) thorax done on the same day showed a CT severity Index (CTSI) of 20/25 and CORADS 5. On day 3 of admission patient had an increased requirement of oxygen and shifted on to venturi mask. He received Injection of Ramdesivir 200 mg 10 days regimen and injection dexamethasone 6 mg once a day. The patient was discharged after symptomatic improvement. The patient was being followed up periodically as a part of the institutional protocol. (Table 1 and 2)

Case 2: A 50-year-old male health care worker, a known diabetic and hypertensive with 10 years of duration, has presented with fever and cough. Tested to be COVID positive by RT-PCR with normal baseline vitals and was in home isolation for 14 days and took standard care regimen for mild disease (favipiravir, vitamin c, levocetirizine) then the RT-PCR report was negative on day 14th of illness. Day 26th after the RT-PCR report was negative for the patient, he developed tachypnea with a respiratory rate of 34/min and presented to casualty. On examination, he was hemodynamically stable with room air saturation of 89%, and CT thorax revealed subpleural opacities with CTSI of 18/25. He fitted to the moderate category as of our institutional protocol and started injection Dexamethasone 6 mg OD. The patient stayed in the hospital (ICU, Ward) for 10 days and discharged on the 11th day. (Table 1 and 2).

Case 3: A 22-year-old female, a known case of thalassemia, had come for routine blood transfusion. As a protocol for admission, COVID RT-PCR was done, and it turned out to be positive. The patient had a history of recurrent admission. The patient has admitted to the COVID ward. The patient was asymptomatic and fitted into a mild-grade disease category, received multivitamins and vitamin C, and was discharged home on day 14 after tested negative for RT-PCR. The patient developed severe dyspnea and come to a casualty with room air saturation of 86% on room air. She was admitted in Isolation ICU and CT severity index 20/25 14 days after discharge. The patient received Injection Ramdesivir 200 mg (Viral replication inhibitor, used for COVID- 19 Pnemonia) and Injection Dexamethasone 6 mg, iv for 10 days. She was discharged home after clinical improvement on the 14th day of readmission. (Table 1 and 2).

Table 1 Tabular representation of the case details .

	Case 1	Case 2	Case 3
Age (years)	28	50	22
Symptoms on Day 1	Fever with cough	Fever with cough	Asymptomatic
Relapse of symptoms	Shortness of breath with room air saturation 90%	Tachypnea with Room air saturation of 89%	Dyspnea
CT severity Day 1	3/25	5/25	4/25
CT severity (readmission) Comorbidities	20/25 Obesity (BMI 28 kg/m^2) (Quetelets Index)	18/25 Diabetes and hypertension	20/25 Thalassemia on frequent blood transfusions
Probable anticipated source of infection	Health care associated	Health care associated	Health care associated
Treatment received on first admission	Flavipiravir and levocitirazine	Flavipiravir and levocitirazine and Vitamin C	Vitamin C Levocetirizine
Treatment received after relapse of symptoms	Ramdesivir and Dexamethasone	Dexamethasone	Ramdesivir Dexamethasone
Follow-up (6 months)	Stable	Stable	Stable

Table 2 Tabular representation of the case details .

	Symptoms	Treatment
Mild	Without evidence of breathlessness and hypoxemia.	Symptomatic treatment Flavipiravir Vitamin C antihistamines.
Moderate	With evidence of breathlessness and hypoxia SpO_2 <94% (90-94%).	Anticoagulation with low molecular heparin 40 IU, sc. Dexamethasone 6 mg, IV, OD Awake proning.
Severe	Clinical signs of pneumonia plus one of the following tachypnea >30 breaths/min, and hypoxemia SpO_2 <90%.	Anticoagulation with low molecular heparin 40 IU, sc. Ramdesivir 400 mg stat f/b 200 mg, OD Dexamethasone 6 mg, IV, OD High Flow Nasal Oxygen Mechanical ventilation.

Discussion

The three cases were treated between July 2020 to September 2020 with symptomatology mentioned above and were enrolled after obtaining ethical clearance from Institutional Ethical Committee of IMS & SUM Hospital, SOA University and informed consent was obtained from the clients. All these cases were admitted with mild symptoms (Table 1), and we had a severity based standard treatment protocol (Table 2).[3] Home quarantine was provided as per patient preference with regular teleconsultations. Our treatment protocol incorporated dexamethasone as a part in moderate to severe categories five along with Ramdesivir (Table 2).

SARS COV-2 virus belongs to the beta coronavirus group with a highly contagious nature comparing to another beta virus-like MERS, with a median incubation period of 2-14 days. Virus spike protein attaches to the Angiotensin-converting enzyme-2 (ACE), leading to increased Angiotensin II levels, ultimately with exaggerated host immune response leading to cytokine storm (Kawasaki like syndrome) with the hypercoagulable response from host.[4,5,6] The primary mode of transmission of SARSCOV-2 is the direct person to person respiratory transmission; when an infected person coughs or sneezes, the virus shredded in respiratory secretions might infect another person if he inhales or if it comes in direct contact with the mucous membranes.[7] The other mode of transmission where patient secretions might contaminate the surfaces like cots, lift bells, doors by touching the contaminated surfaces one's hands might get contaminated and takes a systemic root by rubbing eyes and touching mucous membranes.[8] The later cause has less potential to become an infection source in the general public, but this has its mark of incidence among health care workers, which might probably cause reinfection. Interesting, even though all three cases had no comorbidities matched, case 1 & 2 are healthcare workers who resumed back to work after normalizing the symptoms and both the cases had the step-up symptomatology after resuming back to work. Case-3 was a case of thalassemia, which incidentally detected to be positive. We have not given a blood transfusion to avoid transfusion-related immunological complications during this ongoing hyperimmune response condition, and later she visited the hospital for blood transfusion.

In *The Lancet*, Christian Holm Hansen and colleagues conducted a population-level observational study in Denmark.[9] Among eligible RT-PCR positive individuals from the first surge of the epidemic, 72 (0.65%) tested positive again during the second surge compared with 16 819 (3.27%) of 514 271 who tested negative during the first surge and found that protection against repeat infection was 80·5% among the patients who were previously infected with COVID-19 and 47.1% among subjects more than 65 years. This study concluded only based on RT-PCR, where the chances of false positivity are high, especially among naturally infected and immunized subjects. Considering this 20% chance of reinfection, which can be more commonly seen in geriatric patients than authors, they can also occur in health care workers who have a high chance of exposure to high viral load. The protective immunity obtained by natural infection to the reinfection remained unanswered. The new variants with altered phenotype unlikely to be covered under the immunological natural T cell-mediated immunity. Rosemary J Boyton supported the chances of reinfection after natural infection.[10] In an early report by Wang D et al., from China, it was estimated that among the incidence of COVID-19, 43% were hospital-acquired.[11,12] The study extended to evaluate incidence among the USA residents, which showed near identical results to the previous study conducted by Wang D colleagues proving health care individuals are more prone to infection even with less common modes of transmissions like fomites, fecal shedding.

In all our three subjects RT-PCR was negative on the 14th day of illness and discharged from hospital. A few days later all of them were presented with increase in severity of symptoms (clinical) and a rise in CTSI score after a brief asymptomatic period. The study could not conform the reinfection at genomic level analysis due lack of development of specific marker against the new strains of Corona Virus. This cannot be considered as "long COVID syndrome" as the symptoms regressed, after a certain period the clinical symptoms reappeared with increase in severity.[13] However, this cases series can only act as a driving tool for future RCTs (Randomised Controlled Trail). A statistically significant and adequately powered sample size would give better evidence with detailed mapping of immune parameters.

Consent

Consent has been obtained from the patients and the study was approved by IRB of IMS & SUM Hospital (DMR/IMS/SH/SOA/22/338).

Conflict of interest

The authors disclose that they have no conflicts of interest among them.

Funding Source

Nil.

Acknowledgements

The authors are highly grateful to the chairman of Siksha O Anusandhan (Deemed to be) University, Prof. Manoj Ranjan Nayak for providing the support during the study. The authors are also thankful to the Dean, IMS and Sum Hospital, Siksha O Anusandhan (Deemed to be) University, Prof. Gangadhar Sahoo for encouraging and supporting.

References

[1] Mehta Y, Chaudhry D, Abraham OC, Chacko J, Divatia J, Jagiasi B, et al. Critical Care for COVID-19 Affected Patients: Position Statement of the Indian Society of Critical Care Medicine. Indian J Crit Care Med. 2020; 24(4): 222-41. doi: 10.5005/jp-journals-10071-23395.

[2] Adukia SA, Ruhatiya RS, Maheshwarappa HM, Manjunath RB, Jain GN. Extrapulmonary Features of COVID-19: A Concise Review. Indian J Crit Care Med. 2020; 24(7): 575-80. doi: 10.5005/jp-journals-10071-23476.

[3] COVID-19 Treatment Guidelines Panel. Coronavirus disease 2019 (COVID-19) treatment guidelines. 2020 [cited 2022 January 26]. Available from:https://files.covid19treatmentguidelines.nih.gov/guidelines/covid19treatmentguidelines.pdf.

[4] RECOVERY Collaborative Group, Horby P, Lim WS, Emberson JR, Mafham M, Bell JL, Linsell L, et al. Dexamethasone in Hospitalized Patients with Covid-19. N Engl J Med.2021; 384(8), 693-704. doi.org/10.1056/NEJMoa2021436.

[5] Grasselli G, Tonetti T, Protti A, Langer T, Girardis M, Bellani G, et al. Pathophysiology of COVID-19-associated acute respiratory distress syndrome: a multicentre prospective observational study. Lancet Respir Med. 2020; 8(12): 1201-8. doi: 10.1016/S2213-2600(20)30370-2.

[6] Wiersinga WJ, Rhodes A, Cheng AC, Peacock SJ, Prescott HC. Pathophysiology, Transmission, Diagnosis, and Treatment of Coronavirus Disease 2019 (COVID-19): A Review. JAMA. 2020; 324(8): 782-93. doi: 10.1001/jama.2020.12839.

[7] Bi Q, Wu Y, Mei S, Ye C, Zou X, Zhang Z, et al. Epidemiology and transmission of COVID-19 in 391 cases and 1286 of their close contacts in Shenzhen, China: a retrospective cohort study. Lancet Infect Dis. 2020; 20(8): 911-9. doi: 10.1016/S1473-3099(20)30287-5.

[8] World Health Organization. Transmission of SARS-CoV-2: implications for infection prevention precautions: scientific brief. 2020 [Cited 2022 January 26]. Available from: https://apps.who.int/iris/handle/10665/333114

[9] Hansen CH, Michlmayr D, Gubbels SM, Mølbak K, Ethelberg S. Assessment of protection against reinfection with SARS-CoV-2 among 4 million PCR-tested individuals in Denmark in 2020: a population-level observational study. Lancet. 2021; 397(10280): 1204-12. doi: 10.1016/S0140-6736(21)00575-4.

[10] Boyton RJ, Altmann DM. Risk of SARS-CoV-2 reinfection after natural infection. Lancet. 2021; 397(10280): 1161-3. doi: 10.1016/S0140-6736(21)00662-0.

[11] Wang D, Hu B, Hu C, Zhu F, Liu X, Zhang J, et al. Clinical Characteristics of 138 Hospitalized Patients With 2019 Novel Coronavirus-Infected Pneumonia in Wuhan, China. JAMA. 2020; 323(11): 1061-9. doi: 10.1001/jama.2020.1585.

[12] Kuanar A, Kabi SK, Satapathy S, Mishra S, Bhuyan R, Kar D. Corona Virus-A review concerns about the present scenario. Ann. Romanian Soc. Cell Biol. 2021; 25(2): 1301-15.

[13] Taribagil P, Creer D, Tahir H. 'Long COVID' syndrome. BMJ Case Rep. 2021; 14(4): e241485. doi: 10.1136/bcr-2020-241485.

Journal of Associated Medical Sciences 2022; 55 (3): 109-115

JAMS
Journal of Associated Medical Sciences

Thai-Journal Citation Index Centre (TCI) & ASEAN Citation Index (ACI)

Journal of Associated Medical Sciences

Journal homepage: https://www.tci-thaijo.org/index.php/bulletinAMS/index

Correlation between cardio ankle vascular index, body mass index and pressure parameters in normal and overweight/obesity subjects

Phatiwat Chotimol* **Kanokwan Demeekul**

Department of Cardio-Thoracic Technology, Faculty of Allied Health Sciences at Naresuan University, Phitsanulok Province, Thailand.

ARTICLE INFO

Article history:
Received 27 January 2022
Accepted as revised 30 June 2022
Available online 2 August 2022

Keywords:
Cardio ankle vascular index, ankle brachial index, body mass index, pressure parameters, overweight/obesity

ABSTRACT

Background: Obesity and overweight are a risk factors and related to the arteriosclerosis mechanism. However, it has not been fully elucidated whether cardio ankle vascular index (CAVI) is closely associated with body mass index (BMI) and pressure parameters.

Objectives: This study aimed to compare CAVI and BMI with normal weight and overweight/obesity group, and to investigate the correlation between CAVI, ankle brachial index (ABI), BMI and pressure parameters.

Materials and methods: One hundred and twenty-four participants were divided into normal weight group (n=52), aged 47±12 years and overweight/obesity group (n=72), aged 48.50±13 years. Both CAVI and ABI were measured with a VaSera VS-1500N®; blood pressures were measured with an Omron M7®.

Results: Average ABI and mean arterial pressure (MAP) of overweight/obesity group was higher than the normal weight group. In the univariable analysis, there was a significant negative correlation between BMI and the average CAVI (r=-0.194; *p*=0.031), and the association between the average CAVI and ABI were positively significant (r=0.225, *p*=0.012). Using a multivariate regression analysis, the average CAVI was negatively associated with BMI (β=-0.217, *p*=0.014), while the association between the average CAVI and ABI was positively correlated (β=0.246, *p*=0.005).

Conclusion: The average CAVI and BMI were negatively correlated, while the average CAVI and average ABI were positively related. Using a multivariate regression analysis, the average CAVI is strongly associated with the average ABI and BMI.

Introduction

Obesity is a major public health problem with the number of overweight groups increasing around the world.[1] It is generally understood that excess weight is a risk factor for cardiovascular disease, diabetes, hypertension, dyslipidemia especially, arterial stiffness.[2,3] Arterial stiffness is a consequence of pathology alterations that are associated with endothelial cells, smooth muscle cells and functional arterial walls. These alterations contribute to cardiovascular damage and dysfunction.[4] Several studies used pulse wave velocity (PWV) to evaluate arterial stiffness and to investigate the possible correlation of body mass index (BMI) with vascular function in overweight and obesity subjects.[5-7] However, in the clinical research, the problem with the PWV was itself essentially dependent on blood pressure. There are arterial indexes to investigate vascular damage as the cardio-ankle vascular index (CAVI) and ankle-brachial index (ABI). CAVI is the new arteriosclerotic index and a strong indicator of arterial stiffness. Moreover, CAVI is independent of blood pressure at the time of measurement and an indicator for early arteriosclerosis patients. While ABIs' value is used to diagnose peripheral arterial disease (PAD).[8,9] ABI is defined as the ratio of systolic blood pressure at the ankle and at the arm which demonstrates

* **Corresponding author.**
Author's Address: *Department of Cardio-Thoracic Technology, Faculty of Allied Health Sciences at Naresuan University, Phitsanulok Province, Thailand.*
** **E-mail address:** phatiwatch@nu.ac.th
doi: 10.12982/JAMS.2022.032
E-ISSN: 2539-6056

a high sensitivity and specificity for PAD interpretation.[10]

Several studies illustrated that PWV raised in high blood pressure patients, and positively correlated with BMI.[7,11] Furthermore, Rachel P. and *et al* showed that PWV was strongly correlated with a higher BMI and other parameters of obesity.[6] Many studies showed that overweight/obesity leads to vascular disorder.[12-15] Furthermore, the relationship between arterial indexes and BMI with excess weight remains a controversial debate. A previous study reported that diabetes mellitus without obesity had a significant CAVI.[8] According to this study, CAVI could be used to quantify the severity of arteriosclerosis. Moreover, the lower ankle pressure ABI has a higher sensitivity in detecting PAD.[10] However, the relationship of excess weight on CAVI, ABI and pressure parameters have not been fully reported.

Therefore, this study aimed to compare CAVI and ABI with normal and overweight/obesity group and to investigate the association between CAVI, ABI, BMI, and pressure parameters.

Materials and methods

Study population

This clinical study included the examination of 124 participants, which was conducted between January and June in 2017. "This study was conducted in accordance with the tenets of the Declaration of Helsinki, and the experimental protocol was approved by the Ethical Committee of Naresuan University, Phitsanulok Province, Thailand (Certificate of approval, COA number 352/2016). All participants signed a consent form before the clinical data could be collected. The enrolled participants were divided into normal and overweight/obesity groups and examined for obesity by following the Asia-Pacific BMI classification (BMI 18.5-22.9 kg/m^2 = normal; 23.0-24.9 kg/m^2 = overweight, and ≥25.0 kg/m^2 = obesity).[16] All volunteers answered a medical questionnaire regarding their illness history.

Body composition and blood pressure measurement

Body height was assessed without shoes using an anthropometer with an accuracy of 1 millimeter. BMI was calculated using the weight (kg) divided by the height (m) squared. Blood pressure (BP) measurement was performed after 5 to 10 minutes' rest using a calibrated oscillometric device (Omron M7®, Omron Corporation, Kyoto, Japan). The BP was measured 3 times and then the results were averaged. Mean arterial pressure (MAP) was calculated as [(2×diastolic pressure) + systolic pressure]/3. Hypertension was defined as SBP ≥130 mmHg and/or DBP ≥80 mmHg.[17] Pulsatile stress (PS) was computed as the double result of resting heart rate and pulse pressure (HR x PP).[18]

CAVI and ABI measurement

Both CAVI and ABI can be measured noninvasively using the VaSera VS-1500N® Vascular Screening System (Fukuda Denshi, Tokyo, Japan) by a cardio-thoracic technologist at the Cardio-Thoracic Technological department, Faculty of Allied Health Sciences, Naresuan University, Phitsanulok Province, Thailand. The subjects sat resting for 10 minutes before being measured in the supine position, in a quiet room with the temperature set at about 25°C. Electrocardiography (ECG) electrodes were placed on both wrists and a microphone was attached to the second intercostal space of the sternum, and four blood pressure cuffs were wrapped around the four extremities. CAVI was automatically calculated from 5 to 6 pulses by the following equation: $CAVI = a[(2\rho/PP) \times \ln(SBP/DBP) \times PWV^2] + b$, where ρ is the blood density, PP is SBP-DBP, SBP is systolic blood pressure, DBP is diastolic blood pressure, PWV is pulse wave velocity, and a and b are constants. CAVI was defined as normal (CAVI<8), borderline (8≤CAVI<9), or abnormal with subclinical possible arteriosclerosis (CAVI≥9).[19] ABI was calculated using the SBP from the right and left brachial arteries and posterior tibial artery. An ABI 1.00-1.39 = normal; 0.91-0.99 = borderline; 0.41-0.90 = mild-to-moderate PAD; ≤0.40 = severe PAD; ≥1.40 = non-compressible.[20]

Statistical analysis

Descriptive data was expressed as mean±standard deviation (SD) or median±interquartile rang (IQR), frequencies, or as absolute number and percentages when appropriate. The SPSS software version 17 (SPSS Inc, Chicago, IL, USA) was used for all our analysis. The Kolmogorov-Smirnov test evaluated equality distribution. Univariate comparisons between groups were processed using independent sample t-test for continuous variables and chi-square test for categorical variables. For the variables whose distribution rejected normality, the Mann-Whitney U test and the Wilcoxon rank-sum test were used to analyze. Univariate linear regression analyses were performed and was represented by scatter plot graphs. Multiple regression analysis was analyzed to identify the independent determinants of CAVI, BMI, ABI, and pressure parameters. The p<0.05 were statistically.

Results

A total of 124 participants were used in this study with 52 of them being normal weight and 72 being overweight/obesity. The percentages of normal weight, overweight and obesity was 41.94% (52), 20.16% (25), 37.90% (47), respectively. Age, sex, and heart rate did not differ significantly between the two groups (p=0.425, p=0.564, p=0.696), respectively. In the overweight/obesity group, SBP and DBP were significantly higher than the normal weight group (p=0.002, p=0.000, respectively). BMI in the overweight/obesity group was higher than the normal weight group (26.42±4.69, range 18.65-22.77 versus 20.88±1.74, range 23.16-42.61 kg/m^2; p=0.000). The percentage of smoking, alcohol intake, hypertension and diabetes mellitus did not significantly differ between the two groups. The demographic and personal history of each group is shown in detail in Table 1.

Average CAVI, PP and PS did not differ significantly between the normal weight and the overweight/obesity group as follows: CAVI = 7.48±1.05 vs 7.33±0.94, at p=0.173; PP = 43.00±17.50 mmHg vs 44.75±10.88 mmHg, at p=0.132; PS =2881.80±1172.88 mmHg/min vs 3090.50±1121.50 mmHg/min at p=0.102, respectively. Average ABI and MAP in the overweight/obesity group was higher than the normal weight group; ABI = 1.07±0.11 vs 1.02±0.12 at p=0.017; MAP = 98.84±17.3 mmHg vs 90.58±13.54 mmHg at p=0.001, respectively. The results are shown in Table 2.

In the univariable analysis, there was a significant negative correlation between average CAVI and BMI (r=-0.194; *p*=0.031), (Figure 1), while the association between the average CAVI and ABI are positively significant (r=0.225, *p*=0.012), (Figure 2). A multivariate regression analysis showed that the average CAVI was negatively associated with BMI (β=-0.217, *p*=0.014), while the association between the average CAVI and ABI was positively correlated (β=0.246, *p*=0.005) as shown in Table 3.

Table 1 The demographic characteristics between normal weight and overweight/obesity participants.

	Normal weight (n=52)	Oerweight/obesity (n=72)	*p*-value
Age (years)[b]	47.00±12.00	48.50±13.00	0.425
Male, % (n)	36.54% (19)	41.67% (30)	0.564
BMI (kg/m^2)[b]	20.88±1.74	26.42±4.69	0.000*
SBP (mmHg)[a]	119.50±21.38	127.75±21.88	0.002*
DBP (mmHg)[a]	77.00±11.75	83.25±13.75	0.000*
HR (beats/min)[b]	71.25±15.00	69.50±15.00	0.696
Personal history, % (n)			
Smoking	5.77% (3)	9.72% (7)	0.425
Alcohol intake	5.77% (3)	12.50% (9)	0.211
Hypertension	9.62% (5)	20.83% (15)	0.094
Diabetes mellitus	3.85% (2)	5.56% (4)	0.662

[a]Results expressed as mean±standard deviation (SD), [b]Results expressed as Median±interquartile rang (IQR), BMI: body mass index: SBP. systolic blood pressure, DBP: diastolic blood pressure, HR: heart rate.

Table 2 The CAVI, ABI and pressure parameters of the normal weight group compared with the overweight/obesity group.

	Normal weight (n=52)	Oerweight/obesity (n=72)	*p*-value
Average CAVI[b]	7.48±1.05	7.33±0.94	0.173
Average CAVI ≥9 (%, n)	5.77 % (3)	5.55 % (4)	0.959
Average ABI[a]	1.02±0.12	1.07±0.11	0.017*
Average ABI ≤0.4 (%, n)	0% (0)	0% (0)	1.000
Average ABI ≥ 1.4 (%, n)	0% (0)	0% (0)	1.000
PP (mmHg)[b]	43.00±17.50	44.75±10.88	0.132
MAP (mmHg)[b]	90.58±13.54	98.84±17.30	0.001*
PS (mmHg/min)[b]	2,881.80±1,172.88	3,090.50±1,121.50	0.102

[a]Results expressed as mean±standard deviation (SD), [b]Results expressed as Median±interquartile rang (IQR), CAVI: cardio ankle vascular index, ABI: ankle brachial index, PP: pulse pressure, MAP: mean arterial pressure, PS: pulsatile stress.

Table 3 The CAVI, ABI and pressure parameters of the normal weight group compared with the overweight/obesity group.

	Univariate analysis			Multivariate analysis		
	r	95%CI	*p*-value	β	95%CI	*p*-value
BMI	-0.194	-0.079 - -0.004	0.031*	-0.217	-0.083 - -0.010	0.014*
Average ABI	0.225	0.683 - 5.395	0.012*	0.246	1.00 - 5.64	0.005*
SBP (mmHg)	0.076	-0.006 - 0.015	0.403	-	-	-
DBP (mmHg)	0.076	-0.009 - 0.023	0.404	-	-	-
MAP (mmHg)	0.080	-0.008 - 0.021	0.380	-	-	-
PS (mmHg/min)	0.030	0.000 - 0.000	0.744	-	-	-

CAVI: cardio ankle vascular index, BMI: body mass index, ABI: ankle brachial index, SBP: systolic blood pressure, DBP: diastolic blood pressure, MAP: mean arterial pressure, PS: pulsatile stress.

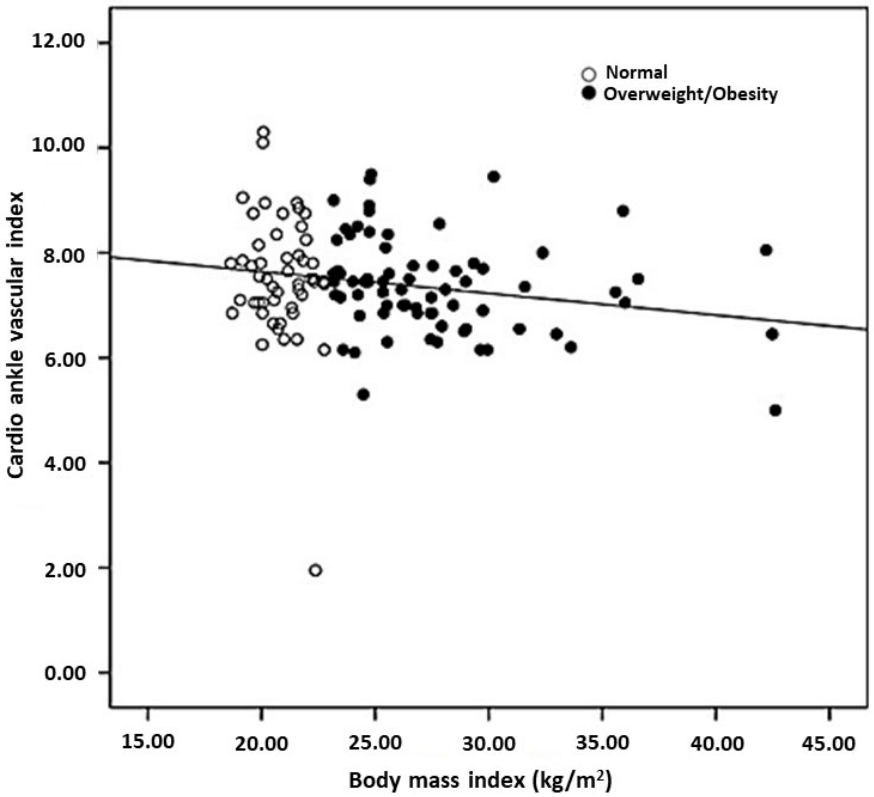

Figure 1. *Correlation between CAVI and BMI. CAVI was negatively correlated with BMI (r= -0.194, p=0.031).*

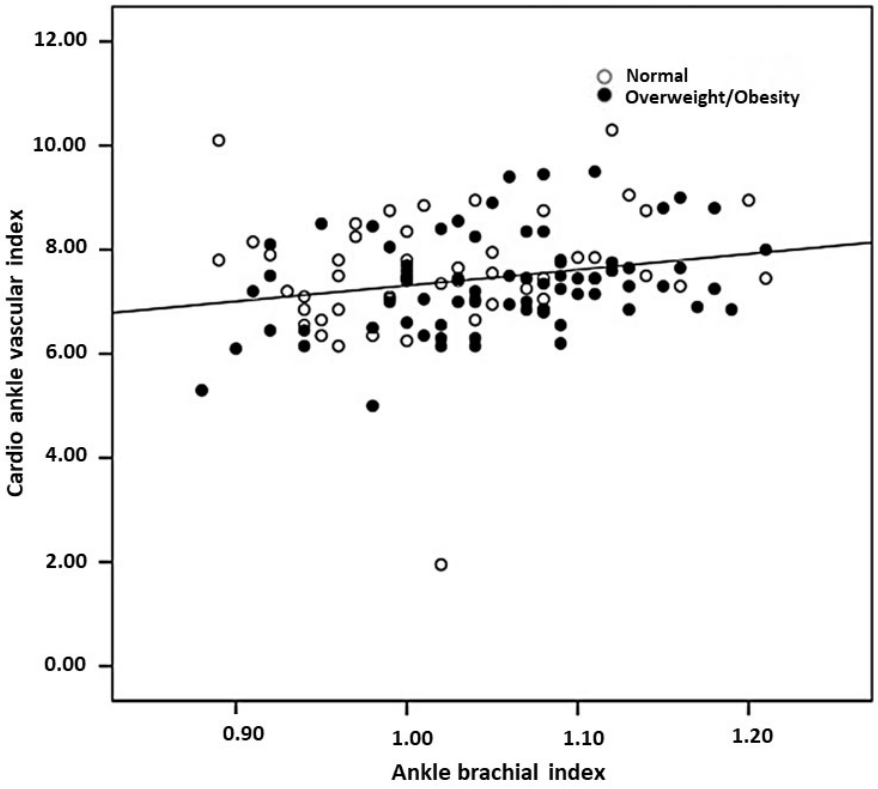

Figure 2. *Correlation between CAVI and ABI. CAVI was positively correlated with ABI (r= 0.225, p=0.012).*

Discussion

This study found that both SBP and DBP, and MAP in overweight/obesity group were significantly higher than the normal weight group. The MAP of this study was calculated according to the following formula: [(2×diastolic pressure) + systolic pressure]/3. Since an elevation of SBP and DBP in the overweight/obesity group, MAP increases due to rising peripheral vascular resistance. In 2002, the Framingham study reported that BMI ≥25 had prevalence rates of hypertension for approximately 34% of men and 62% of women.[21] Elevated blood pressure found in overweight/obesity group is related to systemic vascular resistance. People with an elevated BMI have increased adipose tissue deposition in the vascular wall which increases their systemic resistance, and in turn causes high blood pressure that increases the cardiac workload of pumping blood around the circulatory system.[22] Furthermore, obesity people are at risk of developing hypertension through increased activation of the renin-angiotensin-aldosterone system. In agreement with this mechanism, angiotensinogen, angiotensin I and II are produced which leads to elevated blood pressure that induces vasoconstriction mainly from angiotensin II.[23]

This study has found an average CAVI negatively correlates with BMI (r=-0.194; p=0.031). Many studies found that the CAVI was negatively associated with BMI in healthy subjects. Previous reports demonstrated inverse relationship of CAVI with BMI in healthy adult subjects.[24] Similar to the report from Nagayama D. and et al also found a negative relationship between BMI and CAVI in healthy middle aged Japanese participants.[25] They suggested that almost all subjects in their study were non-obesity without metabolic syndrome. If they had conducted their study on obesity subjects with metabolic disorder, the results may have been better understood. Some studies[26,27] have shown that overweight/obesity associated with elevated LDL-C serum levels induced initial lipidosis, causing soften the vessel walls that may lead to an inverse linear correlation between CAVI and BMI in this research. Furthermore, a negative relation of obesity with both PWV and CAVI has been published regarding adolescents. Dangrdt F. and *et al* found that PWV in obesity lower than lean children.[28] However, the intimal-medial thickness of the dorsal pedal arteries in obesity was more than in lean children. In addition, a previous study showed that BMI was negatively correlated with PWV, with a possibility of not affecting vascular function.[29] Several studies reported that BMI negatively correlated with PWV.[28,29] Consistence with our result found that an average CAVI negatively correlates with BMI. As we can see from the formula "CAVI = a [(2ρ/PP) × ln(SBP/DBP) × PWV2] + b", CAVI is dependent on PWV. So, the association between PWV with BMI and CAVI with BMI are negatively correlated. We expand the effects of overweight/obesity on CAVI. This result may represent the obesity paradox of overweight/obesity on arterial stiffness in the early stage of fat accumulation in Thais subjects. A previous study showed that PWV was inversely associated with BMI in Chinese people and that decreasing arterial stiffness in the overweight population may explain the obesity paradox.[30] Furthermore, the obesity paradox has been demonstrated in population with heart failure, coronary artery disease and hypertension.[31] The average CAVI positively correlates with ABI (r=0.225, p=0.012) in this study. Both PWV and CAVI are well-known indicators for arterial stiffness which is caused by arteriosclerosis. Joo, H. J., and *et al* analyzed brachial-ankle PWV (baPWV) and coronary artery stenosis dependence on ABI.[32] Several studies[33,34] have shown that an increased baPWV is significantly associated with the presence of coronary artery stenosis. Furthermore, the previous studies using a simple correlation analysis demonstrated that both CAVI and baPWV were related with Intima–media thickness, and they also concluded that a high CAVI causes the development of vascular arteriosclerosis, especially in the carotid and coronary artery.[35] Therefore, this study found that CAVI is closely linked to arteriosclerosis index with ABI. Overall, CAVI was negatively correlated with BMI. However, average CAVI and ABI was positively correlated. High CAVI has been widely used to evaluate arterial stiffening, while an abnormally low value of ABI was an indicator of stenosis of the vascular wall in the lower extremities. The stenosis of vessels may develop for many years with various arteriosclerosis risk factors before the obstruction of vascular. Also an ABI greater than 1.3 was incompressible vessels and may lead to artificially high value of the ABI.[36] We suggested that increasing of CAVI and ABI is associated with an increased risk of arterial stiffness and incompressible vessels .

Study limitations

Our study has main limitations to be considered. The history of illness was collected using a health questionnaire, and the lack of medication and biochemical tests were not collected. Further investigations of other obesity parameters, such as body fat percentage and waist-hip ratio, are warranted to strongly understand the pathophysiology of arteriosclerosis with CAVI and ABI in longitudinal cohort studies, and these conditions require elucidation in future studies.

Conclusion

The average CAVI and BMI was negatively correlated, while the average CAVI and ABI was positively related. A multivariate regression analysis showed that the average CAVI is strongly associated with both ABI and BMI.

Acknowledgements

This study was supported by grants from the Faculty of Allied Health Sciences Fund at Naresuan University. We would like to thank Mr. Peter Baton, at the Language Center (NULC), Naresuan University, for editing and correcting our manuscript.

Conflict of interest

The authors have no conflicts to declare.

References

[1] Hruby A, Hu FB. The Epidemiology of Obesity: A Big Picture. Pharmacoeconomics. 2014; 33(7): 673-89. doi: 10.1007/s40273-014-0243-x.

[2] Din-Dzietham R, Liu Y, Bielo MV, Shamsa F. High blood pressure trends in children and adolescents in national surveys, 1963 to 2002. Circulation. 2007; 116(13): 1488-96. doi.org/10.1161/CIRCULATIONAHA.106.683243.

[3] Van Gaal LF, Mertens IL, Christophe E. Mechanisms linking obesity with cardiovascular disease: Obesity and diabetes. Nature. 2006; 444(7121): 875-80. doi: 10.1038/nature05487.

[4] Jia G, Aroor AR, DeMarco VG, Martinez-Lemus LA, Meininger GA, Sowers JR. Vascular stiffness in insulin resistance and obesity. Front. Physiol. 2015; 6: 231. doi: 10.3389/fphys.2015.00231.

[5] Tomlinson LA. Methods for assessing arterial stiffness: technical considerations. Curr Opin Nephrol. Hypertens. 2012; 21(6): 655-60. doi: 10.1097/MNH.0b013e32835856e3.

[6] Wildman RP, Mackey RH, Bostom A, Thompson T, Sutton-Tyrrell K. Measures of obesity are associated with vascular stiffness in young and older adults. Hypertension. 2003; 42(4): 468-73. doi: 10.1161/01.HYP.0000090360.78539.CD.

[7] Huisman HW, Schutte R, Venter HL, van Rooyen JM. Low BMI is inversely associated with arterial stiffness in Africans. Br. J. Nutr. 2015; 113(10): 1621-7. doi: 10.1017/S0007114515000975. Epub 2015 Apr 13.

[8] Shirai K, Utino J, Otsuka K, Takata M. A novel blood pressure-independent arterial wall stiffness parameter; cardio-ankle vascular index (CAVI). J Atheroscler Thrombo. 2006; 13(2): 101-7. doi: 10.5551/jat.13.101.

[9] Ibata J, Sasaki H, Kakimoto T, Matsuno S, Nakatani M, Kobayashi M, et.al. Cardio-ankle vascular index measures arterial wall stiffness independent of blood pressure. Diabetes Res Clin Pract. 2008; 80(2): 265-70.

[10] Khan TH, Farooqui FA, Niazi K. Critical review of the ankle brachial index. Curr. Cardiol. Rev. 2008; 4(2): 101-6. doi: 10.1016/j.diabres.2007.12.016. Epub 2008 Feb 1. doi: 10.2174/157340308784245810.

[11] Benetos A, Buatois S, Salvi P, Marino F, Toulza O, Dubail D, et al. Blood pressure and pulse wave velocity values in the institutionalized elderly aged 80 and over: baseline of the PARTAGE study. J. Hypertens. 2010; 28(1): 41-50. doi: 10.1097/HJH.0b013e328332b879.

[12] Kyrou I, Randeva HS, Tsigos C, Kaltsas G, Weickert MO. Clinical problems caused by obesity. In Endotext [Internet].2018; MDText. com, Inc.

[13] Stapleton PA, James ME, Goodwill AG, Frisbee JC. Obesity and vascular dysfunction. Pathophysiology. 2008; 15(2): 79-89. doi.org/10.1016/j.pathophys.2008.04.007.

[14] Barton M, Baretella O, Meyer MR. Obesity and risk of vascular disease: importance of endothelium-dependent vasoconstriction. Br. J. Pharmacol. 2012; 165(3): 591-602. doi: 10.1111/j.1476-5381.2011.01472.x.

[15] Kappus RM, Fahs CA, Smith D, Horn GP, Agiovlasitis S, Rossow L, et al. Obesity and overweight associated with increased carotid diameter and decreased arterial function in young otherwise healthy men. Am. J. Hypertens. 2013; 27(4): 628-34. doi: 10.1093/ajh/hpt152.

[16] World Health Organization. The Asia-Pacific perspective: redefining obesity and its treatment. 2000. [cited 22 Jan 8]. Available from: https://apps.who.int/iris/bitstream/handle/10665/206936/0957708211_eng.pdf.

[17] Flack JM, CalhounD, Schiffrin EL. The New ACC/AHA Hypertension Guidelines for the prevention, detection, evaluation, and management of high blood pressure in adults. Am J Hypertens. 2018; 12;31(2): 133-35. doi: 10.1093/ajh/hpx207.

[18] Jae SY, Heffernan KS, Yoon ES, Park SH, Choi YH, Fernhall B, et al. Pulsatile stress, inflammation and change in arterial stiffness. J Atheroscler Thrombo. 2012; 19(11): 1035-42. doi: 10.5551/jat.13516. Epub 2012 Jul 14.

[19] Shirai K, Hiruta N, Song M, Kurosu T, Suzuki J, Tomaru T, et al. Cardio-ankle vascular index (CAVI) as a novel indicator of arterial stiffness: theory, evidence and perspectives. J Atheroscler Thrombo. 2011; 18(11): 924-38. doi: 10.5551/jat.7716.

[20] Gerhard-Herman MD, Gornik HL, Barrett C, Barshes NR, Corriere MA, Drachman DE, et al. 2016 AHA/ACC guideline on the management of patients with lower extremity peripheral artery disease: executive summary: a report of the American College of Cardiology/American Heart Association Task Force on Clinical Practice Guidelines. J Am Coll Cardiol. 2017; 69(11): 1465-508. doi: 10.1161/CIR.0000000000000470.

[21] Wilson PW, D'agostino RB, Sullivan L, Parise H, Kannel WB. Overweight and obesity as determinants of cardiovascular risk: the Framingham experience. Arch. of intern. med. 2002; 162(16): 1867-72. doi: 10.1001/archinte.162.16.1867.

[22] Schmieder RE, Messerli FH. Does obesity influence early target organ damage in hypertensive patients?. Circulation. 1993; 87(5): 1482-88. doi: 10.1161/01.cir.87.5.1482.

[23] Vukelic S, Griendling KK. Angiotensin II, from vasoconstrictor to growth factor: a paradigm shift. Circ. Res. 2014; 114(5): 754-57. doi: 10.1161/CIRCRESAHA.114.303045.

[24] Nagayama D, Watanabe Y, Saiki A, Shirai K, Tatsuno I. Lipid Parameters are Independently Associated with Cardio–Ankle Vascular Index (CAVI) in Healthy Japanese Subjects. J. Atheroscler. Thrombo. 2018; 25(7): 621-33. doi: 10.5551/jat.42291.

[25] Nagayama D, Imamura H, Sato Y, Yamaguchi T, Ban N, Kawana H, et al. Inverse relationship of cardioankle vascular index with BMI in healthy Japanese subjects: a cross-sectional study. Vasc. Health Risk Manag. 2017; 13: 1-9. doi: 10.2147/VHRM.S119646.

[26] Dobsak P, Soska V, Sochor O, Jarkovsky J, Novakova M, Homolka M, et al. Increased cardio-ankle vascular index in hyperlipidemic patients without diabetes or hypertension. J. Atheroscler. Thrombo. 2015; 22(3): 272-83. doi: 10.5551/jat.24851. Epub 2014 Oct 22.

[27] Wang H, Liu J, Zhao H, Zhao X, Li L, Shi H, et al. Relationship between cardio-ankle vascular index and plasma lipids in hypertension subjects. J. Hum. Hypertens. 2015; 29(2): 105-8. doi.org/10.1038/jhh.2014.37.

[28] Dangardt F, Osika W, Volkmann R, Gan LM, Friberg P. Obese children show increased intimal wall thickness and decreased pulse wave velocity. Clin Physiol Funct Imaging. 2008; 28(5): 287-93. doi: 10.1111/j.1475-097X.2008.00806.x. Epub 2008 May 12.

[29] Lurbe E, Torro I, Garcia-Vicent C, Alvarez J, Fernández-Fornoso JA, Redon J. Blood pressure and obesity exert independent influences on pulse wave velocity in youth. Hyper. 2012; 60(2): 550-55. doi.org/10.1161/HYPERTENSIONAHA.112.194746.

[30] Yang H, Zhao J, Deng X, Tan I, Butlin M, Avolio A, et al. Pulse wave velocity is decreased with obesity in an elderly Chinese population. J Clin Hypertens. 2019; 21(9): 1379-85. doi: 10.1111/jch.13659.

[31] Uretsky S, Messerli FH, Bangalore S, Champion A, Cooper-DeHoff RM, Zhou Q, et al. Obesity paradox in patients with hypertension and coronary artery disease. Am J Med. 2007; 120(10): 863-70. doi: 10.1016/j.amjmed.2007.05.011.

[32] Joo HJ, Cho SA, Cho JY, Park JH, Hong SJ, Yu, CW, et al. The Relationship between Pulse Wave Velocity and Coronary Artery Stenosis and Percutaneous Coronary Intervention: a retrospective observational study. BMC Cardiovasc. Disord. 2017; 17(1): 45. doi.org/10.1186/s12872-017-0476-7.

[33] Chae MJ, Jung IH, Jang DH, Lee SY, Hyun JY, Jung JH, et al. The brachial ankle pulse wave velocity is associated with the presence of significant coronary artery disease but not the extent. Korean Circ Journal. 2013; 43(4): 239-45. doi: 10.4070/kcj.2013.43.4.239.

[34] Imanishi R, Seto S, Toda G, Yoshida M, Ohtsuru A, Koide Y, et al. High brachial-ankle pulse wave velocity is an independent predictor of the presence of coronary artery disease in men. Hypertens Res. 2004; 27(2): 71-8. doi: 10.1291/hypres.27.71.

[35] Izuhara M, Shioji K, Kadota S, Baba O, Takeuchi Y, Uegaito T, et al. Relationship of cardio-ankle vascular index (CAVI) to carotid and coronary arteriosclerosis. Circ J. 2008; 72(11): 1762-8. doi: 10.1253/circj.cj-08-0152. Epub 2008 Sep 18.

[36] Khan TH, Farooqui FA, Niazi K. Critical review of the ankle brachial index. Curr Cardiol Rev. 2008; 4(2): 101-6. doi: 10.2174/157340308784245810.

Journal of Associated Medical Sciences 2022; 55 (3): 116-122

JAMS
Journal of Associated Medical Sciences

Thai-Journal Citation Index Centre (TCI) & ASEAN Citation Index (ACI)

Journal of Associated Medical Sciences

Journal homepage: https://www.tci-thaijo.org/index.php/bulletinAMS/index

Dose deviations induced by fractional image guidance system errors in intensity-modulated radiotherapy for brain tumor treatment

Siriprapa Somboon[1*] Wannita Malila [2] Surasak Tamon[2] Jumneanphan Rueansri[2] Supoj Ua-apisitwong[1]

[1]Department of Radiologic Technology, Faculty of Associated Medical Sciences, Chiang Mai University, Chiang Mai Province, Thailand.
[2]Department of Radiation Oncology, Lampang Cancer Hospital, Lampang province, Thailand.

ARTICLE INFO

Article history:
Received 27 April 2022
Accepted as revised 28 July 2022
Available online 1 August 2022

Keywords:
Dose, image registration, IMRT, kV-CBCT, EPID

ABSTRACT

Background: Intensity-modulated radiotherapy (IMRT) techniques have a steep dose distribution, leading to large dosimetric errors caused by incorrect daily patient setup. Image-guided radiotherapy (IGRT) is an essential technique to verify accurate patient setup. The accuracy of verifying a patient's position depends on many factors including the image guidance system and image registration software.

Objectives: This study investigated the dosimetric and geometric differences between the original plan and simulated plans with setup errors associated with kilovoltage cone-beam computed tomography (kV-CBCT), kV, kV planar image, and electronic portal imaging detector (EPID) for brain tumor treatment using IMRT.

Materials and methods: A PIXY Anthropomorphic Training/Teaching Phantom was used in this study. IMRT treatment plans with five co-planar fields from a 6 MV Elekta Versa HD linear accelerator were generated using the RayStation computer treatment planning system. Three image guidance systems, including kV-CBCT, kV planar imager, and EPID were used to perform image registration. To evaluate the efficiency of each image guidance system, a simulated setup error by couch was shifted 0, ±2, and ±4 mm in the lateral, longitudinal, and vertical planes. Errors in the image registration from the actual couch shift were collected. Measured errors were used to generate the treatment plans of 25 fractions using the IMRT technique by random shifts of the isocenter of each fraction while maintaining other planning parameters of the original plan. The dose deviation in planning target volume (PTV) and geometric deviation compared to original plan were recalculated and analyzed.

Results: Accuracy of image registration in all image guidance systems indicated that the registration errors were less than 1.7, 2.0, and 1.0 mm for the kV-CBCT, kV planar, and EPID, respectively. The average PTV dosimetric deviation induced by the setup error ranged from -2 to 2 mm per fraction; this study showed dosimetric deviation at $D_{98\%}$ approximately -6%, $D_{95\%}$ approximately -4% and $D_{2\%}$ below -1%, while the average of isodose distribution shift of -5% inside the PTV of the isocenter region were -1.58±0.67, -1.28±0.52 and -1.30±0.80 mm in the cerebella, parasagittal, and convex areas, respectively. An isodose shift of -10% was <1 mm in all PTV locations.

Conclusion: The efficiency of image guidance resulted in small errors within ±2 mm using kV-CBCT, kV planar, and EPID. The setup error influenced daily dose distribution, while the PTV recorded underdose of about 4% in the brain IMRT technique.

* **Corresponding author.**
Author's Address: *Department of Radiologic Technology, Faculty of Associated Medical Sciences, Chiang Mai University, Chiang Mai Province, Thailand.*
** **E-mail address:** siriprapa.s@cmu.ac.th
doi: 10.12982/JAMS.2022.033
E-ISSN: 2539-6056

Introduction

The highly conformal radiation treatment technique allows for high doses to be given to the target volume while sparing the surrounding tissue. Intensity-modulated radiotherapy (IMRT) techniques are widely used in radiotherapy because they can deliver a highly conformal dose distribution to the target volume while sparing the normal tissue.[1] However, the steep dose distribution of the IMRT technique can lead to large dosimetric errors caused by incorrect patient positioning. Therefore, the accuracy of patient positioning is the main factor for radiotherapy treatment success. Any shift from the intra-inter fraction can result in dose variation in the target volume and organs at risk (OAR) between planned and delivered doses. Positioning verification by image-guided radiotherapy (IGRT) is used to improve the position accuracy. Modern image guidance techniques offer more precise patient positioning with different image modalities such as kilovoltage cone-beam computed tomography (kV-CBCT), kV x-ray planar imaging, and electronic portal imaging detector (EPID) systems. However, these modalities offer different pre-treatment position accuracy, which can impact system error and estimation of CTV-PTV margins.[2-6] The delivered dose of the kV planar image is lower and image quality is better than an MV image but its isocenter is not in the same direction as the linear accelerator (Linac). CBCT provides high resolution 3D patient anatomy which helps to achieve high position verification accuracy[7] and a lower dose than two MV planar images (AP-lateral). Devereux *et al*.[8] suggested kV imaging as the method of choice for head and neck IGRT but the setup errors of kV-CBCT are smaller than for the kV planar image, and the CTV-PTV margin could be reduced.[9] Ideally, the patient's position should be controlled and corrected for every fraction but fractional imaging comprises additional doses for the patient.

Metastatic brain tumors are commonly found in the northern region of Thailand.[10] For brain metastatic patient treatment, long-term survival and neurocognitive improvements were found to be correlated with lesion control. Treatment dose compromise could partially preserve the neurocognitive memory functions.[11-12] Therefore, the treatment of patients with metastatic brain tumors using IMRT presents challenges to improve potential long-term survival. Clinical studies have shown that IMRT techniques reduce complications compared to whole-brain radiotherapy (WB-RT) or 3D conformal radiotherapy. Brain treatment requires a rigid immobilization technique, and daily inter-fractional setup errors may cause an underdose in the target volume and overdose in normal tissues near the target. Matching of the planning CT and in-room images is limited by the modality and algorithms of image registration.

This study investigated the dosimetric and geometric differences between the original plan and the simulated plans with setup errors using kV-CBCT, , kV planar image, and EPID for brain tumor treatment using IMRT techniques.

Materials and methods

CT simulation and planning

The experiment was performed at Lampang Cancer Hospital using a Philips Brilliance Big Bore CT simulator (Philips Medical System, Cleveland, OH) to scan a supine PIXY Anthropomorphic Training/Teaching Head Phantom with a short thermoplastic mask placed on a B head rest with a 2-mm slice thickness. CT image data were then transferred to the RayStation computer treatment planning system version 11B (RaySearch Laboratories, Stockholm, Sweden) for target delineation and dose distribution calculation in the brain. The radiation oncologist drew the simulated target volume and organs at risk (OARs) contours from the CT images slice-by-slice on each axial slice plane, with slice thickness of 5 mm. The spherical target volume included three locations at the cerebella and parasagittal regions of the brain and a convex shape near the skull vertex, with an approximate size of 2.5 cm in diameter. The planning target volume (PTV) was created by symmetrically expanding the target volume or clinical target volume (CTV) with a 5-mm margin in all directions. The prescribed dose was 5,000 cGy in 25 conventional fractions and normalized dose to $D_{95\%}$ of PTV. IMRT treatment plans with five co-planar fields from a 6 MV Elekta Versa HD linear accelerator (Elekta, Stockholm, Sweden) were generated using the RayStation treatment planning system. The Elekta Versa HD linear accelerator has 160 tungsten Agility multi-leaf collimators (MLC) with 9 cm thickness and 0.5 cm width and a leaf speed of 3.5 cm/s. The carriage can travel at up to 3 cm/s, thus giving a maximum MLC speed of 6.5 cm/s.

Evaluation of image guidance system accuracy

Image guidance systems such as kV-CBCT, kV planar imager, and EPID can be attached to the Elekta linear accelerator for position verification according to the machine's protocol. The kV-CBCT imaging and kV planar image were performed using an x-ray volumetric imaging (XVI) system mounted on a linear accelerator. The kV-CBCT imaging technique operates at 100 kV, 10 mA, with the angular range of 200° and the angular separation of 0.54°. The kV planar imaging technique uses 100 kV and 0.5 mAs. The MV imaging technique with the EPID used 2 MUs of 6 MV x-rays. Simulation of the intentional setup error by moving the couch in each plane was performed at 0, ±2, and ±4 mm in the lateral (X), longitudinal (Y), and vertical (Z) planes, including combinations of ±2 mm and ±4 mm in all planes, and was used to verify the accuracy of the image registration software for each image guidance system. The planning CT images and in-room images of each image guidance system were automatically registered in XVI software based on the Feldkamp-Davis-Kress algorithm, using bone matching and soft tissue-gray value matching followed by manual correction by the same technician. The results of phantom setup errors from the actual translation are shown in Table 1. The accuracy of the image guidance system presented extremes in setup errors different to the actual translation below 1.7 mm, 2.0 mm, and 1.0 mm for the kV-CBCT, kV planar, and EPID images, respectively.

Simulation of dosimetric deviation induced by the errors of the image guidance systems

This study simulated a plan with a setup error as the isocenter of each fraction shifted based on the image guidance system errors in the previous process of evaluation of the image guidance system accuracy. The simulated plans with the setup error were created for all 25 fractions (200

cGy/fraction) using the isocenters of the simulated plans which were randomly shifted from -2 to 2 mm in three dimensions from the original treatment isocenter on the translation plane for all 25 simulated fractions. The other parameters of planning remained unchanged and the dose distribution for each fraction was recalculated. Dosimetric deviations in terms of the PTV as $D_{98\%}$, $D_{95\%}$, and $D_{2\%}$ and the geometric deviation between the original plan and simulated plans with the setup errors were evaluated in RayStation. The geometric deviation of isodose distribution shift from the PTV surface was evaluated slide by slide in the axial plane in three regions as: (1) at the isocenter 10 slices were evaluated by ±5 slides from the isocenter; (2) the last 5 slides from the inferior end of the PTV, and (3) the last 5 slides from the superior end of the PTV. The geometric deviation was averaged for all investigated planes.

Table 1 Setup errors along the lateral, longitudinal and vertical planes of each image guidance system in the PIXY head phantom.

Translation (mm)	Registration error in mm (Lateral/Longitudinal/Vertical)				
	kV-CBCT	kV planar		MV planar	
		AP-Rt. lateral	AP-Lt. lateral	AP-Rt. lateral	AP-Lt. lateral
2.0, 0.0, 0.0	0.3/0.0/0.1	0.6/0.0/0.0	1.0/0.0/0.0	0.0/0.0/0.0	-0.2/0.0/0.0
4.0, 0.0, 0.0	0.2/0.0/0.1	0.3/0.6/0.0	0.0/0.0/0.0	-0.8/0.4/0.0	-0.8/0.0/0.0
-2.0, 0.0, 0.0	0.4/0.1/0.1	-0.2/0.2/0.0	-0.2/0.0/-0.8	-0.4/-0.2/0.0	0.0/-0.4/0.0
-4.0, 0.0, 0.0	0.2/0.1/0.1	-0.3/0.0/0.0	-0.4/0.2/1.0	-0.6/-0.4/0.0	-0.6/-0.4/0.0
0.0, 2.0, 0.0	0.0/0.6/0.1	-0.4/0.2/-0.6	-0.4/0.0/1.0	-0.2/-0.2/0.0	0.0/-0.3/0.0
0.0, 4.0, 0.0	0.1/0.4/0.1	0.0/-0.1/-0.8	0.0/-0.4/0.8	0.0/-0.4/0.0	0.0/-0.1/-0.4
0.0, -2.0, 0.0	0.0/0.1/0.1	0.0/-0.2/-0.2	-0.2/-0.2/1.0	0.0/0.0/0.0	-0.4/-0.2/-0.2
0.0, -4.0, 0.0	0.1/0.7/0.1	-0.6/-0.3/-0.2	-0.4/-0.3/0.8	-0.2/-0.3/-0.3	-0.2/-0.1/-0.2
0.0, 0.0, 2.0	-0.2/-0.1/1.4	-0.4/0.0/-1.0	-0.4/-0.2/-1.0	0.0/-0.4/0.8	0.2/-0.4/-0.8
0.0, 0.0, 4.0	-0.1/0.0/0.9	-0.8/0.2/0.8	-0.8/0.4/-1.0	0.0/-0.2/-0.6	0.0/-0.4/-0.3
0.0, 0.0, -2.0	-0.2/0.0/1.5	-0.8/0.2/0.8	-0.8/0.4/-1.1	-0.2/0.0/-0.2	0.0/0.0/-0.2
0.0, 0.0, -4.0	0.0/-0.1/1.5	-0.8/0.0/0.9	-0.8/0.0/-0.9	-0.6/-0.2/-0.9	-0.6/-0.2/-0.9
2.0, 2.0, 2.0	0.4/0.5/1.5	0.2/0.2/-0.4	0.4/0.4/-0.8	0.4/0.2/-0.6	0.6/-0.4/-0.2
4.0, 4.0, 4.0	0.7/0.6/1.6	-0.3/0.3/-0.4	0.5/0.5/-1.0	-0.8/-0.1/-0.4	0.4/-0.3/-0.6
-2.0, -2.0, -2.0	0.4/0.4/1.4	-0.6/0.0/-0.8	2.0/0.2/-1.4	0.0/0.0/-0.8	0.0/-0.4/ -0.4
-4.0, -4.0, -4.0	0.6/0.4/1.7	-0.4/0.3/0.9	-0.4/0.1/-0.9	-1.0/-0.1/-0.1	-1.0/-0.9/0.3

Results

The setup errors were found to be less than 2 mm for all image guidance systems. As a result, the dose deviations between the original plan and simulated plans with setup errors are shown in Table 2. Dose 95% coverage of the PTV was reduced by approximately 4%, while the setup error had a greater effect on $D_{98\%}$ (about 6%) than on $D_{2\%}$ (less effect than 1%). Ranges of $D_{95\%}$ variation were 187-198 cGy/fraction, 188-198 cGy/fraction and 185-198 cGy/fraction, and the ranges of $D_{98\%}$ variation were 176-194 cGy/fraction, 178-196 cGy/fraction and 174-195 cGy/fraction in the cerebella, parasagittal, and convex areas, respectively. Figure 1 shows examples of dose deviation between the original plan and the simulated plans with setup errors of a 2 mm shift in the lateral, longitudinal, and vertical directions simultaneously. The hot and cold colors on the heat maps indicate the overdose and underdose relative to the original dose plan as no isocenter shift, respectively.

The geometric deviations of the isodose distribution of the PTV at the cerebella, parasagittal, and convex shape are shown in Tables 3, 4, and 5, respectively. The average of isodose distribution shifts of -5% inside the PTV surface of the isocenter region were -1.58±0.67 (ranged from -0.17 to -3.65 mm), -1.28±0.52 (ranged from -0.33 to -2.47 mm) and -1.30±0.80 (ranged from -0.20 to -4.24 mm) in the cerebella, parasagittal, and convex areas, respectively. The average of isodose distribution shift of -10% inside the PTV surface of the isocenter region was less than 1 mm, except for the parasagittal area which saw no dose deviation (range within -2 mm). For the inferior end and superior end, the isodose distribution shift of -5% and -10% inside the PTV surface were on average less than 5 mm in all PTV locations. The isodose distribution shift of 5% and 10% were found on the outside of the PTV, but small when found on the inside of the PTV. The difference of means of the isodose distribution shift of -5% between the different three locations (cerebella, parasagittal, and convex areas) of the PTV was not significant (p>0.05) using one-way ANOVA with SPSS version 17 (FB7E105EFD8A514130CC).

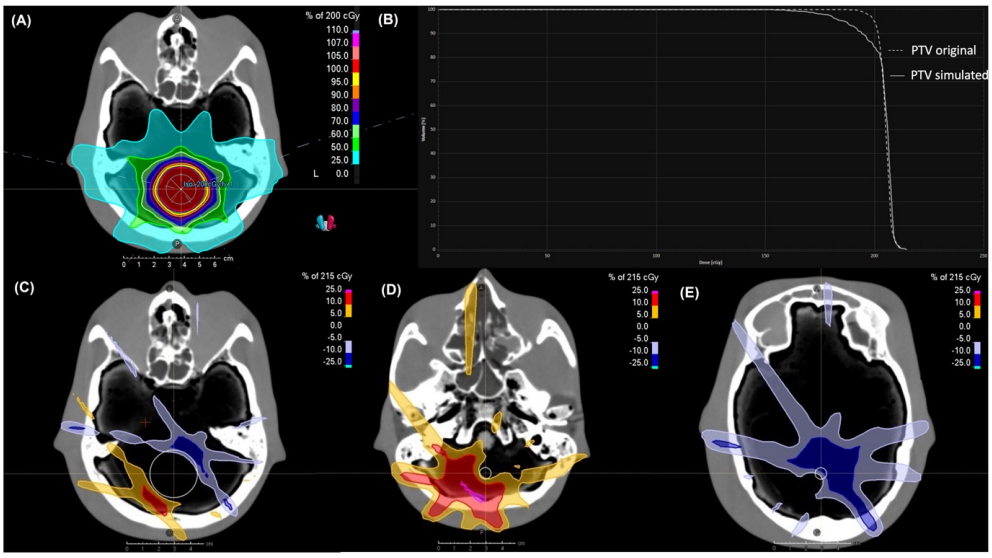

Figure 1. *Examples of dose deviations between the original plan and simulated plans with setup errors by a 2 mm, 2 mm, and 2 mm shift on the X, Y, and Z planes in PTV at the cerebella. A: dose distribution of original plan at the isocenter, B: DVH of PTV, C: dose deviation at the isocenter, D: dose deviation at the inferior end from the isocenter, and E: dose deviation at the superior end from the isocenter. A positive percentage difference is an overdose (red color zone) and a negative percentage difference is an underdose (blue color zone) compared to the original plan.*

Table 2 Comparison of dosimetric parameters between the original plan and simulated plans with setup errors. Prescription dose in 25 fraction is 5000 cGy, therefore the dose per fraction is 200 cGy per fraction.

Dosimetric parameter	Original plan		Dose of simulated plans with setup errors.				Different of accumulation dose (%)
	Dose for all 25 fractions (cGy)	Dose per fraction (cGy)	Avg/fraction (cGy)	Min (cGy)	Max (cGy)	Accumulation Dose (cGy)	
PTV at cerebella (spherical)							
$D_{98\%}$	4923	197	185±5.01	176	194	4621	-6.13
$D_{95\%}$	5000	200	192±3.35	187	198	4796	-4.08
$D_{2\%}$	5271	211	210±0.93	209	212	5256	-0.28
PTV at para-sagittal (spherical)							
$D_{98\%}$	4927	197	187±4.65	178	196	4669	-5.24
$D_{95\%}$	5000	200	193±3.04	188	198	4823	-3.54
$D_{2\%}$	5256	210	210±0.65	208	211	5238	-0.34
PTV at vertex (convex)							
$D_{98\%}$	4943	198	186±5.18	174	195	4657	-5.79
$D_{95\%}$	5000	200	193±3.74	185	198	4824	-3.52
$D_{2\%}$	5219	209	209±0.84	207	210	5218	-0.02

Table 3 Geometric deviation of isodose distribution of the PTV at cerebella.

Region	Distance (mm)	-5% difference of isodose distribution (Origi - Simulated)		-10% difference of isodose distribution (Origi-Simulated)		5% difference of isodose distribution (Origi-Simulated)		10% difference of isodose distribution (Origi-Simulated)	
		Inside PTV	Outside PTV	Inside PTV	Outside PTV	Inside PTV	Outside PTV	Inside PTV	Outside PTV
Inferior end	Range for all 25 fractions	-7.14 to -0.63	0.46 to 7.34	-4.15 to -0.46	0.36 to 6.63	-1.43 to -0.36	0.28 to 8.23	No dev.	1.52 to 10.61
	Avg	-4.05±1.95	2.33±1.98	-2.01±1.02	2.68±1.67	-0.89±0.39	2.47±2.13		4.29±1.77
Isocenter	Range for all 25 fractions	-3.65 to -0.17	0.13 to 2.89	-1.42 to -0.28	0.18 to 8.10	No dev.	0.13 to 2.99	No dev.	1.62 to 3.95
	Avg	-1.58 ±0.67	0.96±0.57	-0.63±0.29	1.25±0.99	No dev.	1.18±1.19		2.61±1.04
Superior end	Range for all 25 fractions	-7.59 to -0.72	0.28 to 7.55	-4.71 to -0.63	0.40 to 6.84	-9.54 to -0.36	0.36 to 8.50	No dev.	1.59 to 9.24
	Avg	-4.06±2.21	2.74±2.09	-2.93±1.16	3.21±1.73	-1.01±1.55	1.80±1.81		3.77±1.92

Note: Origi: original plan, No dev.: no deviation from original plan.

Table 4 Geometric deviation of isodose distribution of the PTV at parasagittal.

Region	Distance (mm)	-5% difference of isodose distribution (Origi-Simulated)		-10% difference of isodose distribution (Origi-Simulated)		5% difference of isodose distribution (Origi-Simulated)		10% difference of isodose distribution (Origi-Simulated)	
		Inside PTV	Outside PTV	Inside PTV	Outside PTV	Inside PTV	Outside PTV	Inside PTV	Outside PTV
Inferior end	Range for all 25 fractions	-7.12 to -0.40	0.25 to 6.85	-3.62 to -0.32	1.01 to 6.71	No dev.	0.24 to 11.43	No dev.	2.67 to 8.60
	Avg	-3.85±2.00	3.56±2.47	-1.94±1.22	3.30±1.93		2.48±2.40		5.01±1.96
Isocenter	Range for all 25 fractions	-2.47 to -0.33	0.35 to 5.58	No dev.	0.35 to 6.80	No dev.	0.94 to 4.79	No dev.	2.74 to 7.09
	Avg	-1.28±0.52	2.26±1.04		2.22±1.27		2.08±0.94		4.59±0.77
Superior end	Range for all 25 fractions	-8.02 to -0.80	0.60 to 9.50	-4.64 to -1.27	0.46 to 8.00	-2.12 to -0.25	0.25 to 9.32	No dev.	1.50 to 8.50
	Avg	-4.52±2.43	3.92±2.30	-2.85±0.92	3.77±1.82	-0.99±0.52	2.47±2.21		3.84±1.63

Note: Origi: original plan, No dev.: no deviation from original plan.

Table 5 Geometric deviation of isodose distribution of the PTV at convex shape.

Region	Distance (mm)	-5% difference of isodose distribution (Origi-Simulated)		-10% difference of isodose distribution (Origi-Simulated)		5% difference of isodose distribution (Origi-Simulated)		10% difference of isodose distribution (Origi-Simulated)	
		Inside PTV	Outside PTV	Inside PTV	Outside PTV	Inside PTV	Outside PTV	Inside PTV	Outside PTV
Inferior end	Range for all 25 fractions	-8.51 to -1.29	0.32 to 7.41	-4.56 to -0.52	0.32 to 8.52	-2.29 to -0.32	0.32 to 8.06	No dev.	2.86 to 11.22
	Avg	-4.94±2.04	3.00±1.98	-3.07±1.41	3.47±2.57	-1.08±0.88	2.63±1.80		5.87±1.95
Isocenter	Range for all 25 fractions	-4.24 to -0.20	0.20 to 5.32	-1.92 to -0.20	0.32 to 5.33	No dev.	0.61 to 5.66	No dev.	2.34 to 7.31
	Avg	-1.30±0.80	1.57±1.14	-0.85±0.55	1.18±1.26		1.98±0.82		4.51±1.04
Superior end	Range for all 25 fractions	-6.08 to -0.40	0.32 to 6.52	-3.09 to -0.57	0.91 to 6.62	-1.54 to -0.64	0.52 to 4.77	No dev.	1.04 to 8.44
	Avg	-2.63±1.49	2.52±1.79	-1.54±0.75	2.85±1.30	-1.09±0.30	1.96±1.18		3.67±1.39

Note: Origi: original plan, No dev.: no deviation from original plan.

Discussion

IGRT has been introduced as a treatment procedure to decrease patient positioning setup errors. The actual treatment position can be accurately confirmed through image guidance systems such as kV-CBCT, kV planar imager, and EPID. The efficiency of all image guidance systems to detect setup errors was below 2 mm, with simulation setup errors of 0, ±2, and ±4 mm in all planes. As a result, the newly simulated plans were created by the random shift of the isocenter from -2 to 2 mm from the original treatment isocenter on three translation plane dimensions for all 25 fractions. The three image guidance systems (kV-CBCT, kV planar image, and EPID) had different image data and image quality for image registration. The kV-CBCT had higher accuracy correction in the lateral and longitudinal planes compared with the vertical plane, especially when the vertical planes were shifted. The phantom's weight may affect the translation of the actual position in the vertical plane. The same isocenter of the Linac and EPID devices detected good geometrical uncertainty with a smaller error than the onboard imager (OBI), while the lowest MV image resolution still achieved high accuracy of image registration. Therefore, frequent QC checks and strict adherence to the QA program are necessary when using OBI. However, the kV image beam had a lower additional dose compared with the treatment beam (MV), leading to the use of the kV beam image for verification of the patient setup.[13] The image registration algorithm has the potential to improve the patient verification in radiotherapy.[14] This result shows that recently developed image registration software achieves accurate and precise image fusion between the reference image and in-room image for brain treatment. The image guidance systems can detect deviations of less than 1 mm in 96.25%, 100%, and 80% of cases for the X, Y, and Z planes, respectively. Guckenberger *et al*.[15] concluded that the translational setup errors using the CB-CT scanner and an EPID device differed by <1 mm in 70.7% and <2 mm in 93.2% of all cases. This

study showed the EPID device differed by <1 mm in 97.5% and <2 mm in 100% of cases.

Setup errors influenced the dose distribution between the reference position and the actual treatment position. This usually has the effect of underdosing the target volume and overdosing the OAR. The results showed that the average dosimetric deviation of the PTV due to setup errors ranging from -2 to 2 mm per fraction were approximately -6% for $D_{98\%}$, -4% for $D_{95\%}$, and less than -1% for $D_{2\%}$. Errors in fractional delivery dose led to a large underdose in the $D_{98\%}$ correlation, as found by Utena *et al*.,[16] while dose deviation was caused by a high isodose line shift from the PTV. Siebers *et al*.[17] have shown that the dose changes in gross target volume of head-and-neck squamous cell carcinomas treated with simultaneous integrated boost (SIB)-IMRT techniques were about 3-5% and the $D_{98\%}$ is the parameter that is most sensitive to patient position uncertainties. The PTV margin used in Lampang Cancer Hospital for head and neck planning has following RTOG protocol 0225.[18] From the geometric deviation of isodose distribution of -5% inside the PTV surface of the isocenter region, inducing the cold spot in PTV can reduce the PTV margin to less than 5 mm for brain treatment using the IMRT technique. The magnitudes of geometric deviation were 3.65 mm, 2.47 mm, and 4.24 mm in the cerebella, parasagittal, and convex areas, respectively. Therefore, we recommend CTV to PTV margins of 3.70 mm for spherical target volume but convex shapes should still have CTV to PTV margins of 5 mm. Cubillos *et al*.[19] concluded that CTV to PTV margins had a range of 3.30-3.70 mm in the brain region. However, the ICRU[20] recommends estimating the magnitude of uncertainties in every radiotherapy unit to apply appropriate CTV to PTV margins for individual institutes. The anatomy of the brain as the cranial bone is easy to match for all image guidance systems but the limits of image registration software and mechanisms of imaging have errors of at least ±2 mm. These factors can affect dose coverage by approximately 4%.

The number of beams also affects PTV dose coverage. IMRT brain treatment usually uses a high number of beams.[21] Five beams were used in this study because this number simulates brain metastasis and the hospital had huge patient loads and a limited number of Linac machines. Five beam IMRT was adopted as this gave faster treatment. This study has several limitations. We used a solid phantom since actual patients are non-rigid and vary in physique, which affects the accuracy of image registration. In clinical practice, the dose distribution in TPS is not related to actual dose distribution in patients. Further research using actual patients is required to confirm dose variation from setup errors.

Conclusion

Accuracies of phantom setup error from actual translation using image registration software in kV-CBCT, kV planar, and EPID images were within a tolerance limit of ±2 mm for all image guidance systems. Setup errors influenced dose deviation between the original plan and simulated plans with setup errors in all the PTV locations of approximately -6% for $D_{98\%}$, -4% for $D_{95\%}$, and less than -1% for $D_{2\%}$. The average of isodose distribution shifts of -5% inside the PTV surface of the isocenter area were -1.58±0.67 (3.65 mm in magnitude), -1.28±0.52 (2.47 mm in magnitude), and -1.30±0.80 (4.24 mm in magnitude) in the cerebella, parasagittal, and convex areas, respectively, and the isodose distribution shift of -10% inside the PTV surface was less than 1 mm in all PTV locations.

Acknowledgements

This research was supported by the Associated Medical Sciences scholarship.

References

[1] Marta GN, Silva V, de Andrade Carvalho H, de Arruda FF, Hanna SA, Gadia R, et al. Intensity-modulated radiation therapy for head and neck cancer: systematic review and meta-analysis. Radiother Oncol. 2014; 110(1): 9-15.

[2] Dawson LA, Jaffray DA. Advances in image-guided radiation therapy. J Clin Oncol. 2007; 25(8): 938-46.

[3] Bissonnette JP, Purdie TG, Higgins JA, Li W, Bezjak A. Cone beam computed tomographic image guidance for lung cancer radiation therapy. Int J Radiat Oncol Biol Phys. 2009; 73(3): 927-34.

[4] Snir JA, Battista JJ, Bauman G, Yartsev S. Evaluation of inter-fraction prostate motion using kilovoltage cone beam computed tomography during radiotherapy. Clin Oncol. 2011; 23(9): 625-31.

[5] Guckenberger M. Image-guided radiotherapy based on kilovoltage cone-beam computed tomography – A review of technology and clinical outcome. Eur Oncol Haematol. 2011; 7(2): 121-4.

[6] Pisani L, Lockman D, Jaffray D, Yan D, Martinez A, Wong J. Setup error in radiotherapy: on-line correction using electronic kilovoltage and megavoltage radiographs. Int J Radiat Oncol Biol Phys. 2000; 47(3): 825-39.

[7] Somboon S, Malila W, Tamon S, Nueangwong W, Yeenang N, Rueansri J. Evaluation of optimal kilovoltage-cone beam technique on image quality, registration accuracy, time of imaging and relative dose for head radiotherapy: A phantom study. J Assoc Med Sci. 2022; 55(2): 10-5.

[8] Devereux B, Frantzis J, Sisson T, Jones M, Martin J, Middleton M. A comparison of kV and imaging in head and neck imaged radiotherapy. Radiography. 2010; 16: 8-13.

[9] Martin L, Couto JG, Barbosa B. Use of planar kV vs. CBCT in evaluation of setup errors in oesophagus carcinoma radiotherapy. Rep Pract Oncol Radiother. 2016; 21: 57-62.

[10] Veerasarn K, Yuthagovit S, Chailorrat RN. Prevalence of Brain tumor in Thailand from 2005 to 2014: data from the National Health Security Office. J Med Assoc Thai. 2016; 99 Suppl3: 62-73.

[11] Li Z, Shen D, Zhang J, Zhang J, Yang F, Kong D et al. Relationship between WBRT total dose, intracranial tumor control, and overall survival in NSCLC patients with brain metastases- a single-center retrospective analysis. BMC cancer. 2019; 19(1): 1104.

[12] Li J, Bentzen SM, Renschler M, Mehta MP. Regression after whole-brain radiation therapy for brain metastases correlates with survival and improved neurocognitive function. J Clin Oncol. 2007; 25(10): 1260-6.

[13] Ding XG, Alaei P, Curran B, Flynn R, Gossman M, Mackie TR et al. Image guidance doses delivered during radiotherapy: Quantification, management, and reduction: Report of the AAPM Therapy Physics Committee Task Group 180. Med Phys. 2018; 45(5): e84-e99.

[14] Brock KK, Mutic S, McNutt RT, Li H, Kessler LM. Use of image registration and fusion algorithms and techniques in radiotherapy: Report of the AAPM Radiation Therapy Committee Task Group No.132. Med Phys. 2017; 44(7): e43-76.

[15] Guckenberger M, Meyer J, Vordermark D, Baier K, Wilbert J, Flentje M. Magnitude and clinical relevance of translational and rotational patient setup errors: a cone-beam CT study. Int J Radiat Oncol Biol Phys. 2006; 65(3): 934-42.

[16] Utena Y, Takatsu J, Sugimoto S, Sasai K. Trajectory log analysis and cone-beam CT-based daily dose calculation to investigate the dosimetric accuracy of intensity-modulated radiotherapy for gynecologic cancer. J Appl Clin Med Phys. 2021; 22(2): 108-17.

[17] Siebers JV, Keall PJ, Wu Q, Williamson JF, Schmidt-Ullrich RK. Effect of patient setup errors on simultaneously integrated boost head and neck IMRT treatment plans. Int J Radiat Oncol Biol Phys. 2005; 2: 422-33.

[18] Group RTO. A phase II study of intensity modulated radiation therapy (IMRT) +/−chemotherapy for nasopharyngeal cancer, RTOG 0225[2011-03-05]. http://208.251.169.72/members/protocols/0225/pdf_fle.html.

[19]Cubillos Mesias M, Boda-Heggemann J, Thoelking J, Lohr F, Wenz F, Wertz H. Quantification and Assessment of Interfraction Setup Errors Based on Cone Beam CT and Determination of Safety Margins for Radiotherapy. PLoS One. 2016; 11(3): e0150326.

[20] International Commission on Radiation Units and Measurements. Prescribing, Recording, and Reporting Photon Beam Therapy ICRU Report 50, ICRU Report 62 (Supplement to ICRU Report 50) 1993. Bethesda:ICRU,1999.

[21] Bell K, Licht N, Rube C, Dzierma Y. Image guidance and positioning accuracy in clinical practice: influence of positioning errors and imaging dose on the real dose distribution for head and neck cancer treatment. Radiat Oncol. 2018; 13(1): 190.

Journal of Associated Medical Sciences 2022; 55 (3): 123-128

JAMS
Journal of Associated Medical Sciences

Thai-Journal Citation Index Centre (TCI) & ASEAN Citation Index (ACI)

Journal of Associated Medical Sciences

Journal homepage: https://www.tci-thaijo.org/index.php/bulletinAMS/index

Musculoskeletal pain in ambulatory patients with spinal cord injury who walking with or without walking devices: Prevalence and impact on walking speed

Lugkana Mato[1, 2,3*] **Narongsak Khamnon**[1,2] **Wilairat Namwong**[1,2] **Thiwabhorn Thaweewannakij**[1,2] **Sugalya Amatachaya**[1,2]

[1]*School of Physical Therapy, Faculty of Associated Medical Sciences, Khon Kaen University, Khon Kaen Province, Thailand.*
[2]*Improvement of Physical Performance and Quality of Life (IPQ) research group, Khon Kaen Province, Thailand.*
[3]*Khon Kaen University Under Incubation Researcher Project, Khon Kaen Province, Thailand.*

ARTICLE INFO

Article history:
Received 14 June 2022
Accepted as revised 3 August 2022
Available online 5 August 2022

Keywords:
Musculoskeletal pain, spinal cord injury, walking speed

ABSTRACT

Background: Musculoskeletal pain in spinal cord injury (SCI) is a common problem. However, not much research exists on the prevalence of pain in ambulatory patients with SCI walking either with or without ambulatory assistive devices (AAD).

Objectives: This study aimed to explore the prevalence of musculoskeletal pain and to investigate the impact of pain on walking speed in ambulatory patients with SCI walking with or without AAD.

Materials and methods: There were 86 patients with SCI who were able to walk independently with or without AAD. All the patients were evaluated for musculoskeletal pain using a visual analogue scale (VAS). Then their walking speed was assessed using a 10-meter walk test (10MWT).

Results: The proportion of patients with pain was high in both groups (63% in patients using AAD and 55% in patients not using AAD). For those with AAD, the fastest walking speed was significantly different in patients with mild, moderate, and severe pain compared to patients with no pain while for those without AAD, the fastest speed was significantly different in patients with moderate and severe pain compared to patients with no pain (p<0.05).

Conclusion: Musculoskeletal pain was commonly found in ambulatory patients with SCI walking with or without AAD, and this pain impacted their walking speeds. The finding of musculoskeletal pain in both patients walking with or without AAD could raise healthcare professionals' awareness of the debilitating impact of musculoskeletal pain. Thus, the development of improved therapeutic approaches for reducing this impact is needed.

Introduction

Musculoskeletal pain is defined as an aching, dull sensation that increases with limb movements and arises from the musculoskeletal structure.[1] When musculoskeletal pain occurs, it can potentially interfere with the ability to perform daily activities-especially walking, the improvement of which is a primary rehabilitation goal in patients with neurological deficits.[2-4] Spinal cord injury (SCI) commonly distorts sensorimotor or autonomic functions and-depending on the severity and levels of the injury-results in various degrees of diminished functional ambulation.[3-5] After SCI, 80% of patients can regain walking ability after participation in rehabilitation.[5] Among patients with SCI who regained walking ability, a previous study reported that 64% of those walked with assistive walking devices including walker crutches or cane, and 34% walked without AAD.[6] Moreover, patients with SCI who had regained walking function also

* **Corresponding author.**
Author's Address: *School of Physical Therapy, Faculty of Associated Medical Sciences, Khon Kaen University, Khon Kaen Province, Thailand.*
** **E-mail address:** yui@kku.ac.th
doi: 10.12982/JAMS.2022.034
E-ISSN: 2539-6056

walked non-functional e.g., household ambulation, slow gait speed, abnormal gait pattern, and compensatory movement that subsequently increase the risk of musculoskeletal pain.[5,6] The prevalence of musculoskeletal pain in SCI patients has been reported to be approximately 68-71.1%.[2,7] Although several studies have reported problems with musculoskeletal pain in patients with SCI, most of the patients featured were wheelchair users and placed in the same category as overall ambulatory patients with SCI.[2,5,8,9] In addition, patients who walk with AAD have remaining muscle weakness and walking asymmetry after SCI.[10] Therefore, the upper extremities are used to aid in locomotion. Barbetta *et al*. (2016) reported that the increased use of upper extremities has been associated with a higher occurrence of musculoskeletal pain among individuals with SCI who walk with AAD.[11] In contrast to AAD patients, non-AAD patients can walk independently, but the ability to walk is diminished and asymmetrical patterns emerge.[10] Therefore, when non-ADD patients walk, the increased strain on their lower extremities may lead to musculoskeletal pain. However, there was no evidence of musculoskeletal pain in ambulatory patients with SCI walking with or without AAD. Therefore, we hypothesized that patients with SCI walking with or without AAD might experience musculoskeletal pain and that the areas of musculoskeletal pain in each group would differ. Therefore, the objectives of this study were to investigate the extent of musculoskeletal pain in ambulatory patients with SCI walking with or without AAD and to determine the areas of pain in those patients. Moreover, this study investigated the impact of musculoskeletal pain on walking speeds in these patients.

Materials and methods

Participants

One hundred and twelve SCI patients were enrolled from a tertiary rehabilitation centre and community in the northeast area of Thailand during January 2017 and October 2018. The sample size calculation (using proportion of prevalence musculoskeletal pain from pilot study in 54 participants with SCI=0.66 with precision of estimation =0.1, levels of significant level at 0.05, and power of test at 0.80) indicated that the study required 86 participants.

The participants were ambulatory patients at least 18-years old with SCI stemming from both traumatic and non-traumatic causes who scored from A to D on the American Spinal Injury Association [ASIA] Impairment Scale (AIS).[12] The exclusion criteria included inability to understand and follow commands, leg-length discrepancy, pregnancy, brain involvement and any underlying disease that caused pain. The study was approved by the Khon Kaen University Ethics Committee for Human Research (HE551077), and eligible participants provided their written informed consent before participating in the study.

Protocol

Eligible patients were interviewed and assessed for baseline demographic and SCI characteristics, including the cause of the injury, the severity of SCI according to the AIS criteria, the time of injury, the level and completeness of the injury (using the ASIA motor and sensory score) and the walking devices used.[12] Pain intensity was assessed with a visual analogue scale (VAS), and areas of pain were determined using a body chart diagram.[13-15]

For this study, the reasons for musculoskeletal pain caused by problems with the muscles, joints or bones were injury, overuse or strain, arthritic changes or wear and tear. Musculoskeletal pain usually gets worse with movement and better with rest.[1,15] We collected VAS data using visuals analog scale from interviews with the participants. When participants had multiple areas with different VAS scales, we confirmed pain data in those areas using palpation and active and passive movement; in such cases, we selected the area of most severe pain as the measure of the patient's severity of pain. Patients with SCI who had a VAS scale >1 were classified into the pain group, whereas those with a VAS <1 was assigned to the no-pain group.[16] To differentiate musculoskeletal pain from neurological pain in this study, active, passive, and accessory movement tests were used.[1]

After the patients were interviewed and assessed for their baseline demographics and the SCI characteristics and musculoskeletal pain analyses were completed, the patients were divided into four groups according to the severity of their pain: no pain (VAS=0), mild pain (VAS=1-3), moderate pain (VAS=4-6) and severe pain (VAS=7-10).[16] Patients were assessed for their walking speed using a 10-metre walk test (10MWT).[17]

The 10-metre walk test (10MWT)

Patients walked at both their preferred and fastest gait speeds along a 10-metre walkway. The time required during the middle four metres of the walkway was recorded to minimise the inclusion of acceleration and deceleration effects.[17] Patients performed three trials at each speed, and average times in the seconds were recorded.[17] When assessing preferred walking speed and fastest gait speed, all participants were given time to rest between each test for 5 minutes or until their tired disappear. We observed no decline in the walking speed of patients asked to walk at a fast speed.

Statistical analysis

Descriptive statistics were applied to explain the baseline demographics, SCI characteristics and the prevalence of musculoskeletal pain. Findings among groups were compared using nonparametric Mann-Whitney U tests when the data were not normally distributed for continuous data. For variables were categorized data, chi-square test was used to compare differences between groups. The one-way analysis of variance (ANOVA) was used to compare walking speeds among groups of patients who had no pain, mild pain, moderate pain and severe pain, with a p-value of less than 0.05.

Results

There were 112 patients with SCI who were interested in participating in this study. However, 26 patients were excluded due to osteoarthritis of the knee (n=7) brain involvement (n=3) and inability to ambulate (n=16). There were ultimately 86 ambulatory patients with SCI who participated in this study.

The patients' demographic and SCI characteristics are presented in Table 1. There were no significant differences among the groups in terms of demographic data or SCI

characteristics, except for the motor score and gender (Table 1). In addition, the average duration of AAD use was 24 months. The severity of pain ranged from no pain to severe pain in both the AAD (no pain=21, mild pain=8, moderate pain=19, and severe pain=9) and the non-AAD groups (no pain=13, mild pain=4, moderate pain=8, and sever pain=4).

Table 1 Demographic and spinal cord injury (SCI) characteristics of patients with SCI who walked with or without assistive devices (AAD).

Variable	AAD group (n = 57)			Non-AAD group (n = 29)		
	Pain (n=35)	No pain (n=21)	*p* value	Pain (n=16)	No pain (n=13)	*p* value
Age (years)[a]	49.0 (36.0 – 67.5)	61.0 (48.0 - 67.0)	0.312	51.0 (41.0 – 57.0)	55.0 (32.0–58.0)	0.812
Body mass index (kg/m2)[a]	20.9 (18.6 – 24.0)	21.90 (20.1 - 25.7)	0.227	20.3 (18.7 – 23.7)	22.5 (19.1–24.4)	0.682
Post-injury time (months)[a]	48.01 (24.0 – 99.0)	48.04 (25.0 - 98.0)	0.921	57.5 (29.0 – 111.0)	63.5 (48.0–180.0)	0.215
Gender:						
- Male, n (%)[b]	24 (67)	17 (80)	0.726	15 (94)	8 (61)	0.033*
- Female, n (%)[b]	12 (33)	4 (20)		1 (6)	5 (39)	
Motor score:						
- Upper motor scores (scale)[a]	32.50 (18.6–23.7)	40.0 (19.1–25.1)	0.017*	37.0 (33.0 – 44.5)	46.0 (44.0–48.0)	0.004***
- Lower motor scores (scale)[a]	34.0 (19.5–40.0)	38.0 (27.0–43.0)	0.097	37.40 (34.0 – 44.5)	46.03 (44.6–48.0)	0.008**
Sensory scores (scale)[a]	180.0 (164.0–196.0)	188.0 (160.0 –99.0)	0.697	197.0 (189.0 – 204.0)	208.0 (188.0–216.0)	0.308
Cause of injury:						
- traumatic, n (%)[b]	23 (64)	13 (62)	0.582	7 (44)	6 (46)	0.377
- non-traumatic, n (%)[b]	13(36)	8(38)		9 (56)	7 (54)	
Severity of injury:						
- AIS A and B, n (%)	6 (17)	2 (9)	0.836	-	-	-
- AIS C, n (%)	10 (28)	5 (24)		-	-	-
- AIS D, n (%)	20 (55)	14 (67)		16	13	0.310

***Abbreviations**: AIS: American Spinal Injury Association (ASIA) Impairment Scales, AIS A: No sensory or motor function is preserved in the sacral segments S4–S5, AIS B: Sensory but not motor function is preserved below the neurological level and extends through the sacral segments S4–S5, AIS C: Motor function is preserved below the neurological level, and most key muscles below the neurological level have a muscle grade less than three, AIS D: Motor function is preserved below the neurological level, and most key muscles below the neurological level have a muscle grade greater than or equal to three.*

***Note**: [a]Data were presented in terms of median (interquartile range: Q1–Q3). The findings between the groups were compared using the Mann–Whitney U test. [b]These variables were categorised data, and a chi-square test was used to compare differences between groups. * Indicates a significant difference between groups (p<0.05). ** Indicates a significant difference between groups (p<0.01). *** Indicates a significant difference between groups (p<0.001).*

The proportion of patients who experienced pain was high for both the AAD (63%) and the non-AAD groups (55%); however, the areas where pain was experienced varied. Moderate severity of upper limb (36%) pain was more common in the AAD group, moderate severity pain of trunk (59%) and lower limb (36%) pain was more common in the non AAD group (Figure 1).

We examined walking speed and reported pain in patients in the AAD and non-AAD groups separately. Within the AAD group, a significantly faster gait speed was observed in patients with no pain than in those with mild, moderate, and severe pain (p<0.05, Figure 2A). In the non-AAD group, there was no significant difference in gait speed between those with mild and no pain and no significant difference in gait speed between those with severe and moderate pain (Figure 2B). In addition, there were no differences found in the preferred walking speed, both AAD and non-AAD group.

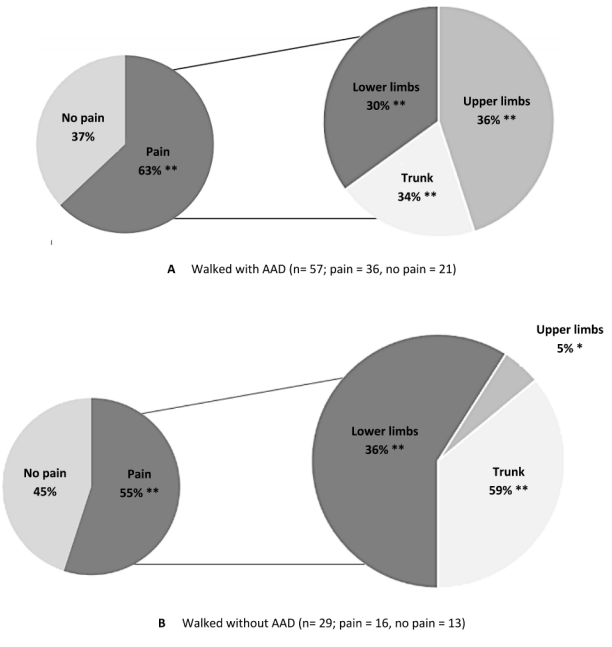

***Figure 1**. Prevalence, severity, and area of pain in ambulatory patients with SCI who walked with or without AAD. A: walked with AAD, B: walked without AAD.*

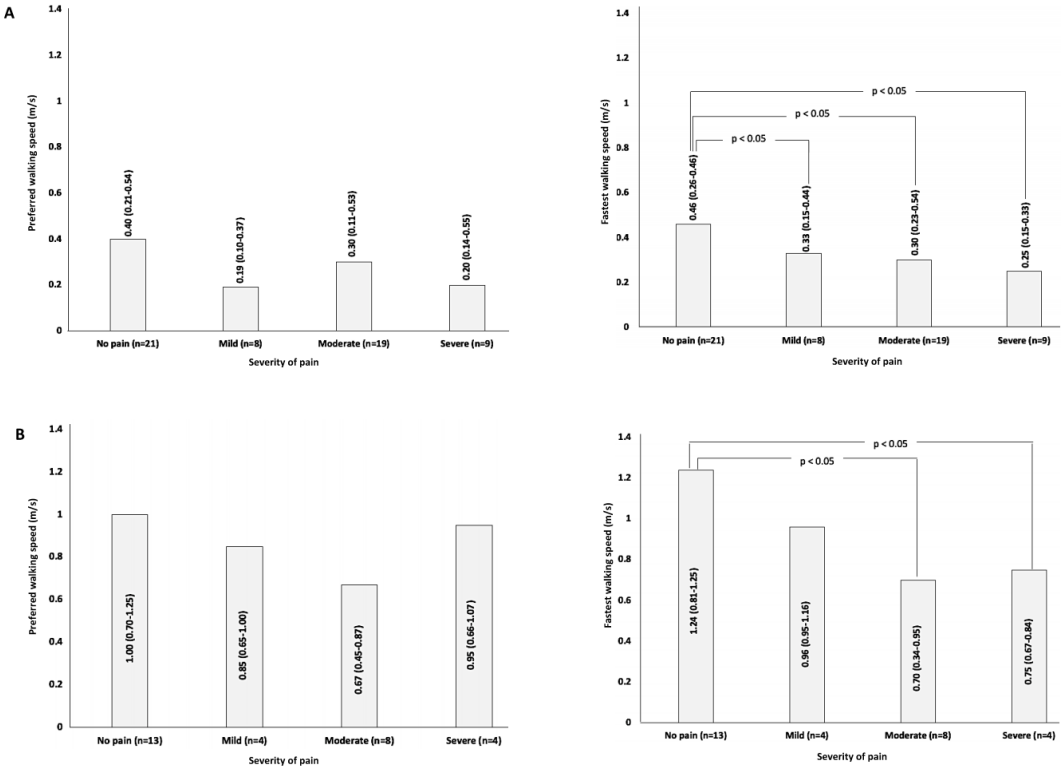

***Figure 2**. Comparison of walking speeds associated with different pain severities among patients with SCI who walked with and without AAD. A: AAD group, B: non- AAD group.*

Discussion

Musculoskeletal pain is a serious problem and is commonly found in those with neurological conditions, especially in patients with SCI. A previous study reported that patients with SCI had the highest prevalence of chronic pain when compared with other patients with neurological deficits.[18]

The present study has shown that SCI patients with or without an AAD who participated in this study had problems with musculoskeletal pain. An important finding of the present study is the high prevalence of pain in the non-AAD group (55%, Figure. 1). We found that the areas of pain in this group were mostly reported in the lower limbs and trunk. This may be explained by the fact that patients with SCI have sensorimotor deficits as indicated by the data showing significantly lower upper and lower motor scores in patients who had pain than those who had none (Table 1). Although these patients can walk independently, their sensorimotor impairments are likely to cause them to walk asymmetrically and with an abnormal gait pattern. Kumprou *et al*. reported that different degrees of impairment between the limbs is one important cause of asymmetrical walking in those with neurological disorders whereas the levels of asymmetrical walking in ambulatory participants with SCI who had bilateral sensorimotor impairments were reported around 78–94%.[10] Asymmetrical walking can increase the risk of injury to the musculoskeletal structures and ultimately result in lower limb pain in SCI patients who walk without AAD.[10] In addition, the SCI patients experience lingering muscle weakness. Walking in non-AAD patients seems to increase the demand on lower-extremity muscles. Therefore, walking with an abnormal gait pattern and walking asymmetrically while there is still muscle weakness after SCI could-especially in the case of ambulatory patients with SCI who walk without AAD-lead to chronic arthritis causing by repetitive abnormal movements and putting direct strain on musculoskeletal structures.

In addition, the present study found a high prevalence of pain in the AAD group (63%, Figure 1A). The AAD group showed a high prevalence of upper limb pain. This may be explained by the fact that SCI patients who walk with an AAD are more likely to have impaired lower limb functions, which can increase their dependence on the upper extremity functions for mobility.[19] The muscles of the upper limbs are primarily composed of small muscle fibre groups, whereas lower limb muscles primarily consist of large muscle fibre groups.[2,19] Thus, the extra work of the upper limbs that compensates for loss of strength and/or mobility in lower limbs might induce an injury to the upper limbs structures.[19] Previous studies reported that repetitive compressive forces on the upper limbs in chronic arthritis patients could be caused by long-term use of a walker or cane.[19-21] These repetitive forces can, in turn, contribute to pathologies, such as osteoarthritis, carpal tunnel syndrome and tendonitis.[19] Another study reported the prevalence of upper limb musculoskeletal pain in patients with poliomyelitis, which prolonged the use of AAD.[22] Therefore, medical care and prevention of musculoskeletal pain should

be of concern to patients who walk with and without AAD.

Walking speed is considered a measurement of the overall quality of a person's gait.[17] Furthermore, adequate velocity is only one criterion that should be met for independent community ambulation to be considered safe for patients with SCI.[23] However, a previous study showed no evidence of a link between musculoskeletal pain and walking speed in ambulatory SCI patients.[2,4] Therefore, this study considers the effects of musculoskeletal pain on walking speed in SCI patients walking with or without AAD. The results indicate that mild-to-severe musculoskeletal pain may influence the fastest gait speed in ambulatory patients with SCI who walk with AAD (p<0.05, Figure 2A). In non-AAD group, moderate to severe pain influenced fastest gait speed (p<0.05, Figure. 2B). Musculoskeletal pain, especially in parts of the lower limbs, influences walking abilities in patients with SCI.[4] Sawa *et al*. reported that people with pain commonly alter their gait pattern to avoid pain.[24] Furthermore, individuals with musculoskeletal pain typically limit the range of joint movement during walking to minimise pain severity, which could cause a decrease in gait speed. One study has reported that problems with musculoskeletal pain affect patients who pay more attention to the pain side, which could distract the patient during walking. These individuals have been shown to walk more slowly when performing other tasks or encountering challenging walking conditions.[25] Patients using AAD and suffering mild-to-severe pain exhibited a pain-related decline in walking speed (p<0.05, Figure 2A). The impact of musculoskeletal pain on the fastest gait speed in patients with AAD might be attributed to upper limb, trunk, and lower limb pain (Figure 1A). Furthermore, the patients using AAD required more work from the upper limbs rather than the lower limbs for walking.[19] Therefore, the impact of musculoskeletal pain on the fastest gait speed in patients with AAD was probably due to both upper limb and lower limb pain (Figure 1) which since upper and lower limbs are both important in controlling walking functions in these patients. The reduction in fastest gait speed suffered by SCI patients with musculoskeletal pain could result in limited community ambulation skills-such as difficulties crossing streets with traffic lights-in addition to producing other detrimental effects in these patients.[23]

There are some potential concerns regarding this study's data collection and interpretation methods. For instance, the small sample size for comparing walking speeds may have contributed to the fact that no significant difference was found in terms of the preferred gait speed of patients. Further studies should use a larger sample to confirm the effects of musculoskeletal pain on walking speed. Therefore, the results could not be generalised to the entire population of SCI patients. Further research involving longitudinal study is required to explain the causes of musculoskeletal pain. In addition, this study did not report AAD types and the different types of AAD could affect whole-body control while walking. Future study could consider the different types of AAD.

Conclusion

The findings of this study show a high prevalence of musculoskeletal pain in ambulatory patients with SCI who walk with and without AAD. Upper limb pain was more common in those using AAD, whereas patients in non-AAD group experienced more lower limb pain. Moreover, this study finds that musculoskeletal pain might be the cause of difficulty in changing walking speeds, which is related to walking ability in SCI patients. With greater awareness of problems related to musculoskeletal pain, healthcare professionals will be able to more effectively prevent this pain and ensure that it does not interfere with these patients' improvement in walking ability.

Conflicts of interest

The authors declare no conflict of interest.

Ethical approval

The participants gave their informed consent before enrolling in the study. The study was approved by the Khon Kaen University Ethics Committee for Human Research (no. HE551077).

Acknowledgment

This study was supported by Research and Graduate Studies Khon Kaen University.

References

[1] Siddall PJ, McClelland JM, Rutkowski SB, Cousins MJ. A longitudinal study of the prevalence and characteristics of pain in the first 5 years following spinal cord injury. Pain 2003; 103: 249-57. doi: 10.1016/S0304-3959(02)00452-9.

[2] Das A, Equebal A, Kumar S. Incidence of musculoskeletal pain and its impact on daily and functional activities in Indian spinal cord injury patients. Int J Physioth Res 2013; 3: 99-106. ISSN 2321-1822.

[3] Scivoletto G, Romanelli A, Mariotti A, Marinucci D, Tamburella F, Mammone A, et al. Clinical factors that affect walking level and performance in chronic spinal cord lesion patients. Spine 2008; 33: 259-64. doi: 10.1097/BRS.0b013e3181626ab0.

[4] Hassanijirdehi M, Khak M, Afshari-Mirak S, Holakouie-Naieni K, Saadat S, Taheri T, et al. Evaluation of pain and its effect on quality of life and functioning in men with spinal cord Injury. Korean J Pain 2015; 28: 129-36. PMID: 25852835.

[5] Melis EH, Torres-Moreno R, Barbeau H, Lemaire ED. Analysis of assisted-gait characteristics in persons with incomplete spinal cord injury. Spinal Cord. 1999; 37(6):430-9. doi: 10.1038/sj.sc.3100850.

[6] Saensook W, Phonthee S, Srisim K, Mato L, Wattanapan P, Amatachaya S. Ambulatory assistive devices and walking performance in patients with incomplete spinal cord injury. Spinal Cord. 2014; 52: 216-9. doi: 10.1038/sc.2013.120.

[7] Muller R, Brinkhof MW, Arnet U, Hinrichs T, Landmann G, Jordan X, et al. Prevalence and associated factors of pain in the Swiss spinal cord injury population. Spinal Cord. 2017; 55:346-54. doi: 10.1038/sc.2016.157.

[8] Kentar Y, Zastrow R, Bradley H, Bruner M, Pepke W, Bruckner T, et al. Prevalence of upper extremity pain in a population of people with paraplegia. Spinal Cord. 2018; 56(7): 695-703. doi: 10.1038/s41393-018-0062-6.

[9] Akbar M, Balean G, Brunner M, Seyler TM, Bruckner T, Mun- zinger J, et al. Prevalence of rotator cuff tear in paraplegic patients compared with controls. J Bone Joint Surg Am. 2010; 92: 23-30. doi: 10.2106/JBJS.H.01373.

[10] Kumprou M, Amatachaya P, Sooknuan T, Thaweewannakij T, Mato L. Amatachaya S. Do ambulatory patients with spinal cord injury walk symmetrically? Spinal cord. 2017; 55: 204-7. doi: 10.1038/sc.2016.149.

[11] Barbetta DC, Lopes AC, Chagas FN, Soares PT, Casaro FM, Poletto MF, et al. Predictors of musculoskeletal pain in the upper extremities of individuals with spinal cord injury. Spinal Cord. 2016; 54: 145-9. doi: 10.1038/sc.2015.126.

[12] Roberts TT, Leonard GR, Cepela DJ. Classifications in brief: American Spinal Injury Association (ASIA) Impairment Scale. Clin Orthop Relat Res. 2017; 475: 1499-504. doi: 10.1007/s11999-016-5133-4.

[13] Bryce TN, Budh CN, Cardenas DD, Dijkers M, Felix ER, Finnerup NB, et al. Pain after spinal cord injury: an evidence-based review for clinical practice and research. Report of the National Institute on Disability and Rehabilitation Research Spinal Cord Injury Measures meeting. J Spinal Cord Med. 2007; 30(5): 421-40. doi: 10.1080/10790268.2007.11753405.

[14] Siddall, PJ, Yezierski RP, Loeser JD. Taxonomy and epidemiology of spinal cord injury pain. In: Yezierski RP. and Burchiel K, editor. Spinal cord injury pain: assessment, mechanisms. Seattle, WA: IASP Press; 2002: 137-54.

[15] Siddall PJ, Loeser JD. Pain following spinal cord injury. Spinal cord. 2001; 39: 63-73. doi: 10.1038/sj.sc.3101116.

[16] Jones KR, Vojir CP, Hutt E, Fink R. Determining mild, moderate, and severe pain equivalency across pain- intensity tools in nursing home residents. J Rehabil Res Dev. 2007; 44: 305-14. doi: 10.1682/jrrd.2006.05.0051.

[17] Poncumhak P, Saengsuwan J, Kumruecha W, Amatachaya S. Reliability and validity of three functional test in ambulatory patients with spinal cord injury. Spinal Cord. 2013; 51: 214-7. doi: 10.1038/sc.2012.126.

[18] Cragg JJ, Warner FM, Shupler MS, Jutzeler CR, Cashman N, Whitehurst -GT, et al. Prevalence of chronic pain among individuals with neurological conditions. Health Rep. 2018; 29 (3): 11-6. PMID: 29561565.

[19] Saunders LL, Krause JS, DiPiro ND, Kraft S, Brotherton S. Ambulation and complications related to assistive devices after spinal cord injury. J Spinal Cord Med. 2013; 36 (6): 652-9. doi: 10.1179/2045772312Y.0000000082.

[20] Bateni H, Maki BE. Assistive devices for balance and mobility: benefits, demands, and adverse consequences. Arch Phys Med Rehabil. 2005; 86: 134-45. doi: 10.1016/j.apmr.2004.04.023.

[21] Dalyan M, Cardenas DD, Gerard B. Upper extremity pain after spinal cord injury. Spinal Cord. 1999; 37: 191-5. doi: 10.1038/sj.sc.3100802.

[22] Koh ES, Williams AJ, Povlsen B. Upper-limb pain in long-term poliomyelitis. QJM. 2002; 95: 389-95. doi: 10.1093/qjmed/95.6.389.

[23] Lapointe R, Lajoie Y, Serresse O, Barbeau H. Functional community ambulation requirements in incomplete spinal cord injury subjects. Spinal Cord. 2001; 39: 327-35. doi: 10.1038/sj.sc.3101167.

[24] Sawa R, Doi T, Misu S, Satio T, Saito T, SugimotoT, et al. The severity and number of musculoskeletal pain associated with gait in community-dwelling elderly individuals. Gait Posture. 2017; 54: 242-7. doi: 10.1016/j.gaitpost.2017.03.013.

[25] Ogawa EF, Shi L, Bean JF, Hausdorff JM, Dong Z, Manor B, et al. Chronic pain characteristics and gait in older adults The MOBILIZE Boston Study II. Arch Phys Med Rehabil.2020; 101(3): 418-25. doi: 10.1016/j.apmr.2019.09.010.

Instructions for Authors

Instructions for Authors

Original article/thesis can be submitted through the on-line system via website https://www.tci-thaijo.org/index.php/bulletinAMS/

General Principles

Journal of Associated Medical Sciences is a scientific journal of the Faculty of Associated Medical Sciences, Chiang Mai University. The articles submitted to the journal that are relevant to any of all aspects of Medical Technology, Physical Therapy, Occupational Therapy, Radiologic Technology, Communication Disorders, and other aspects related to the health sciences are welcome. Before publication, the articles will go through a system of assessment and acceptance by at least three experts who are specialized in the relevant discipline. All manuscripts submitted to Journal of Associated Medical Sciences should not have been previously published or under consideration for publication elsewhere. All publications are protected by the Journal of Associated Medical Sciences' copyright.

Manuscript categories

1. **Review articles** must not exceed 20 journal pages (not more than 5,000 words), including 6 tables/figures, and references (maximum 75, recent and relevant).
2. **Original articles** must not exceed 15 journal pages (not more than 3,500 words) including tables, figures, and 40 references (maximum 40, recent and relevant).
3. **Short communications** including technical reports, notes, and letter to editor must not exceed 5 journal pages (not more than 1,500 words), including 2 tables/figures, and references (maximum 10, recent and relevant).

Manuscript files

To submit your manuscripts, you will need the following files:

1. A Title page file with the names of all authors and corresponding authors*
2. Main document file with abstract, keywords, main text and references
3. Figure files
4. Table files
5. Any extra files such as Supplemental files or Author Biographical notes

Manuscript Format

1. **Language**: English, Caribri 10 for text and 7 for all symbols. PLEASE be informed that the Journal only accept the submission of English manuscripts.
2. **Format**: One-side printing, double spacing. Use standard program and fonts and, add page and line number for all pages.
3. **A Title page**: Include article title, names of all authors and co-authors, name of the corresponding author and acknowledgements. Prepare according to following contents;
   - *Title of the article*: Concise and informative. Titles are often used in information-retrieval systems. Avoid abbreviations and formulate where possible.
   - *Author names and affiliation*: Where the family name may be ambiguous (e.g. a double name), please indicate this clearly. Present the authors' affiliation addresses (where the actual work was done) below the names. Indicate all affiliations with superscript number immediately after author's name and in front of appropriate address. Provide the full postal address of each affiliation, including the province, country and, if available, the e-mail address of each author.
   - *Corresponding author*: Clearly indicate who will handle correspondence at all stages of refereeing and publication, also post-publication, ensure that telephone and fax numbers (with postal area code) are provided in addition to the e-mail address and the complete postal address. Contact details must be kept up to date by the corresponding author.
   - *Acknowledgements*: Acknowledgements will be collated in a separate section at the end of the article before the references in the stage of copyediting. Please, therefore, include them on the title page, List here those individuals who provided help during the research (e.g. providing language help, writing assistance or proof reading the article, etc.)
4. **Main article structure**: The manuscripts should be arranged in the following headings: Title, Abstract, Introduction, Materials and Methods, Results, Discussion and Conclusion, and Reference. Prepare according to following contents;
   - *Abstract*: Not exceeding 400 words, abstract must be structured with below headings in separated paragraph:
     - Background,
     - Objectives,
     - Materials and methods,
     - Results,
     - Conclusion, and
     - Keywords (3-5 keywords should be included)
   - *Introduction*: State the objectives of work and provide an adequate background, avoiding a detailed literature survey or a summary of the results.
   - *Materials and Methods*: Provide sufficient detail to allow the work to be reproduced. Methods already published should be indicated by a reference, only relevant modifications should be described. Ensure that each table, graph, or figure is referred in the text. According to the policy of ethical approval, authors must state the ethical approval code and conduct informed consent for human subject research (If any) and for animal research, authors must include a statement or text describing the experimental procedures that affirms all appropriate measures (if any) in this section.
   - *Results*: Results should be clear and concise. Present the new results of the study such as tables and figures mentioned in the main body of the article and numbered in the order in which they appear in the text or discussion.
   - *Discussion*: This should explore the significance of the results of the work, not repeat them. A combined Results and Discussion

section is often appropriate. Avoid extensive citations and discussion of published literature.
- *Conclusion*: The main conclusions of the study may be presented in a short Conclusions section, which may stand alone or form a subsection of a "Discussion" or "Results and Discussion".
- *Conflict of interes*t: All authors must declare any financial and personal relationship with other people or organization that could inappropriately influence (bias) their work. If there is no interest to declare, then please state this: "The authors declare no conflict of interest".
- *Ethic approval*: Ethic clearance for research involving human and animal subjects.
- *References*: Vancouver's style.

5. **Artwork Requirements**
   - Each table, graph and figure should be self-explanatory and should present new information rather than duplicating what is in the text. Prepare one page per each and submit separately as supplementary file(s).
   - Save the figures as high resolution JPEC or TIFF files.

Note: Permission to reprint table(s) and/or figure(s) from other sources must be obtained from the original publishers and authors and submitted with the typescript.

Ensuring a blind peer review

To ensure the integrity of the double-blinded peer-review for submission to this journal, every effort should be made to prevent the identities of the authors and reviewers from being known to each other. The authors of the document have deleted their names from the main text, with "Author" and year used in the references and footnotes, instead of the authors' name, article title, etc. After the journal was accepted, the name of authors and affiliation and the name of the corresponding author must be included into the document and re-submitted in the copyediting stage.

Proof correction

The Proofs of final paper approved for publication are to be returned by email to the researcher before publication.

Page charge

No page charge.

References Format

1. References using the Vancouver referencing style (see example below).
2. In-text citation: Indicate references by number(s) in the order of appearance in the text with superscript format. Reference numbers are to be placed immediately after the punctuation (with no spacing). The actual authors can be referred to, but the reference number(s) must always be given. When multiple references are cited at a given place in the text, use a hyphen (with no spacing) to join the first and last numbers that are inclusive. Use commas (with spaces) to separate non-inclusive numbers in a multiple citation e.g. (2-5, 7, 10). Do not use a hyphen if there are no citation numbers in between inclusive statement e.g. (1-2). Use instead (1, 2).
3. References list: number the references (numbers in square brackets) in the list must be in the order in which they are mentioned in the text. In case of references source from non-English language, translate the title to English and retain "in Thai" in the parentheses.
4. Please note that if references are not cited in order the manuscript may be returned for amendment before it is passed on to the Editor for review.

Examples of References list

Multiple Authors: List up to the first 6 authors/editors, and use "et al." for any additional authors.

Journal Articles (print): In case of reference source contains Digital Object Identifier (DOI), retain doi: at the end of reference. Vancouver Style does not use the full journal name, only the commonly-used abbreviation: "Physical Therapy" is cited as "Phys Ther". As an option, if a journal carries continuous pagination throughout a volume (as many medical journals do) the month and/or issue number may be omitted. Allow one space after semi-colon and colon then end each reference with full stop after page number.

[1] Pachori P, Gothalwal R, Gandhi P. Emergence of antibiotic resistance Pseudomonas aeruginosa in intensive care unit; a critical review. Genes Dis. 2019; 6(2): 109-19. doi: 10.1016/j.gendis.2019.04.001.

[2] Hung Kn G, Fong KN. Effects of telerehabilitation in occupational therapy practice: A systematic review. Hong Kong J Occup Ther. 2019; 32(1): 3-21. doi: 10.1177/1569186119849119.

[3] Wijesooriya K, Liyanage NK, Kaluarachchi M, Sawkey D. Part II: Verification of the TrueBeam head shielding model in Varian VirtuaLinac via out-of-field doses. Med Phys. 2019; 46(2): 877-884. doi: 10.1002/mp.13263.

[4] Velayati F, Ayatollahi H, Hemmat M. A systematic review of the effectiveness of telerehabilitation interventions for therapeutic purposes in the elderly. Methods Inf Med. 2020; 59(2-03): 104-9. doi: 10.1055/s-0040-1713398.

[5] Junmee C, Siriwachirachai P, Chompoonimit A, Chanavirut R, Thaweewannakij T, Nualnetr N. Health status of patients with stroke in Ubolratana District, Khon Kaen Province: International Classification of Functioning, Disability and Health-based assessments. Thai J Phys Ther. 2021; 43(1): 45-63 (in Thai).

Journal Articles on the Internet

[1] Siegel PM, Bojti I, Bassler N, Holien J, Flierl U, Wang X, et al. A DARPin targeting activated Mac-1 is a novel diagnostic tool and potential anti-inflammatory agent in myocarditis, sepsis and myocardial infarction. Basic Res Cardiol [Internet]. 2021; 116(1): 1-25. Available from: https://doi.org/10.1007/s00395-021-00849-9.

Journal Articles from an Online Database

[1] Jackson D, Firtko A, Edenborough M. Personal resilience as a strategy for surviving and thriving in the face of workplace adversity: A literature review. J Adv Nurs [serial online]. 2007;60(1):1-9. DOI: 10.1111/j.1365-2648.2007.04412.x.

Book / Chapter in an Edited Book References

PLEASE be informed that references of books and chapter in edited book should not be include in the research article, but others manuscript categories.

[1] Grove SK, Cipher DJ. Statistics for nursing research: A workbook for evidence-based practice. 3rd ed. St. Louis, Missouri: Elsevier; 2019.

[2] Haznadar M, editor. Cancer metabolism: Methods and protocols. New York: Humana Press; 2019. doi: 10.1007/978-1-4939-9027-6.

[3] Perrin DH. The evaluation process in rehabilitation. In: Prentice WE, editor. Rehabilitation techniques in sports medicine. 2nd ed. St Louis, Mo: Mosby Year Book; 1994: 253–276.

E-book

[1] Dehkharghani S, editor. Stroke [e-book]. Brisbane (AU): Exon Publications; 2021 [cited 2021 Jul 31]. Available from: https://www.ncbi.nlm.nih.gov/books/NBK572004/ doi: 10.36255/exonpublications.stroke.2021

[2] Tran K, Mierzwinski-Urban M. Serial X-Ray radiography for the diagnosis of osteomyelitis: A review of diagnostic accuracy, clinical utility, cost-effectiveness, and guidelines [e-book]. Ottawa (ON): Canadian Agency for Drugs and Technologies in Health; 2020 [cited 2021 Jul 31]. Available from: https://www.ncbi.nlm.nih.gov/books/NBK562943/

Dissertation/Thesis

[1] On-Takrai J. Production of monoclonal antibody specific to recombinant gp41 of HIV-1 subtype E [Term paper]. Faculty of Associated Medical Sciences: Chiang Mai University; 2001 [in Thai].

[2] Seale AC. The clinical and molecular epidemiology of streptococcus agalactiae in Kenya: maternal colonization and perinatal outcomes [Dissertation on the Internet]. [Oxford (England)]: University Oxford; 2015 [cited 2015 Jul 28]. Available from: http://ora.ox.ac.uk/objects/uuid:6e7d952a-dc5b-4af0-b0bb-f2ae2184eed0.

.

Conference Proceedings

[1] Lake M, Isherwood J, Clansey. Determining initial knee joint loading during a single limb drop landing: reducing soft tissue errors. Proceedings of 34th International Conference of Biomechanics in Sport; 2016 Jul 18-22; Tsukuba, Japan, 2016. Available from: https://ojs.ub.uni-konstanz.de/cpa/article/view/7126

[2] Ellis MD, Carmona C, Drogos J, Traxel S, Dewald JP. Progressive abduction loading therapy targeting flexion synergy to regain reaching function in chronic stroke: preliminary results from an RCT. Proceedings of the 38th Annual International Conference of the IEEE Engineering in Medicine and Biology Society; 2016: 5837-40. doi: 10.1109/EMBC.2016.7592055.

Organization as Author / Government Document

[1] Australian Government, Department of Health. Physical activity and exercise guidelines for all Australian. 2021 [updated 2021 May 7; cited 2021 Jul 15]. Available from: https://www.health.gov.au/health-topics/physical-activity-and-exercise/physical-activity-and-exercise-guidelines-for-all-australians.

[2] Department of Health. Situation survey on policy and implementation of physical activity promotion in schools for first year 2005. Nonthaburi: Ministry of Public Health; 2005. (in Thai).

[3] Department of Local Administration, Ministry of Interior Affairs. Standard of Sports Promotion. Bangkok. 2015: 7–9. (in Thai).

[4] World Health Organization. WHO guidelines on physical activity and sedentary behaviour. Geneva: World Health Organization; 2020. Licence: CC BY-NC-SA 3.0 IGO.

[5] World Health Organization. The epidemiology and impact of dementia: current state and future trends. 2015 [cited 2021 Mar 8]. Available from: http://www.who.int/mental_health/neurology/dementia/dementia_thematicbrief_epidemiology.pdf.

Journal History

Established in 1968

- 1968-2016 As the Bulletin of Chiang Mai Associated Medical Sciences
  - Vol1, No1 - Vol.49, No3
- 2017, the Journal of Associated Medical Sciences
  - Vol.50, No1 and forward.

Journal Sponsorship Publisher

Faculty of Associated Medical Sciences, Chiang Mai University

Sponsors

Faculty of Associated Medical Sciences, Chiang Mai University

Sources of support

Faculty of Associated Medical Sciences, Chiang Mai University


JOURNAL OF ASSOCIATED
MEDICAL SCIENCES
JAMS